

Sheffield Hallam University

Novel supramolecular assemblies based on sulfur-nitrogen radicals.

HARGREAVES, Stephen.

Available from the Sheffield Hallam University Research Archive (SHURA) at:

<http://shura.shu.ac.uk/19755/>

A Sheffield Hallam University thesis

This thesis is protected by copyright which belongs to the author.

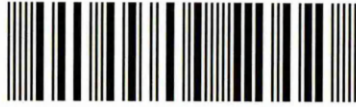
The content must not be changed in any way or sold commercially in any format or medium without the formal permission of the author.

When referring to this work, full bibliographic details including the author, title, awarding institution and date of the thesis must be given.

Please visit <http://shura.shu.ac.uk/19755/> and <http://shura.shu.ac.uk/information.html> for further details about copyright and re-use permissions.

LEARNING CENTRE
CITY CAMPUS, POND STREET,
SHEFFIELD, S1 1WB.

101 651 883 8



Fines are charged at 50p per hour

- 5 FEB 2002

8.51.p.m

20 MAR 2002

4.23p.m



ProQuest Number: 10697057

All rights reserved

INFORMATION TO ALL USERS

The quality of this reproduction is dependent upon the quality of the copy submitted.

In the unlikely event that the author did not send a complete manuscript and there are missing pages, these will be noted. Also, if material had to be removed, a note will indicate the deletion.



ProQuest 10697057

Published by ProQuest LLC (2017). Copyright of the Dissertation is held by the Author.

All rights reserved.

This work is protected against unauthorized copying under Title 17, United States Code
Microform Edition © ProQuest LLC.

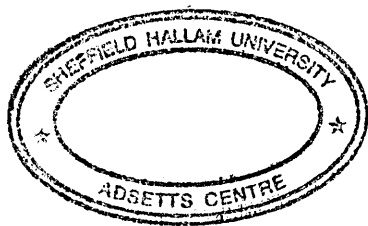
ProQuest LLC.
789 East Eisenhower Parkway
P.O. Box 1346
Ann Arbor, MI 48106 – 1346

Novel Supramolecular Assemblies Based on Sulfur-Nitrogen Radicals

Stephen Hargreaves (BSc Hons)

A thesis submitted in partial fulfilment of the requirements of
Sheffield Hallam University
for the degree of Doctor of Philosophy

November 2000



Abstract

This thesis describes the synthesis of a range of novel dithiadiazolyl radicals. The structures of these compounds are discussed. The physical properties of several compounds have been investigated using EPR spectroscopy and magnetic susceptibility studies.

Chapter one begins with an overview of the chemistry of 1,2,3,5-dithiadiazolyl radicals. A general discussion of the history of organic conductors and magnets, and the terms involved in some of the techniques used is given in order to provide a background to the work presented.

The second chapter outlines the synthesis and general characterisation of all the dithiadiazolyl radicals discussed in this thesis. A proposed mechanism for the conversion of parent nitriles into dithiadiazolyl radicals has been included.

The third chapter describes the solid state structures of three dichlorophenyl dithiadiazolyl derivatives (2,4-, 2,5- and 3,5-dichlorophenyl-1,2,3,5-dithiadiazolyl). A further polymorph of 3,5-dichlorophenyl-1,2,3,5-dithiadiazolyl has also been included. The magnetic susceptibility of 2,4- and 3,5-dichlorophenyl-1,2,3,5-dithiadiazolyl has been investigated and the EPR analysis of all three compounds has been performed. These compounds are the first examples of neutral dithiadiazolyl radicals that form evenly spaced, segregated stacks in the solid state.

Chapter four describes the dimer stacking structures of two further dichlorophenyl dithiadiazolyl derivatives (2,3- and 3,4-dichlorophenyl-1,2,3,5-dithiadiazolyl).

The fifth chapter discusses the association of 3,5-dibromophenyl-1,2,3,5-dithiadiazolyl in the solid state. An investigation of this compound by EPR spectroscopy is also presented.

Chapter six describes the *trans* cofacial association of *p*-iodophenyl-1,2,3,5-dithiadiazolyl in the solid state, only the second published example of this mode of dimerisation. The synthesis of *o*- and *p*-iodobenzonitrile are also described. An investigation of the EPR signal of this compound has also been included.

Chapter seven describes the specialised techniques used in the synthesis of all the compounds. A list of the instruments used for analysis is also included.

Acknowledgements

Firstly I would like to thank my supervisor Neil Bricklebank for his help during my PhD, Norman Bell for his time taken to read my work and the Materials Research institute for financial support.

I am deeply indebted to Harry Adams and Sharon Spey who have work above and beyond the call of duty to complete my crystal structures. Frank Mabbs has shown enthusiasm and has spent a considerable amount of time trying to gain a clear picture of EPR measurements of my compounds. I would also like to thank Fernando Palacio and his students for completing my magnetic susceptibility measurements.

Thanks to all of my colleagues namely Donna, Jo, Matt, Jackie, Chris, John, Sarah, Bob (Rory), Anna, Cristina and Tahir. They have all played a part in keeping me sane but not always sober. The technical staff of the Division of Chemistry have also played an important role in the support of my research, especially Kev (I will never say no) Osbourne.

My girlfriend, Monica has tirelessly supported me throughout my work and has been a constant source of tea during my writing up.

Finally I would like to thank my parents for supporting me even though I still haven't got a proper job and often find it difficult to balance my books.

Contents

CHAPTER 1

INTRODUCTION

1.0	INTRODUCTION	2
1.1	BRIEF HISTORY OF SULFUR NITROGEN COMPOUNDS	2
1.2	DITHIADIAZOLYLS	4
1.3	SYNTHETIC METHODS FOR DITHIADIAZOLYLIUM SALTS.....	5
1.4	SYNTHETIC METHODS FOR DITHIADIAZOLYLS.....	9
1.5	STRUCTURAL ASPECTS OF DITHIADIAZOLYL RADICALS.....	10
1.5.1	<i>Cis-cofacial Type Configurations</i>	11
1.5.2	<i>Twisted Type Configurations</i>	13
1.5.3	<i>Trans-antarafacial Configurations</i>	13
1.5.4	<i>Trans-cofacial Configurations</i>	14
1.5.5	<i>Other Conformations</i>	14
1.6	MAGNETISM AND NON-METALLIC MAGNETS.....	18
1.7	CONDUCTION IN ORGANIC MATERIALS.....	25
1.8	ELECTRON PARAMAGNETIC RESONANCE.....	28
1.8.1	<i>Experimental Considerations</i>	29
1.8.2	<i>g-value</i>	30
1.8.3	<i>Fine, Hyperfine and Superfine Structure</i>	30
1.8.4	<i>EPR Spectroscopic Studies of Dithiadiazolyl Radicals</i>	31
1.9	AIMS OF THE PRESENT WORK.....	34
1.10	REFERENCES	34

CHAPTER 2

SYNTHESIS

2.0	INTRODUCTION	42
2.1	SYNTHESIS AND MECHANISMS	44
2.2	EXPERIMENTAL.....	48
2.2.1	<i>Preparation of 3,5-dichlorophenyl-1,2,3,5-dithiadiazolyl (1)</i>	48
2.2.2	<i>Preparation of 2,5-dichlorophenyl-1,2,3,5-dithiadiazolyl (2)</i>	49
2.2.3	<i>Preparation of 2,4-dichlorophenyl-1,2,3,5-dithiadiazolyl (3)</i>	50
2.2.4	<i>Preparation of 3,4-dichlorophenyl-1,2,3,5-dithiadiazolyl (4)</i>	51
2.2.5	<i>Preparation of 2,3-dichlorophenyl-1,2,3,5-dithiadiazolyl (5)</i>	52
2.2.6	<i>Preparation of 3,5-dibromophenyl-1,2,3,5-dithiadiazolyl (6)</i>	53
2.2.7	<i>Preparation of 4-iodophenyl-1,2,3,5-dithiadiazolyl (7)</i>	54
2.2.8	<i>Preparation of 2-iodophenyl-1,2,3,5-dithiadiazolyl (8)</i>	55
2.3	REFERENCES	56

CHAPTER 3

STACKING MOTIFS FOR DICHLOROPHENYL DITHIADIAZOLYL RADICALS

3.0	INTRODUCTION	58
3.1	X-RAY CRYSTAL STRUCTURES	61
3.1.1	<i>X-ray Crystal Structure of 2,4-dichlorophenyl-1,2,3,5-dithiadiazolyl</i>	66
3.1.2	<i>X-ray Crystal Structure of 2,5-dichlorophenyl-1,2,3,5-dithiadiazolyl</i>	72
3.1.3	<i>X-ray Crystal Structure of 3,5-dichlorophenyl-1,2,3,5-dithiadiazolyl</i>	77
3.1.3.1	<i>Structure of β-3</i>	78
3.1.3.2	<i>Structure of α-3</i>	84
3.2	MAGNETIC MEASUREMENTS	90
3.2.1	<i>The Diamagnetic Contribution</i>	90
3.2.2	<i>Features at Low Temperature</i>	94
3.2.3	<i>Features at High Temperature</i>	95
3.2.4	<i>Conclusion</i>	98
3.3	ELECTRON PARAMAGNETIC RESONANCE.....	98
3.3.1	<i>Frozen Glass Studies</i>	98
3.3.2	<i>Powder Studies</i>	103
3.3.3	<i>Single Crystal EPR Measurements on Compound 3</i>	107
3.4	CONCLUSIONS.....	111
3.5	REFERENCES	112

CHAPTER 4

DIMER STACKING MOTIFS FOR DICHLOROPHENYL DITHIADIAZOLYL RADICALS

4.0	INTRODUCTION	116
4.1	X-RAY CRYSTAL STRUCTURES	118
4.1.1	<i>X-ray Crystal Structure of 2,3-dichlorophenyl-1,2,3,5-dithiadiazolyl</i>	122
4.1.2	<i>X-ray Crystal Structure of 3,4-dichlorophenyl-1,2,3,5-dithiadiazolyl</i>	126
4.2	CONCLUSIONS.....	130
4.3	REFERENCES	131

CHAPTER 5

THE STRUCTURE AND PHYSICAL PROPERTIES OF 3,5-DIBROMOPHENYL-1,2,3,5-DITHIADIAZOLYL

5.0	INTRODUCTION	133
5.1	X-RAY CRYSTAL STRUCTURE.....	134
5.2	ELECTRON PARAMAGNETIC RESONANCE STUDY	141
5.2.1	<i>Frozen Glass Studies</i>	141
5.3	CONCLUSIONS	143
5.4	REFERENCES	144

CHAPTER 6

THE SYNTHESIS, STRUCTURE AND PHYSICAL PROPERTIES OF IODOPHENYL DITHIADIAZOLYL RADICALS

6.0	INTRODUCTION	147
6.1	SYNTHESIS OF <i>PARA</i> AND <i>ORTHO</i> -IODOBENZONITRILE	148
6.2	X-RAY CRYSTAL STRUCTURE OF <i>P</i> -IODOPHENYL-1,2,3,5-DITHIADIAZOLYL.....	149
6.3	EPR STUDY OF <i>P</i> -IODOPHENYL-1,2,3,5-DITHIADIAZOLYL	156
	6.3.1 <i>Frozen Glass Studies</i>	156
6.4	EXPERIMENTAL.....	158
	6.4.1 <i>Preparation of p-Iodobenzonitrile</i>	158
	6.4.2 <i>Preparation of o-Iodobenzonitrile</i>	159
6.5	CONCLUSIONS.....	160
6.6	REFERENCES	161

CHAPTER 7

GENERAL EXPERIMENTAL

7.0	INTRODUCTION	164
7.1	PHYSICAL METHODS	164
7.1.1	<i>Infra-Red Spectroscopy</i>	164
7.1.2	<i>Mass Spectrometry</i>	164
7.1.3	<i>¹H and ¹³C NMR Spectroscopy</i>	165
7.1.4	<i>Differential Scanning Calorimetry</i>	165
7.1.5	<i>Electron Paramagnetic Resonance</i>	165
7.1.6	<i>Single Crystal X-Ray Diffraction</i>	165
7.1.7	<i>Elemental Analysis</i>	166
7.1.8	<i>Magnetic Measurements</i>	166
7.2	SOLVENTS	166
7.2.1	<i>Diethyl ether (Fisher)</i>	166
7.2.2	<i>Tetrahydrofuran (Sigma-Aldrich)</i>	166
7.2.3	<i>Dichloromethane (Fisher)</i>	167
7.2.4	<i>Acetonitrile (Fisher)</i>	167
7.2.5	<i>Dimethylformamide</i>	167
7.2.6	<i>Toluene (Fisher)</i>	167
7.3	REAGENTS.....	167
7.4	REFERENCES	168
	OVERALL CONCLUSIONS AND SUGGESTIONS	169

APPENDICES

APPENDIX 1	171
<i>Crystal data and structure refinement:</i>	
2,4-dichlorophenyl-1,2,3,5-dithiadiazolyl	171
APPENDIX 2	173
<i>Crystal data and structure refinement:</i>	
2,5-dichlorophenyl-1,2,3,5,-dithiadiazolyl	173
APPENDIX 3	175
<i>Crystal data and structure refinement:</i>	
β -(3,5-dichlorophenyl-1,2,3,5,-dithiadiazolyl)	175
APPENDIX 4	178
<i>Crystal data and structure refinement:</i>	
α -(3,5-dichlorophenyl-1,2,3,5,-dithiadiazolyl)	178
APPENDIX 5	184
<i>Supporting data for magnetic measurement plots</i>	184
Figure 3.25 $M(T)$ at 10,000 Oe (no Correction) Curie-Weiss fit for 3	184
Figure 3.26 $M(T)$ at 10,000 Oe (no correction) Curie-Weiss fit for 1	185
Figure 3.27 $M(H/T)$ (low temperature) diamagnetism removed Brillouin fit for 3 ...	186
Figure 3.28 $M(H/T)$ (low temperature) diamagnetism removed Brillouin fit for 1 ...	187
Figure 3.29 χT (T) (diamagnetism removed) “dimer” fit for 3	188
Figure 3.30 χT (T) (diamagnetism removed) “dimer” fit for 1	189
APPENDIX 6	190
<i>Crystal data and structure refinement:</i>	
2,3-dichlorophenyl-1,2,3,5-dithiadiazolyl	190
APPENDIX 7	192
<i>Crystal data and structure refinement:</i>	
3,4-dichlorophenyl-1,2,3,5-dithiadiazolyl	192
APPENDIX 8	194
<i>Crystal data and structure refinement:</i>	
3,5-dibromophenyl-1,2,3,5-dithiadiazolyl	194
APPENDIX 9	196
<i>Crystal data and structure refinement:</i>	
<i>p</i> -iodophenyl-1,2,3,5-dithiadiazolyl	196
APPENDIX 10	198
<i>Published paper</i>	198

1.0 Introduction

The search for non-metallic conductors and magnets has become a significant field of research over the past few decades. The first purely organic conductor was a perylene-bromine salt, discovered in 1954.¹ Experimental observations of co-operative magnetic effects in a purely organic material were first reported in 1985.² Since the discovery of these two unusual organic compounds, the number of organic materials exhibiting conductive or magnetic properties has increased dramatically.

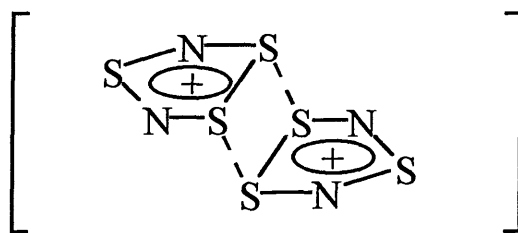
1.1 Brief History of Sulfur Nitrogen Compounds

The study of sulfur-nitrogen compounds has attracted the attention of chemists for decades. Unusual structures that pose considerable problems in terms of simple bonding theory have been observed in many novel cyclic and acyclic compounds. Tremendous additional interest was stimulated by the discovery of the polymer $(SN)_x$ that has a metal-like conductivity at room temperature and which becomes superconducting below 0.3 K.³ Although many recent discoveries have heightened the interest in this group of compounds the field is not new. In 1835, W. Gregory⁴ added sulfur dichloride to an aqueous solution of ammonia to give a yellow precipitate of sulfur contaminated with S_4N_4 . It was not until 1851 and 1896 that the stoichiometry and tetrameric nature, respectively, of pure S_4N_4 was elucidated. Its cyclic, pseudo-cluster structure was not revealed until 1944.

Nitrogen and sulfur are diagonally related in the periodic table and therefore might be expected to have similar electronic charge densities for similar co-ordination numbers. Likewise, they have similar electronegativities ($N = 3.0$, $S = 2.5$)⁵ that can become even closer when additional electron withdrawing groups are bonded to the S atom. Extensive

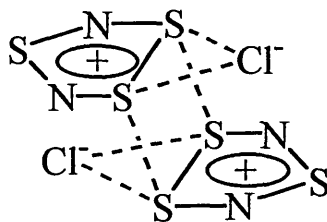
covalent bonding into acyclic, cyclic and polycyclic molecular structures is therefore expected.

The first sulfur nitrogen radical $[S_3N_2^{+\bullet}]Cl^-$ was reported in 1880.⁶ The deep green powder was thought to be in the form of S_3N_2Cl and the ESR spectra of this compound indicated the presence of a monomeric radical.⁷ Further studies contradicted this, showing little solubility in a variety of solvents and the absence of a Nuclear Quadrupole Resonance signal, consistent with an oligomeric, ionic, structure. The structure of $[S_3N_2^{+\bullet}]Cl^-$ was finally elucidated in 1974⁸ in the form of the $S_6N_4^{2+}$ cation [1].



[1]

The monomeric component of this structure ($S_3N_2^{+\bullet}$) provides a single electron to form a $\pi^*-\pi^*$ interaction crossing the four sulfur atoms. There are also secondary interactions between the sulfur and the chloride anion [2]. Such interactions inhibit the dissolution of these salts in organic solvents.



[2]

Since then many such structures have been reported,^{9,10,11,12,13,14,15} all showing the overlap of two singly occupied molecular orbitals (SOMO) at sulfur to form dimers. The heat of dimerisation is small ($-47 \pm 3 \text{ kJ mol}^{-1}$ for $[\text{S}_3\text{N}_2^+] \text{Cl}$),⁷ which is enough to show some paramagnetic behaviour even in the solid state.^{7,16}

1.2 Dithiadiazolyls

As a development of the $[\text{S}_3\text{N}_2^+]$ radical, it was thought that similar iso-electronic radicals could be obtained by substituting one of the sulfurs by an RC unit (R = alkyl, aryl or halogen). The physical and chemical properties could then be investigated for a large variety of structures in which the properties could be modified by the variation of the R substituent. This replacement leads to four possible isomers of a 7π RCN_2S_2 ring [3] – [6], which are commonly known as dithiadiazolyls.

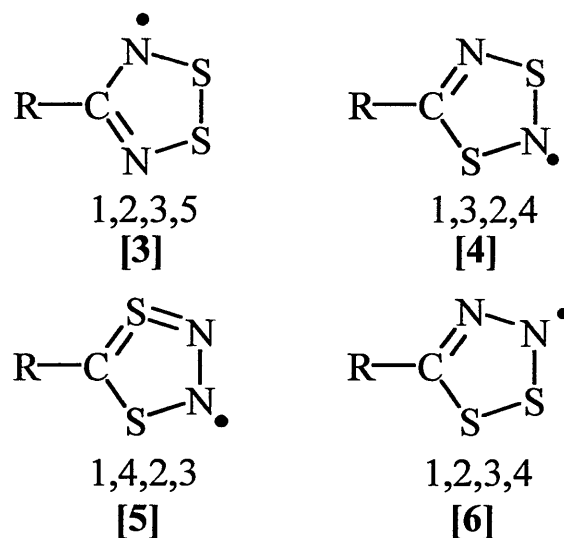
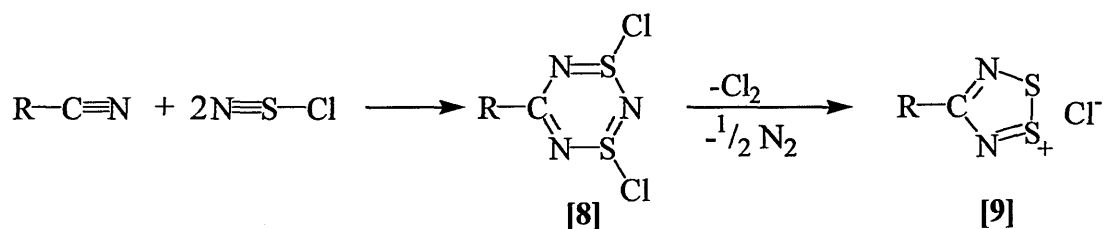


Figure 1.1 Isomers of dithiadiazolyl

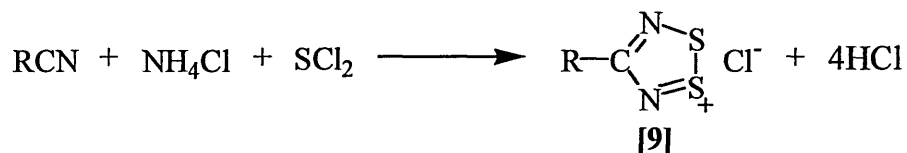
Molecular orbital calculations indicate that all of the four isomers (Figure 1.1) could be formed although only the 1,2,3,5- and 1,3,2,4-isomers have been isolated to date.¹⁷ The possible loss of di-nitrogen may have an important effect on the stability of the 1,2,3,4- and 1,4,2,3-isomers.

complicated, forms several different intermediates, and can often give much lower yields than 50%.



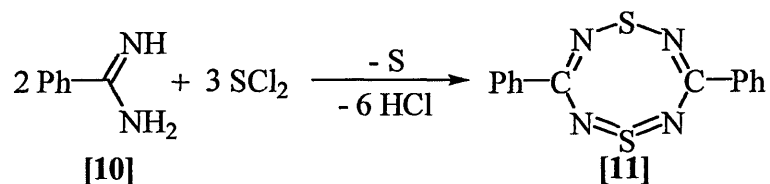
Scheme 1.2 Reaction of organic nitrile with (NSCl)₃

These problems led to the investigation of different routes for the synthesis of [9]. One important step was the discovery that a refluxing mixture of parent nitrile and sulfur dichloride containing ammonium chloride, creates an *in situ* source of thiazyl chloride (Scheme 1.3).^{23,27} The reaction proceeds *via* [S₃N₂Cl]Cl, which can be converted to thiazyl chloride [7] under an atmosphere of chlorine.²⁸



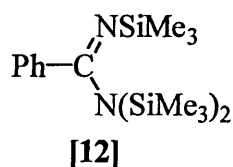
Scheme 1.3 *in situ* synthesis of thiazolyl chloride

It was predicted that during the reaction the nitrile was converted to the corresponding amidine and amidinium salt. An investigation of the reaction of various amidines with sulfur dichloride was then performed.²³ Subsequently a range of dithiadiazolylum salts were made in this way.^{29,30,31,32} Woodward and co-workers³³ conducted the attempted synthesis of a linear polymeric sulfur nitride. It was discovered that if benzamidine was condensed with sulfur dichloride then the desired precursor to a polymer was not produced, and only a complex mixture of heterocycles could be isolated. On further investigation²⁹ the sulfur nitrogen heterocycle 3,7-diphenyl-1,5,2,4,6,8-dithiatetrazocine [11] was found (Scheme 1.4).

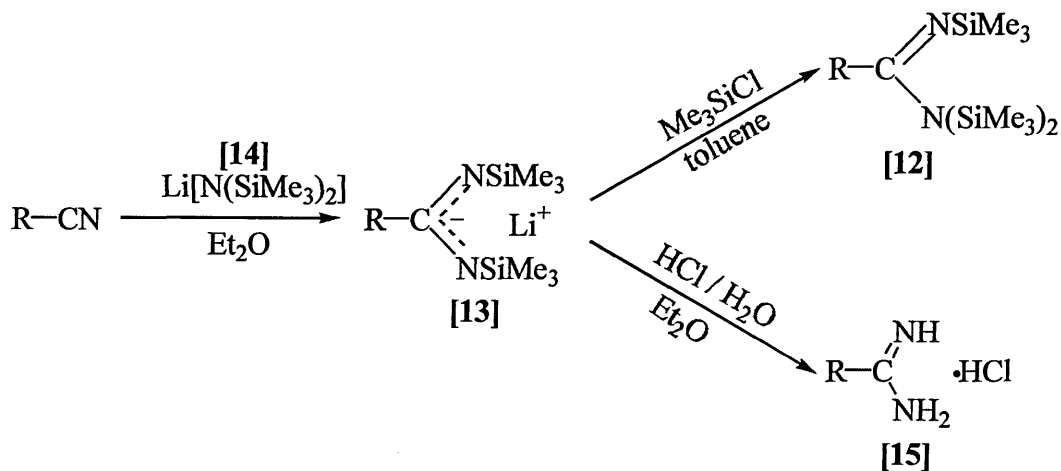


Scheme 1.4 Reaction of an amidine with sulfur dichloride

A further study of the reaction showed that another product was 4-phenyl-1,2,3,5-dithiadiazolylum chloride [9].³¹ The yield was improved by the addition of a base like diazabicycloundecane (DBU) to react with the hydrochloric acid produced during the course of the reaction.^{33,32} It was also shown that changing sulfur dichloride with disulfur dichloride and benzamidine [10] with its tris(trimethylsilyl) derivative [12], greatly improved the yield of the reaction (60 and 54% respectively).³⁴

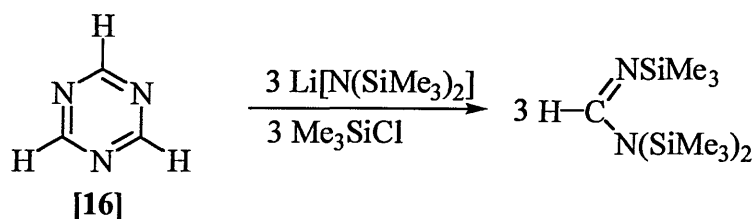


The precursor to [12], *N*-lithio salt [13], was first reported in 1973 by A.R. Sanger *et al.*³⁵ A further study of this group of compounds was published in 1987.³⁶ The reaction of lithium bis(trimethylsilyl)amide [14] with benzonitrile in diethyl ether allowed the isolation of the respective lithiated benzamidine derivative (Scheme 1.5). This could then be hydrolysed with ethanolic HCl to yield an un-substituted amidine hydrochloride [15] by precipitation. The reaction of the lithiated benzamidine with chlorotrimethylsilane in toluene afforded tris(trimethylsilyl)benzamidine [12]. Compound [12] has been found very useful for high yielding synthesis of sulfur-nitrogen heterocycles.^{31,37,38,39,40,41,42,43,44}



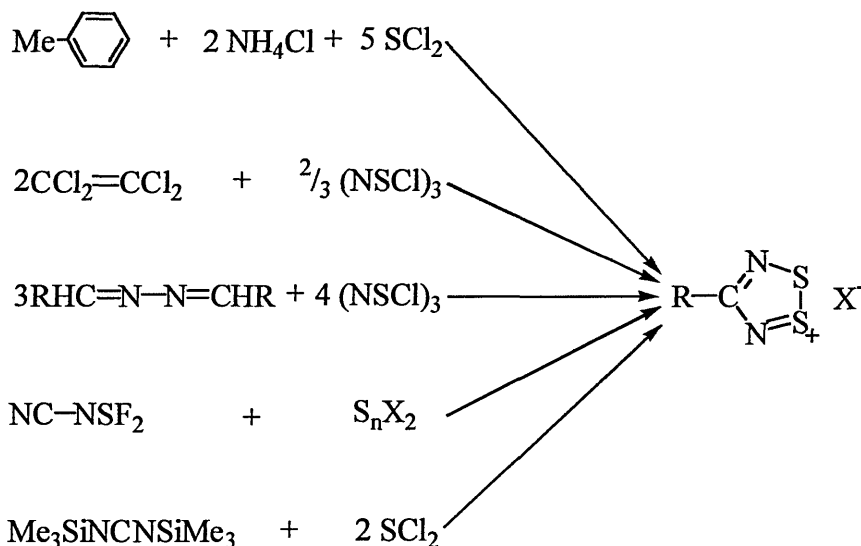
Scheme 1.5 Amidine synthesis

The conversion of benzamidines such as [12] into the 1,2,3,5-dithiadiazolylium chlorides [9] can be achieved by the addition of excess sulfur dichloride. The reaction will proceed whether the amidine itself or its *N*-lithio salt [13] is used. Further purification by Soxhlet extraction of the dithiadiazolylium salt with sulfur dioxide is necessary when proceeding *via* the *N*-lithio salt [13]. The reaction, although giving high yields, has limitations especially for compounds containing protons in the α -position, due to complex side reactions. One method of solving this problem has been to use *sym*-triazines [16] as the starting material (Scheme 1.6).⁴⁵



Scheme 1.6 Amidine synthesis *via sym*-triazine

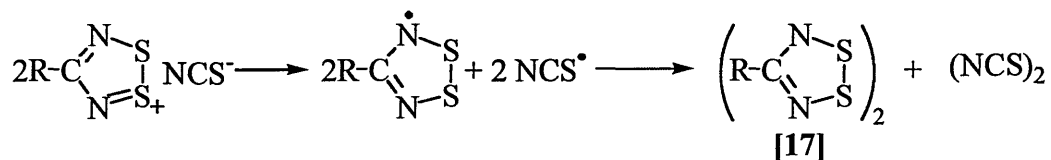
In addition to the routes outlined earlier, other methods have been reported in the literature for making dithiadiazolylium salts. Selections of these are outlined in (Scheme 1.7).^{23,25,27,46,47,48}



Scheme 1.7 Other synthetic methods for 1,2,3,5- dithiadiazolylium salts

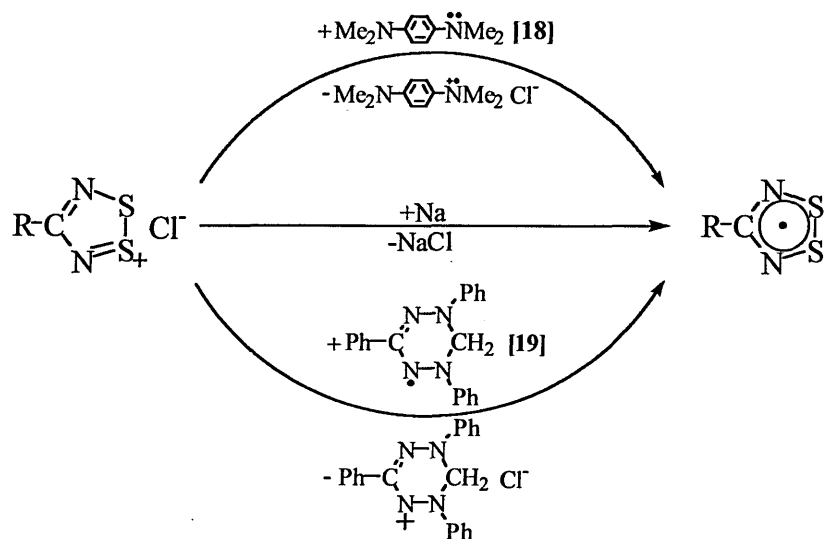
1.4 Synthetic Methods for Dithiadiazolyls

The first dithiadiazolyl radical dimer was reported in 1980 by A.J. Banister *et al.*¹⁹ It was prepared by the metathesis of 4-phenyl-1,2,3,5-dithiadiazolylium chloride with sodium thiocyanate. After refluxing in 1,2-dimethoxyethane for 12 hours disproportionation occurred and the neutral dimer was isolated (Scheme 1.8).



Scheme 1.8 Disproportionation of 1,2,3,5-dithiadiazolylium salts

This phenomenon is particularly common with soft anions especially NCS^- and I^- .^{27,17} The first chemical reduction of a dithiadiazolylium salt was reported using either sodium dust, tetramethyl-*p*-phenylene diamine [18] or triphenylverdazyl [19] (Scheme 1.9).²⁰



Scheme 1.9 Chemical reduction of 1,2,3,5-dithiazolium chloride

Since this discovery, many other materials have been investigated as reducing agents, including zinc/copper couple, potassium, mercury, zinc, potassium cyanide, LiN_3 , PhMgBr , $n\text{BuLi}$ and SnCl_2 .^{27,40,49} They all work well in oxygen-donor solvents at room temperature (*e.g.* THF or monoglyme). In recent years, triphenylstibine in dichloromethane has become a common reducing agent.^{27,32,40} Reduction can also take place electrochemically.¹⁷

1.5 Structural Aspects of Dithiadiazolyl Radicals

Like (S_3N_2^+) , dithiadiazolyls tend to display a complex array of secondary 'intermolecular' $\text{S}\cdots\text{S}$ and $\text{S}\cdots\text{N}$ interactions in the solid state. X-ray diffraction studies of this group of compounds has moved on from studying the mode of association in the solid state, to study the factors affecting the molecular packing of the compounds. More recently, an emphasis has been made on the effects of particular R substituents to steer the radicals towards specific solid state motifs.

Most dithiadiazolyls associate in the solid state to form *cis*-cofacial dimers. The S...S interactions linking the dimers are normally in the range 2.9 - 3.2 Å. The energy of dimerisation is approximately 35 kJ mol⁻¹.⁷ This energy is small on the scale of bond energies (for example a typical S-S covalent bond has a dissociation energy of 226 kJ mol⁻¹),⁵⁰ but is large in comparison with other intermolecular interactions. Other modes of association observed include *trans*-antarafacial and twisted dimer motifs, and very recently a compound displaying a *trans*-cofacial mode has been identified (Figure 1.2).

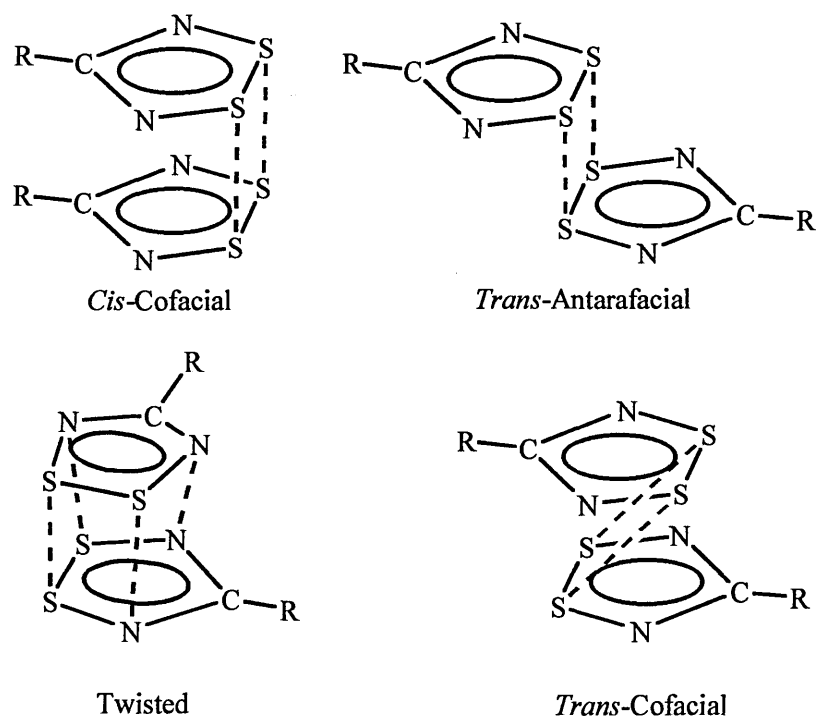


Figure 1.2 Conformations of dithiadiazolyl dimers in the solid state

1.5.1 *Cis-cofacial Type Configurations*

Many of the dithiadiazolyls studied to date have aryl substituents and are therefore planar. In the solid state, the materials dimerise through two S...S interactions. In the case of aryl substituents, there is little steric hindrance, which allows the groups to lie directly above

each other. Table 1.1 lists several reported *cis*-cofacial dimers together with their S...S distances.

Table 1.1 Inter dimer distances for some *cis*-cofacial dimers

Dithiadiazolyl Substituent	S...S Dimer Distance	Reference
Ph	3.102 Å	19
<i>p</i> -MeS.C ₆ H ₄	3.061 Å	17
<i>p</i> -Cl.C ₆ H ₄	3.099 Å	51
2-NC.C ₄ H ₂ O	3.126 Å	40
C ₆ F ₅	3.067 Å	17
<i>p</i> -NC.C ₆ H ₄	3.10(2) Å	32
<i>m</i> -NC.C ₆ H ₄ (α -phase)	3.13(2) Å	32

The molecular structures of these compounds are remarkably similar, but all display significantly different molecular packing in the solid state. This phenomenon is extremely important when considering the factors controlling the production of polymeric arrays or chains which may display electronic or magnetic properties. An example of this can be seen with *p*-Cl.C₆H₄. $\overline{\text{CNSSN}}$ ⁵¹ which is a dimer but which also shows secondary S...Cl interactions. In this case, the chlorine acts in much the same way as the chloride ion in C₆H₅. $\overline{\text{CNSSN}}$ ⁺ Cl⁻ and interacts along the plane of the dithiadiazolyl ring with two sulfur atoms within the ring. Another good example of this is observed for *p*-NC.C₆H₄. $\overline{\text{CNSSN}}$ ³² where the secondary interactions between the sulfur atoms within the ring and the nitrile substituent form chains through in-plane CN...S interactions.

1.5.2 Twisted Type Configurations

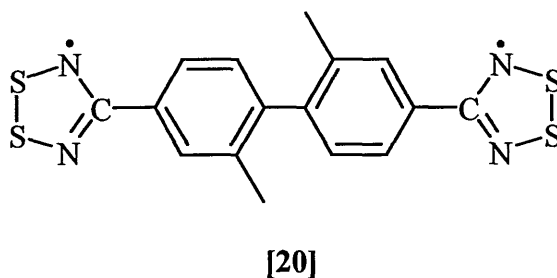
This configuration usually occurs when the substituent is non-planar *e.g.* CF₃,²⁵ Me,⁴⁹ *t*Bu.^{17,52} In order to minimise steric repulsion the molecules adopt a twisted conformation in which there is one strong S··S contact and some weaker S··N interactions. The interdimer distance (S··S distance) is comparable to that of the *cis*-cofacial conformation. It has also been shown that because of the large steric crowding involved in these compounds, the melting points are often low. Indeed the *t*Bu derivative is a paramagnetic liquid at room temperature but upon cooling, the compound associates as a dimer. A further example was also observed in adamantyl-1,2,3,5-dithiadiazolyl.⁵³ The structure was surprisingly similar to that of smaller alkyl substituents, despite its rigidity and significant steric influence. A twisted conformation was also observed for 2,3-F₂.C₆H₃. $\overline{\text{CNSSN}}$ ^{54,55} which had an S··S interdimer distance of 3.020(4) Å. This structure was the first observed when the R substituent was planar and illustrates how electrostatic repulsion can be used to alter the solid state structure.

1.5.3 Trans-antarafacial Configurations

To date, only one compound has been reported with this *trans*-antarafacial conformation. This is despite the fact that the energy difference between the *cis* and *trans* isomers is very small. In the case of *m*-NC.C₆H₄. $\overline{\text{CNSSN}}$ ³² there are two morphologies. The first, (α -phase) shows the *cis*-cofacial dimer with ordered crystal packing through secondary S··CN interactions. The second (β -phase) is the *trans*-antarafacial dimer which shows similar S··S distances and also shows strong S··CN secondary interactions which results in a chain type structure.

1.5.4 *Trans-cofacial Configurations*

Until very recently, no *trans*-cofacial configurations had been published. The 2,2'-dimethylbiphenylene bridged derivative [20],⁵⁶ contains one dithiadiazolyl associated in a dimerised *trans*-cofacial manner across an inversion centre to an equivalent radical on a neighbouring molecule. The contact between these rings is small (3.24 Å), which is well within the distance effected by spin pairing. It is unclear why this cofacial association was favoured in this compound. The other side of the di-radical has no close spin-paired interactions with any neighbouring ring. This renders the compound paramagnetic in the solid state. However, no long range magnetic ordering is observed.



1.5.5 *Other Conformations*

During the past few years, the emphasis in much of the work into these systems has been to control the molecular packing, several notable advances have been made leading to derivatives with novel structures and properties. Oakley and co-workers³⁹ reported the first example of a dithiadiazolyl, 1,3-phenylene-bis-dithiadiazolyl, which crystallised as one-dimensional stacks. However, it was discovered that Peierls distortion caused a subtle rocking at opposite ends of each molecule. This in turn produced long and short centroid-to-centroid distances (*i.e.* S...S distances of 3.140Å and 3.966Å) alternating throughout the stack (Figure 1.3).

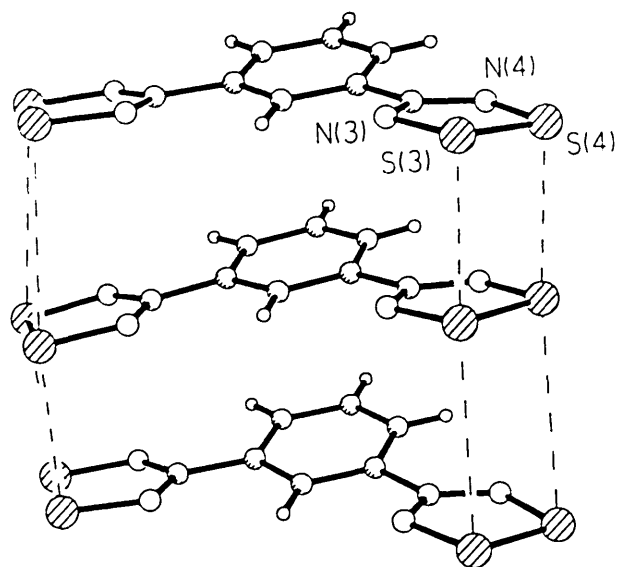


Figure 1.3 The Solid State Structure of 1,3[$\overline{\text{NSSNC}} \cdot \text{C}_6\text{H}_4 \cdot \overline{\text{CNSSN}}$]

Subsequently, the same workers co-sublimed simple dithiadiazolyls such as Ph. $\overline{\text{CNSSN}}$ with iodine.⁵⁷ The result was a p-doped charge transfer complex, where stacks of dithiadiazolyls associated with iodide or triiodide anions. The complex of 1,3- $[\overline{\text{NSSNC}} \cdot \text{C}_6\text{H}_4 \cdot \overline{\text{CNSSN}}]$ with iodine was observed to be a semi-conductor at room temperature with a conductivity of 100 Scm^{-1} .

The first paramagnetic dithiadiazolyl was discovered by A.J. Banister *et al.*^{58,59} The structure of this fluorinated 1,2,3,5-dithiadiazolyl radical [*p*-NC. C_6F_4 . $\overline{\text{CNSSN}}$] \cdot displayed two distinct polymorphs. Both structures showed strong S \cdots N interactions to form polymeric chain structures and F \cdots F repulsion preventing dimerisation (Figure 1.4). The main difference between the two structures is the direction of the dithiadiazolyl within adjacent chains. In the α -phase, adjacent chains align in antiparallel directions. In the β -phase, all the chains lie in the same direction. This subtle difference in the crystal packing has great consequences for the overall properties of the β -phase, which becomes ferromagnetic at 36 K, whereas the α -phase is antiferromagnetic. The properties of this compound are discussed in more detail later in this chapter.

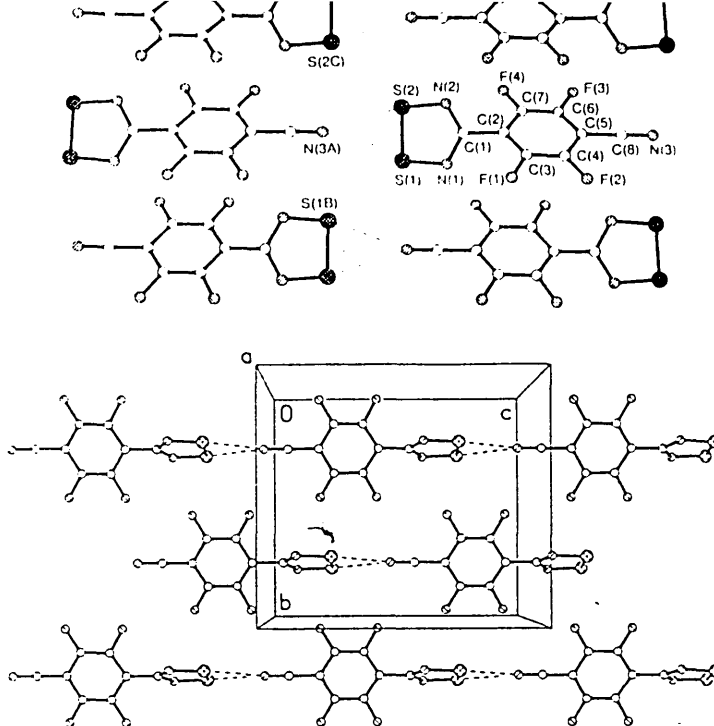


Figure 1.4 The α (above) and β (bottom) structures of $p\text{-CN.C}_6\text{F}_4.\overline{\text{CNSSN}}$

Further work by Banister and co-workers^{54,55} into the repulsion of fluorinated substituents attached to a phenyl ring resulted in the first example of an intrinsic, ordered dithiadiazolyl stack (2,5-difluorophenyl-1,2,3,5-dithiadiazolyl). However, this year, a study by Oakley and co-workers⁶⁰ has suggested that the reported structure was incorrect. The inaccurate assignment of the original structure was attributed to the presence of a superlattice, common in other stacked forms of dithiadiazolyls.⁶⁰ After re-examination, a molecular structure of π -stacked dimers was reported (Figure 1.5). This has been used to explain why the compound was essentially diamagnetic up to 300K. This new structure showed a striking similarity to previously reported stacks which displayed alternating short intradimer distances (2.9 - 3.0 Å) and long interdimer distances (3.9 - 4.1 Å) through the stack. The dimerisation of dithiadiazolyls has been suppressed by p-type doping *e.g.* iodine doped $[\text{H}.\overline{\text{CNSSN}}].0.18\text{I}_2$,⁶¹ displayed a stacking structure along with increased conductivity.

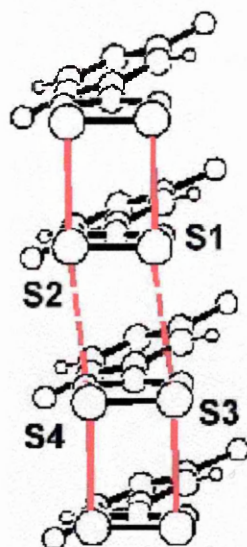
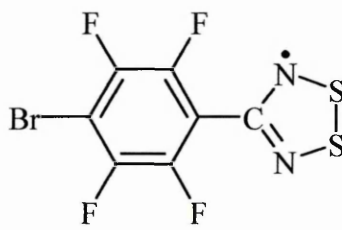


Figure 1.5 The solid state structure of $2,5\text{-F}_2\text{C}_6\text{H}_3\text{.}\overline{\text{CNSSN}}$ ⁶⁰

More recently, a monomeric dithiadiazolyl **[21]** has been reported.⁶²



[21]

Compound **[21]** has a molecular structure showing columns of radicals perpendicular to the crystallographic a -axis. The association out of plane takes the form of a twisted motif with each dithiadiazolyl ring lying directly above the next. The interaction mimics that of the twisted dithiadiazolyls described earlier (Section 1.5.2) but shows a larger angle between dithiadiazolyl units, approaching the *trans*-antarafacial configuration. In this case, the out of plane contacts fall in the range 3.675 – 3.999 Å which is well above the normal dimer separation (2.9 – 3.1 Å). Compound **[21]** has an effective magnetic moment at room temperature of $1.45 \mu_{\text{B}}$. Above 60 K, the magnetic susceptibility follows the Curie-Weiss law ($\theta = -27 \text{ K}$); however, there is no evidence for long-range magnetic order down to 1.8 K.

1.6 Magnetism and non-Metallic Magnets

If two objects attract each other and also repel each other (depending on their relative orientations), then these objects might be called magnets. In addition, when certain objects are attracted to, but not repelled by each other then these objects may be said to consist of magnetic materials. Magnetic phenomena has been known and exploited for centuries. Since the first known magnetic material, magnetite, many other magnetic materials have been used and investigated.^{63,64} One of the main challenges in the field of molecular materials concerns the design and synthesis of compounds exhibiting spontaneous magnetisation.^{65,66} Compounds of this type have only been described in the past decade, and despite much effort, this class of compound is still small in size.

It is important first to understand some of the definitions as a background to magnetic behaviour.^{67,68} Although magnetism has been known and used for hundreds of years it was not until the nineteenth century that a link was found between electricity and magnetism. Michael Faraday stated that the force driving a current around a circuit, *i.e.* the electromotive force (Volts) is equal to the rate of change of flux through a circuit. The effect of a magnetic field on a material can be defined in several equations. It can be shown that in a vacuum the magnetic induction of a material, B , is directly proportional to the field, H (Am^{-1}) (Equation 1.1).

$$B = \mu_0 H \quad \text{Equation 1.1}$$

where μ_0 is a universal constant, the *permeability of a vacuum*. In a vacuum, B and H are always parallel to each other. When a material is present, this equation is not followed as the material acquires a dipole moment. In this case the material has a magnetisation, M , which is the dipole moment per unit volume. The relationship can then be shown to be:

$$B = \mu_0 (H + M)$$

Equation 1.2

The magnetisation of a material in general depends on the magnetic field acting upon it.

For most materials M is proportional to H and is related by:

$$M = \chi H$$

Equation 1.3

where χ is the magnetic susceptibility and is a property of the material. The cgs units of molecular susceptibility (used in this thesis) are $\text{emu.Oe}^{-1}.\text{mol}^{-1}$. The emu is an electromotive unit with dimensions of volume so that 1 emu is equivalent to 1 cm^3 . Another way of characterising the material magnetically is to use the magnetic permeability, μ . This is related to the magnetic susceptibility by:

$$\mu = 1 + \chi$$

Equation 1.4

It then follows that the magnetic permeability is related to the magnetic induction by the following equation:

$$B = \mu_0 \mu H$$

Equation 1.5

Both magnetic susceptibility and magnetic permeability can be used to characterise the nature of a magnetic material. For small values of χ then μ becomes very close to 1 and is of very little use. However, for larger values, and therefore materials of more practical interest, μ can be used.

The classification of magnetic materials can be aided by studying the magnetic susceptibility of materials as a function of temperature. Compounds which contain only pairs of electrons are repelled by magnetic field and are said to be diamagnetic. Their susceptibility is negative and independent of temperature. Compounds which contain unpaired electrons are attracted into the magnetic field and their susceptibility is positive. These compounds are described as paramagnetic and have a susceptibility which is temperature dependent (discussed in more detail later). In reality, all paramagnetic compounds contain some electron pairs (core electrons and electrons involved in bond formation) and so the observed susceptibility is the sum of the diamagnetic and paramagnetic components (Equation 1.6).

$$\chi_{\text{obs}} = \chi_{\text{p}} + \chi_{\text{d}} \qquad \text{Equation 1.6}$$

If we are interested in the paramagnetism arising from the unpaired electrons (χ_{p}) then a careful correction for the sample diamagnetism must be made. This is often estimated using Pascal's constants, although more elaborate methods can be applied. For now, we will concentrate on the sample paramagnetism.

Pierre Curie found an empirical relationship between the value of χ_{p} and the absolute temperature, T. For many paramagnetic compounds there is an inverse-relationship between χ and T (Equation 1.7). Thus as a sample is cooled its susceptibility rises rapidly. At low temperatures some deviation from the *Curie-Weiss* behaviour (Equation 1.7) is often observed.

$$\chi = \frac{C}{T \pm \theta} \qquad \text{Equation 1.7}$$

If $\theta = 0$ the compound behaves as a perfect paramagnet, *i.e.* each molecule acts independently from its neighbours. However in many compounds, there may be some degree of communication between neighbours (often referred to as a magnetic exchange interaction). This communication may try to align the unpaired electrons on neighbouring molecules anti-parallel to one another. These molecules are said to be antiferromagnetically coupled and in this case $\theta < 0$. In contrast, local co-parallel alignment of electrons gives rise to ferromagnetic coupling, signified by $\theta > 0$. The sign and magnitude of θ give an indication of the type and strength of the coupling between neighbouring molecules.

In the mean field approach, for ferromagnetically coupled compounds when $T = \theta$, then $\chi \rightarrow \infty$, *i.e.* all the unpaired electrons move co-operatively and this is known as a magnetically ordered state. This temperature is known as the critical temperature. In reality many compounds begin to deviate from *Curie-Weiss* behaviour and will usually order somewhat below $|\theta|$. Since the co-operativity is essentially required to propagate throughout the three-dimensional solid, it requires communication in three dimensions. For compounds exhibiting strong communication between spins in only one or two dimensions, then magnetic order is frequently not observed at any finite temperature. Some common forms of long range magnetic order are briefly outlined:-

In a ferromagnet, all the electrons align co-parallel at absolute zero ($T = 0$ K) giving rise to a spontaneous magnetisation, M , even in the absence of an applied field, H . Under these circumstances, Equation 1.3 is no longer applicable and the sample susceptibility is meaningless. Instead, we discuss the spontaneous magnetisation. At 0 K all the electrons align perfectly and we observe saturation magnetisation, M_s . On warming above 0K some thermal energy leads to electron motion away from perfect alignment and the saturation

magnetisation steadily decreases, reaching zero at the magnetic ordering temperature or *Curie temperature*, T_c . Above the ordering temperature the material is paramagnetic and χ becomes meaningful once more. At temperatures well above the ordering temperature the compound will obey Equation 1.7 with $\theta > 0$.

In an antiferromagnet, the spins align antiparallel throughout the solid below the *Neel temperature*, T_N . An antiferromagnet is often characterised by a sharp maximum in the susceptibility. On cooling a paramagnet, χ is expected to increase but, as the antiferromagnetic interactions become stronger (in relation to the thermal energy kT) then the electrons begin to align antiparallel to each other rather than all parallel with the applied field and the susceptibility begins to decrease. For a three-dimensional order the transition is usually sharp whereas low-dimensional magnetic interactions give rise to broad maxima in the susceptibility. Well above the ordering temperature an antiferromagnet is expected to follow Equation 1.7 with $\theta < 0$.

In a ferrimagnet, electrons on neighbouring molecules interact antiferromagnetically (*i.e.* $\theta < 0$). However, the interacting molecules may bear spins of differing size (*e.g.* two unpaired electrons on one molecule, $S = 1$, interacting a neighbouring molecule bearing one unpaired electron, $S = \frac{1}{2}$). In this case, antiparallel alignment will lead to a greater number of spins pointing in one direction. Below the critical temperature, T_c , the compound behaves much like a ferromagnet, although the magnitude of the saturation magnetisation is lower [*cf* $2S$ for a ferromagnet *vs* $2(S_A - S_B)$ for a ferrimagnet].

More esoteric types of magnetic order and partially ordered states are also known. These include asperomagnetism, canted antiferromagnetism and spin-glass behaviour and are

beyond the scope of introductory remarks. The different types of magnetic order are shown schematically in Figure 1.6.

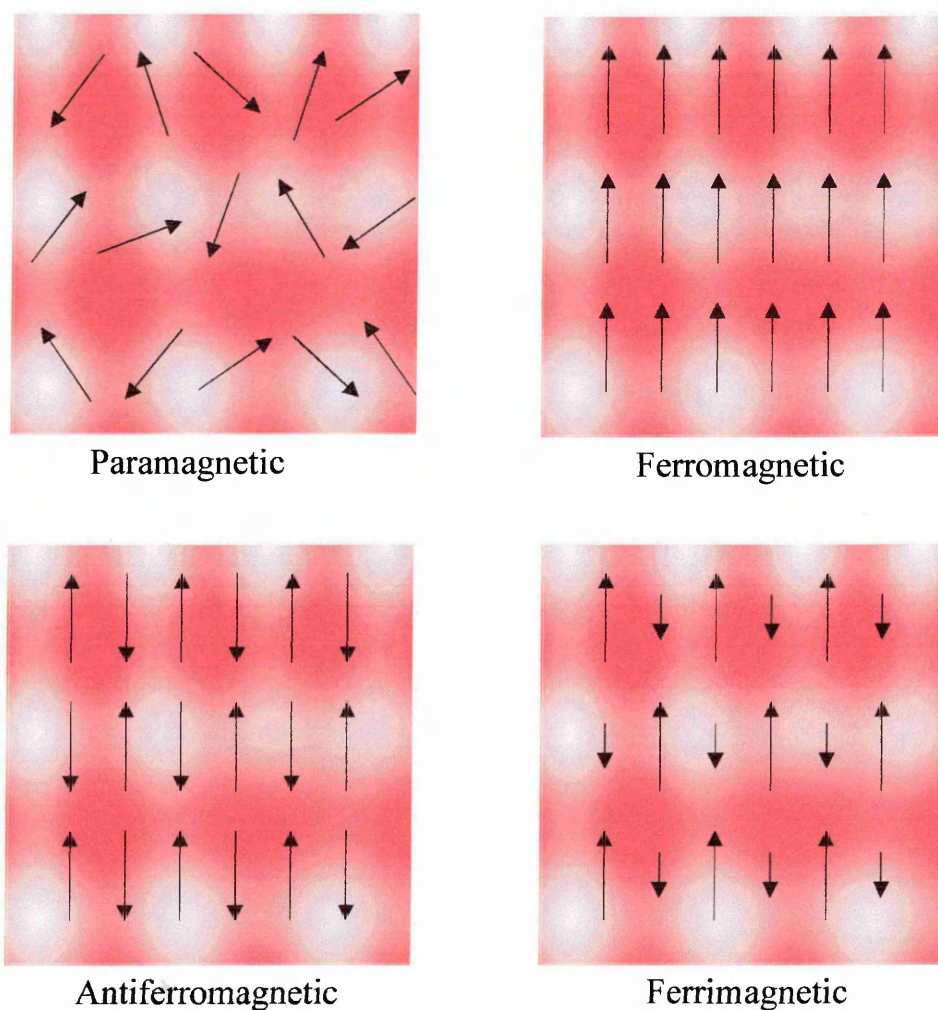


Figure 1.6 The alignment of magnetic moments

Spontaneous ferromagnetic ordering in purely organic compounds was not expected. Indeed, in 1928 Heisenberg⁶⁹ concluded that ferromagnetism could not exist in compounds consisting only of light elements. It was not until 1991 that the first organic ferromagnet, *p*-nitrophenyl nitroxide [22] (β -phase) was discovered.⁷⁰ This compound orders ferromagnetically with a critical temperature (T_c) of just 0.48 K. Since then the major challenge within this field has been to increase the value of T_c . Several more organic materials have been reported, which exhibit ferromagnetic behaviour and most of these have been based on nitroxide radicals.^{71,72} The highest reported T_c in a nitroxide based

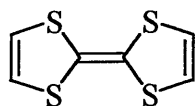
1.7 Conduction in Organic Materials

The classic electron conduction model for a metal considers that a valence electron of an atom can move freely between all the atoms within the solid. The energy band model for partially filled bands (metals) shows that the energy required to excite valence electrons so that they are mobile is very small. For filled bands, the energy required to excite the valence electrons to make them mobile is much greater, which leads to materials that are either semiconductors or insulators. These models are based on interaction between atoms in a solid lattice. Thus the extension of electrical conductivity models from atom based systems to those made up of molecules is dependent on the interactions in the solid state. Molecular based materials which have electrons delocalised over the entire solid may exhibit high metal-like conductivities. It was postulated, as far back as 1911,⁷⁷ that molecule-based compounds could exhibit conductivities similar to those of metals. These predictions were realised in 1954¹ and since then there has been extraordinarily large interests in this area.⁷⁸

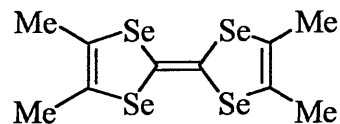
The primary motivation for the extensive interest in the synthesis of this group of molecular conductors is the potential technological applications of these materials. The simple fact that many of the materials have a much lower density (about 1.5 g/cm³) than metals (9 g/cm³ for copper) makes their use very appealing. Moreover, a combination of different physical properties and their ease of fabrication also makes them very inviting.

Over the past 20 years research into the design of molecular conducting materials has focused primarily on organic donor molecules like TTF [25], TMTSF [26], BEDT-TTF [27] and acceptors such as TCNQ [28]. For these systems, conductivity is only possible after oxidation (p-doping) of the neutral molecule, to form a charge transfer (CT) salt. This conductivity arises from the generation of a partially filled energy band, which is

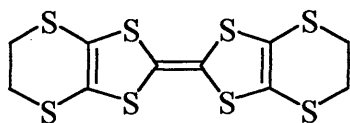
associated with the overlap of π -orbitals within the stacks of radical ions. Modifications to the conductive properties of the materials can be achieved by the variation of the molecular structure of the organic donor or the inorganic acceptor. Most of these materials have highly one-dimensional structures.



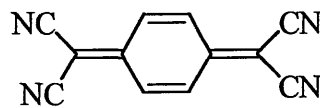
TTF
[25]



TMTSF
[26]



BEDT-TTF
[27]



TCNQ
[28]

All neutral π -radicals, including dithiadiazolyls, by definition give rise to a half-filled energy band. However, in a one-dimensional stack of dithiadiazolyls, Peierls distortion,⁷⁹ driven by charge density waves (CDWs), produces an essentially dimerised system.

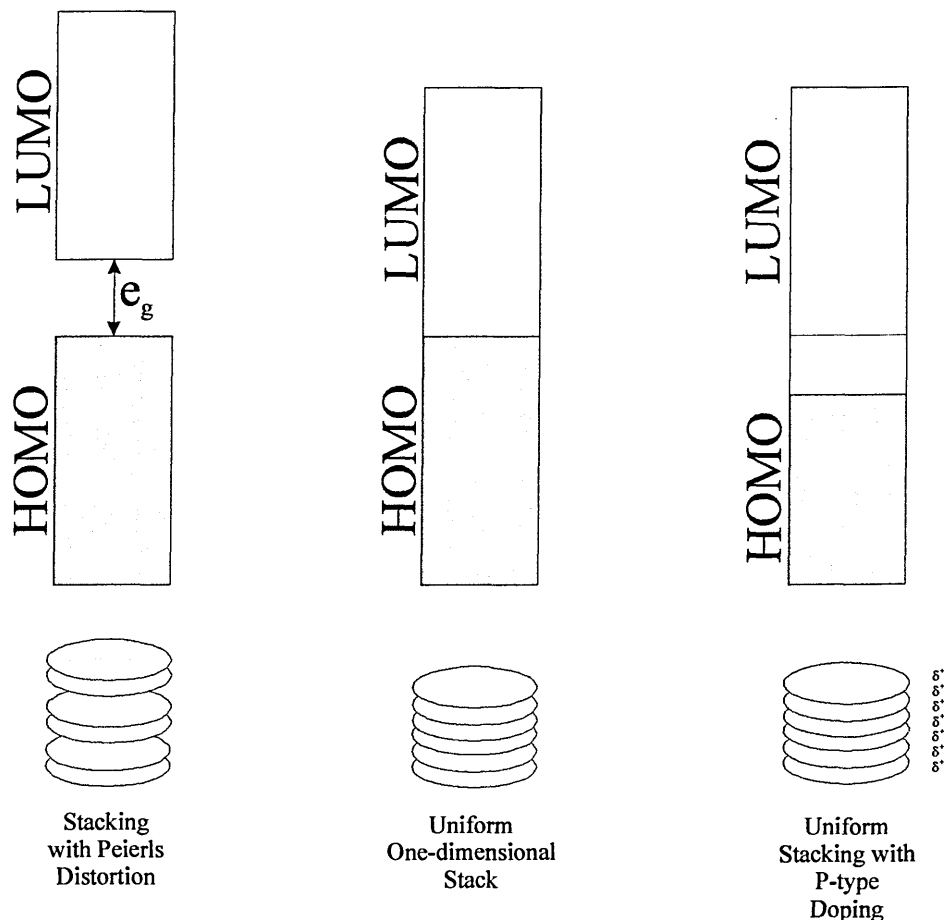


Figure 1.7 Representations of the energy bands in stacked dithiadiazolyis

The uniformly spaced stack shown above (Figure 1.7) was described by R.T. Oakley *et al*⁸⁰ as the ‘metallic state’. It shows no energy gap (e_g) between the highest occupied molecular orbital (HOMO) and the lowest unoccupied molecular orbital (LUMO). One can therefore consider it to have the ability to conduct. It was reasoned that if the dithiadiazolyis, $\overline{\text{HCNSSN}}$ ⁶¹ was co-sublimed with elemental iodine, partial oxidation would take place. Oxidation suppresses the Peierls distortion, which occurs in the neutral radical. The conductivity at room temperature of the charge transfer salt $[\overline{\text{HCNSSN}}]\text{I}$ was found to be 15 Scm^{-1} . Similarly, iodination of 1,4-⁵⁷ and 1,3-⁸¹($\overline{\text{NSSNC}} \cdot \text{C}_6\text{H}_4 \cdot \overline{\text{CNSSN}}$), both of which exist as diamagnetic dimers in the solid state, produced the charge transfer salts $[\text{1,4-}(\overline{\text{NSSNC}} \cdot \text{C}_6\text{H}_4 \cdot \overline{\text{CNSSN}})]\text{I}$ and $[\text{1,3-}(\overline{\text{NSSNC}} \cdot \text{C}_6\text{H}_4 \cdot \overline{\text{CNSSN}})]\text{I}$ respectively. The conductivity of $[\text{1,4-}(\overline{\text{NSSNC}} \cdot \text{C}_6\text{H}_4 \cdot \overline{\text{CNSSN}})]\text{I}$ was particularly outstanding being in excess of 200 S cm^{-1} at room temperature.⁵⁷

1.8 Electron Paramagnetic Resonance

Electron Paramagnetic Resonance (EPR) spectroscopy is a technique used to study materials that contain unpaired (paramagnetic) electrons⁸² and is invaluable for investigating free radicals such as dithiadiazolyls.⁸³

The technique is often considered more difficult to obtain detailed information from than experiments such as NMR and Mössbauer spectroscopy. More knowledge about the specific ion in question is often needed for detailed interpretation. In addition, some systems may give weak or broad signals that require cooling to low temperatures to gain high quality spectra. Despite these difficulties, the technique is considered complementary to NMR, which cannot be used with paramagnetic samples under normal conditions.

Considerable parallels exist between NMR and EPR because both depend on the magnetic moment of a spinning particle, either the nucleus or the electron. For electrons with a spin $\frac{1}{2}$, two energy states are produced by the interaction with a magnetic field, B. They differ in energy by:

$$\Delta E = g\mu B \quad \text{Equation 1.8}$$

The value of g depends on the identity of the particle and μ is its magnetic moment. For a free electron, g is 2.0023 and for a proton, the value is 5.5856.⁸² The magnetic moment varies considerably because of its dependence on mass.

$$\mu = \frac{eh}{4\pi m} \quad \text{Equation 1.9}$$

In the case of EPR μ_B (the Bohr magneton) is $9.274 \times 10^{-24} \text{ JT}^{-1}$. The spectra obtained by EPR depend on determining the g-values for the unpaired electrons in the sample, which are different to those of the free electrons and are dependent on the chemical environment of the paramagnetic atom. This is usually achieved by using a fixed frequency, usually 9 GHz, and varying the applied field. The method used is the opposite to that of NMR because the chamber where the sample is kept has to be tuned to the particular wavelength used. It is therefore not possible to adjust the wavelength without an adjustable chamber. The frequency of 9GHz was chosen because similar systems using this frequency were already being used for marine radar (X-band), and were well understood. Some spectrometers operate at 36GHz (Q-band) because the technology of airport radar can be utilised.

1.8.1 Experimental Considerations

EPR studies can be performed on liquids, solids and solutions. The technique is very sensitive so only a small sample is required. Because of this high sensitivity, every effort must be made to omit all traces of additional paramagnetic impurities. Solid samples are measured in silica tubes rather than glass to avoid the contamination from iron (III) in the glass. Air is often removed from the tubes prior to analysis to avoid line broadening from the presence of molecular oxygen. Line broadening due to spin-spin relaxation effects can be minimised by dissolving the sample in a solvent at a concentration of about 5 mmol dm^{-3} . A small amount of another solvent such as dimethylsulfoxide or glycerol is useful to encourage the formation of a glass when cooling. This in turn helps to prevent the crystallisation of the solid sample from the solvent during cooling.

In order to reduce noise, most spectrometers use a modular technique, which superimposes a cyclic variation on the magnetic field. The detection of the signal involves examining the

phase of the resultant wave using a phase-sensitive detector.⁸³ The graphical results are displayed in the first derivative form (Figure 1.8).

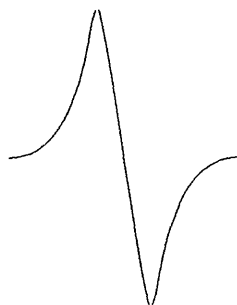


Figure 1.8 An example of a first derivative EPR signal

The position of maximum absorption is at the point where the curve crosses the baseline and the signal width is the distance between the maximum and minimum. The second derivative can often be used to determine the fine structure of the sample.

1.8.2 *g-Value*

For a free electron in a vacuum g is 2.0023.¹⁶ In chemical systems, the unpaired electron occupies an orbital almost exclusively localised on a single atom or can be strongly delocalised across a molecule. It then follows that the g -value reflects the nature of the orbital. In the case of free radicals, the value of g approaches that of a free electron. Orbital contributions are most common in compounds containing a transition metal ion.

1.8.3 *Fine, Hyperfine and Superfine Structure*

A species which has the spin S has a total of $2S + 1$ energy states, characterised by the quantum numbers M_s . In the absence of a magnetic field all states with $M_s \neq 0$ are expected to remain doubly degenerate (*i.e.* M_s and $-M_s$ are the same energy). However, the electric fields produced by other atoms usually separate these doublets and act *via* spin-orbital

coupling. This is known as *zero field splitting* and depend on the structure of the sample under investigation. The presence of a magnetic field removes the remaining degeneracy and allows transitions between adjacent states to be observed. The appearance of more than one line (when $S = \frac{1}{2}$) is known as *fine structure*.

The spectra produced by EPR may have some additional fine structure when the atom on which the unpaired spin is centred also has a spin (exactly analogous to NMR). A nucleus of spin I gives rise to the splitting of the EPR line into $2I + 1$ components, all with equal intensity and separated with a coupling constant, A . This phenomenon is known as *hyperfine structure*. In an analogous way, nuclei on adjacent atoms may give splitting of the spectrum. This is known as *superfine structure* and is dependent on the extent of delocalisation of the unpaired electron on to these atoms, decreasing rapidly with the number of bonds involved. It is usually only detectable for nuclei of atoms directly bound to that containing the unpaired electrons.

1.8.4 EPR Spectroscopic Studies of Dithiadiazolyl Radicals

Free radicals, whether organic or inorganic, usually give sharp spectra with g close to 2. It may be possible to see hyperfine and superfine structure, both of which are usually well resolved.

The structural study of inorganic ring systems by EPR spectroscopy has received significant interest in recent years¹⁶ and has proved to be a vital tool in the study of dithiadiazolyls. Reviews of the technique and the characterisation of spectra in relation to sulfur nitrogen radicals have been published.^{16,83,84} The technique has been described⁸³ as being unrivalled as a probe of the structure of paramagnetic molecules, leading to unequivocal assignment of ground state geometry and electronic wavefunction.

Isotropic and powder EPR spectra have been obtained for a range of 1,2,3,5-dithiadiazolyl derivatives. Some of the data is summarised in Table 1.2.

Table 1.2 EPR data for different substituents attached to 1,2,3,5-dithiadiazolyl

Substituent	Temperature	Solvent	g	a_N
C_6H_5 ²⁰	298 K	C_6H_6 /THF	2.0104	0.49
C_6H_5 ⁷	205 K	<i>d</i> ₈ -toluene	2.01019	0.517
C_6F_5 ⁸⁵	219 K	<i>d</i> ₈ -toluene	2.01012	0.505
<i>t</i> Bu ⁸⁶	203 K	<i>d</i> ₈ -toluene	2.01059	0.51
<i>t</i> Bu ⁵²			2.0121	0.52
Me ⁷	203 K	<i>d</i> ₈ -toluene	2.0104	0.538
CF ₃ ⁸⁵	193 K	<i>d</i> ₈ -toluene	2.00939	0.49
CF ₃ ²⁵	298 K	liquid SO ₂		0.51
CCl ₃ ²⁰	298 K	C_6H_6 /THF	2.0104	0.49
1,4- C_6H_4 - ³⁸	273 K	CHCl ₃	2.011	0.51 mT
1,3- C_6H_4 - ³⁹	213 K	CHCl ₃	2.011	0.51 mT
$\overline{NSSNC - CNSSN}$ ⁸⁷	273 K	CHCl ₃	2.011	0.5 mT
F ²⁵	298 K	liquid SO ₂		0.506
Cl ²⁵	298 K	liquid SO ₂		0.53
Br ²⁵	298 K	liquid SO ₂		0.5
I ⁸⁸	298 K	SO ₂ /CFCl ₃	2.0106	0.5

Simple solution state measurements give well resolved isotropic spectra with hyperfine splitting to two equivalent ¹⁴N nuclei ($a_N \approx 0.5$ mT), to yield 1:2:3:2:1 quintet. An example of the spectrum for $\overline{PhCNSSN}^\bullet$ is shown below (Figure 1.9). Although the coupling to sulfur is also large ($a_S \approx 0.62$ mT), the low abundance of ³³S means that this frequency is not normally observed. Further splitting has also been observed as a result of the R

substituent *e.g.* in CF_3 . $\overline{\text{CNSSN}}$,⁸⁵ coupling to fluorine produces a superfine splitting with a 1:3:3:1 pattern.

All the dithiadiazolyls analysed to date have shown large isotopic *g*-values of approximately 2.01. There is little variation in g_{iso} and a_{N} for dithiadiazolyls. EPR has also been used to investigate the thermodynamic nature of the monomer-dimer equilibrium in solution.^{7,52} Anisotropic spectra of frozen glass, powder and single crystal samples have been obtained in order to separate the hyperfine coupling into *x*, *y* and *z* directions (similar to solid state NMR). It has been used to calculate the percentage occupancy (spin density) of the radical on the ring atoms. Single crystal measurements on $\text{Ph}.\overline{\text{CNSSN}}$ ⁸⁹ and $1,3-(\overline{\text{NSSNC}}.\text{C}_6\text{H}_4.\overline{\text{CNSSN}})$ ³⁹ have revealed the orientations of the SOMO and further splitting due to dipolar coupling.

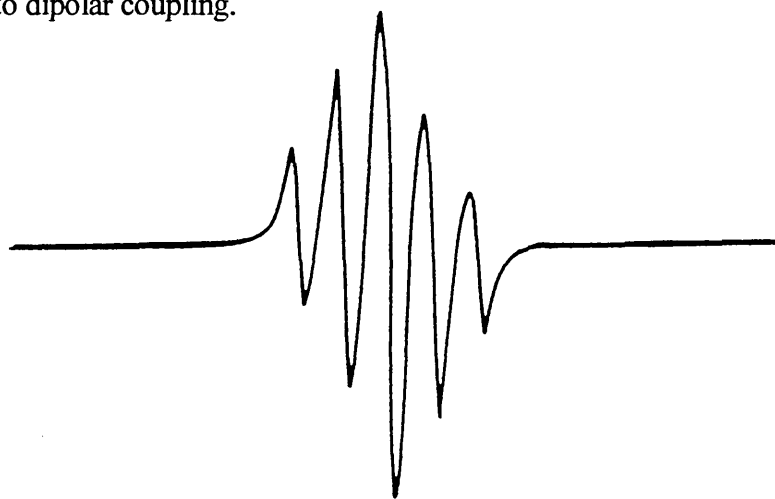


Figure 1.9 EPR solution spectrum of $\text{Ph}.\overline{\text{CNSSN}}$

1.9 Aims of the Present Work

The project aimed to synthesise several novel dithiadiazolyl radicals possessing various halogenated phenyl substituents. The effect of the halogen substituents and isomers on the molecular packing was to be investigated. Information on the intermolecular interactions of particular halogen atoms in the solid state, and the significance of their position on the phenyl ring will be discussed.

Products with interesting structures were then examined for their physical properties (*i.e.* magnetic or electrical). A comparison could then be drawn between the physical properties and the packing structure to learn more about electron mobility between adjacent dithiadiazolyl rings in the solid state.

1.10 References

-
- 1 H. Akamatsu, H. Inokuchi and Y. Matsunaga, *Nature*, 1954, **173**, 168.
 - 2 (a) J.S. Miller, A.J. Epstein and W.M. Reiff, *Mol. Liq. Cryst.*, 1985, **120**, 27;
(b) J.S. Miller, A.J. Epstein and W.M. Reiff, *Mol. Liq. Cryst.*, 1986, **120**, 234;
(c) J.S. Miller, J.C. Calabrese, A.J. Epstein, R.W. Bigelow, J.H. Zhang and W.M. Reiff, *J. Chem. Soc., Chem. Commun.*, 1986, 1026; (d) J.S. Miller, J.C. Calabrese, H. Rommelmann, S. Chittapeddi, J.H. Zhang, W.M. Reiff and A.J. Epstein, *Mol. Liq. Cryst.*, 1987, **109**, 769.
 - 3 M. Schlüter, J. R. Chelikowsky and M. L. Cohen, *Phys. Rev. Lett.*, 1975, **35**, 869.
 - 4 W. Gregory, *J. Pharm. Chim.*, 1835, **21**, 315.
 - 5 F.A. Cotton, G. Wilkinson and P.L. Gaus, *Basic Inorganic Chemistry*, second edition, John Wiley and Sons, 1987, 62.

-
- 6 E. Demarcay, *Compt. Rend.* 1880, **91**, 854.
 - 7 S.A. Fairhurst, K.M. Johnson, L.H. Sutcliffe, K.F. Preston, A.J. Banister, Z.V. Hauptman and J. Passmore, *J. Chem. Soc., Dalton Trans.*, 1986, 1465.
 - 8 A.J. Banister, H.G. Clarke, I. Rayment and H.M.M. Shearer, *Inorg. Nucl. Chem. Lett.*, 1974, **10**, 647.
 - 9 R.W.H. Small, A.J. Banister and Z.V. Hauptman, *J. Chem. Soc., Dalton Trans.*, 1984, 1377.
 - 10 R.J. Gillespie, P.R. Ireland and J.E. Vekris, *Can. J. Chem.*, 1975, **53**, 3147.
 - 11 R. Gleiter, R. Bartetzko and P. Hoffmann, *Z. Naturforsch. B*, 1980, **35B**, 1166.
 - 12 B. Krebs and G. Henkel, *Chem. Ber.*, 1980, **113**, 226.
 - 13 R.J. Gillespie, J.P. Kent and J.F. Sawyer, *Inorg. Chem.*, 1981, **20**, 3784
 - 14 U. Thewalt and M. Burger, *Z. Naturforsch. B*, 1981, **36B**, 293.
 - 15 B. Ayres, A.J. Banister, P.D. Coates, M.I. Hansford, J.M. Rawson, C.E.F. Rickard, M.B. Hursthouse, K.M.A. Malik and M. Motevalli, *J. Chem. Soc., Dalton Trans.*, 1992, 3097.
 - 16 K.F. Preston and L.H. Sutcliffe, *Magn. Reson. Chem.*, 1990, **28**, 189.
 - 17 J.M. Rawson, A.J. Banister and I. Lavender, *Adv. Heterocycl. Chem.*, 1995, **62**, 137.
 - 18 G.G. Alange, A.J. Banister, B. Bell and P.W. Millen, *Inorg. Nucl. Chem. Lett.*, 1977, **13**, 143.
 - 19 A. Vegas, A. Pérez-Salazar, A.J. Banister and R.G. Hey, *J. Chem. Soc., Dalton Trans.*, 1980, 1812.
 - 20 L.N. Markovski, O.M. Polumbrik, V.S. Talanov and Yu.G. Shermolovich, *Tetrahedron Lett.*, 1982, **23**, 761.
 - 21 R.L. Patton and W.L. Jolly, *Inorg. Chem.*, 1970, **9**, 1079.
 - 22 J. Passmore and M. Schriver, *Inorg. Chem.*, 1988, **27**, 2749.

-
- 23 G.G. Alange, A.J. Banister, B. Bell and P.W. Millen, *J. Chem. Soc., Perkin Trans. 1*, 1979, 1192.
- 24 H.-U. Höfs, R. Mews and G.M. Sheldrick, *Angew. Chem., Int. Ed. Engl.*, 1984, **23**, 988.
- 25 H.-U. Höfs, J.W. Bats, R. Gleiter, G. Hartmann, R. Mews, M. Eckert-Maksic, H. Oberhammer and G.M. Sheldrick, *Chem. Ber.*, 1985, **118**, 3781.
- 26 T. Chivers, J.F. Richardson and N.R.M. Smith, *Inorg. Chem.*, 1986, **25**, 47.
- 27 A.J. Banister, N.R.M. Smith and R.G. Hey, *J. Chem. Soc., Perkin Trans. 1*, 1983, 1181.
- 28 W.L. Jolly and K.D. Maguire, *Inorg. Synth.*, 1967, **9**, 102.
- 29 M. Amin and C.W. Rees, *J. Chem. Soc., Chem. Commun.*, 1989, 1137.
- 30 A.W. Cordes, J.D. Goddard, R.T. Oakley and N.P.C. Westwood, *J. Am. Chem. Soc.*, 1989, **111**, 6147.
- 31 M. Amin, C.W. Rees, *J. Chem. Soc., Perkin Trans. 1*, 1989, 2495.
- 32 A.W. Cordes, R.C. Haddon, R.G. Hicks, R.T. Oakley and T.T.M. Palstra, *Inorg. Chem.*, 1992, **31**, 1802.
- 33 I. Ernest, W. Holick, G. Rihs, D. Schomburg, G. Shoham, D. Wenkert and R.B. Woodward, *J. Am. Chem. Soc.*, 1981, **103**, 1540.
- 34 U. Scholz, H.W. Roesky, J. Schimkowiak and M. Noltemeyer, *Chem. Ber.*, 1989, **122**, 1067.
- 35 A.R. Sanger, *Inorg. Nucl. Chem. Lett.*, 1973, **9**, 351.
- 36 R.T. Boéré, R.T. Oakley and R.W. Reed, *J. Organomet. Chem.*, 1987, **331**, 161.
- 37 P.D.B. Belluz, A.W. Cordes, E.M. Kristov, S.W. Liblong and R.T. Oakley, *J. Am. Chem. Soc.*, 1989, **111**, 9276.
- 38 A.W. Cordes, R.C. Haddon, R.T. Oakley, L.F. Schneemeyer, J.V. Waszczak, K.M. Young and N.M. Zimmerman, *J. Am. Chem. Soc.*, 1991, **113**, 582.

-
- 39 M.P. Andrews, A.W. Cordes, D.C. Douglas, R.M. Fleming, S.H. Glarum, R.C. Haddon, P. Marsh, R.T. Oakley, T.T.M. Palstra, L.F. Schneemeyer, G.W. Trucks, R. Tycko, J.V. Waszczak, K.M. Young and N.M. Zimmerman, *J. Am. Chem. Soc.*, 1991, **113**, 3559.
- 40 A.W. Cordes, C.M. Chamchoumis, R.G. Hicks, R.T. Oakley, K.M. Young and R.C. Haddon, *Can. J. Chem.*, 1992, **70**, 919.
- 41 A.W. Cordes, R.C. Haddon, R.G. Hicks, R.T. Oakley, T.T.M. Palstra, L.F. Schneemeyer and J.V. Waszczak, *J. Am. Chem. Soc.*, 1992, **114**, 5000.
- 42 A.J. Banister, I. Lavender, J.M. Rawson, and R.J. Whitehead, *J. Chem. Soc., Dalton Trans.*, 1992, 1449.
- 43 C.M. Aherne, A.J. Banister, I.B. Gorrell, M.I. Hansford, Z.V. Hauptman, A.W. Luke and J.M. Rawson, *J. Chem. Soc., Dalton Trans.*, 1993, 967.
- 44 A.J. Banister, I. Lavender, J.M. Rawson, W. Clegg, B.K. Tanner and R.J. Whitehead, *J. Chem. Soc., Dalton Trans.*, 1993, 1421.
- 45 A.W. Cordes, S.H. Glarum, R.C. Haddon, R. Hallford, R.G. Hicks, D.K. Kennepohl, R.T. Oakley, T.T.M. Palstra and S.R. Scott, *J. Chem. Soc., Chem. Commun.*, 1992, 1265.
- 46 H.W. Roesky and T. Müller, *Chem. Ber.*, 1978, **111**, 2960.
- 47 P. Klinzing, A. El-Kohli, U. Patt-Siebel, U. Müller and K. Dehnicke, *Z. Anorg. Allg. Chem.*, 1988, **562**, 31.
- 48 H.-U. Höfs, R. Mews, W. Clegg, M. Noltemeyer, M. Schmidt and G.M. Sheldrick, *Chem. Ber.*, 1983, **116**, 416.
- 49 A.J. Banister, M.I. Hansford, Z.V. Hauptman, S.T. Wait and W. Clegg, *J. Chem. Soc., Dalton Trans.*, 1989, 1705.

-
- 50 J.E. Huheey, E.A. Keiter and R.L. Keiter, *Inorganic chemistry: principles of structure and reactivity*, 4th ed., Harper Collins, 1993.
- 51 R.T. Boéré and K.H. Moock, *Z. Anorg. Allg. Chem.*, 1994, **620**, 1589.
- 52 W.V.F. Brookes, N. Burford, J. Passmore, M.J. Schriver and L.H. Sutcliffe, *J. Chem. Soc., Chem. Commun.*, 1987, 69.
- 53 J.N. Bridson, S.B. Copp, M.J. Schriver, S. Zhu and M.J. Zaworotko, *Can. J. Chem.*, 1994, **72**, 1143.
- 54 A.J. Banister, A.S. Batsanov, O.G. Dawe, P.L. Herbertson, J.A.K. Howard, S. Lynn, I. May, J.N.B. Smith, J.M. Rawson, T.E. Rogers, B.K. Tanner, G. Antorrena and F. Palacio, *J. Chem. Soc., Dalton Trans.*, 1997, 2539.
- 55 A.J. Banister, A.S. Batsanov, O.G. Dawe, J.A.K. Howard, J.E. Davies, J.M. Rawson and J.N.B. Smith, *Phosphorus, Sulfur, and Silicon*, 1997, **124**, 553.
- 56 T.M. Barclay, A.W. Cordes, N.A. George, R.C. Haddon, M.E. Itkis and R.T. Oakley, *Chem. Commun.*, 1999, 2269.
- 57 C.D. Bryan, A.W. Cordes, R.M. Fleming, N.A. George, S.H. Glarum, R.C. Haddon, R.T. Oakley, T.T.M. Palstra, A.S. Perel, L.F. Schneemeyer and J.V. Waszczak, *Nature*, 1993, **365**, 821.
- 58 A.J. Banister, N. Bricklebank, W. Clegg, M.R.J. Elsegood, C.I. Gregory, I. Lavender, J.M. Rawson and B.K. Tanner, *J. Chem. Soc., Chem. Commun.*, 1995, 679.
- 59 A.J. Banister, N. Bricklebank, I. Lavender, J.M. Rawson, C.I. Gregory, B.K. Tanner, W. Clegg, M.R.J. Elsegood and F. Palacio, *Angew. Chem. Int. Ed. Engl.*, 1996, **35**, 2533.
- 60 L. Beer, A.W. Cordes, D.J.T. Myles, R.T. Oakley and N.J. Taylor, *Cryst. Eng. Comm.*, 2000, 20.

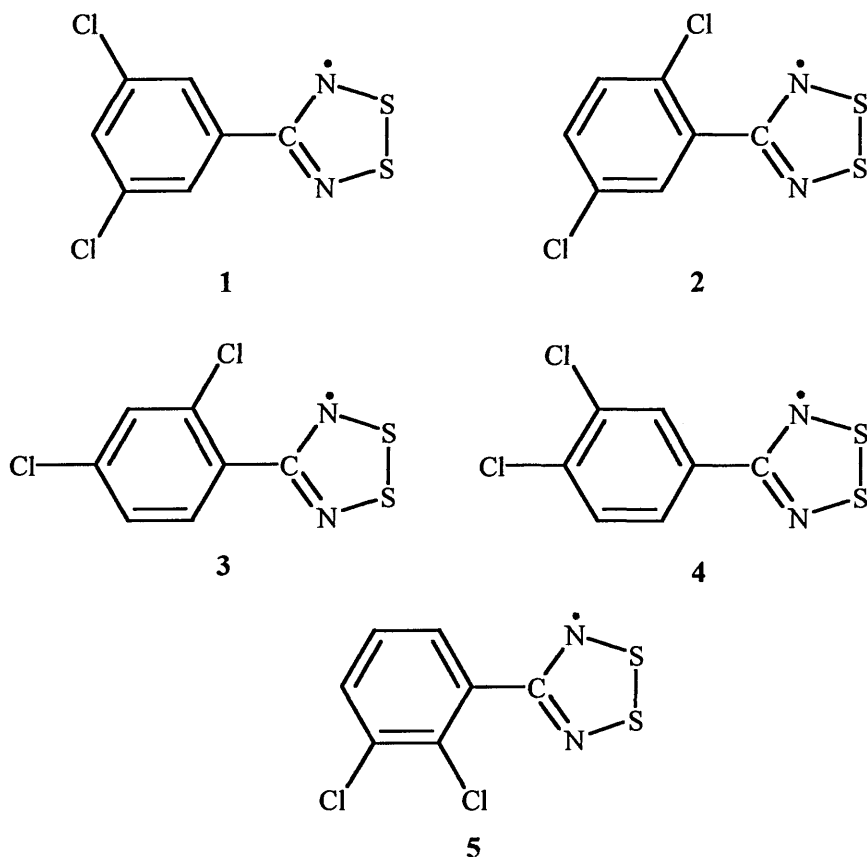
-
- 61 C.D. Bryan, A.W. Cordes, R.C. Haddon, R.G. Hicks, D.K. Kennepohl, C.D. MacKinnon, R.T. Oakley, T.T.M. Palstra, A.S. Perel, S.R. Scott, L.F. Schneemeyer and J.V. Waszczak, *J. Am. Chem. Soc.*, 1994, **116**, 1205.
- 62 G. Antorrena, J.E. Davies, M. Hartley, F. Palacio, J.M. Rawson, J.N.B. Smith and A. Steiner, *Chem. Commun.*, 1999, 1393.
- 63 O. Kahn, J.S. Miller and F. Palacio, *Magnetic Molecular Materials*, Kluwer Acad. Publ., 1991, **E198**, 1.
- 64 J.S. Miller and A.J. Epstein, *Angew. Chem. Int. Ed. Engl.*, 1994, **33**, 385.
- 65 R.C. Carlin, *Magnetochemistry*, Springer-verlag, Berlin Heidelberg, 1986.
- 66 J. Crange, *The Magnetic Properties of Solids*, Edward Arnold, London, 1977.
- 67 L. Smart and E. Moore, *Solid State Chemistry: An introduction*, Chapman & Hall.
- 68 L.V. Interrante and M.J. Hampden-Smith, *Chemistry of Advanced Materials, an Overview*, Wiley-VCH, 1998
- 69 W. Heisenberg, *Z.Phys.*, 1928, **49**, 619.
- 70 M. Tamura, Y. Nakazawa, D. Shiomi, K. Nozawa, Y. Hosokoshi, M. Ishikawa, M. Takahashi, M. Kinoshita, *Chem. Phys. Lett.*, 1991, **186**, 401.
- 71 R. Chiarelli, M.A. Novak, A. Rassat and J.L. Thorlence, *Nature*, 1993, **363**, 147.
- 72 J. Veciana, *Adv. Mater.*, 1995, **7**, 221.
- 73 T. Tomoyoshi, *Phys. Rev.*, 1994, **B49**, 16301.
- 74 P.-M. Allemand, K.C. Khemani, A.Koch, F. Wudl, K. Holczer, S. Donovan, G. Grüner and J.D. Thompson, *Science*, 1991, **253**, 301.
- 75 F. Palacio, G. Antorrena, M. Castro, R. Burriel, J.M. Rawson, J.N.B. Smith, N. Bricklebank, J. Novoa and C. Ritter, *Physical Review Letters*, 1997, **79**, 2336.
- 76 P.J. Langley, J.M. Rawson, J.N.B. Smith, M. Schuler, R. Bachmann, A. Schweiger, F. Palacio, G. Antorrena, G. Gescheidt, A. Quintel, P. Rechsteiner and J. Hulliger, *J. Mater. Chem.*, 1999, **9**, 1431.

-
- 77 H.N. McCoy and W.C. Moore, *J. Am. Chem. Soc.*, 1911, **33**, 273.
- 78 M.R. Bryce, *Chem. Soc. Rev.*, 1991, **20**, 355 and references therein.
- 79 R.E. Peirels, *Quantum Theory of Solids*, Oxford University Press, London, 1955, 108.
- 80 A.W. Cordes, R.C. Haddon, and R.T. Oakley, *Adv. Mater.*, 1994, **6**, 798.
- 81 C.D. Bryan, A.W. Cordes, R.M. Fleming, N.A. George, S.H. Glarum, R.C. Haddon, C.D. MacKinnon, R.T. Oakley, T.T.M. Palstra and A.S. Perel, *J. Am. Chem. Soc.*, 1995, **117**, 6880.
- 82 J.E. Wertz and J.R. Bolton, *Electron Spin Resonance, Elementary Theory and Practical Applications*, McGraw-Hill, 1972.
- 83 S.A. Fairhurst, K.F. Preston and L.H. Sutcliffe, *Phosphorus, Sulfur and Silicon*, 1994, **93-94**, 105.
- 84 J. Grassman and J. Fabian, *Magn. Reson. Chem.*, 1996, **34**, 913.
- 85 S.A. Fairhurst, L.H. Sutcliffe, K.F. Preston, A.J. Banister, A.S. Partington, J.M. Rawson, J. Passmore and M. Schriver, *Magn. Reson. Chem.*, 1993, **31**, 1027.
- 86 Y.-L. Chung, S.A. Fairhurst, D.G. Gillies, K.F. Preston and L.H. Sutcliffe, *Magn. Reson. Chem.*, 1992, **30**, 666.
- 87 C.D. Bryan, A.W. Cordes, J.D. Goddard, R.C. Haddon, R.G. Hicks, C.D. MacKinnon, R.C. Mawhinney, R.T. Oakley, T.T.M. Palstra and A.S. Perel, *J. Am. Chem. Soc.*, 1996, **118**, 330.
- 88 N. Burford, J. Passmore and M.J. Schriver, *J. Chem. Soc., Chem. Commun.*, 1986, 141.
- 89 F.L. Lee, K.F. Preston, A.J. Williams, L.H. Sutcliffe, A.J. Banister and S.T. Wait, *Magn. Reson. Chem.*, 1989, **27**, 1161.

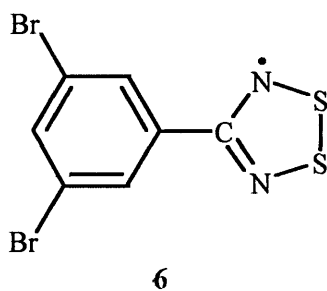
2.0 Introduction

This chapter reports the synthesis of neutral radical dithiadiazolyls with varying R-groups. On each occasion, an investigation of the crystal structure was performed in collaboration with H. Adams and S. Spey at the Department of Chemistry, University of Sheffield. Derivatives with interesting structures were examined further by electron paramagnetic resonance (EPR) in collaboration with Dr F. Mabbs and co-workers at the EPSRC cwEPR service, Department of Chemistry, University of Manchester. Magnetic susceptibility experiments were performed by Professor F. Palacio at the University of Zaragoza. This chapter will discuss the synthesis of all the dithiadiazolyls described in this thesis.

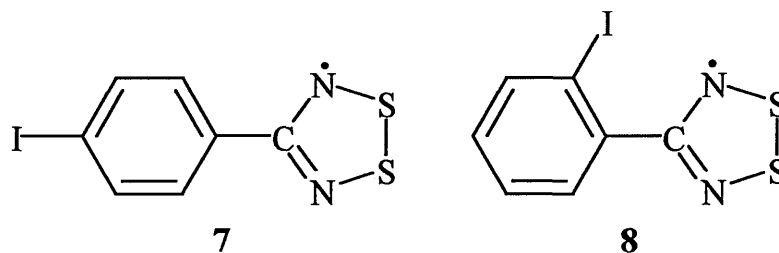
The main section of work undertaken was the synthesis of a range of dichlorophenyl dithiadiazolyls 1-5. Preparation of all the possible isomers of $\text{Cl}_2\text{C}_6\text{H}_3\text{.}\overline{\text{CNSSN}}$ were attempted (except $2,6\text{-Cl}_2\text{C}_6\text{H}_3\text{.}\overline{\text{CNSSN}}$)¹ and all have an assigned crystal structure.



The synthesis and structure of 3,5-dibromophenyl-1,2,3,5-dithiadiazolyl **6** is reported and a comparison of the structure has been made with relevant examples from the literature and that of the chloro-derivatives.

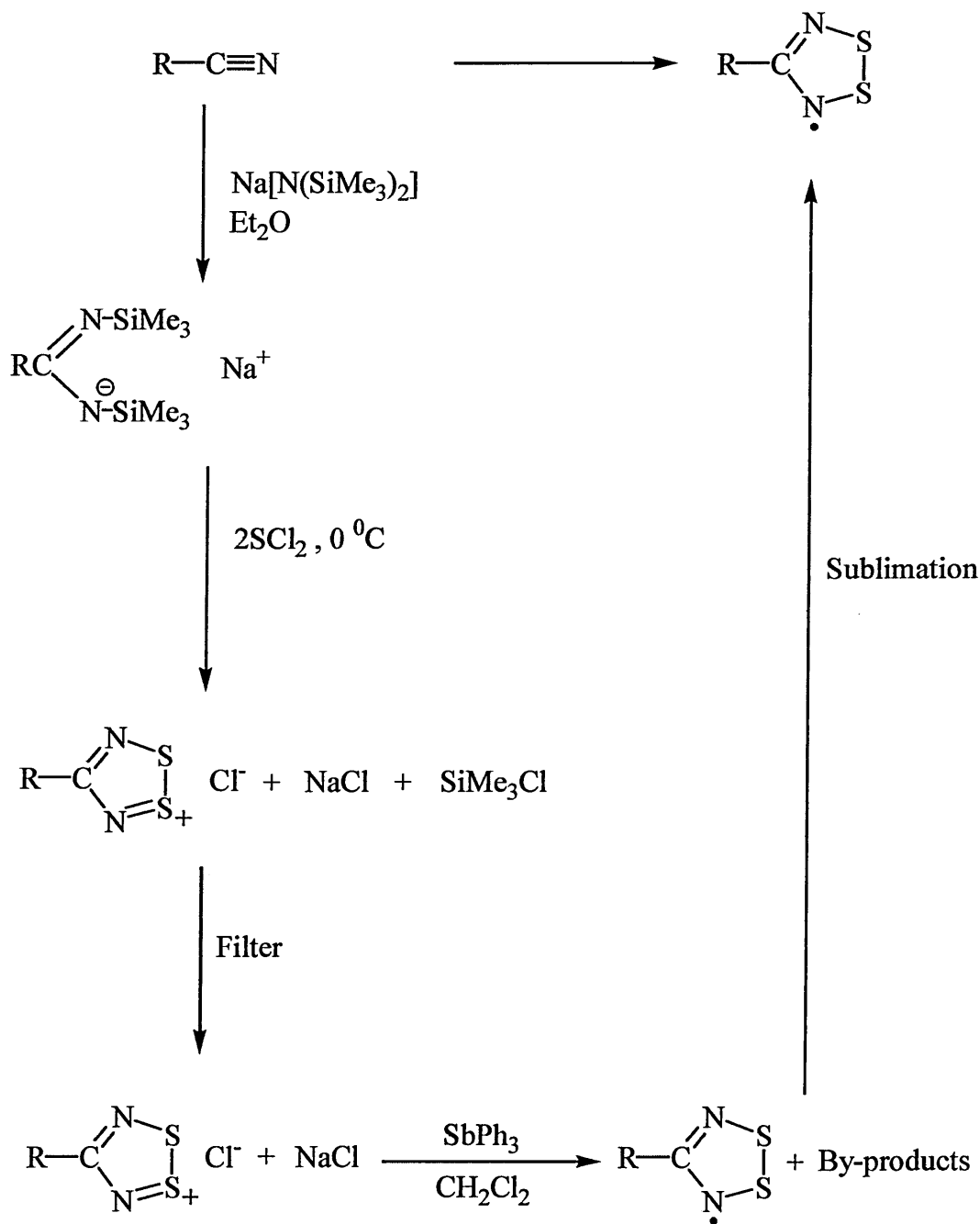


The syntheses of two iodophenyl dithiadiazolyls **7** and **8** are described. The crystal structure of **7** is reported.

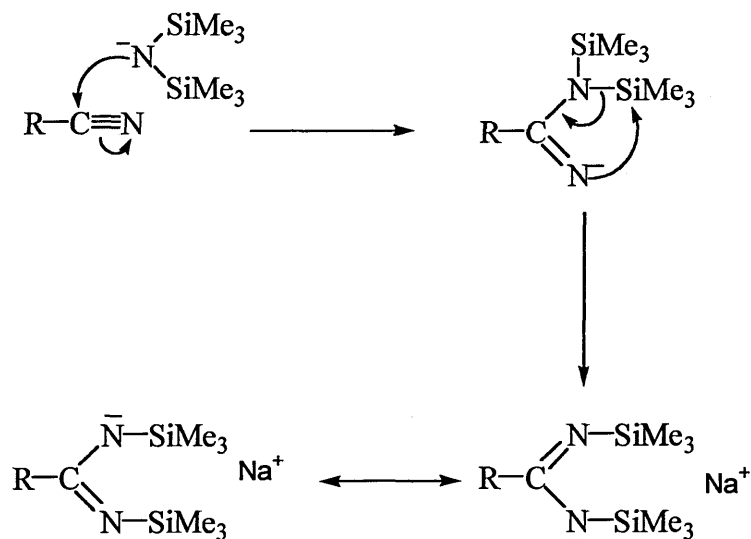


2.1 Synthesis and Mechanisms

As outlined in the previous chapter (Section 1.3) there are several published methods² for the synthesis of dithiadiazolylium salts and for their subsequent reduction to the corresponding dithiadiazolyl radical. The chosen method for these compounds was from the appropriate halogenated benzonitrile derivative *via* an amidinium salt,³ as shown in Scheme 2.1.

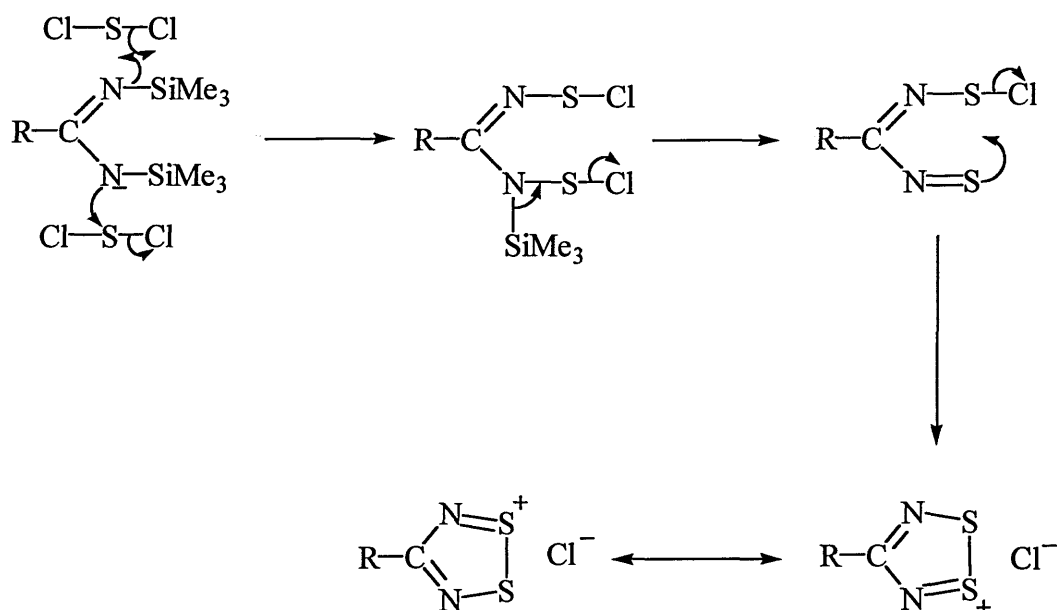


Scheme 2.1 Synthetic strategy for the preparation of 1,2,3,5-dithiadiazolyls



Scheme 2.2 The formation of an amidine salt

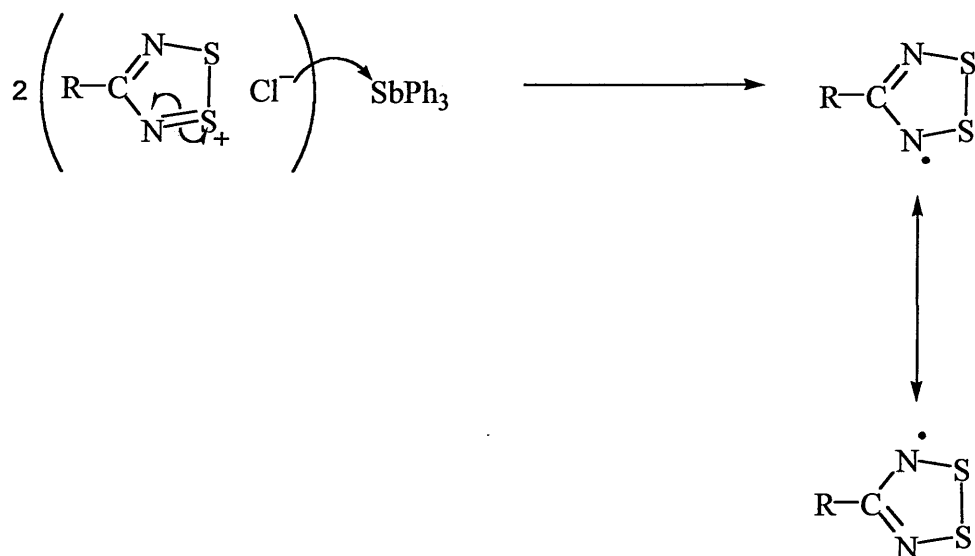
The addition of sulfur dichloride to the metalated amidinium salt eliminates chlorotrimethyl silane (SiMe_3Cl) and sodium chloride. A proposed mechanism for the formation of the dithiadiazolylium ring system is outlined below. Ring closure occurs because of the stabilisation of the resulting ring system due to resonance (Scheme 2.3).



Scheme 2.3 The formation of the dithiadiazolylium ring system

Reduction of the dithiadiazolylium chloride to the neutral radical is outlined below (Scheme 2.4). The triphenylantimony reacts with two chloride ions to yield pentavalent dichlorotriphenylantimony. The stability of the neutral radical is thought to be due to its

resonance stabilisation and aromaticity. In addition, Peierls distortion causing dimerisation of the radicals may further explain their unexpected stability in the solid state.

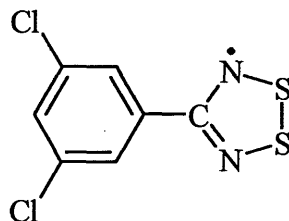


Scheme 2.4 The reduction of a dithiadiazolylium salt

The intermediate dithiadiazolylium chloride can be purified by recrystallisation and by soxhlet extraction with liquid SO₂. However, I chose to eliminate the purification step because the sodium chloride by-product of the reaction does not affect the formation of the radical during the reduction stage⁷ and the chlorotrimethyl silane is removed by washing with diethyl ether. After the reduction, the dithiadiazolyl radical is purified by vacuum sublimation. The production of crystals suitable for x-ray analysis can then be achieved by sublimation under a temperature gradient.

2.2 Experimental

2.2.1 Preparation of 3,5-dichlorophenyl-1,2,3,5-dithiadiazolyl (1)



Sodium bis(trimethylsilyl) amide (1 g, 5.1 mmol) was dissolved in diethyl ether (50 ml). 3,5-Dichlorobenzonitrile (0.88 g, 5.1 mmol) was added to give an immediate dark blue coloured solution which was left to stir at room temperature overnight. The reaction mixture was cooled to 0 °C and sulfur dichloride (0.79 ml, 12.5 mmol) was added. The resulting orange-red precipitate was stirred for 5 hours, filtered, washed (3 x 20 ml diethyl ether) and dried *in vacuo* for approximately 3 hours. The orange dithiadiazolylum chloride (0.94 g, 3.22 mmol) was dissolved in dichloromethane (50ml) and triphenylantimony (0.57 g, 1.61 mmol) was added to give an immediate purple solution that was stirred for approximately 6 hours. The dichloromethane was removed *in vacuo* leaving an oily purple/red solid which was sublimed on to a cold finger at 95 °C to yield a purple microcrystalline solid. This solid was further sublimed under gradient temperature (105 - 25 °C) to yield lustrous dark red crystals.

DSC: Sublimation 73-74.7 °C (α) 95-97 °C (β) Mpt 124-126 °C

 Decomp. 200-250 °C

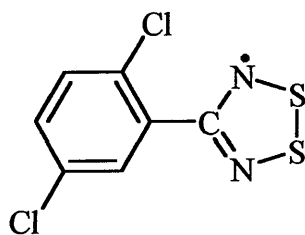
MS (EI) 248.8 (M^+), 202.9 ($M^+ - SN$), 170.9 ($M^+ - S_2N$), 77.9 (S_2N^+)

Infrared 1720(br), 1565(m), 1307(sh), 1156(w), 1176(w), 1021(w), 955(w), 891(w),
864(m), 805(s), 667(w), 598(w), 469(s).

Elemental analysis:

	Carbon	Hydrogen	Nitrogen
Calculated	33.61	1.21	11.19
Experimental	33.61	1.24	11.00

2.2.2 Preparation of 2,5-dichlorophenyl-1,2,3,5-dithiadiazolyl (2)



Sodium bis(trimethylsilyl) amide (1 g, 5.1 mmol) was dissolved in diethyl ether (50 ml). 2,5-Dichlorobenzonitrile (0.88 g, 5.1 mmol) was added to give an immediate dark blue coloured solution which was left to stir at room temperature overnight. The reaction mixture was cooled to 0 °C and sulfur dichloride (0.79 ml, 12.5 mmol) was added. The resulting red/brown precipitate was stirred for 5 hours, filtered, washed (3 x 20 ml diethyl ether) and dried *in vacuo* for approximately 3 hours. The brown dithiadiazolylium chloride (0.94 g, 3.22 mmol) was dissolved in dichloromethane (50 ml) and triphenylantimony (0.57 g, 1.61 mmol) was added to give an immediate purple solution that was stirred for approximately 6 hours. The dichloromethane was removed *in vacuo* leaving an oily purple/red solid which was sublimed on to a cold finger at 95 °C to yield a purple/red microcrystalline solid. This solid was further sublimed under gradient temperature (95 - 25 °C) to yield lustrous dark red crystals.

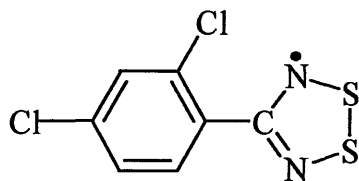
DSC: Sublimation 75-80 °C Mpt 100-103 °C Decomp. 120-226 °C

MS (EI) 248.8 (M⁺), 202.9 (M⁺ - SN), 170.9 (M⁺ - S₂N), 77.9 (S₂N⁺)

Infrared 1720(br), 1565(m), 1307(sh), 1156(w), 1176(w), 1021(w), 955(w), 891(w), 864(m), 805(s), 667(w), 598(w), 469(s).

Accurate mass calculated for C₇H₃S₂N₂³⁵Cl₂ 248.91147, found 248.91112

2.2.3 Preparation of 2,4-dichlorophenyl-1,2,3,5-dithiadiazolyl (3)



Sodium bis(trimethylsilyl) amide (1 g, 5.1 mmol) was dissolved in diethyl ether (50 ml). 2,4-Dichlorobenzonitrile (0.88 g, 5.1 mmol) was added to give an immediate dark blue coloured solution which was left to stir at room temperature overnight. The reaction mixture was cooled to 0 °C and sulfur dichloride (0.79 ml, 12.5 mmol) was added. The resulting light yellow precipitate was stirred for 5 hours, filtered, washed (3 x 20 ml diethyl ether) and dried *in vacuo* for approximately 3 hours. The yellow dithiadiazolylium chloride (0.94 g, 3.22 mmol) was dissolved in dichloromethane (50 ml) and triphenylantimony (0.57 g, 1.61 mmol) was added to give an immediate purple solution that was stirred for approximately 6 hours. The dichloromethane was removed *in vacuo* leaving an oily purple/red solid which was sublimed on to a cold finger at 95 °C to yield a purple microcrystalline solid. This solid was further sublimed under gradient temperature (105 - 25 °C) to yield lustrous dark red crystals.

DSC: Sublimation 60-61 °C Mpt 79-80 °C Decomp. 140-165 °C

MS (EI) 248.9 (M⁺), 202.8 (M⁺ - SN), 171.0 (M⁺ - S₂N), 78.0 (S₂N⁺)

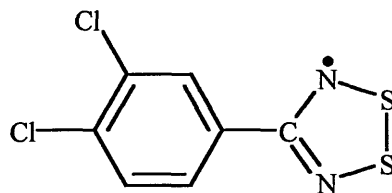
IR (nujol) 1401(s), 1342(s), 1262(w), 1227(w), 1154(w), 1103(s), 1071(m), 1050(s),
1024(sh), 935(m), 886(m), 826(s), 806(m), 782(s), 664(w).

Accurate mass calculated for C₇H₃S₂N₂³⁵Cl₂ 248.91147, found 248.91144

Elemental analysis:

	Carbon	Hydrogen	Nitrogen
Calculated	33.61	1.21	11.19
Experimental	33.69	1.27	11.04

2.2.4 Preparation of 3,4-dichlorophenyl-1,2,3,5-dithiadiazolyl (4)



Sodium bis(trimethylsilyl) amide (1 g, 5.1 mmol) was dissolved in diethyl ether (50 ml). 3,4-Dichlorobenzonitrile (0.88 g, 5.1 mmol) was added to give an immediate dark purple coloured solution which was left to stir at room temperature overnight. The reaction mixture was cooled to 0 °C and sulfur dichloride (0.79 ml, 12.5 mmol) was added. The resulting orange precipitate was stirred for 5 hours, filtered, washed (3 x 20 ml diethyl ether) and dried *in vacuo* for approximately 3 hours. The orange dithiadiazolylum chloride (0.94 g, 3.22 mmol) was dissolved in dichloromethane (50 ml) and triphenylantimony (0.57 g, 1.61 mmol) was added to give an immediate purple solution that was stirred for approximately 6 hours. The dichloromethane was removed *in vacuo* leaving an oily purple/red solid which was sublimed on to a cold finger at 100°C to yield a purple microcrystalline solid. This solid was further sublimed under gradient temperature (110 - 25 °C) to yield lustrous dark red crystals.

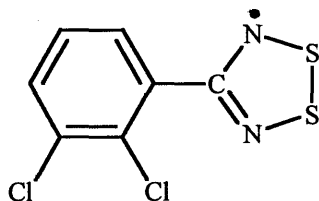
DSC: Sublimation 86-89 °C Mpt 156-158 °C Decomp. 220°C (onset)

MS (EI) 249.0(M⁺), 203.0(M⁺ - SN), 171.0 (M⁺ - S₂N), 77.9(S₂N⁺)

IR (nujol) 1403(s), 1348(s), 1262(w), 1225(w), 1154(w), 1106(s), 1068(m), 1053(s),
1024(m), 938(m), 886(m), 826(s), 806(m).

Accurate mass calculated for C₇H₃S₂N₂³⁵Cl₂ 248.91147, found 248.91195

2.2.5 Preparation of 2,3-dichlorophenyl-1,2,3,5-dithiadiazolyl (5)



Sodium bis(trimethylsilyl) amide (1 g, 5.1 mmol) was dissolved in diethyl ether (50 ml). 2,3-Dichlorobenzonitrile (0.88 g, 5.1 mmol) was added to give an immediate green/brown coloured solution which was left to stir at room temperature overnight. The reaction mixture was cooled to 0 °C and sulfur dichloride (0.79 ml, 12.5 mmol) was added. The resulting bright yellow precipitate was stirred for 5 hours, filtered, washed (3 x 20 ml diethyl ether) and dried *in vacuo* for approximately 3 hours. The bright yellow dithiadiazolylium chloride (0.94 g, 3.22 mmol) was dissolved in dichloromethane (50 ml) and triphenylantimony (0.57 g, 1.61 mmol) was added to give an immediate purple solution that was stirred for approximately 6 hours. The dichloromethane was removed *in vacuo* leaving an oily purple/red solid which was sublimed on to a cold finger at 100 °C to yield a purple microcrystalline solid. This solid was further sublimed under gradient temperature (95 – 25 °C) to yield lustrous dark red crystals.

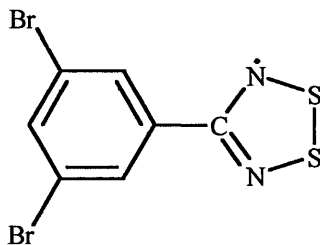
DSC: Sublimation 73-75 °C Mpt 119-120.5 °C Decomp. 190-226 °C

MS (EI) 248.8 (M⁺), 203.0 (M⁺ - SN), 171.0 (M⁺ - S₂N), 78.0 (S₂N⁺)

IR (nujol) 1411(s), 1337(s), 1263(w), 1215(w), 1159(w), 1109(s), 1063(m), 1044(s),
1023(sh), 935(m), 892(m), 844(s), 801(m).

Accurate mass calculated for C₇H₃S₂N₂³⁵Cl₂ 248.91147, found 248.91007

2.2.6 Preparation of 3,5-dibromophenyl-1,2,3,5-dithiadiazolyl (6)



Sodium bis(trimethylsilyl) amide (0.71 g, 3.3 mmol) was dissolved in diethyl ether (50 ml). 3,5-Dibromobenzonitrile (1 g, 3.3 mmol) was added to give an immediate brown coloured solution which was left to stir at room temperature overnight. The reaction mixture was cooled to 0 °C and sulfur dichloride (0.48 ml, 6.6 mmol) was added. The resulting orange precipitate was stirred for 5 hours, filtered, washed (3 x 20 ml diethyl ether) and dried *in vacuo* for approximately 3 hours. The orange dithiadiazolylium chloride (1.38 g, 3.22 mmol) was dissolved in tetrahydrofuran (50 ml) and Zn/Cu couple (0.24 g, 1.61 mmol) was added to give an immediate red solution that was stirred for approximately 6 hours. The dichloromethane was removed *in vacuo* leaving an oily red solid which was sublimed on to a cold finger at 125 °C to yield a purple microcrystalline solid. This solid was further sublimed under gradient temperature (110 – 25 °C) to yield lustrous dark red crystals.

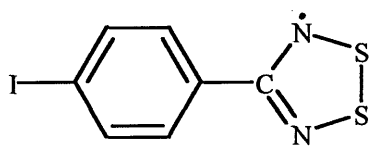
DSC: Sublimation 91-93 °C Mpt 148-150 °C Decomp.230 °C (onset)

MS (EI) 339.1 (M⁺), 292.9 (M⁺ - SN), 161.0 (M⁺ - S₂N), 78.0 (S₂N⁺)

Elemental analysis:

	Carbon	Hydrogen	Nitrogen
Calculated	24.80	0.89	8.26
Experimental	24.65	0.90	8.22

2.2.7 Preparation of 4-iodophenyl-1,2,3,5-dithiadiazolyl (7)



Sodium bis(trimethylsilyl) amide (0.89 g, 4.8 mmol) was dissolved in diethyl ether (50 ml). 4-iodobenzonitrile⁸ (1.11 g, 4.8 mmol) was added to give an immediate yellow coloured solution which was left to stir at room temperature overnight. The reaction mixture was cooled to 0 °C and sulfur dichloride (0.61 ml, 9.6 mmol) was added. The resulting orange-red precipitate was stirred for 5 hours, filtered, washed (3 x 20 ml diethyl ether) and dried *in vacuo* for approximately 3 hours. The orange dithiadiazolylum chloride (1.32 g, 3.85 mmol) was dissolved in dichloromethane (50 ml) and triphenylantimony (0.68 g, 1.9 mmol) was added to give a black solution that was stirred for approximately 12 hours. The dichloromethane was removed *in vacuo* leaving an oily purple/red solid which was sublimed on to a cold finger at 130 °C to yield a purple microcrystalline solid. This solid was further sublimed under gradient temperature (120 – 25 °C) to yield lustrous dark red crystals.

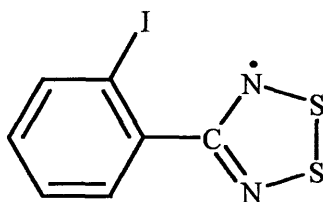
DSC: Sublimation 120-121 °C Mpt 171-172 °C Decomp. 210-239 °C

MS (EI) 307.1 (M⁺), 261.1 (M⁺ - SN), 229.0 (M⁺ - S₂N), 77.9 (S₂N⁺)

Elemental analysis:

	Carbon	Hydrogen	Nitrogen
Calculated	27.37	1.31	9.12
Experimental	27.13	1.32	9.05

2.2.8 Preparation of 2-iodophenyl-1,2,3,5-dithiadiazolyl (8)



Sodium bis(trimethylsilyl) amide (0.66 g, 3.6 mmol) was dissolved in diethyl ether (50 ml). 2-iodobenzonitrile (0.82 g, 3.6 mmol) was added to give an immediate yellow coloured solution which was left to stir at room temperature overnight. The reaction mixture was cooled to 0 °C and sulfur dichloride (0.45 ml, 7.2 mmol) was added. The resulting orange-red precipitate was stirred for 5 hours, filtered, washed (3 x 20 ml diethyl ether) and dried *in vacuo* for approximately 3 hours. The orange dithiadiazolium chloride (1.19 g, 3.5 mmol) was dissolved in dichloromethane (50 ml) and triphenylantimony (0.61 g, 1.75 mmol) was added to give a light brown solution that was stirred for approximately 12 hours. The dichloromethane was removed *in vacuo* leaving an oily red solid which was sublimed on to a cold finger at 90 °C to yield a purple oil. This solid was further sublimed under gradient temperature (90 - 25 °C) to yield purple oil.

DSC: Mpt 40-57 °C Decomp. 110-164 °C

MS (EI) 306.9 (M⁺), 261.1 (M⁺ - SN), 229.0 (M⁺ - S₂N), 77.9 (S₂N⁺)

Accurate mass calculated for C₇H₃S₂N₂I 306.88606, found 306.88612

2.3 References

- 1 Synthesis was unsuccessful
- 2 J.M. Rawson, A.J. Banister and I. Lavender, *Adv. Heterocycl. Chem.*, 1995, **62**, 137 and references therein.
- 3 A.R. Sanger, *Inorg. Nucl. Chem. Letters*, 1973, **9**, 351.
- 4 R.T. Boéré, R.T Oakley and R.W. Reed, *J. Organomet. Chem.*, 1987, **331**, 161.
- 5 R.T. Boéré, R.T Oakley and R.W. Reed, *J. Organomet. Chem.*, 1987, **331**, 161.
- 6 M. Amin and C.W. Rees, *J. Chem. Soc., Perkin Trans. 1*, 1989, 2495.
- 7 I. May, PhD Thesis, Univeristy of Durham, 1995.
- 8 (a) N. Bricklebank, S. Hargreaves and S.E. Spey, *Polyhedron*, 2000, **19**, 1163.
(b) E.O. Schlemper and D.Britton, *Acta. Cryst.*, 1965, **18**, 419.

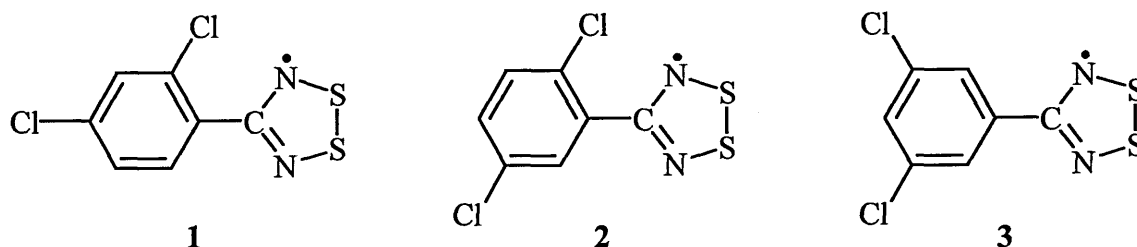
Chapter 3

Stacking Motifs for Dichlorophenyl Dithiadiazolyl Radicals

3.0 Introduction

The assembly of molecular species into ordered supramolecular arrays, which display useful physical phenomena, provides a goal for much contemporary research.^{1,2} Relatively minor changes to the structures of the constituent molecules can lead to pronounced changes in the crystal packing and hence to the overall physical properties of the compound.

In this chapter, the structures and physical properties of three dichlorophenyl dithiadiazolyls, **1**, **2** and **3**, the first examples of dithiadiazolyls that crystallise in uniformly spaced, segregated, stacks in their neutral radical form are presented. A second polymorph of **3** has also been isolated and its crystal structure is described.



As discussed above (Section 1.5, page 10), one of the primary aims of dithiadiazolyl research has been to produce infinite arrays of dithiadiazolyl molecules either in the form of paramagnetic chains or segregated stacks.

Previous studies have investigated the effect of di-^{3,4} and tri⁵-fluorinated phenyl groups on the molecular packing of dithiadiazolyl radicals. Studies by Rawson and co-workers revealed that 3,5- and 2,4-difluorophenyl-1,2,3,5-dithiadiazolyl associated in stacks of dimers, containing alternated short intradimer and long interdimer S...S interactions. In contrast, 2,5-difluorophenyl-1,2,3,5-dithiadiazolyl was found to crystallise in stacks

containing uniformly spaced radical units with an unexpectedly long intermolecular S...S distance of 3.554(3) Å. However, a re-examination of the structure of 2,5-difluorophenyl-1,2,3,5-dithiadiazolyl by Oakley and co-workers⁶ discovered that the original structure was a superlattice and the true structure was actually segregated stacks of dimer pairs, like those of the analogous 2,4- and 3,5-difluorophenyl isomers. This conclusion is supported by the absence of paramagnetic or conductive behaviour that might be expected for an evenly spaced (undimerised) radical.⁶ Stacking motifs within dithiadiazolyls have also been observed in the form of partially oxidised radicals,^{7,8,9} which exhibit conductivity at room temperature.

Fluorine...Fluorine interactions are generally considered to be of a repulsive nature.¹⁰ It has been suggested that homonuclear interactions between heavier halogens are attractive¹⁰ and that Cl...Cl interactions can have a marked effect on the solid state structure.¹¹

It has long been accepted that many intermolecular X...X (X= Cl, Br and I) distances in molecular crystals are significantly less than the sum of the accepted van der Waals radii.¹² These X...X interactions have special significance in crystal engineering or the deliberate design of organic crystal structures because they may be used to create layered motifs,¹³ which are associated with specific solid state reactivity patterns. These have previously been described as “donor-acceptor”, “secondary” and “charge transfer” interactions. More recently, the interactions have been described in terms of highest occupied molecular orbital and lowest unoccupied molecular orbital (HOMO-LUMO) and nucleophilic attack.¹⁴ In all such cases, it has been noticed that there is a directional preference in which contacting groups position themselves. Indeed, it has been shown¹¹ that in organic molecular solids, association is only *via* certain geometrical motifs.¹⁰ This is thought to be due to either specific attractive forces of chlorine in certain directions (*i.e.* increased

attraction) or non-spherical shapes with polar flattening¹² in a close packed structure (*i.e.* decreased repulsion). A statistical approach employed by Desiraju and Parthasarathy concluded that there were indeed attractive (and anisotropic) forces within Cl...Cl interactions.¹⁰ Irrespective of the origin of the effect, it would appear that chlorine atoms attached directly to an organic group tend to “steer” the crystal structure to a so-called “ β -mode”.¹¹ This is characterised by a short crystallographic axis of *c.a.* 4 Å with the molecules packing in layered sheets and stacks. This phenomenon has been observed for at least one hundred published polychlorinated-aromatics.¹⁰ The β -structure may therefore have great significance in the design of low dimensional organic metals and superconductors.

To date only one chlorine-substituted phenyl derivative of a dithiadiazolyl radical has been reported, *p*-chlorophenyl-1,2,3,5-dithiadiazolyl.¹⁵ In the solid state it is a dimer (Figure 3.1) but exhibits packing of an unusual type for dithiadiazolyls. The discrete dimers form into two *interpenetrating* ribbons, which are orthogonal to one another. The ribbons are connected by a triangle of S...Cl contacts along the plane of the dithiadiazolyl ring of 3.38Å and 3.52Å. These distances are less than the sum of the van der Waals radii (3.5 - 3.7 Å). The publication noted the similarity of interaction between this compound and cyano substituents attached to aryl dithiadiazolyls.^{16,17}

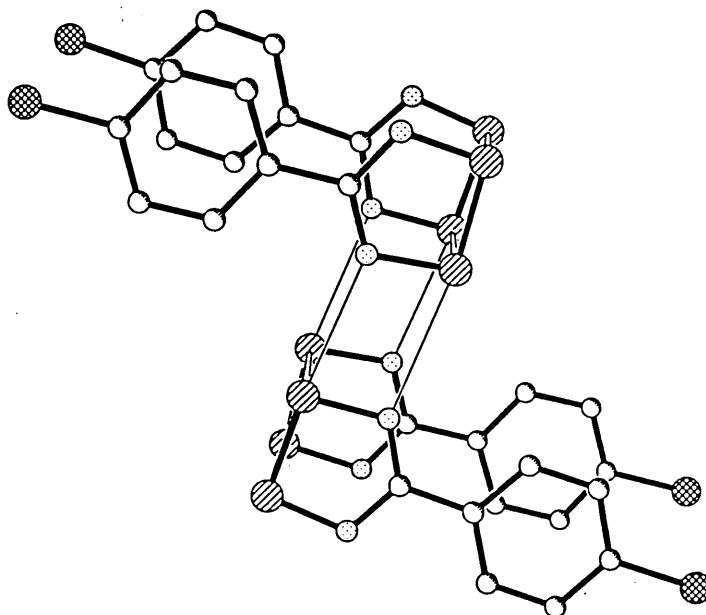


Figure 3.1 Crystal structure of *p*-chlorophenyl-1,2,3,5-dithiadiazolyl

3.1 X-Ray Crystal Structures

X-ray structural determinations were undertaken on compounds **1** - **3**. All of the determinations were carried out by Sharon Spey and Harry Adams from the University of Sheffield. An Ortep structural plot of one molecule from each of the three isomers, including two polymorphs of **3** (α -**3** and β -**3**) are shown in Figures 3.2 – 3.5. The bond lengths and angles in **1** - **3** are listed in Tables 3.1 and 3.2 together with data for phenyl-1,2,3,5-dithiadiazolyl¹⁸ and *p*-chlorophenyl-1,2,3,5-dithiadiazolyl¹⁵ for comparative purposes. The full crystallographic data for these compounds can be found in appendices 1-4 at the end of this thesis.

The molecular structures of **1** - **3** are, as expected, similar to those of most previously published aryl substituted dithiadiazolyls. The chlorine-carbon bond distances are reasonably similar to those observed for *p*-chlorophenyl-1,2,3,5-dithiadiazolyl,¹⁵ (Figure 3.1) which has a Cl-C bond length of 1.750 Å. The most significant difference observed between the four structures is the torsion angle between the two planar rings

(Cl₂C₆H₃-CNSSN). As expected, the compounds which have a chlorine in the *ortho* position in relation to the dithiadiazolyl have the largest torsion angles (26° and 27.6° for **1** and **2** respectively). Presumably, this is due to the steric hindrance caused by the close proximity of the chlorine to the nitrogen of the dithiadiazolyl. The twist angle of the two polymorphs of **3** are somewhat smaller (16.15° and 15.4° for β-3 and α-3 respectively) because the chlorine is far enough from the dithiadiazolyl ring not to cause steric hindrance. These values are significantly larger than the equivalent angles in phenyl¹⁸ (7° torsion angle) and the *p*-chlorophenyl derivatives¹⁵ (7° torsion angle) indicating that for **3** at least, packing factors may have an effect on the twist angle.

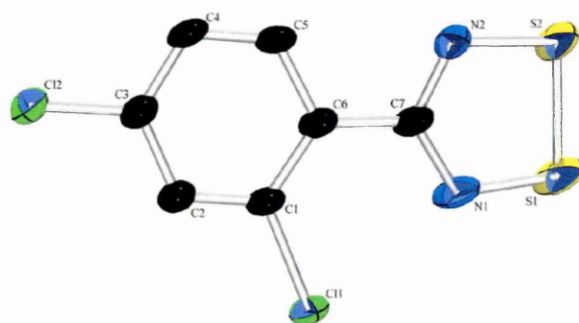


Figure 3.2 2,4-dichlorophenyl-1,2,3,5-dithiadiazolyl (1)

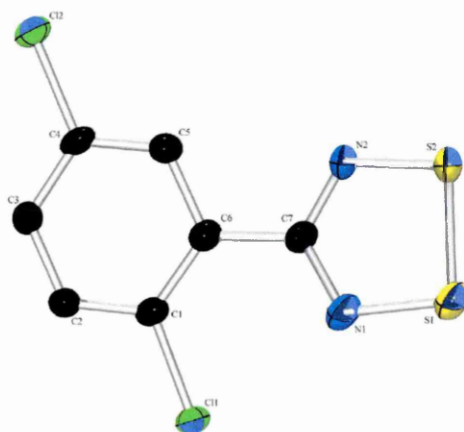


Figure 3.3 2,5-dichlorophenyl-1,2,3,5-dithiadiazolyl (2)

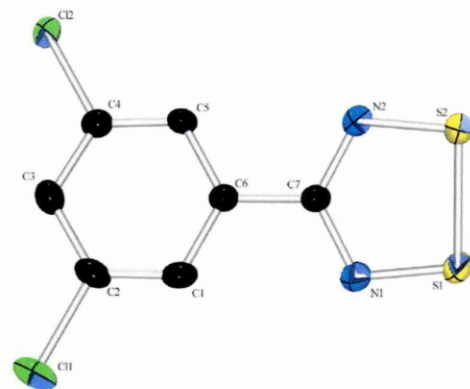


Figure 3.4 β phase of 3,5-dichlorophenyl-1,2,3,5,-dithiadiazolyl (β -3)

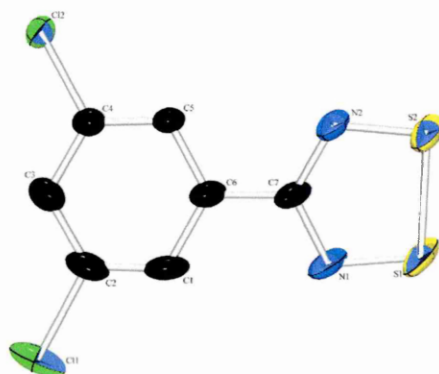


Figure 3.5 α phase of 3,5-dichlorophenyl-1,2,3,5,-dithiadiazolyl (α -3)

Table 3.1 Bond lengths of 1-3 (Å).

Atom No.	Bond Distance (Å)					
	1	2	β -3*	α -3*	Ph	<i>P</i> -ClC ₆ H ₄
Cl(1)-C(1)	1.727(4)	1.735(3)	-	-	-	-
Cl(1)-C(2)	-	-	1.743(5)	1.727(4)	-	-
Cl(1)-C(4)	-	-	-	-	-	1.750(4)
Cl(2)-C(3)	1.727(5)	-	-	-	-	-
Cl(2)-C(4)	-	1.738(3)	1.732(5)	1.743(4)	-	-
S(1)-N(1)	1.620(5)	1.631(3)	1.633(5)	1.626(4)	1.63	1.643(10)
S(1)-S(2)	2.090(2)	2.0973(18)	2.0865(19)	2.0920(16)	2.096	2.103(5)
S(2)-N(2)	1.625(4)	1.623(3)	1.627(5)	1.634(4)	1.63	1.651(10)
N(1)-C(7)	1.332(5)	1.335(5)	1.347(6)	1.336(5)	1.32	1.320(1)
N(2)-C(7)	1.332(6)	1.338(5)	1.339(6)	1.343(5)	1.31	1.340(1)
C(1)-C(2)	1.377(6)	1.387(5)	1.376(7)	1.391(5)	1.37	1.365(7)
C(1)-C(6)	1.406(6)	1.398(5)	1.390(7)	1.398(5)	1.37	1.410(7)
C(2)-C(3)	1.388(6)	1.378(5)	1.386(7)	1.390(5)	1.39	1.385(8)
C(3)-C(4)	1.373(6)	1.380(5)	1.382(7)	1.377(6)	1.42	1.371(7)
C(4)-C(5)	1.384(6)	1.384(5)	1.385(7)	1.376(6)	1.36	1.376(8)
C(5)-C(6)	1.396(5)	1.404(4)	1.397(6)	1.400(5)	1.38	1.401(6)
C(6)-C(7)	1.471(6)	1.484(5)	1.476(7)	1.476(6)	1.50	1.472(7)

* Denotes the bond lengths of a representative molecule within an asymmetric unit containing more than one molecule.

Table 3.2 Bond angles of 1-3 (^o)

Atom Numbers	Angle (degrees)					
	(1)	(2)	α -3*	β -3*	Ph	<i>p</i> -ClC ₆ H ₄
N(1)-S(1)-S(2)	94.61(16)	94.57(13)	94.92(17)	94.16(13)	93.0	95.3(4)
N(2)-S(2)-S(1)	94.16(16)	94.28(14)	94.38(17)	94.74(13)	94.1	93.4(4)
C(7)-N(1)-S(1)	114.2(4)	113.8(3)	113.8(4)	115.0(3)	116	113.2(9)
C(7)-N(2)-S(2)	114.3(3)	114.4(3)	114.8(4)	113.9(3)	115	114.0(8)
C(2)-C(1)-C(6)	121.9(4)	121.2(3)	118.9(4)	118.4(3)	121	121.5(5)
C(2)-C(1)-Cl(1)	116.3(3)	116.4(3)	-	-	-	-
C(6)-C(1)-Cl(1)	121.9(3)	122.3(3)	-	-	-	-
C(3)-C(2)-Cl(1)	-	-	122.4(4)	118.9(3)	-	-
C(1)-C(2)-Cl(1)	-	-	118.3(4)	118.9(3)	-	-
C(4)-C(3)-Cl(1)	-	-	-	-	-	120.6(4)
C(5)-C(4)-Cl(1)	-	-	-	-	-	119.1(4)
C(1)-C(2)-C(3)	118.8(4)	120.3(3)	119.4(4)	122.2(3)	120	119.4(5)
C(4)-C(3)-C(2)	121.7(4)	119.3(3)	117.1(5)	117.6(4)	119	120.3(3)
C(4)-C(3)-Cl(2)	119.5(3)	-	-	-	-	-
C(2)-C(3)-Cl(2)	118.9(3)	-	-	-	-	-
C(3)-C(4)-Cl(2)	-	120.4(3)	123.1(4)	119.5(3)	-	-
C(5)-C(4)-Cl(2)	-	118.5(3)	118.2(4)	117.8(3)	-	-
C(3)-C(4)-C(5)	118.4(4)	121.1(3)	118.6(4)	122.7(4)	120	119.7(5)
C(4)-C(5)-C(6)	122.6(4)	120.4(3)	117.6(4)	118.9(3)	119	120.9(4)
C(5)-C(6)-C(1)	116.7(4)	117.6(3)	120.9(4)	120.2(4)	121	119.1(5)
C(5)-C(6)-C(7)	117.5(4)	116.5(3)	119.5(4)	119.7(3)	119	121.3(5)
C(1)-C(6)-C(7)	125.8(4)	125.9(3)	119.6(4)	120.1(3)	120	121.6(5)
N(1)-C(7)-N(2)	122.7(4)	123.0(3)	122.1(5)	122.1(4)	122	123(1)
N(2)-C(7)-C(6)	120.4(4)	116.8(3)	118.9(4)	118.7(4)	121	116(1)
N(1)-C(7)-C(6)	116.7(4)	120.1(3)	119.0(4)	119.1(3)	117	119(1)
Twist Angle*	26	27.6	16.15	15.4	7	7

* Denotes the bond angles of a representative molecule within an asymmetric unit containing more than one molecule.

** Denotes the torsion angle between C(6) and C(7) based on the planes of both the dithiadiazolyl ring and the phenyl ring.

As with most dithiadiazolyl studies, the interest in the crystal structure does not lie in the molecules themselves, but in the interaction of the molecules with each other in the solid state. Gaining an understanding of these interactions will lead to the controlled design of crystals, which pack with a particular, pre-determined motif.

3.1.1 X-ray Crystal Structure of 2,4-dichlorophenyl-1,2,3,5-dithiadiazolyl

A suitable crystal for x-ray analysis was produced by sublimation. First, the crude oil containing the dithiadiazolyl radical produced from the reduction of the respective dithiadiazolylium chloride, was purified by cold finger sublimation. The resulting needle-like crystals were carefully sublimed for approximately 48 hours under a temperature gradient range of 105 °C - 25 °C (10^{-3} torr), which yielded **1** as small dark red blocks.

The asymmetric unit of **1** contains one molecule and is monoclinic with a space group of $P2_1/n$. As indicated at the start of the chapter, the molecules associate in segregated stacks, containing uniformly spaced radical units. This stack is parallel to the b-axis and the intrastack S...S distance is 3.629 Å. This value is equal to the length of the shortest crystallographic axis and is in close agreement with the chlorinated aromatic structures, which also crystallise in the so-called β -mode. The association within one stack is shown below (Figure 3.6) The distances between the atoms S1a...S1b, S1b...S1c, S2a...S2b and S2b...S2c are all equal (3.629 Å). These intrastack S...S distances are considerably longer than those observed for dimerised dithiadiazolyls, although the distance is still less than twice the van der Waals radius of sulfur (4.06 Å when perpendicular to the bond).¹⁹

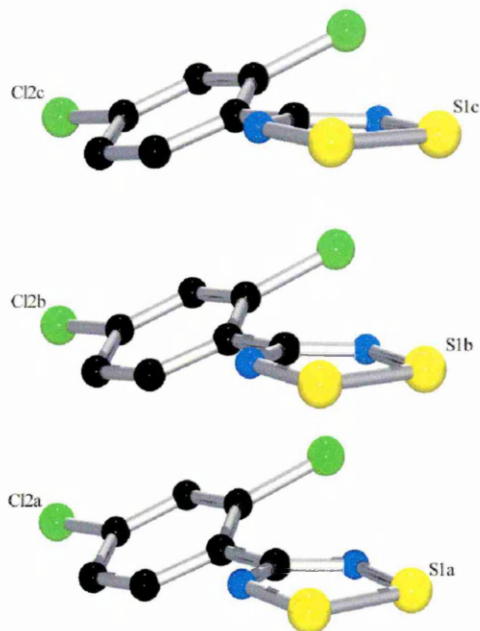


Figure 3.6 Ortep plot of the stacking of **1**, with selected atoms labelled.

As well as the association within the stack, there is also significant interaction between the stacks (*i.e.* in the *a* and *c* directions). Molecules in adjacent stacks are associated in a herringbone fashion, linked by two principal sets of S \cdots Cl contacts (Figure 3.7). These interactions take the form of one short (S1 \cdots Cl2, 3.285 Å) and one long (S2 \cdots Cl2, 3.648 Å) electrostatic S \cdots Cl contact, both of which lie within sum of the van der Waals radii for S and Cl (3.65 Å).¹⁹ In the case of the S1 \cdots Cl2 contact the distance is significantly shorter than the van der Waals and so represents a strong interaction. The molecules are linked into chains parallel to the crystallographic *a*-axis with adjacent chains aligning in an antiparallel manner.

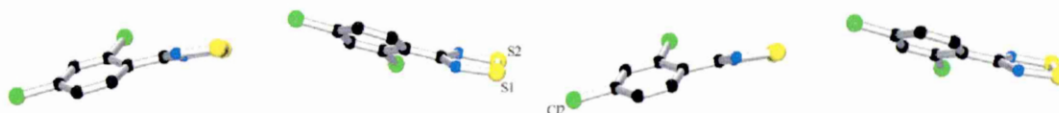


Figure 3.7 Ortep plot of a chain of **1**, with selected atoms have been labelled.

Significant interactions are also observed between adjacent chains (Figure 3.8), the most important being S...N and S...Cl interactions that affect the packing of the chains within the *ac* plane.

Electrostatic interactions are present between the *ortho* chlorine and a sulfur of the dithiadiazolyl ring (S1b...Cl1a, 3.831 Å and S1a...Cl1b, 3.547 Å). This interaction between the sulfur and the chlorine atom in the *ortho* position in turn weakens the S...Cl contact with the chlorine in the *para* position. This is responsible for the asymmetry in the bond lengths between the chlorine in the *para* position and the two sulfurs of the dithiadiazolyl ring (S2a...Cl2d, 3.285 Å and S2...Cl2, 3.648 Å). Moreover, these S...Cl interactions also affect the head-to-head S...N contacts between adjacent heterocycles in the *ac* plane. For example, the S...N distances between molecules which are also linked by S...Cl contacts (S1b...N1a, 3.657 Å and S1a...N1b, 3.907 Å) are much shorter than those between molecules which are not linked by S...Cl contacts (S2c...N2a and S2a...N2c, 3.995 Å). Within the *ac* plane, there is also evidence of Cl...Cl interactions (Cl1b...Cl2d and Cl1d...Cl2b, 3.643 Å)

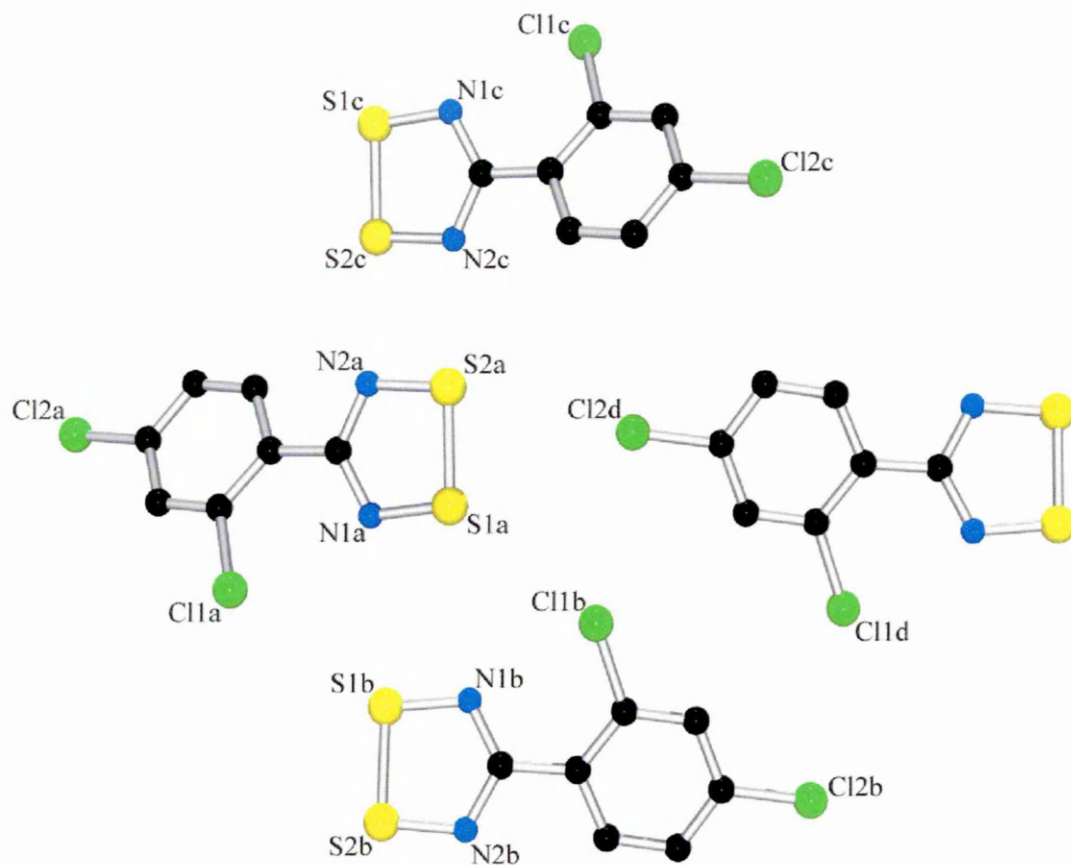


Figure 3.8 Ortep plot of the interactions between chains of **1**, with selected atoms labelled.

The chains formed in this compound are similar to those observed in the α -phase of $p\text{-NC.C}_6\text{F}_4.\overline{\text{CNSSN}}$.²⁰ The molecular packing of this compound also displays sheets of interconnecting chains. Within the molecular packing of $\alpha\text{-}p\text{-NC.C}_6\text{H}_4.\overline{\text{CNSSN}}$, adjacent chains of molecules are linked through electrostatic interactions between the sulfur atoms of the dithiadiazolyl ring and the cyano nitrogen atoms. In this case, the sheets were not then translated into stacks like those I have observed for **1**, instead, the dithiadiazolyl rings are offset between sheets producing a compound that was not spin paired and was therefore paramagnetic.

It is clear that the chloro substituents attached to the aryl ring have a marked effect on the molecular packing. It is not clear whether the stacking is a result of the steric bulk of chlorine counteracting the attractive nature of spin pairing, or because of its reported

directional effects.¹¹ Studies of the literature would suggest that this type of structure is typical of chlorinated aryl groups, many of which exhibit stacked and layered motifs.¹⁰ The structure does show some similarities to that of $p\text{-Cl.C}_6\text{H}_4.\overline{\text{CNSSN}}$ ¹⁵ (Figure 3.1) because of the close proximity of the $\text{S}\cdots\text{Cl}$ interactions within a chain of molecules. Despite this, the molecular packing of **1** and $p\text{-Cl.C}_6\text{H}_4.\overline{\text{CNSSN}}$ are considerably different. This can only be attributed to the interactions of the second chlorine both within the plane and through the stack. Unfortunately, although all the other isomers of the difluorophenyl-1,2,3,5-dithiadiazolyl have been reported,⁴ the 2,4-isomer was not studied so no comparison can be drawn.

Figure 3.9 shows the overall crystal packing of **1** looking down the crystallographic b -axis. In the light of new literature⁶ describing the ability of this type of compound to form a superlattice, great effort was taken to search for this possibility. No superlattice structure could be refined from the data produced.

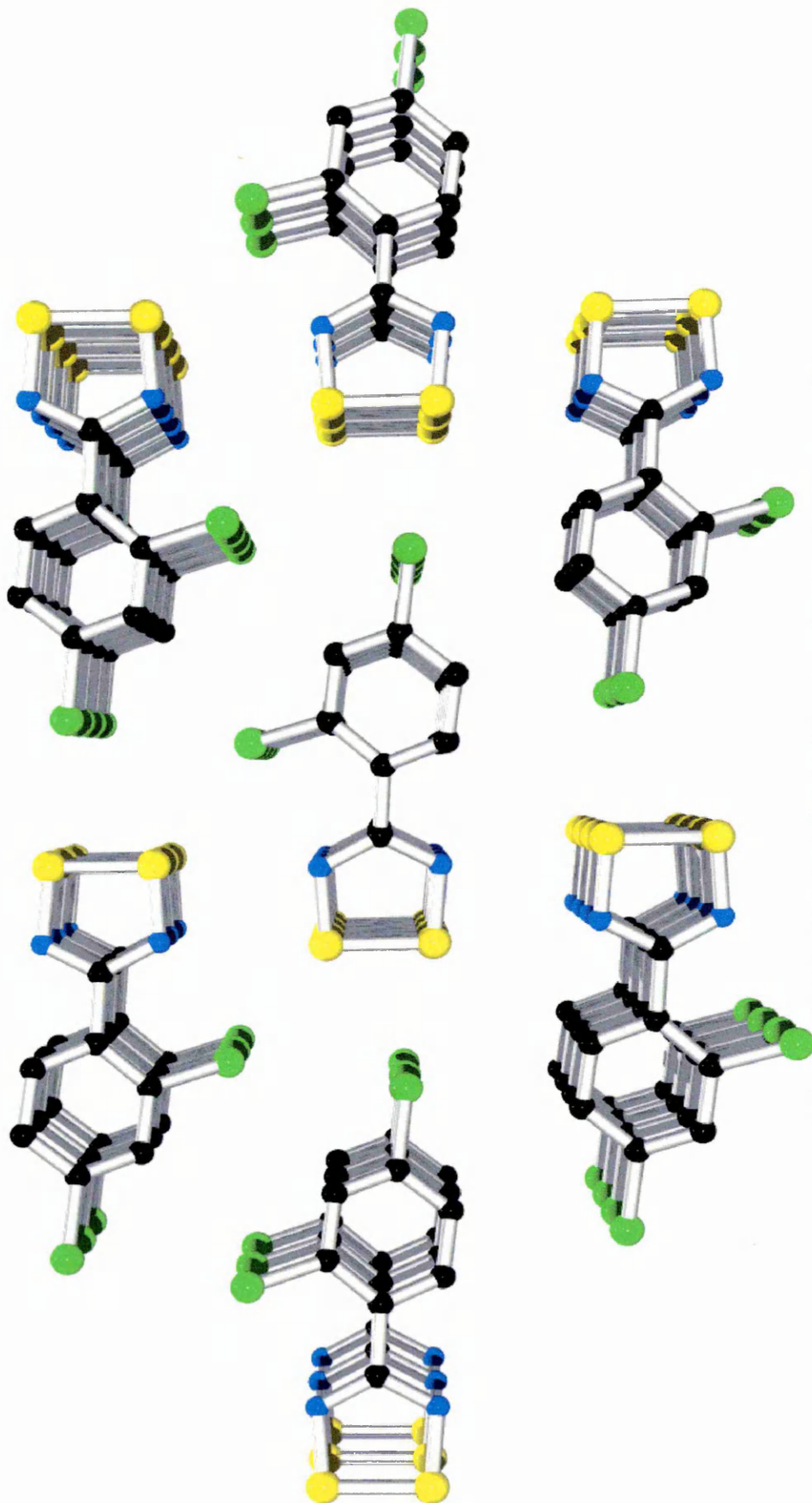


Figure 3.9 Ortep plot of the packing structure of 1

3.1.2 X-ray Crystal Structure of 2,5-dichlorophenyl-1,2,3,5-dithiadiazolyl

Crystals of 2,5-dichlorophenyl-1,2,3,5-dithiadiazolyl suitable for x-ray analysis were produced using a similar method to that described for **1** (Section 3.1.1). The gradient sublimation was completed with a temperature range 95 - 25 °C under a dynamic vacuum (10^{-3} torr). In most cases, only thin fibrous crystals were produced that were both twinned and extremely brittle. Successive sublimations in small bore tubes over several days eventually yielded small, dark red, needle like crystals.

The asymmetric unit of **2** contains one molecule and is monoclinic with space group $P2_1/c$. The packing is also in the form of stacks, in this case parallel to the a-axis. The intrastack S...S (S1a...S1b and S1b...S1c) distance (Figure 3.10) is 3.6685 Å. The length of the a-axis is equal to the intrastack S...S distance. This short axis is known in the literature as the β -structure,¹¹ and is common in many chloro aromatic derivatives. Each molecule lies in a coplanar manner above and below each other (Figure 3.10), which means that the interstack Cl...Cl distances (Cl2a...Cl2b and Cl2b...Cl2c) are also 3.6685 Å. As with **4** the intrastack S...S distances are considerably longer than typical values quoted for dimerised dithiadiazolyls (typically 3.0 – 3.2 Å)¹⁹ and are slightly larger than that of **1**.

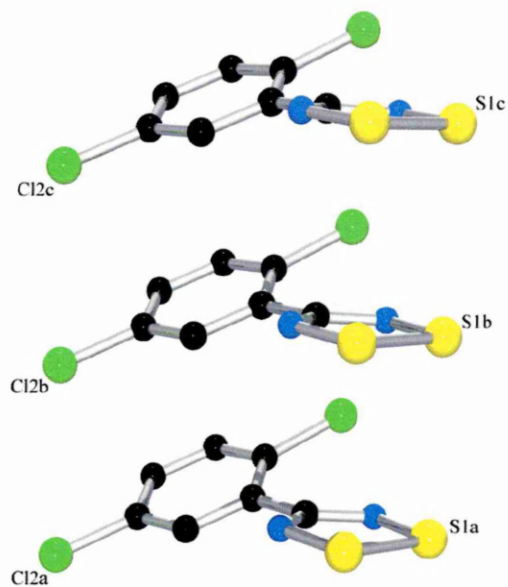


Figure 3.10 Ortep plot of the stacking of **2**, with selected atoms labelled.

The analogous fluorinated dithiadiazolyl (2,5-difluorophenyl-1,2,3,5-dithiadiazolyl)⁶ has also been shown to exhibit a stacking motif, although, in this case, as π -stacked dimers. The predominant interactions perpendicular to the stacks are S...S contacts, forming a ‘pinwheel’ arrangement wrapped around a 4_1 axis (Figure 3.11). There are also significant S...N and S...F interactions perpendicular to the *a* axis.

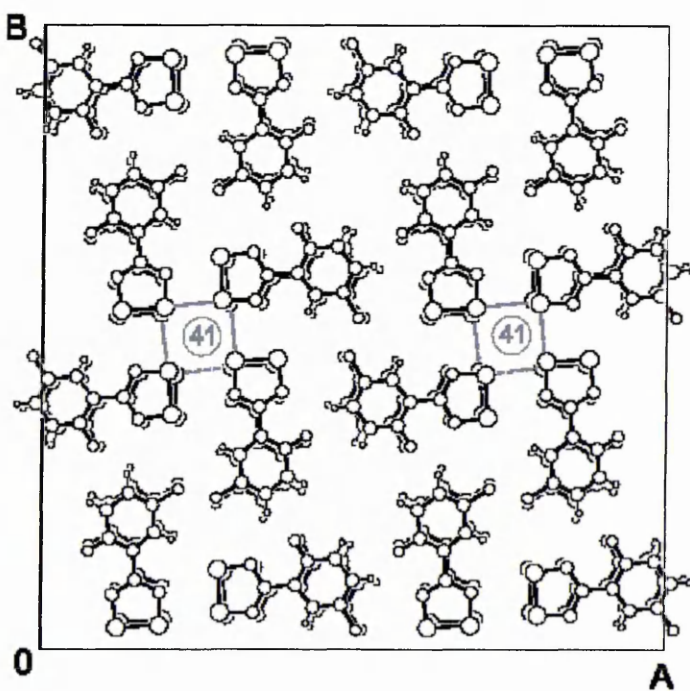


Figure 3.11 ‘Pin wheel’ packing of 2,5-difluorophenyl-1,2,3,5-dithiadiazolyl⁶

The structure of **2** within the *bc* plane consists of a complex array of S...N, S...Cl and Cl...Cl interactions. Chlorines in the *meta* position of the phenyl ring are associated to both of the sulfur atoms within an adjacent dithiadiazolyl ring. The interactions form a triangle of short (S1c...Cl2a, 3.432 Å) and long (S2c...Cl2a, 3.653 Å) electrostatic S...Cl contacts. This compares to the sum of the van der Waals radii for sulfur and chlorine of 3.65 Å. Furthermore, the same chlorine is also involved in a strong tail-to-tail type interaction with a *meta* substituted chlorine on an adjacent molecule (Cl2a...Cl2b, 3.321 Å). The chlorine atoms in the *ortho* position of the phenyl ring are weakly associated to one sulfur atom of an adjacent molecule (S1c...Cl1d, 3.656 Å). Finally, the dithiadiazolyls are linked together in a head-to-head fashion through weak S...N interactions (S2c...N2b, 3.336 Å and S2b...N2c, 3.337 Å). This compares to the sum of the van der Waals radii for sulfur and nitrogen of 3.4 Å. The pin wheel arrangement observed for 2,5-difluorophenyl-1,2,3,5-dithiadiazolyl is not present in the packing of **2** because of the absence of any S...S interactions.

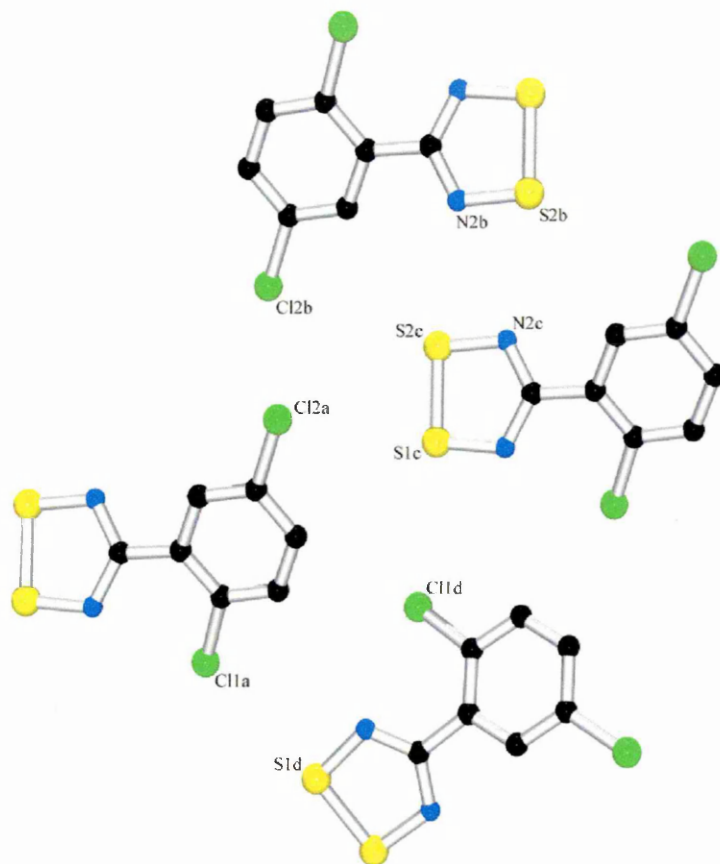


Figure 3.12 Ortep plot of the interactions within the plane of compound **2**.

The overall packing of the molecules reveals the presence of a chain structure steered by the presence of electrostatic $S \cdots Cl$ interactions. Adjacent chains run antiparallel with each other due to the presence of strong tail-to-tail $Cl \cdots Cl$ contacts. It is obvious that the $Cl \cdots Cl$ interactions again have a pivotal role in the packing of **2** in the production of a stack and in the packing within the bc plane. The diagram below (Figure 3.13) shows the crystal packing of **2** viewed down the a -axis. In the light of new literature⁶ describing the ability of this type of compound to form a superlattice, great effort was taken to search for this possibility. No superlattice structure could be refined from the data produced.

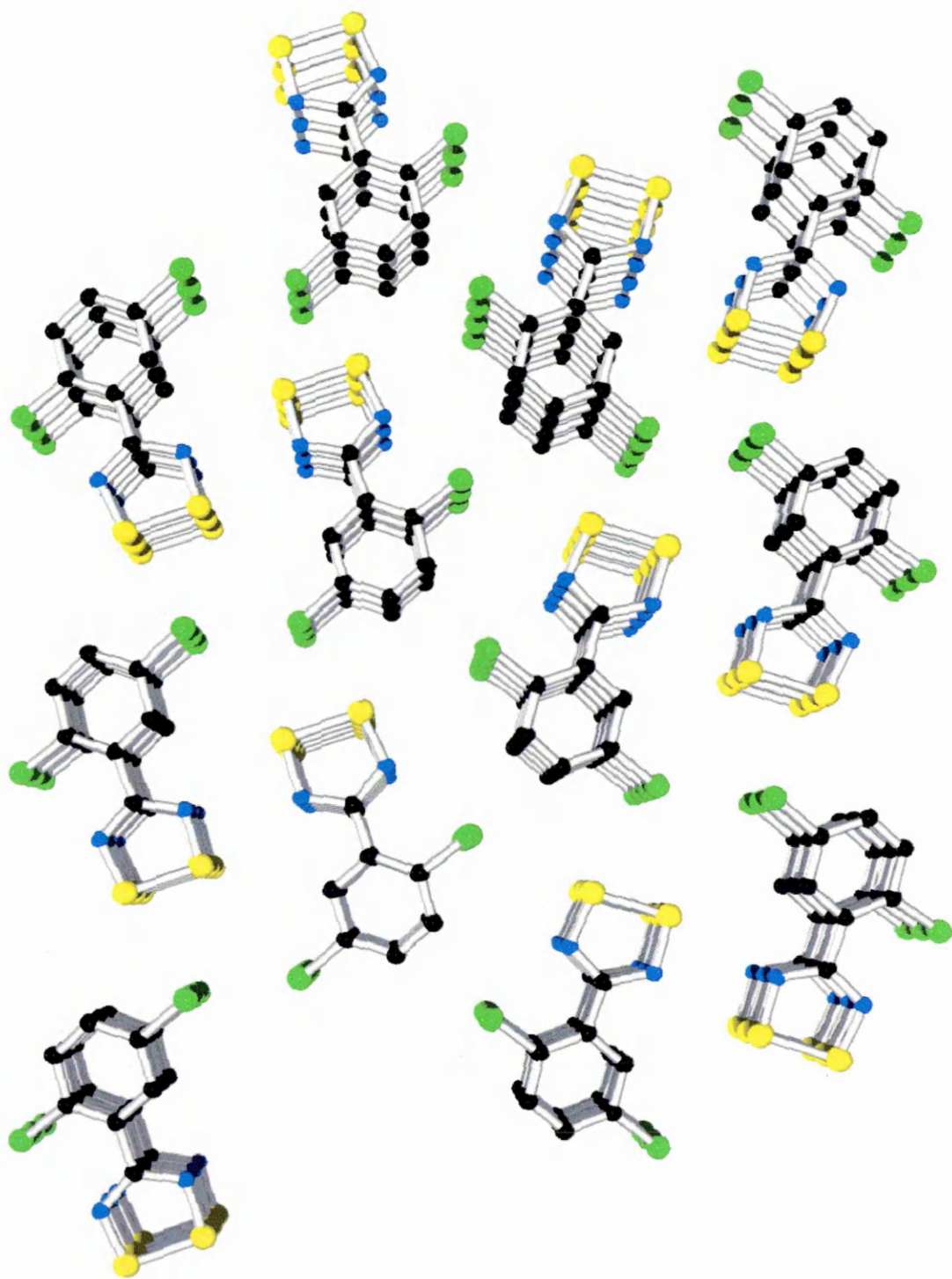


Figure 3.13 Ortep plot of the packing structure of 2

3.1.3 X-ray Crystal Structure of 3,5-dichlorophenyl-1,2,3,5-dithiadiazolyl

The temperature controlled sublimation of 3,5-dichlorophenyl-1,2,3,5-dithiadiazolyl **3**, yielded one of two polymorphs, not distinctive in appearance but possessing very different molecular packing. Gradient sublimation of the cold finger sublimed product at relatively high temperature (145 °C) compared with the melting point of the compound yielded the β -structure. If the isomer was sublimed at low temperature (95 °C) and therefore very slowly over several days the α -structure was formed. The only chemical difference observed between the two polymorphs was in the DSC thermogram (Figure 3.14). Although both forms have very similar melting points, their sublimation points are very different. A third curve has been included showing the thermogram of the product retrieved after sublimation at 120 °C. The sublimation points of the two polymorphs can be observed on the same curve.

The possibility that the polymorphs were actually a product of a superlattice was investigated by determining the structure of several different crystals, from different batches of material, and by the re-analysis of collected data. It was discovered that the two structures would not converge or refine to create any other structures. It was therefore concluded that the structures are correct and true polymorphs. It should also be noted that β -**3** cannot be a superlattice of α -**3** because of its higher order of symmetry in relation to the other polymorph (C2/c and P-1 for β -**3** and α -**3** respectively)

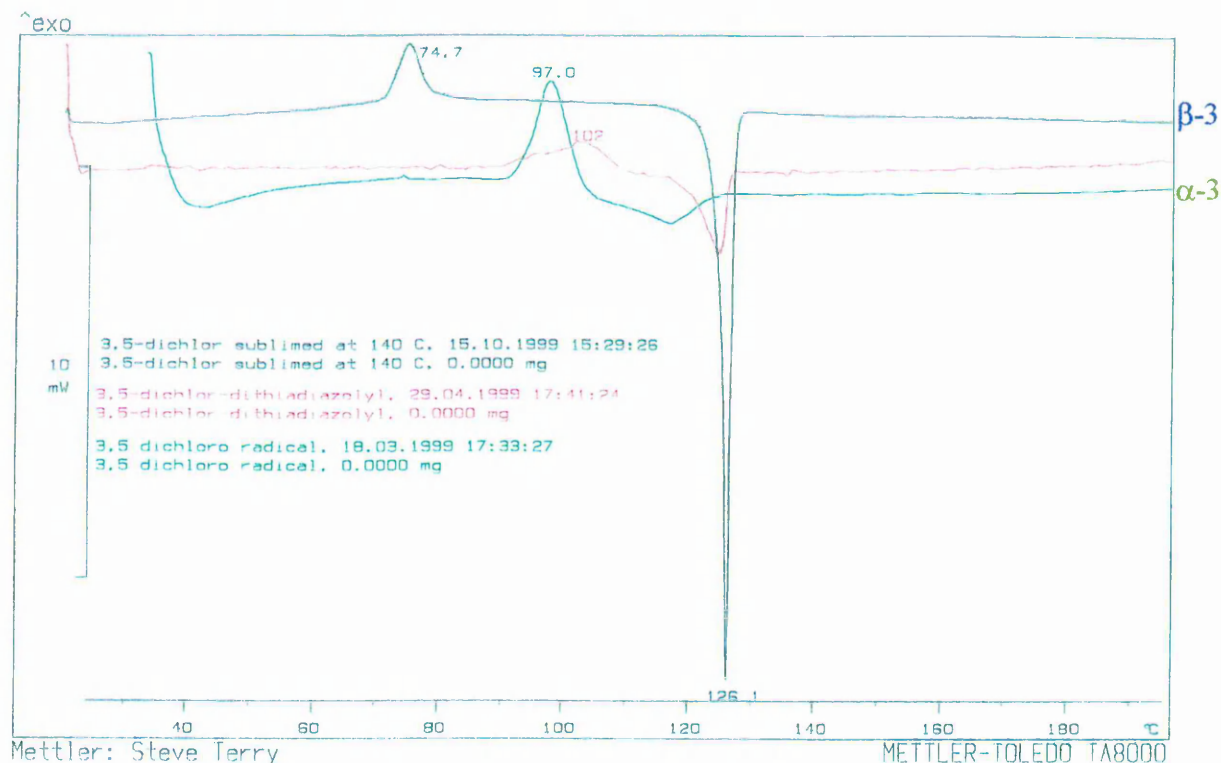


Figure 3.14 DSC plot of the α and β polymorph of **3**

3.1.3.1 Structure of β -**3**

The asymmetric unit of β -**3** consists of three molecules all in approximately the same *ac* plane and is monoclinic with *C2/c* space group. The unit cell is very large containing 24 individual molecules connected by an extensive and complex array of intermolecular interactions. The length of the other crystallographic *b*-axis is, as with the other two isomers discussed earlier (**1** and **2**), equal to the interstack distance (6.628 Å). The packing of the β -structure down the stack is again very similar to that of **1** and **2**. Each heterocycle lies in a co-planar manner with the molecules above and below it in the stack (Figure 3.15) and so the following distances Cl1a...Cl1b, Cl1b...Cl2c, S1a...S1b, S1b...S1c, S2a...S2b and S2b...S2c are all 3.628 Å.

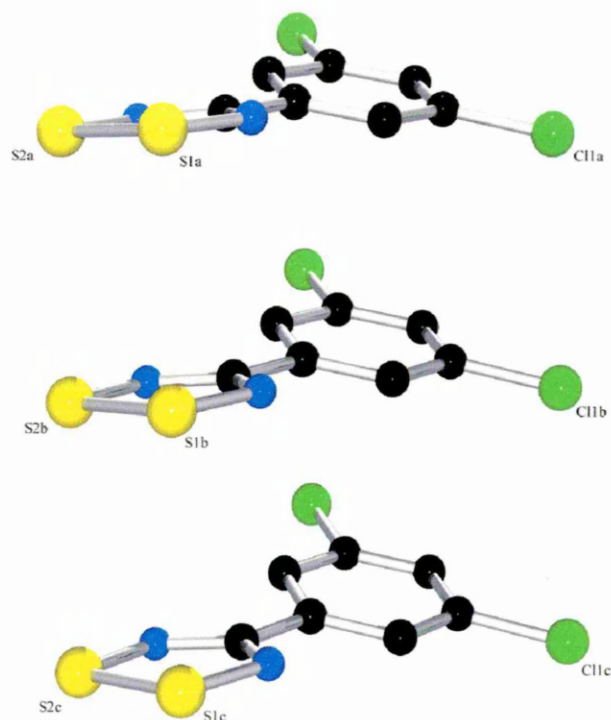


Figure 3.15 Ortep plot of the stacking of β -3

The interactions within the *ac* plane of this molecular structure are considerably more complex than those observed for **1** and **2**. At the centre of the unit cell, four stacks are related by a two-fold rotational symmetry, and associate in a ‘Catherine wheel’ motif (Figure 3.16). The stacks are linked in the centre by two sets of Cl \cdots Cl interactions (Cl1a \cdots Cl1d, Cl1b \cdots Cl1c, 3.538 Å; Cl1a \cdots Cl1b, Cl1c \cdots Cl1d, 3.453 Å). These short non-bonded Cl \cdots Cl interactions take the form of a spiral staircase arrangement linking different layers of the structure together. This phenomenon may add to the stability of the stacking structure. In addition, a series of interleaved S \cdots Cl interactions at the periphery of the pinwheel provides additional linkage between layers (S1d \cdots Cl2a, S1b \cdots Cl2c, 3.457 Å; S1a \cdots Cl2b, S1c \cdots Cl2d, 3.720 Å).

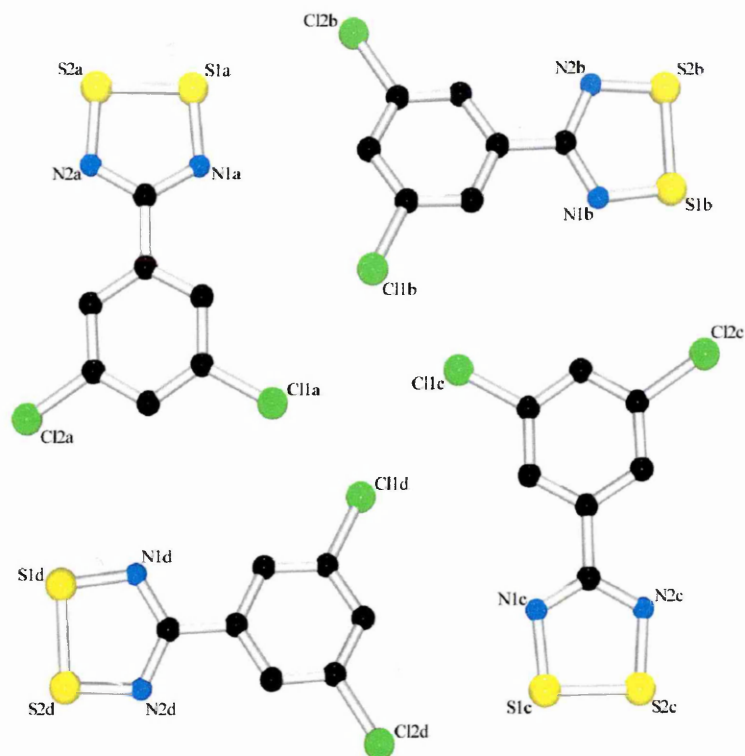


Figure 3.16 Ortep plot of the Cl...Cl interactions within the *ac* plane of β -3.

Two molecules on opposite corner of the chlorine centred pinwheel take part in a second pinwheel arrangement. This time the pinwheel is sulfur centred with interstack S...S interactions creating a spiral staircase arrangement that links different layers together (S2a...S2b and S2c...S2d, 3.696 Å; S2b...S2c and S2a...S2d, 3.471 Å). Across the centre of the pinwheel is another short S...S interaction (S2b...S2d, 3.570 Å) and further from the centre there is a set of S...N interactions holding the 'Catherine wheel' together (Figure 3.17) (S1b...N2a and S1d...N2c, 3.969 Å; S1c...N2b and S1a...N2d, 3.471 Å).

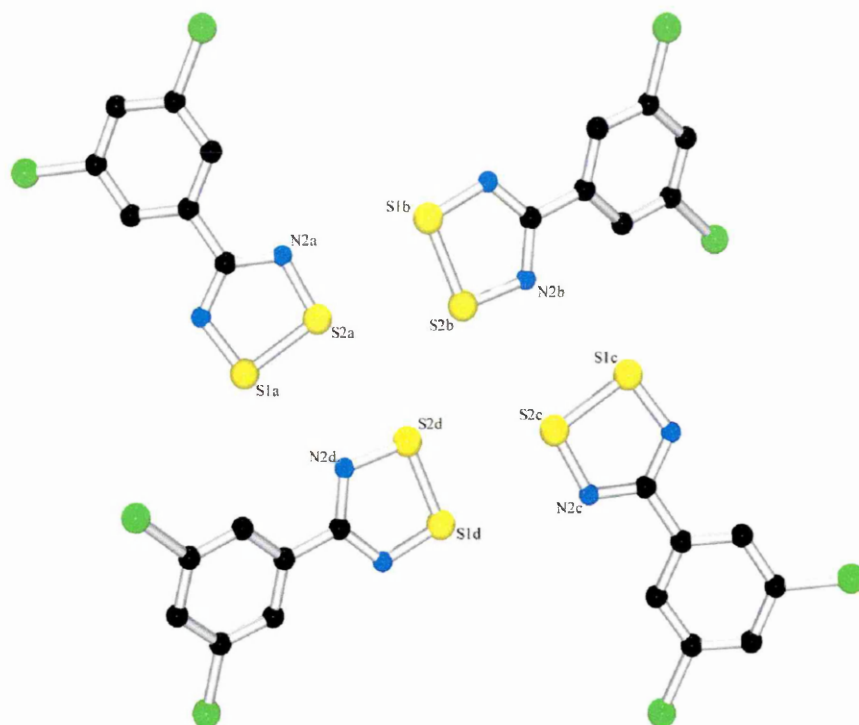


Figure 3.17 Ortep plot of S...S and S...N interactions within the *ac* plane of β -3.

At the other two corners of the chlorine centred ‘Catherine wheel’ (Figure 3.18, S2d and S2b) are some further interactions (Figure 3.18). The first is a familiar head to head type association with two S...N links (S2b...N2a and S2a...N2b, 3.114 Å). There is also evidence of an electrostatic S...Cl interaction (S2a...Cl2c, 3.360 Å; S1a...Cl2c, 3.552 Å) which forms a head to tail motif like that observed for **1**. Each edge of this ‘pinwheel’ is one of the chlorine-centred ‘pinwheels’ described above. Hence, the complicated network of interactions within this molecule.

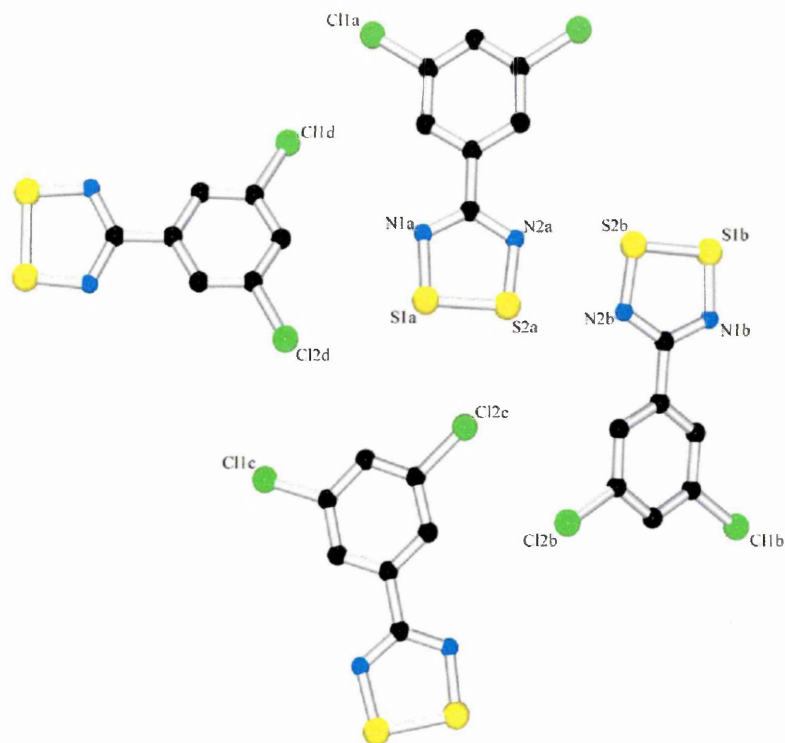


Figure 3.18 Ortep plot of the further interactions of β -3 within the *ac* plane

The interactions involved in the crystal structure of β -3 are very different to those observed for **1** and **2**. The previous structures exhibited a small number of intermolecular interactions holding the units together in an ordered manner. In this case, within one plane, the dithiadiazolyl units seem to lie in almost random directions and several different interactions hold the units together as a network. It is interesting to note that the reported crystal structure of 3,5-difluorophenyl-1,2,3,5-dithiadiazolyl⁴ also displays a stacked structure but one that has suffered from Peierls distortion producing alternating long and short interactions along the stack. The structure of 3,5-difluorophenyl-1,2,3,5-dithiadiazolyl⁴ is more analogous to the structure of α -3, which will be discussed in the next section. The pinwheel arrangement of β -3 shows initial similarities to that reported for 2,5-difluorophenyl-1,2,3,5-dithiadiazolyl⁶ (Figure 3.11) but possesses a lower order of symmetry (space group of monoclinic *C2/c* compared to tetragonal *I4₁/a*) and has not suffered Peierls distortion. Figure 3.19 shows the overall packing of β -3 in the solid state.

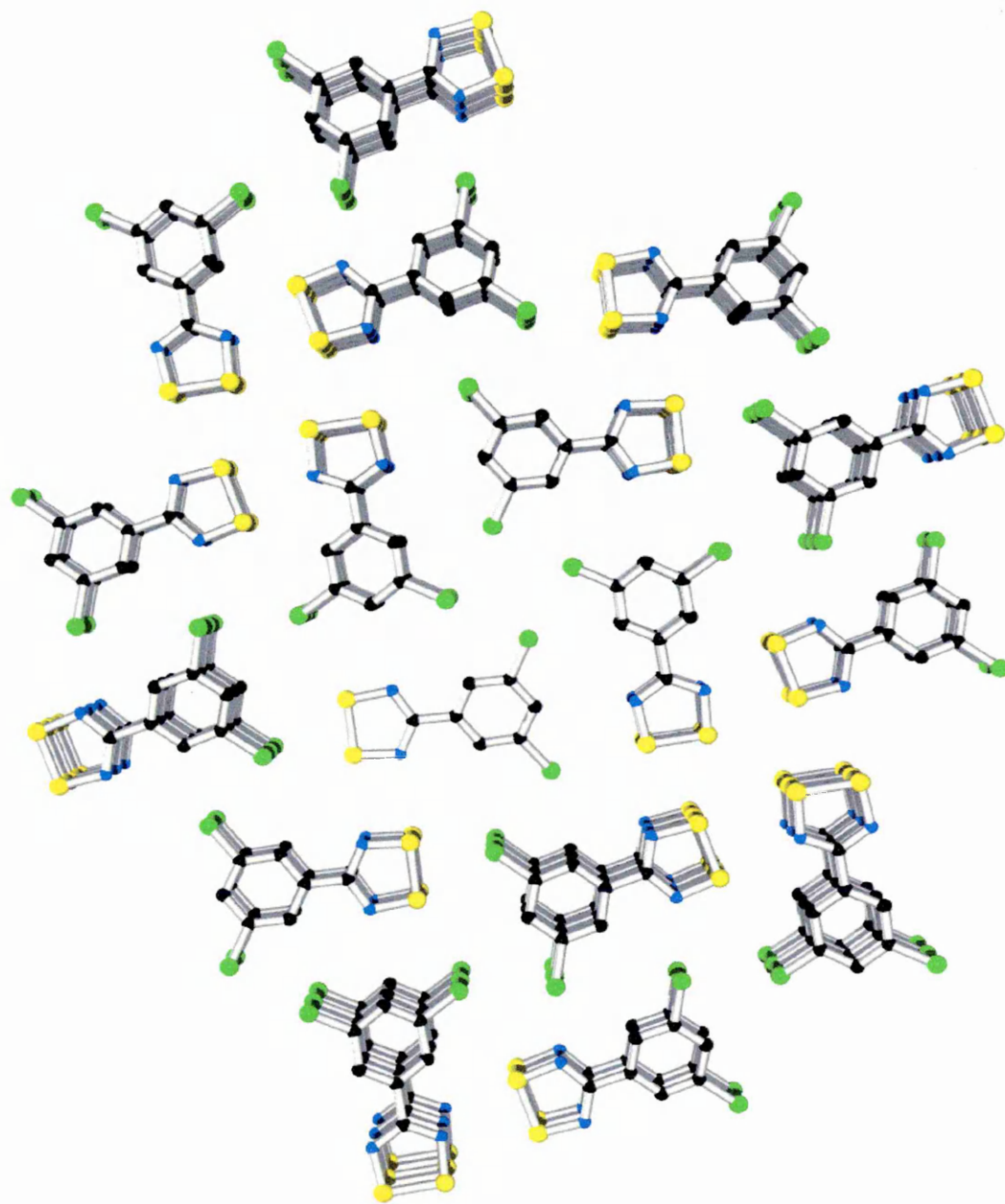


Figure 3.19 Ortep plot of the packing of beta-3

3.1.3.2 Structure of α -3

The asymmetric unit of α -3 consists of twelve molecules linked as π -stacked dimers by short (≈ 3.25 Å) and long (≈ 3.98 Å) S \cdots S interactions. Much like the asymmetric unit for β -3, the groups are also joined within the *bc* plane. The unit cell is triclinic with a space group P-1, which contains an inversion centre that generates a unit cell containing 24 individual molecules connected (like β -3) by an extensive and complex array of intermolecular interactions. In α -3, the length of the shortest crystallographic axis is 7.2484(8) Å, which is much larger than that described for other chloro-aromatic compounds that exhibit a β -type structure. This is seen in the crystal packing which shows stacking interactions, although the individual groups do not eclipse each other throughout the stack and so cannot be described in terms of a π -stack.

Figure 3.20 below shows the intrastack interactions of α -3. The molecular packing contains dimers linked by long S \cdots S contacts. However, adjacent dimers within the stack are not coplanar. The result is a structure that is similar to that of 1,3-phenylene-bis(1,2,3,5-dithiadiazolyl)⁸ which can be described in terms of a zigzag stack. Within the stack, the S \cdots S contacts vary by approximately 0.8 Å between short and long distances. In contrast, the related Cl \cdots Cl contacts only vary by less than 0.1 Å. This again shows that chlorine is having an effect on the packing of the molecules and that the Peierls distortion of the unpaired electrons seems almost localised at the dithiadiazolyl rings. Some selected bond distances to illustrate this point are as follows; S1a \cdots S1b and S1c \cdots S1d, 3.232 Å; S2a \cdots S2b and S2c \cdots S2d, 3.310 Å; S1b \cdots S1c, 4.019 Å; S2b \cdots S2c, 3.941 Å;

Cl1a...Cl1b and Cl1c...Cl1d, 3.615 Å; Cl2a...Cl2b and Cl2c...Cl2d, 3.630 Å;
 Cl1b...Cl1c, 3.637 Å; Cl2b...Cl2c, 3.619 Å.

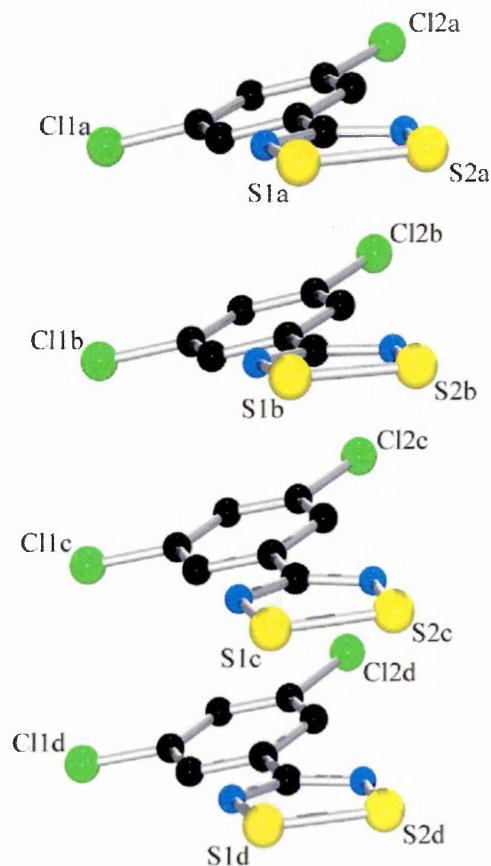


Figure 3.20 Orteplot of the stacking of α -3

The structure of α -3 within the bc plane is similar to that of β -3. Although having a different space group (P-1 compared to C2/c for α -3 and β -3 respectively) the overall crystal packing within the plane is very similar. At the centre of the unit cell is a ‘Catherine wheel’ type association (Figure 3.21). The chlorines are linked in the centre by four principal short Cl...Cl contacts, two of which are 3.439 Å in length, and the others 3.412 Å. These values are slightly shorter than those observed for β -3 (3.538 Å and 3.453 Å). In a similar way to β -3, the Cl...Cl contacts join different layers of the stack through short interstack interactions, which again may in turn help to stabilise the stack.

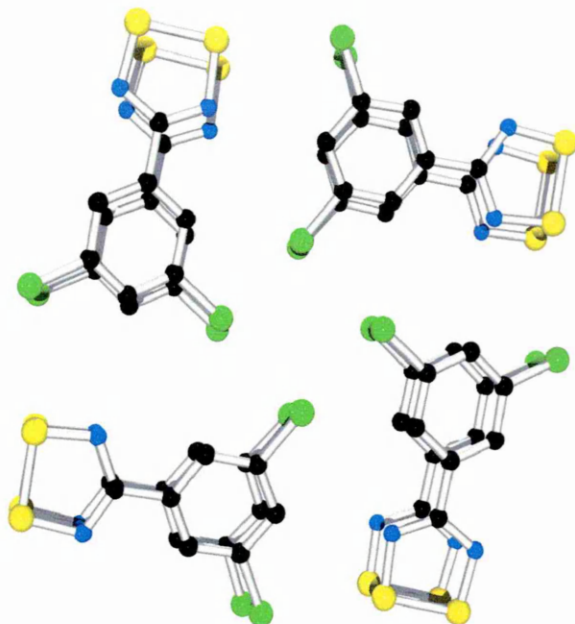


Figure 3.21 Ortep plot of the Cl...Cl 'Catherine wheel' type interactions in α -3

Two corners of the chlorine centred 'Catherine wheel' connect in a further head-to-head (*i.e.* S...S) interaction creating a second 'Catherine wheel' arrangement (Figure 3.22). At the centre of this 'Catherine wheel', there are two principal short S...S contacts (two at 3.383 Å and two at 3.376 Å) and one short contact across the centre of the wheel (3.516 Å). This set of contacts are (like the chlorine interactions) smaller than those observed for β -3 (3.696 Å and 3.471 Å) and shorter than the S...S interaction across the centre (3.570 Å). This set of interactions also exhibit a 'spiral staircase' arrangement linking different layers of the structure together.

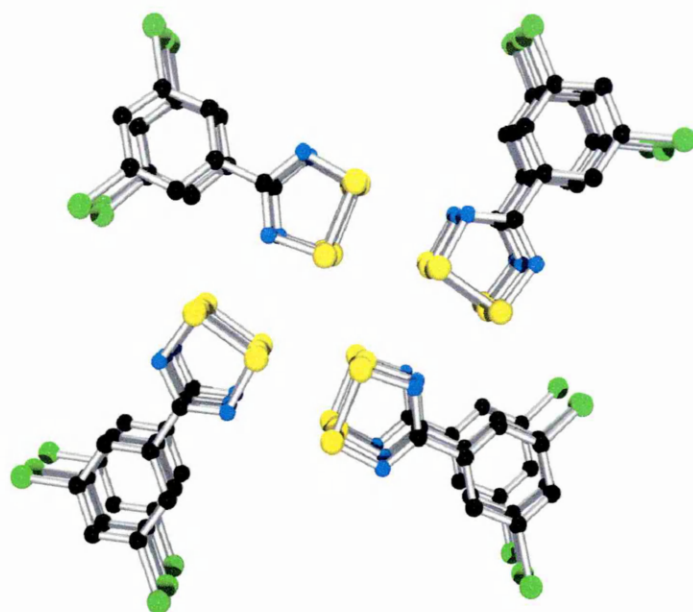


Figure 3.22 Ortep plot of the S...S 'Catherine wheel' type interactions in α -3

At the other two corners of the chlorine centred 'Catherine wheel' are some further interactions (Figure 3.23). The first is a familiar head-to-head type association with two S...N links (shortest contacts 3.126 and 3.128 Å). There is also evidence of an electrostatic S...Cl interaction (S2a...Cl2c, 3.360 Å; S1a...Cl2c, 3.552 Å) which forms a head-to-tail motif similar to that observed for **1**.

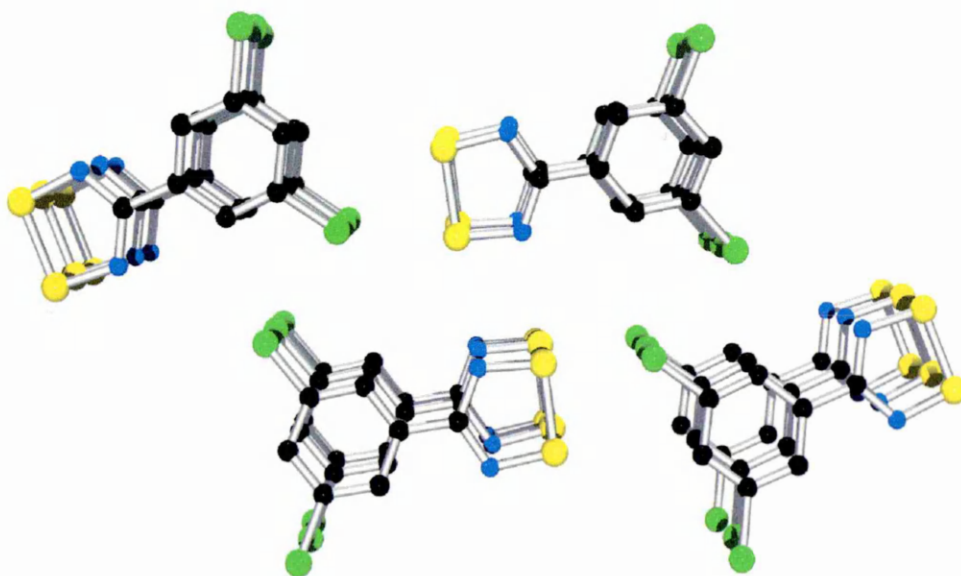


Figure 3.23 Ortep plot of other interactions within α -3

Figure 3.24 shows an Ortep plot of the overall packing in α -3. The crystal packing bears a striking similarity to the reported structure of 2,5-difluorophenyl-1,2,3,5-dithiadiazolyl⁴ which also exhibits a Peierls distortion to form stacks of dimerised radical units (interdimer and intradimer S...S distances are 4.04 Å and 3.16 Å respectively). When compared to β -3 it is noted that the structure within the *ac* plane is very similar. The overall packing only differs because of the short and long S...S contacts in α -3. It would seem reasonable to assume that the two polymorphs are very close in energy to each other, which is also supported by the small differences in sublimation temperature required to change the crystal structure. As described at the beginning of this section the only appreciable physical difference between β -3 and α -3 is the sublimation temperature. The physical data supplied in the remainder of this chapter concerns the β polymorph, as this is of most interest due to its infinite equidistant stacking structure.

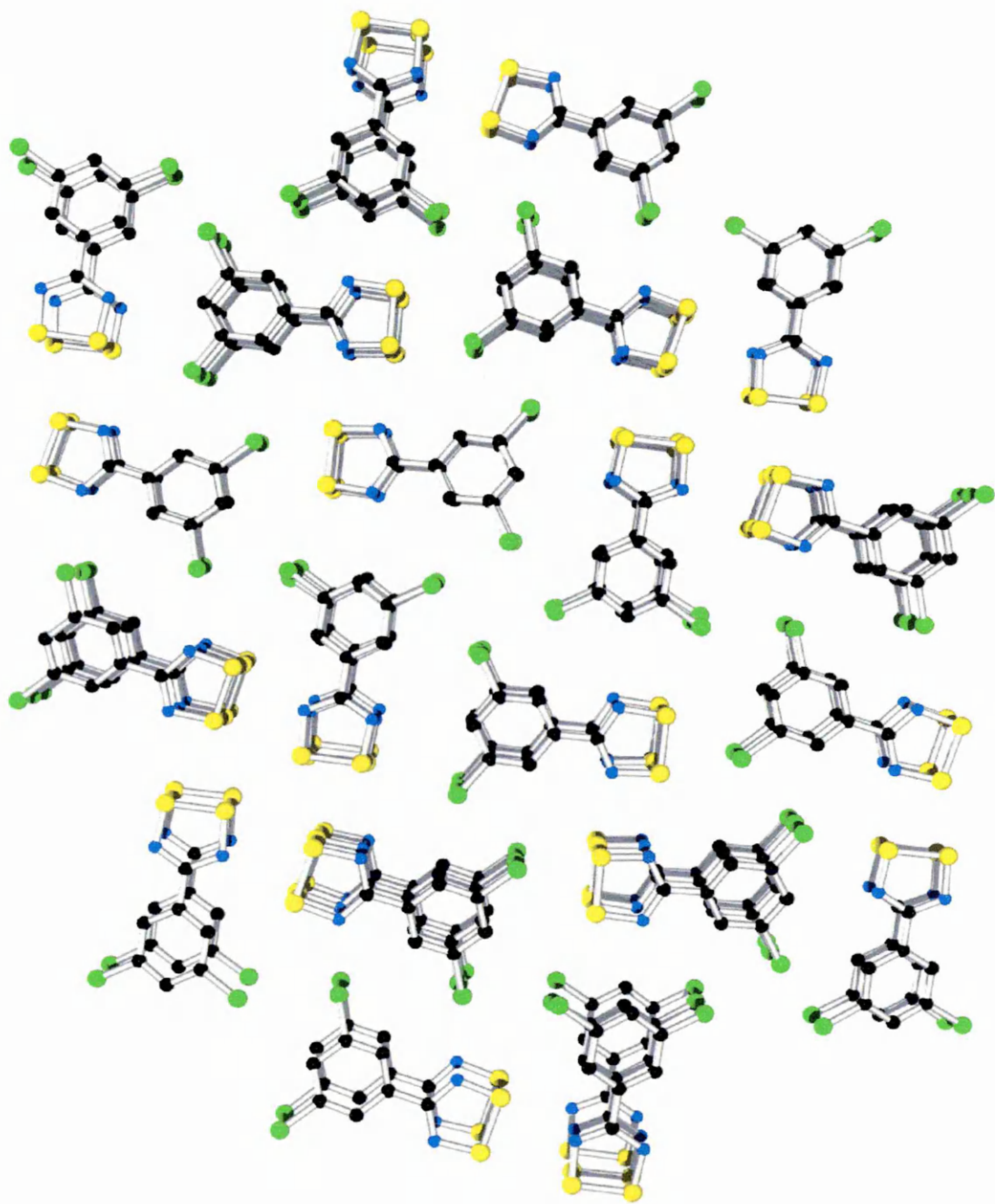


Figure 3.24 Ortep plot of the packing of alpha-3

3.2 Magnetic Measurements

Two types of magnetisation measurements have been made:

- 1) Temperature dependent magnetisation at constant applied field of 10 kOe in the temperature range from 1.8 to 300 K.
- 2) Isothermal magnetisation, from 0 to 50 kOe, at constant temperatures 1.8 and 3 K.

Experimental and numerical data for these experiments are listed appendix 5.

At present two of the samples have been investigated, 2,4-dichlorophenyl-1,2,3,5-dithiadiazolyl (1) and 3,5-dichlorophenyl-1,2,3,5-dithiadiazolyl (3).

The magnetisation of both samples is very weak as shown in the experimental points of Figures 3.25 and 3.26. Between room temperature and about 10K the magnetisation is negative although slowly increasing. Below about 10K it becomes positive and increases more rapidly. A small shoulder observed at about 45K indicates the presence of a very small amount of oxygen in the sample holder. These results are indicative of the presence of a few paramagnetic centres in a mainly diamagnetic sample.

3.2.1 The Diamagnetic Contribution

The diamagnetic contribution from the sample to the magnetisation can be estimated in various ways:

Evaluating the diamagnetic contributions from the capsule and cotton wool,²¹ and estimating that of the sample using Pascal's tables. We then have the gelatine capsule at $-3.92(2) \times 10^{-7}$ emu/Oe.g and the cotton at $-4.56(2) \times 10^{-7}$ emu/O e.g. From Pascal's tables

for both compounds: -122.57×10^{-6} emu/Oe mol (the molecular weight of both samples is 250 g/mol). The results are shown in Table 3.3:

Table 3.3 Evaluation of the diamagnetic contribution

	Compound 3	Compound 1
capsule mass (g)	0.03852	0.03830
cotton mass (g)	0.00994	0.01221
sample mass (g)	0.06928	0.04795
(mole number)	$(2.771 \times 10^{-4}$ mol)	$(1.918 \times 10^{-4}$ mol)
diamagnetism (emu/Oe.mol)	-2.002×10^{-4}	-2.386×10^{-4}

The diamagnetic contribution to the magnetisation can also be calculated from a Curie-Weiss fit of the magnetisation at 10.000 Oe between 1.8 and 300 K. This is shown in Figures 3.25 and 3.26 for compound 3 and 1 respectively. The small rise at high temperature was not taken into account, which will be discussed later in this section. Therefore the estimate for the diamagnetic part of the magnetisation (in emu/Oe mol) is:

(3): -1.723×10^{-4}

(1): -2.062×10^{-4}

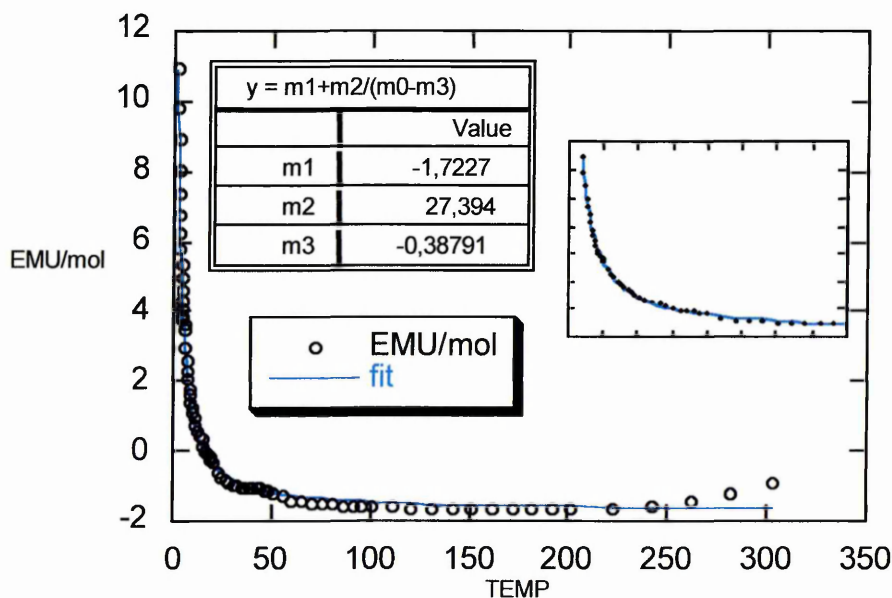


Figure 3.25 M(T) at 10,000 Oe (no Correction) Curie-Weiss fit for 3

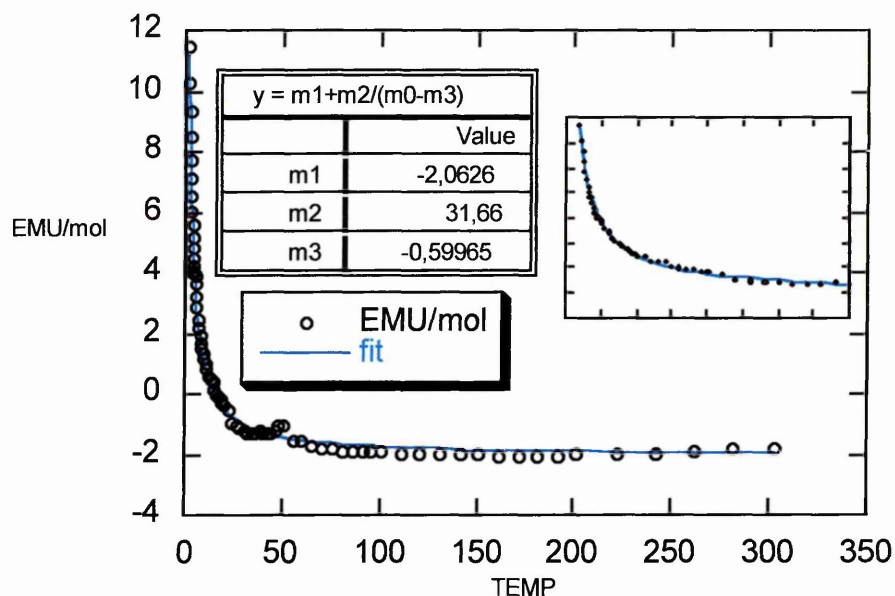


Figure 3.26 M(T) at 10,000 Oe (no correction) Curie-Weiss fit for 1

A final method of assessing the diamagnetic contribution involves the analysis of the magnetisation curves at low temperature. In a purely paramagnetic sample magnetisation is a function of the ratio between the magnetic field and the temperature (H/T), whereas in a diamagnetic sample it is proportional to the magnetic field. The diamagnetic part was then adjusted so that the magnetisation curves from 0 to 50 kOe, 1.8 or 3.0 K, collapses into the same curve when plotted as a function of H/T (see Figures 3.27 and 3.28). In this case the values obtained were:

(3): -1.1×10^{-4} emu/Oe mol

(1): -1.3×10^{-4} emu/Oe mol

The discrepancy using this last method is not unusual since only the low temperature data is used.

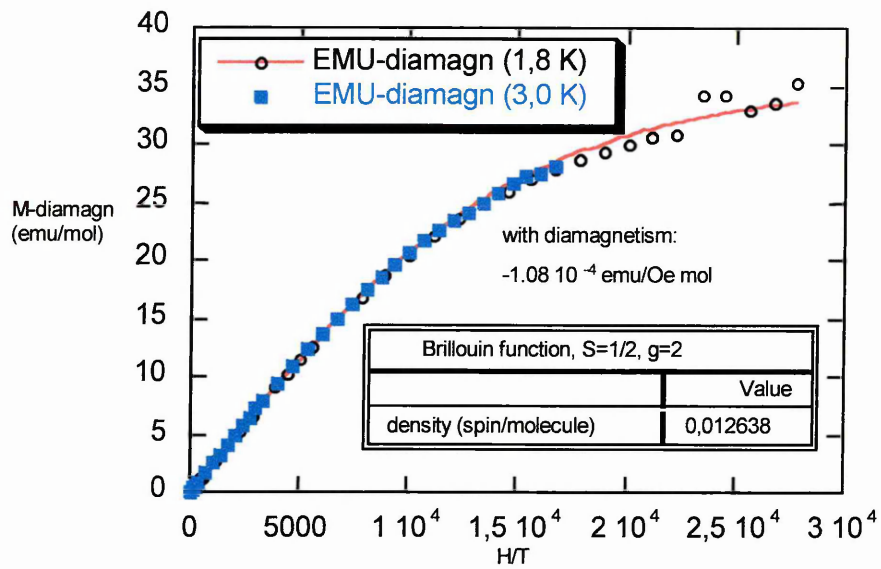


Figure 3.27 M(H/T) (low temperature) diamagnetism removed Brillouin fit for 3

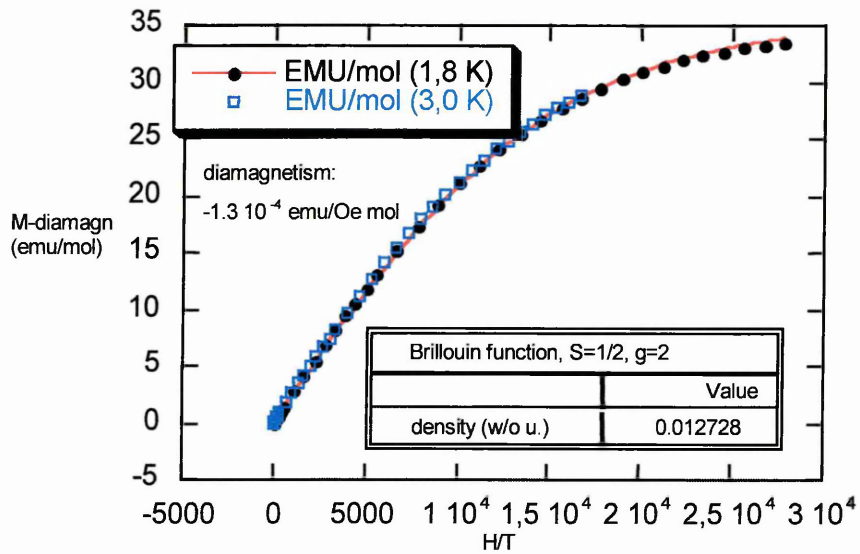


Figure 3.28 M(H/T) (low temperature) diamagnetism removed Brillouin fit for 1

3.2.2 Features at Low Temperature

After removing the diamagnetic contribution, the magnetisation at low temperature is mainly due to paramagnetic impurities. The isotherm curves measured at 1.8 and 3.0 K can be fitted to a Brillouin function. This was done assuming a spin $S = 1/2$ and a Landé Factor $g = 2$ (Figures 3.27 and 3.28), which allowed the following spin densities to be calculated (spin/molecule):

$$(3): n_S = 0.0126$$

$$(1): n_S = 0.0127$$

The magnetisation at a lower field (10.000 Oe), at which the saturation of the spins was not reached, can be adjusted with the Curie-Weiss law:

$$\chi(T) = \chi_{\text{dia}} + C/(T-\theta) \quad \text{Equation 3.1}$$

Assuming that only one type of paramagnetic impurity exists and that there is no magnetic interaction, we would obtain:

$$\theta = 0, \text{ and}$$

$$C = N_A n_S g^2 \mu_B^2 S(S + 1)/(3k_B) \quad (C \text{ in emu K/Oe mol}) \quad \text{Equation 3.2}$$

The fits have been calculated (Figures 3.27 and 3.28), and the results are listed in Table 3.4

Table 3.4 Magnetisation at low temperature

	Compound 3	Compound 1
C from fit	4.77×10^{-3}	4.74×10^{-3}
C from equation 3.2	3.17×10^{-3}	2.74×10^{-3}

The agreement is quite acceptable considering that we have assumed that paramagnetism in the sample was only due to n_S , which has been determined at the lowest temperatures.

One can also notice the characteristic signal caused by the phase transition of oxygen at 50 K, which exists despite the precautions taken in order to minimise the risks of contamination. Nevertheless, this signal is weak, and can be considered as normal.

3.2.3 Features at high temperature

At high temperature ($T > 200$ K), there is an increase in the magnetisation, which is unusual in diamagnetic materials (as well as in paramagnetic or ferromagnetic materials). This increase is particularly noticeable in compound **3** (see Figure 3.25), but once subtracted from the diamagnetic contribution, and represented as χT vs T , it appears clearly in both samples (Figures 3.29 and 3.30).

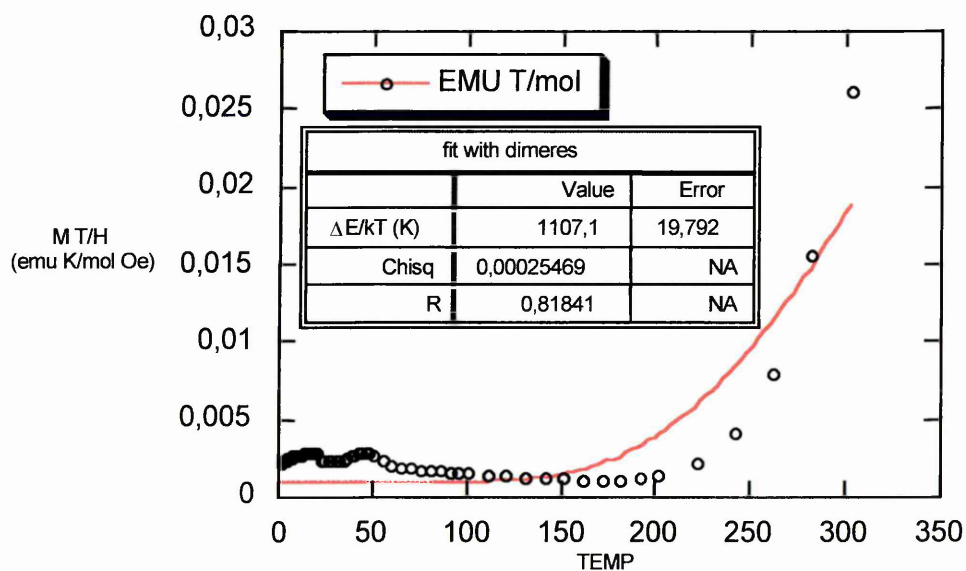


Figure 3.29 χT (T) (diamagnetism removed) “dimer” fit for **3**

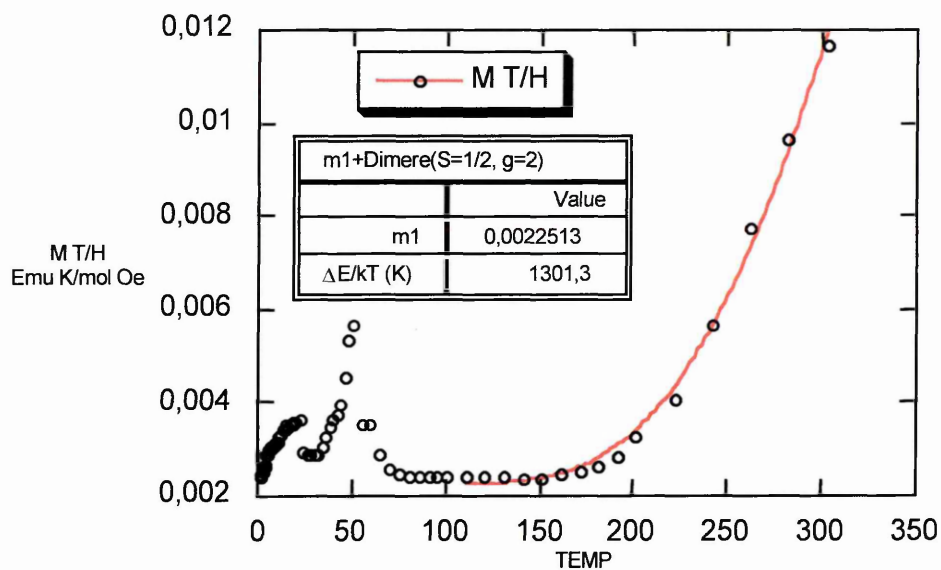


Figure 3.30 χT (T) (diamagnetism removed) “dimer” fit for 1

This is the main peculiarity of these samples and can be explained by the dimerisation of these materials (Figure 3.31).

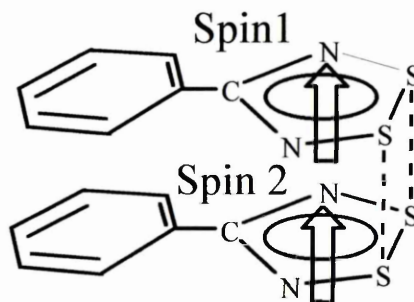


Figure 3.31 An image of a dimer, showing that the spins borne by the two molecules will couple.

The magnetisation measurements show that the ground state resulting from the coupling of the two $1/2$ spins is diamagnetic ($S = 0$), but the excited state ($S = 1$) may appear on heating the sample. We will then consider the following (Figure 3.32):

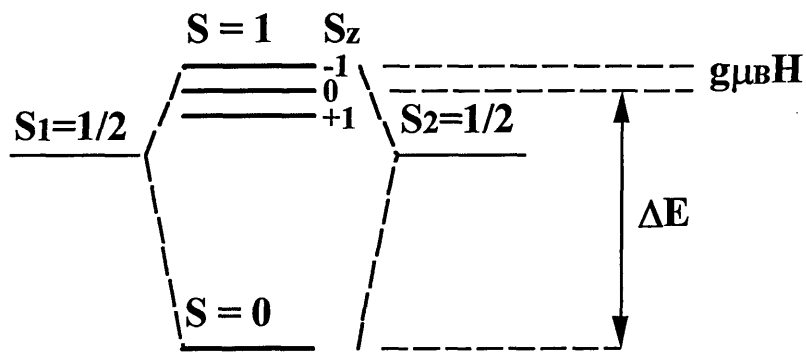


Figure 3.32 The energy level diagram for two interacting $S = 1/2$ spins.

The susceptibility for a pair of interacting $S = 1/2$ ions, as illustrated in Equation 3.3, can be described as:

$$\chi = \frac{2N_A g^2 \mu_B^2}{kT} \cdot \frac{\exp(J/kT)}{1 + 3\exp(J/kT)} \quad \text{Equation 3.3}$$

Taking $g = 2$, we can fit the curves with this formula (Figures 3.29 and 3.30). The only variable parameter is J . For $\beta\text{-3}$, $J/kT = 1107$ K, but the fit is not very good. For 1 , $J/kT = 1302$ K, and fits the experimental data very nicely.

This is an indication that the explanation may be the correct one, but it should be remembered that only very small signals were analysed and very few experimental points were taken, so the uncertainty is quite significant.

3.2.4 Conclusion

These materials mainly show diamagnetic behaviour. At low temperature, a contribution from paramagnetic impurities is observed; this can be estimated at a concentration of about 1 spin per 100 molecules. Finally, a rise of the magnetisation is visible at $T > 200$ K, particularly for β -3. This increase may be assigned to the thermal excitation of the magnetic state of dimers. The explanation is in a good agreement with the experimental data, particularly for **1**, and gives an energy splitting corresponding to 1100 to 1300 K between the $S = 0$ and $S = 1$ states.

3.3 Electron Paramagnetic Resonance

Each of the compounds listed at the start of the chapter (**1**, **2** and **3**) have been studied by electron paramagnetic resonance (EPR) spectroscopy. The properties of the monomeric radicals were investigated by analysis of a frozen glass sample in dimethyl formamide. Preliminary studies of the solid state properties were carried out on powder samples. A single crystal study of compound **3** has also been undertaken.

3.3.1 Frozen Glass Studies

All sample preparation was carried out in a dry nitrogen glove box and sealed prior to analysis. Solution samples were prepared by the dissolution of a few milligrams of **1**, **2** or **3** in approximately 0.5 ml of DMF. The resulting solution was treated with a drop of toluene to aid the formation of a satisfactory 'glass' when analysed. The solution was added to a quartz tube, which was sealed prior to analysis.

As expected for the solution, the spectra observed and values obtained, were very similar to previous studies on dithiadiazolyls. This is because by definition, EPR spectrometry only observes unpaired electrons and these are almost unaffected by the substituent attached to the dithiadiazolyl radical. The aim of the frozen glass study was to gain accurate information about the unpaired electron when the interactions between adjacent radical centres are at a minimum. This in turn leads to spectra exhibiting the properties of the monomer. Table 3.5 shows the calculated g-factors and where applicable the values for hyperfine splitting for **1**, **2**, **3** (K-band) and Ph. $\overline{\text{CNSSN}}$.²²

Table 3.5 Frozen glass study of **1**, **2**, **3** and the Ph. $\overline{\text{CNSSN}}$.

	1	2	3	Ph. $\overline{\text{CNSSN}}$
Temperature	111 K	105 K	111 K	176 K
g_x	2.0019	2.0018	2.0021	2.0021
g_y	2.0085	2.0018	2.0085	2.0078
g_z	2.0215	2.0213	2.0217	2.0218
a_y/G	13.9	13.9	13.6	-

The y-component of the spectra themselves have a peak ratio pattern of 1:2:3:2:1 (from two equivalent nitrogen-14 nuclei), which is typical for 1,2,3,5-dithiadiazolyl radicals. The calculated g-values are also typical for a radical species with some spin orbital coupling. There is no further splitting observed due to the chlorine substituents. This is theoretically possible and has been observed for fluorine derivatives,²³ but the lone electron in chlorine is spread across a larger area (due to the larger atomic radius), this in turn reduces any possible coupling effects. Figures 3.33 - 3.35 show the frozen glass spectra for **1**, **2** and **3** respectively.

Receiver	Signal Channel	Field	9333-4	Microwave
Receiver Gain : 2.50e+03	Conversion : 40.96 ms	Center Field : 8610.00 G		Frequency : 24.15724 GHz
Phase : 0.0 deg	Time Const : 1.28 ms	Sweep Width : 220.00 G		Power : 3.44e+00 mW
Harmonic : 1	Sweep Time : 41.943 s	Resolution : 1024 points		
Mod Frequency : 100.0000 kHz	Scale : 19			
Mod Amplitude : 1.995 G			2178	

Comment: S620, 2,4 dichloro dmf/tol K band, 111K, Freq=24.15724

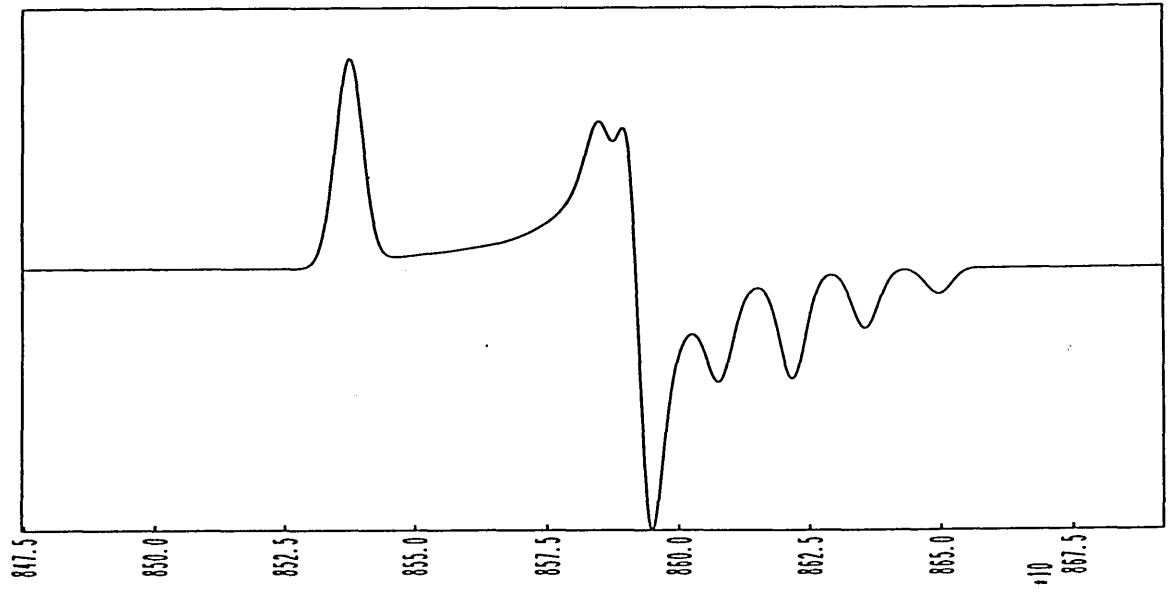
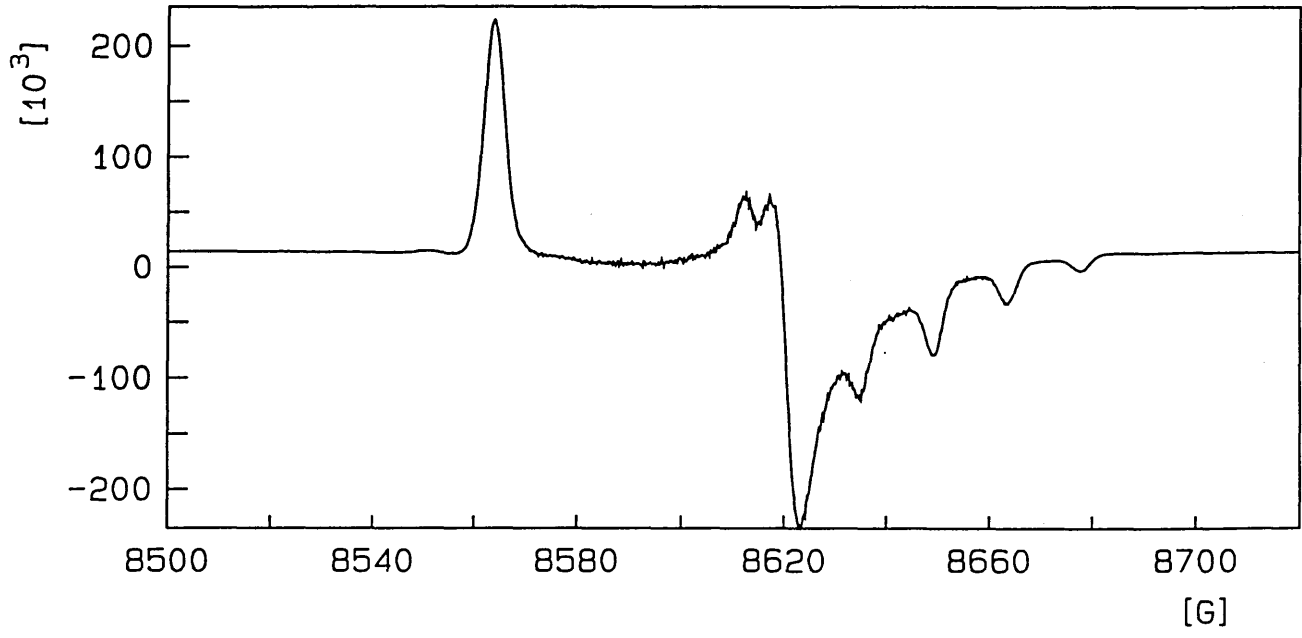


Figure 3.33 K-band EPR frozen glass spectrum of 1, Sample curve (top) and simulation (bottom)

Receiver	Signal Channel	Field	Microwave
Receiver Gain : 8.00e+03	Conversion : 163.84 ms	Center Field : 8510.00 G	Frequency : 23.8643000 GHz
Phase : 0.0 deg	Time Const : 1.28 ms	Sweep Width : 200.00 G	Power : 3.62e+00 mW
Harmonic : 1	Sweep Time : 167.772 s	Resolution : 1024 points	
Mod Frequency : 100.0000 kHz	Scale : 17		
Mod Amplitude : 1.000 G			

Comment: s685 2,5 dichloro/toluene 110K 23.8650GHz

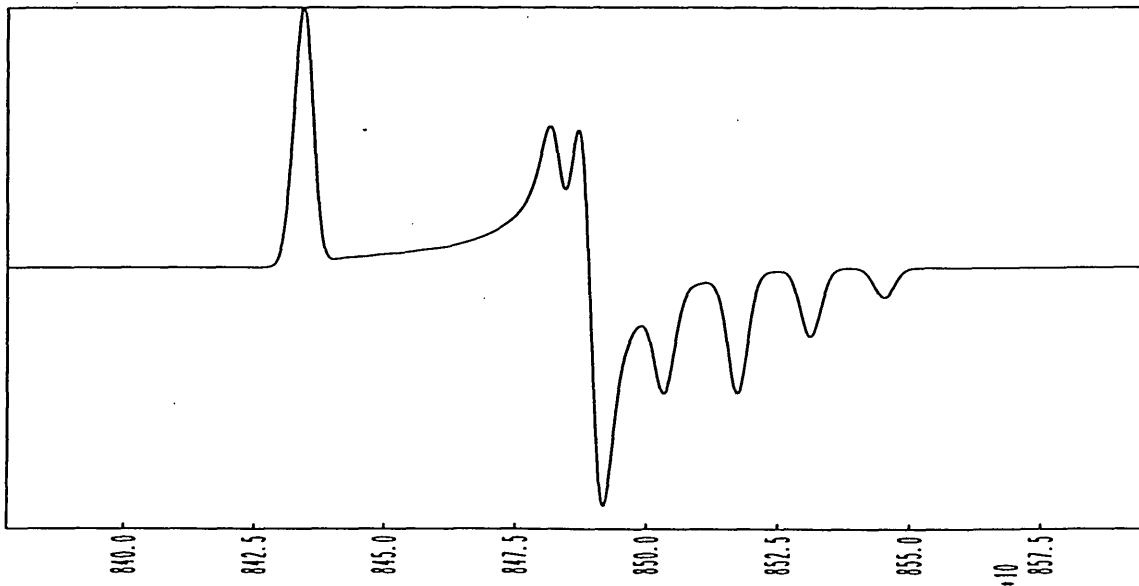
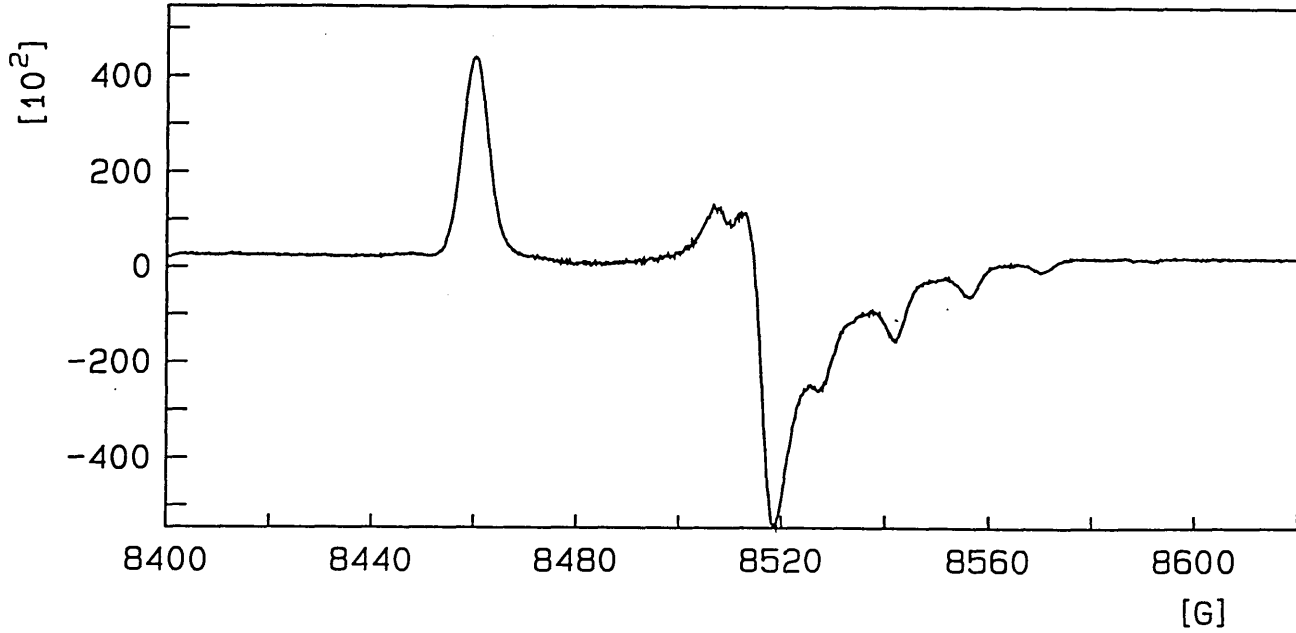


Figure 3.34 K-band EPR frozen glass spectrum of 2, Sample curve (top) and simulation

Receiver	Signal Channel	Field		Microwave
Receiver Gain : 5.00e+03	Conversion : 40.96 ms	Center Field : 8583.4		Frequency : 24.14957 GHz
Phase : 0.0 deg	Time Const : 1.28 ms	Sweep Width : 220.00 G		Power : 3.44e+00 mW
Harmonic : 1	Sweep Time : 41.943 s	Resolution : 1024 points		
Mod Frequency : 100.0000 kHz	Scale : 19			
Mod Amplitude : 1.995 G				

Comment: S618, 3,5 dichloro dmf/tol K band, 111K, Freq=24.14957

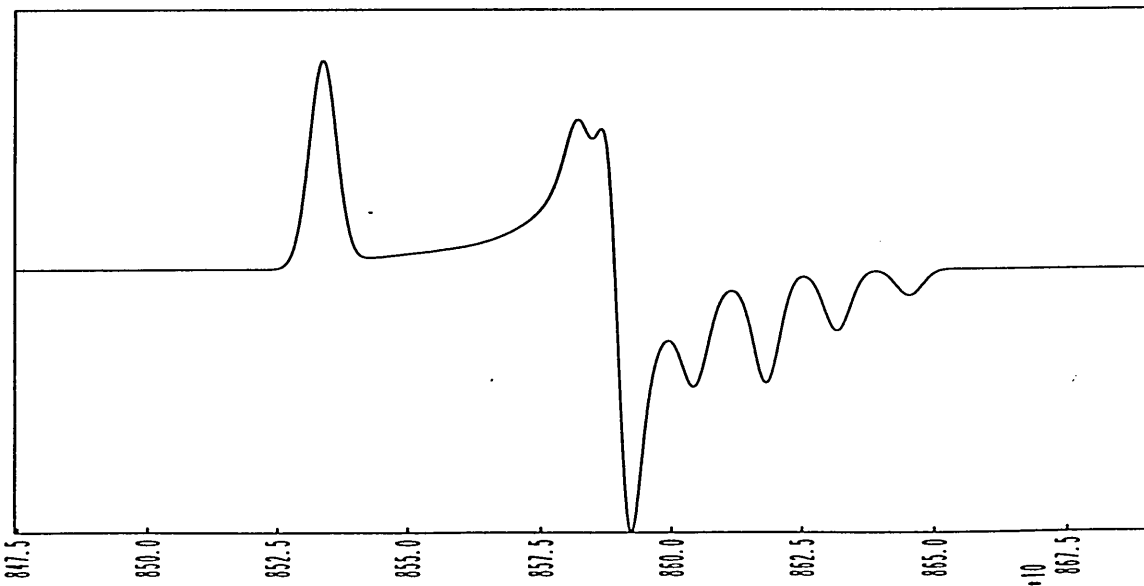
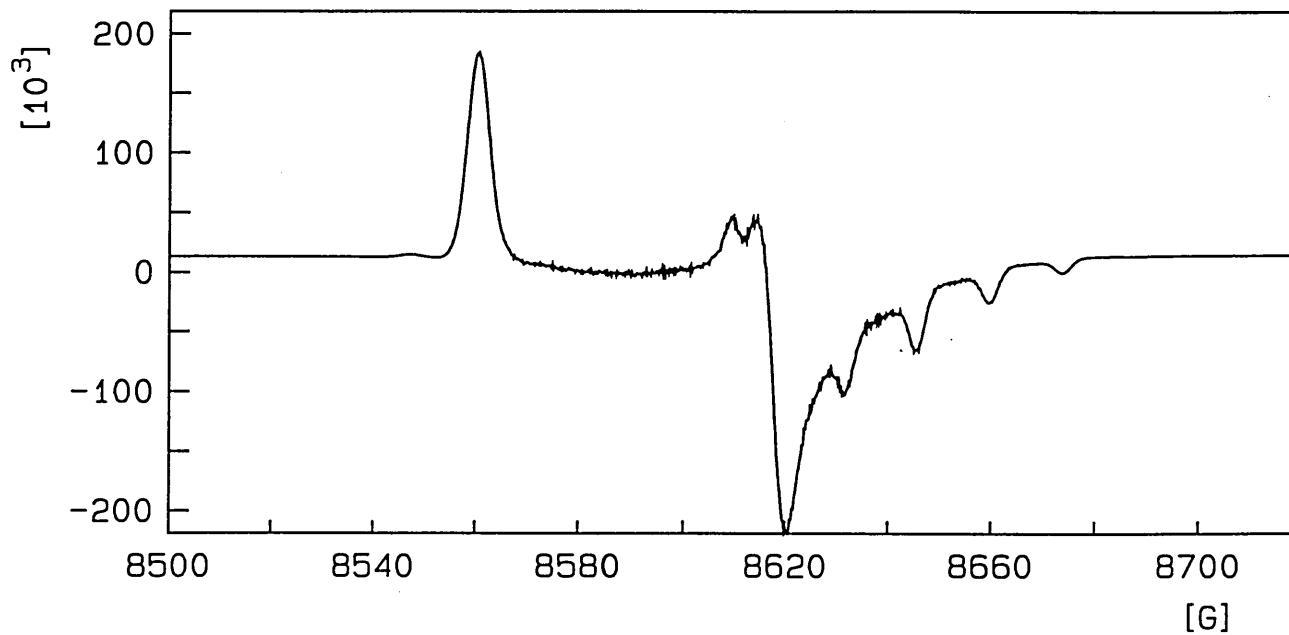


Figure 3.35 K-band EPR frozen glass spectrum of β -3, Sample curve (top) and simulation (bottom)

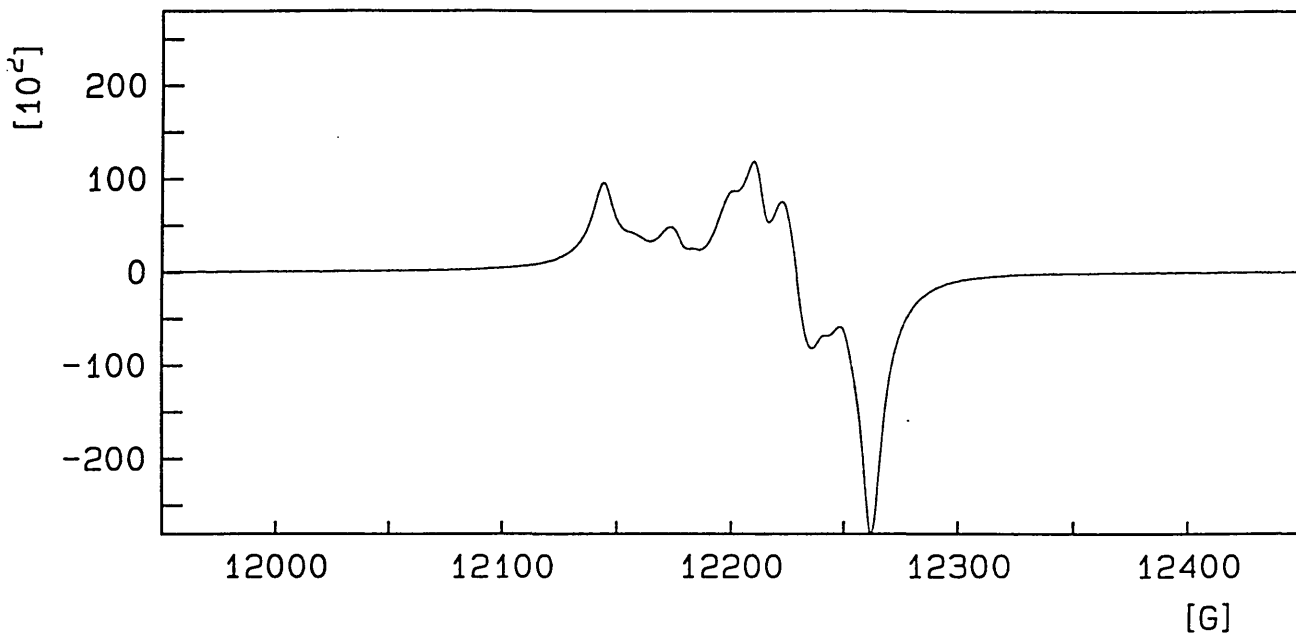
3.3.2 Powder Studies

Powder samples were prepared by grinding approximately 0.5 g of pure crystalline sample into a fine powder. The powder was then transferred into a quartz tube in a glove box to prevent degradation and was sealed prior to analysis. The analysis of the samples was then performed at different temperatures and frequencies.

Figures 3.36 - 3.38 show the powder spectra of **1**, **2** and **3** respectively. At room temperature, there is little fine detail in the spectra of **2** and **3** but on cooling to 105 K there is significant resolution enhancement. This suggests there is some isolated monomeric centres contributing to the spectrum. Compound **1** shows significant fine structure at room temperature which may indicate the presence of monomeric centres at high temperature. All the results obtained for powder measurement appear to contradict the results obtained for the magnetic data that indicated that the samples became more diamagnetic as temperature was decreased. Studies on further powders of the same materials revealed that the measurements were not reproducible. It is thought that the act of grinding the crystalline material to produce a powder actually destroys or modifies the solid state packing of the compounds leading to the inconsistent EPR signals.

Receiver	Signal Channel	Field	Microwave
Receiver Gain : 1.25e+02	Conversion : 40.96 ms	Center Field : 12200.10 G	Frequency : 33.9251000 GHz
Phase : 0.0 deg	Time Const : 1.28 ms	Sweep Width : 500.00 G	Power : 4.53e+00 mW
Harmonic : 1	Sweep Time : 41.943 s	Resolution : 1024 points	
Mod Frequency : 100.0000 kHz	Scale : 16		
Mod Amplitude : 1.000 G			

Comment: 2,4 dichoro s608 powder Q-band 293K, 4.72 mw



Receiver	Signal Channel	Field	Microwave
Receiver Gain : 6.30e+01	Conversion : 40.96 ms	Center Field : 12200.10 G	Frequency : 33.9089000 GHz
Phase : 0.0 deg	Time Const : 1.28 ms	Sweep Width : 500.00 G	Power : 4.59e+00 mW
Harmonic : 1	Sweep Time : 41.943 s	Resolution : 1024 points	
Mod Frequency : 100.0000 kHz	Scale : 15		
Mod Amplitude : 1.000 G			

Comment: 2,4 dichoro s608 powder Q-band 115K

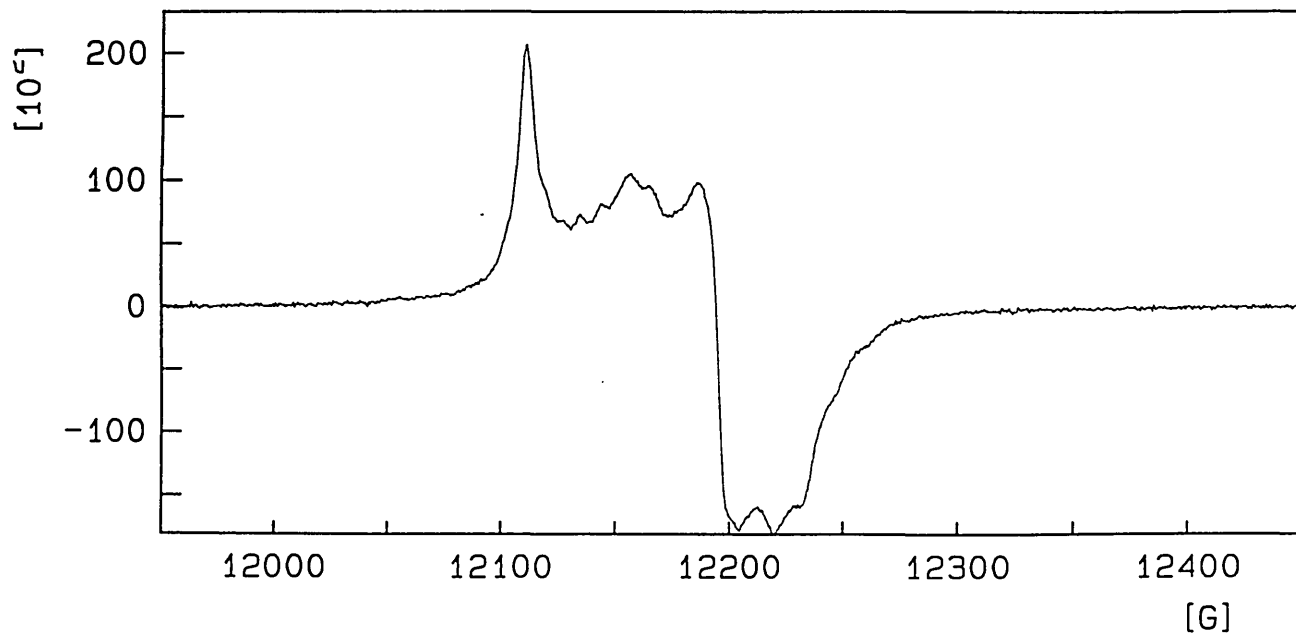


Figure 3.36 Q-band EPR powder spectrum of 1, taken at room temperature (top) and 105K (bottom)

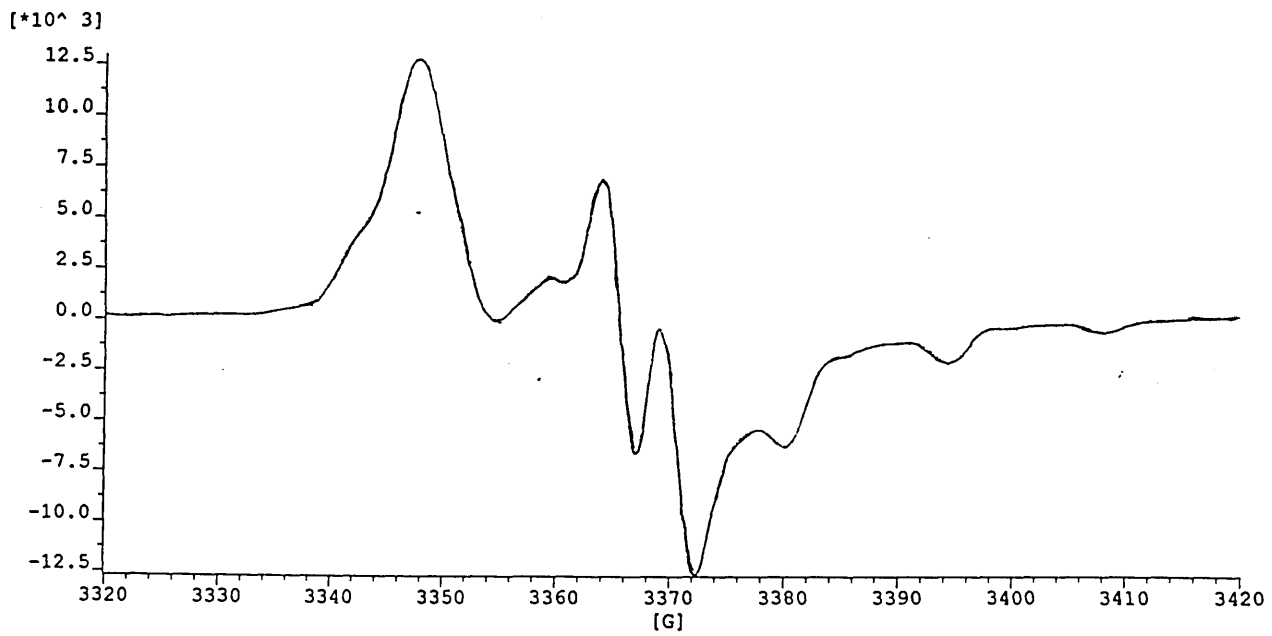
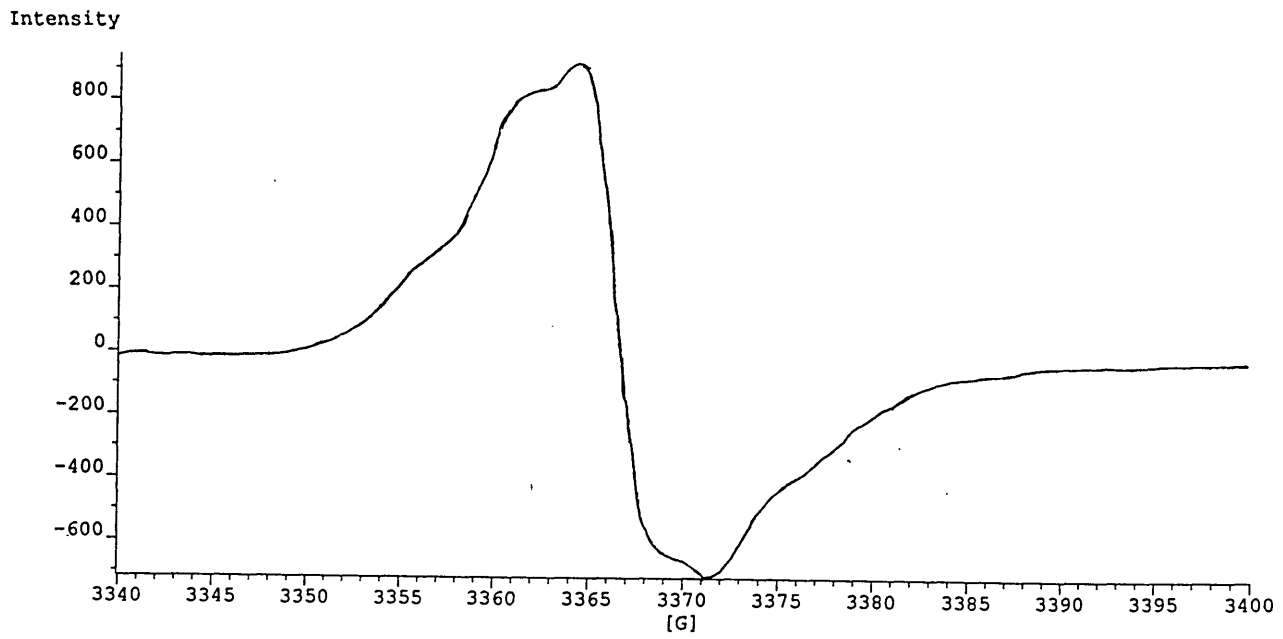
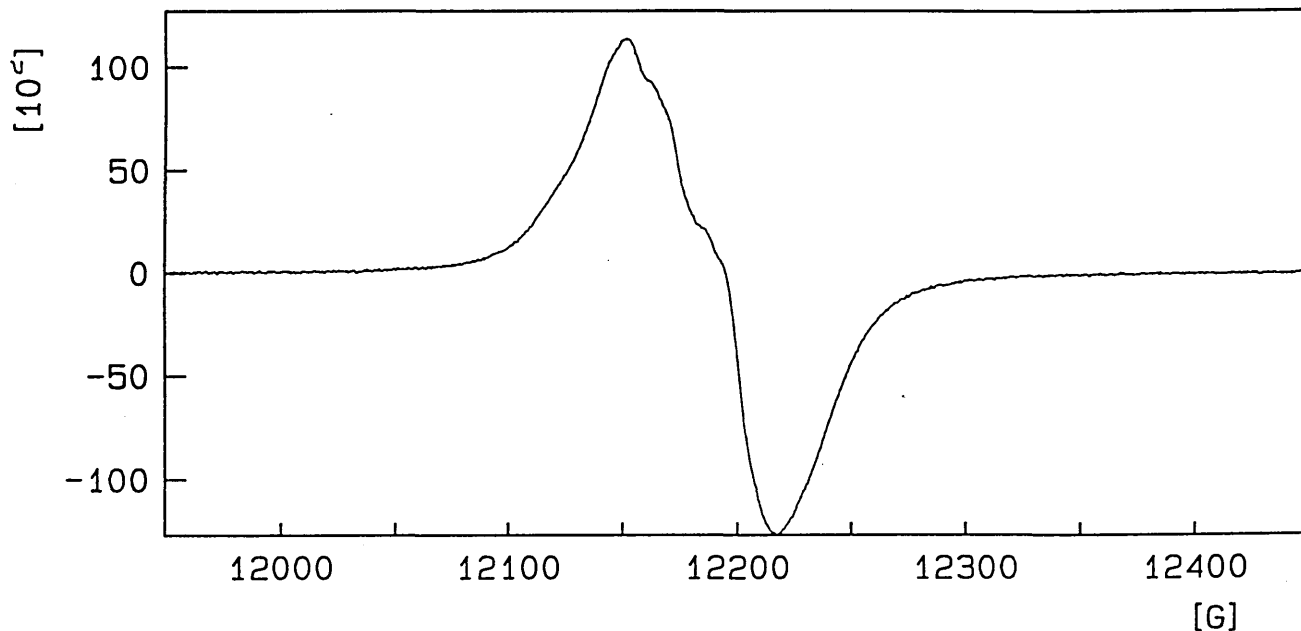


Figure 3.37 X-band EPR powder spectrum of **2**, taken at room temperature (top) and
 105K (bottom)
 105

Receiver	Signal Channel	Field	Microwave
Receiver Gain : 5.00e+01	Conversion : 40.96 ms	Center Field : 12200.10 G	Frequency : 33.8761000 GHz
Phase : 0.0 deg	Time Const : 1.28 ms	Sweep Width : 500.00 G	Power : 4.41e+00 mW
Harmonic : 1	Sweep Time : 41.943 s	Resolution : 1024 points	
Mod Frequency : 100.0000 kHz	Scale : 15		
Mod Amplitude : 1.000 G			

Comment: 3.5 dichoro s610 powder Q-band 295K



Receiver	Signal Channel	Field	Microwave
Receiver Gain : 8.00e+02	Conversion : 40.96 ms	Center Field : 12200.10 G	Frequency : 33.9251000 GHz
Phase : 0.0 deg	Time Const : 1.28 ms	Sweep Width : 500.00 G	Power : 4.53e+00 mW
Harmonic : 1	Sweep Time : 41.943 s	Resolution : 1024 points	
Mod Frequency : 100.0000 kHz	Scale : 15		
Mod Amplitude : 1.000 G			

Comment: 3.5 dichoro s610 powder Q-band 115K, 4.53 mw

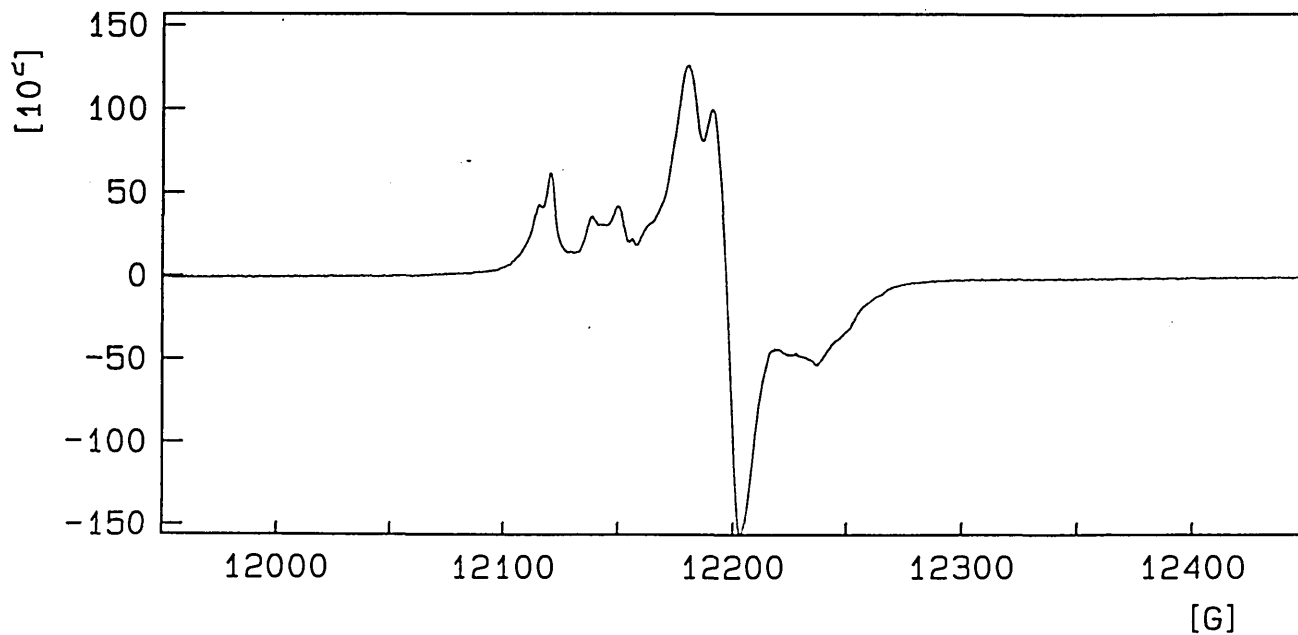


Figure 3.38 Q-band EPR powder spectrum of β -3, taken at room temperature (top) and

105K (bottom)

3.3.3 Single Crystal EPR Measurements on β -3

A small needle shaped crystal of β (approximately 1mm x 0.5mm x 0.5mm) was selected and measurements were taken at different orientations and temperatures within the magnetic field.

Figure 3.39 shows the spectra produced by varying the temperature of data collection between 290 K and 110 K while keeping the orientation constant. The results were unexpected when compared to the powder analysis. At 290 K there is a single line but as the temperature is decreased towards 200 K there is a considerable decrease in the intensity of the signal. This indicates the presence of a strong antiferromagnetic interaction between centres in the crystal that almost certainly becomes diamagnetic at 200 K. This might indicate the presence of strong local antiferromagnetic alignment. However, the pattern of the spectrum is not very different when analysed from a different orientation (Figure 3.40), which may suggest that this assumption is incorrect.

Figure 3.41 shows the temperature variation of the crystal when orientated perpendicular to the direction of the needle. The single line at room temperature breaks down into two weak lines as the temperature decreases. This indicates either a spectrum from the spin-triplet state which is being averaged and broadened or two independently orientated monomeric centres. The source of the averaging at higher temperatures is probably due to the exchange interactions either between adjacent dimers or between adjacent monomers. This exchange, which would be different from the exchange leading to the overall loss of intensity of the spectrum, need only be greater than the field difference between the two resonances being averaged (*i.e.* less than 1 cm^{-1}). This compares to the magnitude of the antiferromagnetic interaction, which is in the order of a few hundred cm^{-1} . This would suggest that the break up of the single line is not due to the monomeric centres being

averaged. Thus, it would seem that that strong interaction between individual centres might produce a spin-triplet state before it finally becomes diamagnetic.

Another point worth noting is that in the crystal data there is evidence of two satellites to the main peak (Figures 3.39 and 3.40). This has been reported previously for 1,3- and 1,4-phenyl-bridged bis(1,2,3,5-dithiadiazoly)^{8,24} which also exhibit a stacking motif. In this case, the peaks were described as the splitting due to dipolar coupling between pairs of electrons. The splitting was also temperature dependent as those observed for compound 3.

The data collected for the crystal is in good agreement with the results obtained for the magnetic data, which may suggest that the act of grinding the sample into a fine powder is somehow altering the crystal structure. This may suggest that from a structural point of view, data collected on the powder samples may not be representative of the overall properties of the crystal. Therefore, the information gathered from such samples may be of little use when describing the magnetic interactions in the solid state.

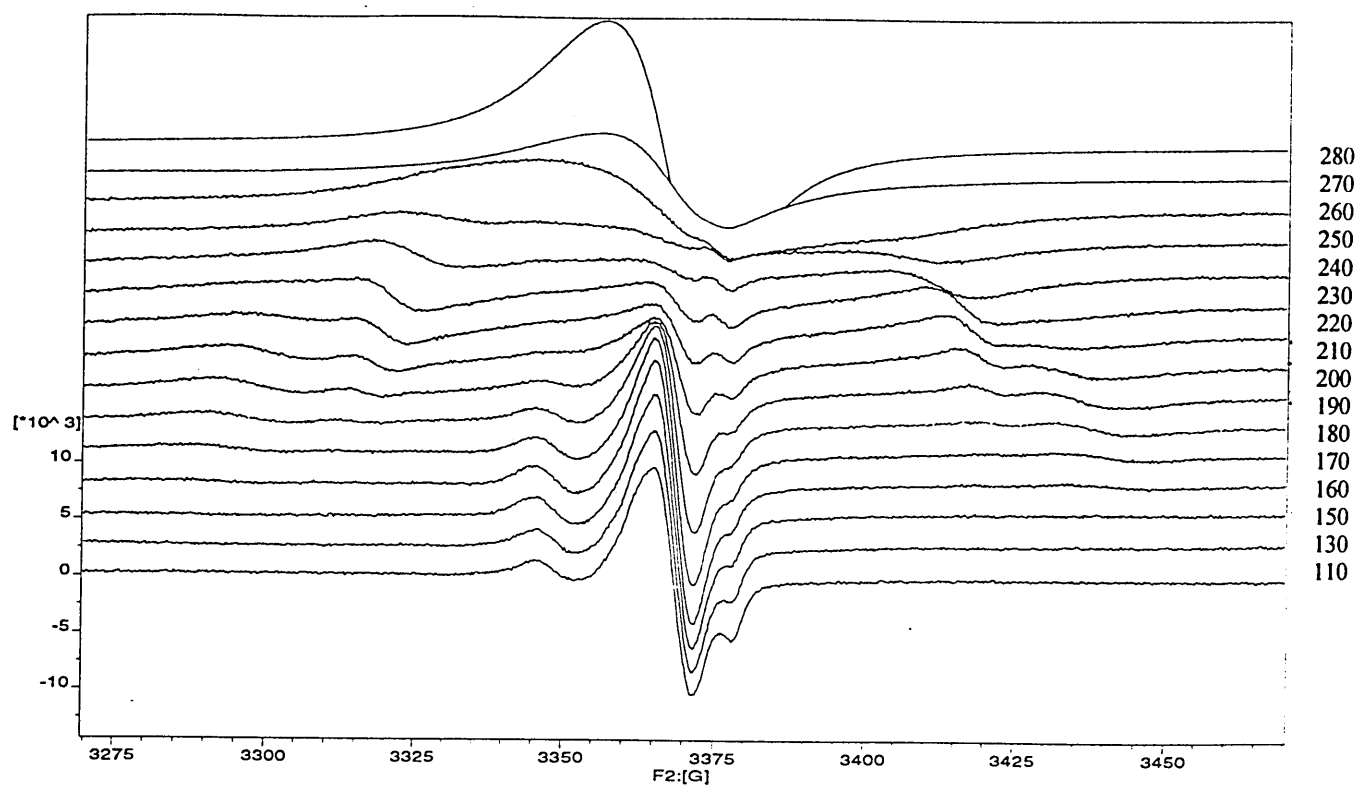


Figure 3.39 X-band EPR spectrum of **3** showing the variation of signal with temperature.

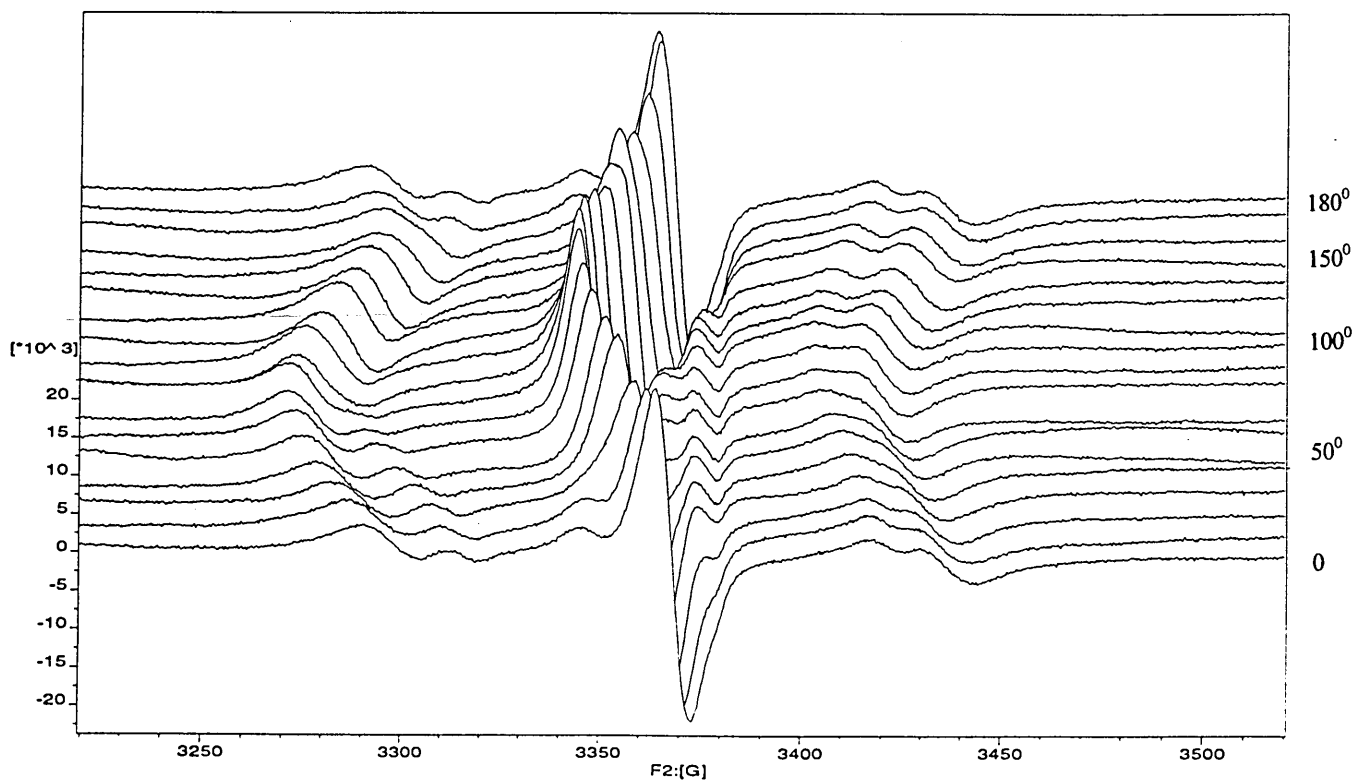


Figure 3.40 X-band EPR spectrum of **3** showing the variation of signal with angle at 200 K.

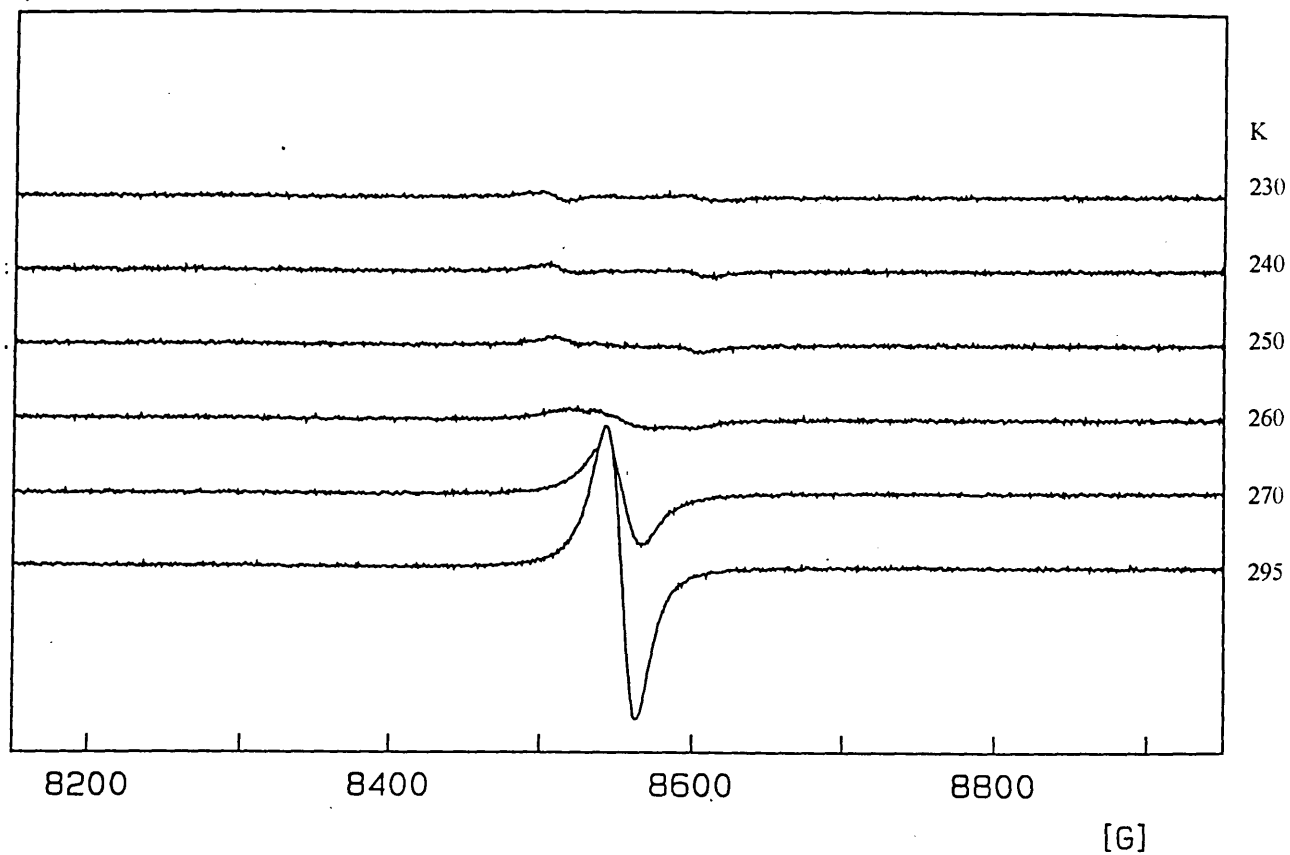


Figure 3.41 K-band EPR spectrum of **3** showing the variation of signal with temperature when orientated perpendicular to the needle.

3.4 Conclusions

In summary, I have successfully characterised the first three examples of neutral dithiadiazolyl radicals displaying a stacked structure containing evenly spaced radical units. I have also shown that chlorine substituents can direct the packing of dithiadiazolyl radicals towards layered/stacked motifs. An investigation of the physical properties of these systems showed the presence of some paramagnetic behaviour within the samples. EPR measurements on crystal samples exhibited dipolar coupling. It is clear that the exchange interactions within these structures are more complex than expected and further solid state EPR measurements are desirable.

3.5 References

- 1 H. Genin and R. Hoffman, *Macromolecules*, 1998, **31**, 444.
- 2 J.S. Miller and A.J. Epstein, *Angew. Chem. Int. Ed. Engl.*, 1994, **33**, 385.
- 3 A.J. Banister, A.S. Batsanov, O.G. Dawe, P.L. Herbertson, J.A.K. Howard, S. Lynn, I. May, J.N.B. Smith, J.M. Rawson, T.E. Rogers, B.K. Tanner, G. Antorrena and F. Palacio, *J. Chem. Soc., Dalton Trans.*, 1997, 2539.
- 4 A.J. Banister, A.S. Batsanov, O.G. Dawe, J.A.K. Howard, J.E. Davies, J.M. Rawson and J.N.B. Smith, *Phosphorus, Sulfur, and Silicon*, 1997, **124**, 553.
- 5 J.E. Davies, R.J. Less, I. May and J.M. Rawson, *New J. Chem.*, 1998, 763.
- 6 L. Beer, A.W. Cordes, D.J.T. Myles, R.T. Oakley and N.J. Taylor, *Cryst. Eng. Comm.*, 2000, 20.
- 7 (a) C.D. Bryan, A.W. Cordes, R.M. Fleming, N.A. George, S.H. Glarum, R.C. Haddon, R.T. Oakley, T.T.M. Palstra, A.S. Perel, L.F. Schneemeyer and J.V. Waszczak, *Nature*, 1993, **365**, 821; (b) C.D. Bryan, A.W. Cordes, R.C. Haddon, R.G. Hicks, D.K. Kennepohl, C.D. MacKinnon, R.T. Oakley, T.T.M. Palstra, A.S. Perel, S.R. Scott, L.F. Schneemeyer and J.V. Waszczak, *J. Am. Chem. Soc.*, 1994, **116**, 1205; (c) A.W. Cordes, R.C. Haddon, and R.T. Oakley, *Adv. Mater.*, 1994, **6**, 798; (d) C.D. Bryan, A.W. Cordes, R.C. Haddon, R.G. Hicks, R.T. Oakley, T.T.M. Palstra, A.S. Perel and S.R. Scott, *Chem. Mater.*, 1994, **6**, 508; (e) C.D. Bryan, A.W. Cordes, R.M. Fleming, N.A. George, S.H. Glarum, R.C. Haddon, C.D. MacKinnon, R.T. Oakley, T.T.M. Palstra and A.S. Perel, *J. Am. Chem. Soc.*, 1995, **117**, 6880; (f) C.D. Bryan, A.W. Cordes, J.D. Goddard, R.C. Haddon, R.G. Hicks, C.D. MacKinnon, R.C. Mawhinney, R.T. Oakley, T.T.M. Palstra and A.S. Perel, *J. Am. Chem. Soc.*, 1996, **118**, 330; (g) A.W. Cordes,

-
- N.A. George, R.C. Haddon, D.K. Kennepohl, R.T. Oakley, T.T.M. Palstra and R.W. Reed, *Chem. Mater.*, 1996, **8**, 2774.
- 8 M.P. Andrews, A.W. Cordes, D.C. Douglas, R.M. Fleming, S.H. Glarum, R.C. Haddon, P. Marsh, R.T. Oakley, T.T.M. Palstra, L.F. Schneemeyer, G.W. Trucks, R. Tycko, J.V. Waszczak, K.M. Young and N.M. Zimmerman, *J. Am. Chem. Soc.*, 1991, **113**, 3559.
- 9 (a) A.W. Cordes, R.C. Haddon, R.G. Hicks, R.T. Oakley, T.T.M. Palstra, L.F. Schneemeyer and J.V. Waszczak, *J. Am. Chem. Soc.*, 1992, **114**, 5000; (b) A.W. Cordes, R.C. Haddon, R.G. Hicks, D.K. Kennepohl, R.T. Oakley, T.T.M. Palstra, L.F. Schneemeyer, S.R. Scott and J.V. Waszczak, *Chem. Mater.*, 1993, **5**, 820; (c) C.D. Bryan, A.W. Cordes, R.C. Haddon, R.G. Hicks, R.T. Oakley, T.T.M. Palstra and A.S. Perel, *J. Chem. Soc., Chem. Commun.*, 1994, 1447.
- 10 G.R. Desiraju and R. Parthasarathy, *J. Am. Chem. Soc.*, 1989, **111**, 8725.
- 11 J.A.R.P. Sarma and G.R. Desiraju, *Acc. Chem. Res.*, 1986, **19**, 222.
- 12 (a) T. Sakurai, M. Sundaralingham and G.A. Jeffrey, *Acta Cryst.*, 1963, **16**, 354; (b) K. Yamasaki, *J. Phys. Soc. Jpn.*, 1962, **17**, 1262; (c) S.C. Nyburg, *J. Chem. Phys.*, 1964, **40**, 2493.
- 13 D.E. Williams and L.-Y. Hsu, *Acta Cryst.*, 1985, **A41**, 296.
- 14 (a) N. Ramasubba, R. Parthasarathy and P. Murray-Rust, *J. Am. Chem. Soc.*, 1986, **108**, 4308. (b) J.D. Dunitz, *Philos. Trans. R. Soc. London*, 1975, **B272**, 99. (c) K. Fukui, T. Yonezawa and H. Shinga, *J. Chem. Phys.*, 1952, **20**, 722.
- 15 R.T. Boéré and K.H. Moock, *Z. anorg. allg. Chem.*, 1994, **620**, 1589.
- 16 A.W. Cordes, C.M. Chamchoumis, R.G. Hicks, R.T. Oakley, K.M. Young and R.C. Haddon, *Can. J. Chem.*, 1992, **70**, 919.

-
- 17 A.W. Cordes, R.C. Haddon, R.G. Hicks, R.T. Oakley and T.T.M. Palstra, *Inorg. Chem.*, 1992, **31**, 1802.
- 18 A. Vegas, A. Pérez-Salazar, A.J. Banister and R.G. Hey, *J. Chem. Soc., Dalton Trans.*, 1980, 1812.
- 19 S.C. Nyburg and C.H. Faerman, *Acta. Cryst.*, 1985, **B41**, 274.
- 20 A.J. Banister, N. Bricklebank, W. Clegg, M.R.J. Elsegood, C.I. Gregory, I. Lavender, J.M. Rawson and B.K. Tanner, *J. Chem. Soc., Chem. Commun.*, 1995, 679.
- 21 G. Antorrena, Ph.D. thesis, Universidad de Zaragoza.
- 22 S.A. Fairhurst, K.M. Johnson, H. Sutcliffe, K.F. Preston, A.J. Banister, Z.V. Hauptman and J. Passmore, *J. Chem. Soc., Dalton Trans.*, 1986, 1465.
- 23 S.A. Fairhurst, L.H. Sutcliffe, K.F. Preston, A.J. Banister, A.S. Partington, J.M. Rawson, J. Passmore and M. Schriver, *Magn. Reson. Chem.*, 1993, **31**, 1027.
- 24 A.W. Cordes, R.C. Haddon, R.T. Oakley, L.F. Schneemeyer, J.V. Waszczak, K.M. Young and N.M. Zimmerman, *J. Am. Chem. Soc.*, 1991, **113**, 582.

Chapter 4

Dimer Stacking Motifs for

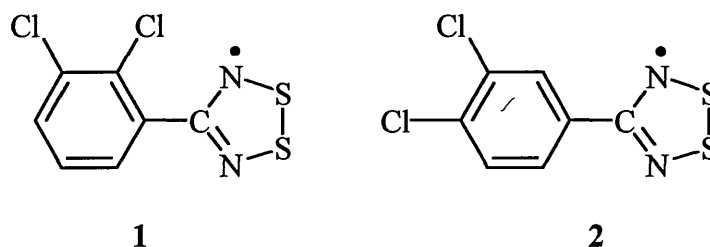
Dichlorophenyl Dithiadiazolyl

Radicals

4.0 Introduction

As shown in chapter 3, dichlorophenyl derivatives can have a significant effect on the molecular packing of dithiadiazolyl radicals. The chlorine atoms appear to steer the compounds towards a stacking motif and, in certain cases, also encourage the formation of chains through electrostatic $S \cdots Cl$ interactions.

This chapter describes the characterisation of two further dichlorophenyl dithiadiazolyls **1** and **2**, which crystallise as stacks of dimer units.



Previous investigations of the structures of difluorophenyl dithiadiazolyls,^{1,2} found that the compounds associated as stacks of dimers containing alternate long interdimer (3.9 - 4.1 Å) and short intradimer (2.9 - 3.1 Å) $S \cdots S$ interactions. Further $F \cdots S$ electrostatic interactions were also observed, facilitating the formation of chains / ribbons of molecules.

Compound **1** may be expected to exhibit different packing properties to the other dichlorophenyl derivatives because of the asymmetric nature of the molecule. Indeed, the analogous difluorophenyl derivative forms discrete twisted dimers^{1,3} (Figure 4.1) induced by a comparatively large molecular dipole across the aromatic group.

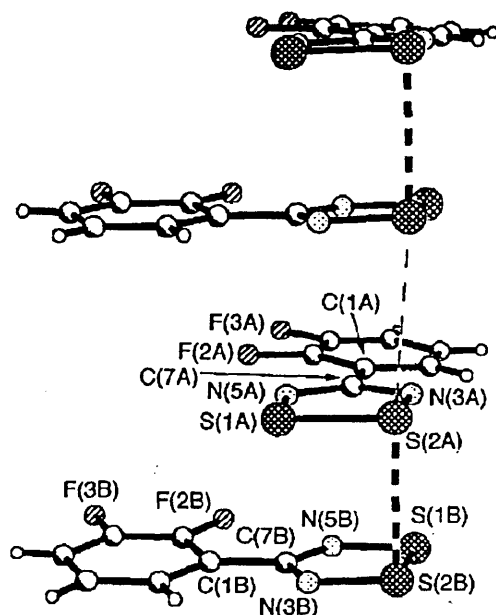


Figure 4.1 Crystal structure of 2,3-difluorophenyl-1,2,3,5-dithiadiazolyl³

In contrast, 3,4-difluorophenyl-1,2,3,5-dithiadiazolyl¹ forms *cis*-cofacial dimers that are linked together by F...S contacts to form a ribbon-type structure (Figure 4.2). Adjacent chains within the structure align in opposite directions. The structure is very similar to 2,3,4-trifluorophenyl-1,2,3,5-dithiadiazolyl which has also been reported.⁴

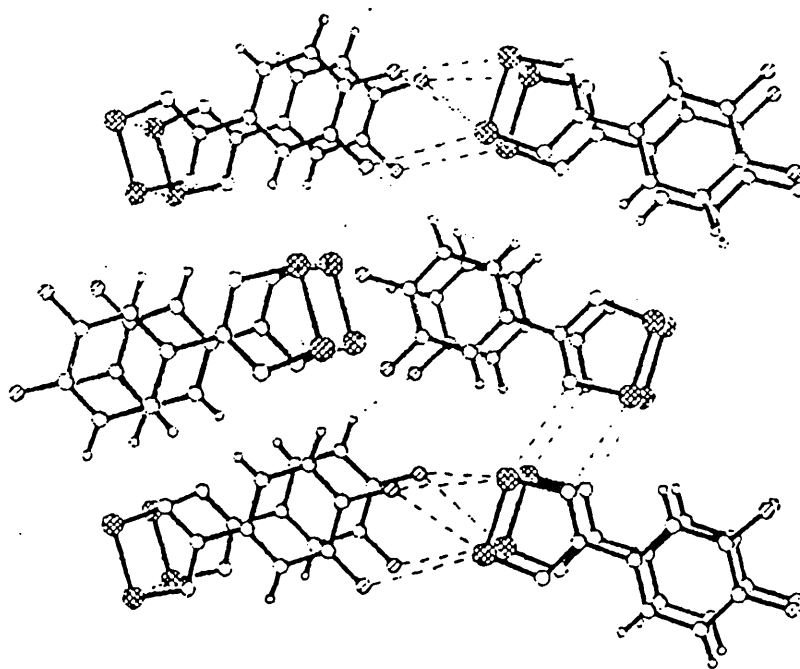


Figure 4.2 Crystal structure of 3,4-difluorophenyl-1,2,3,5-dithiadiazolyl¹

The only chlorine derivative reported to date (*p*-chlorophenyl-1,2,3,5-dithiadiazolyl)⁵ has a crystal structure where S···Cl interactions were observed at a 90⁰ angle with respect to the planes of the two rings (Figure 3.1, page 61). The formation of ribbons was still observed within the structure indicating that chlorine in the *para* position can facilitate this sort of ribbon/chain structure. This was also true for 2,4-dichlorophenyl-1,2,3,5-dithiadiazolyl (Figure 3.9, page 71) that also has significant S···Cl interactions resulting in the formation of ribbons of Cl₂.C₆H₃. $\overline{\text{CNSSN}}$ molecules throughout the structure.

4.1 X-Ray Structures

X-ray structural determinations were undertaken on **1** and **2**. An Ortep structural plot of the asymmetric units from both isomers **1** and **2** are shown in Figure 4.3 and 4.4 respectively. The bond lengths and angles of the two molecules (denoted by a and b) within the asymmetric units of **1** and **2** are listed in Table 4.1 and 4.2 together with data for phenyl-1,2,3,5-dithiadiazolyl⁶ and *p*-chlorophenyl-1,2,3,5-dithiadiazolyl⁵ for comparative purposes. The full crystallographic data for compounds **1** and **2** can be found in appendix 6 and 7 respectively at the end of the thesis.

The molecular structures of **1** and **2** are similar to those of the majority of aryl 1,2,3,5-dithiadiazolyls and to the other isomers of dichlorophenyl-1,2,3,5-dithiadiazolyl described earlier (Chapter 3). The chlorine-carbon bond distances (1.722 – 1.753 Å) are reasonably similar to those observed for *p*-chlorophenyl-1,2,3,5-dithiadiazolyl⁵ [Figure 3.1 (1.750 Å)]. The most significant difference observed between the two structures is the torsion angle between the two planar rings (Cl₂.C₆H₃. $\overline{\text{CNSSN}}$). As might be expected compound **1**, which has chlorine in the *ortho* position, has a relatively large torsion angle (27.5⁰), whereas the torsion angle observed for compound **2** is significantly smaller (13.4⁰). Presumably, this is due to the reduced steric hindrance.

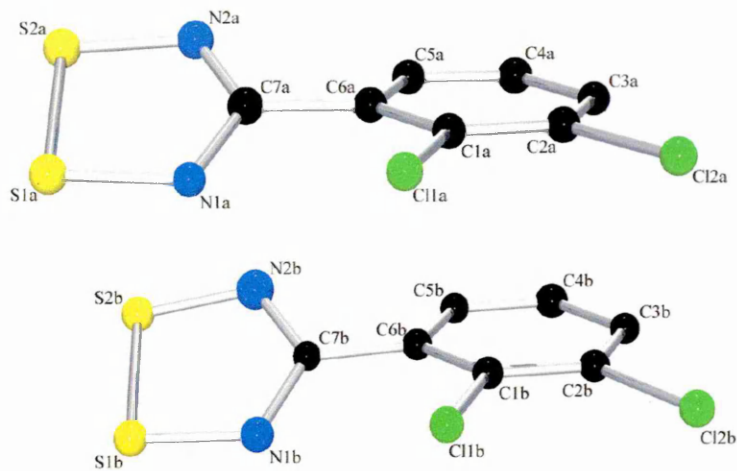


Figure 4.3 2,3-dichlorophenyl-1,2,3,5-dithiadiazolyl (1)

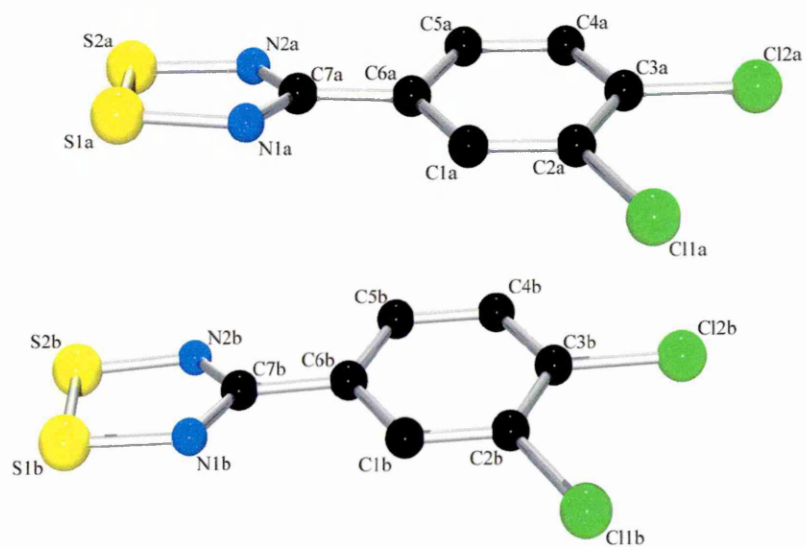


Figure 4.4 3,4-dichlorophenyl-1,2,3,5-dithiadiazolyl (2)

Table 4.1 Bond lengths of 1 and 2 (Å).

Atom No.	Bond Distance (Å)					
	(1)a	(1)b	(2)a	(2)b	<i>p</i> -ClC ₆ H ₄	Ph
Cl(1)-C(1)	1.728(14)	1.735(14)	-	-	-	-
Cl(2)-C(2)	1.753(14)	1.744(13)	-	-	-	-
Cl(1)-C(2)	-	-	1.742(7)	1.735(7)	-	-
Cl(2)-C(3)	-	-	1.722(7)	1.733(6)	-	-
Cl(1)-C(3)	-	-	-	-	1.750(4)	-
S(1)-N(1)	1.643(12)	1.635(12)	1.628(6)	1.637(6)	1.643(10)	1.63
S(1)-S(2)	2.095(5)	2.094(5)	2.092(3)	2.094(3)	2.103(5)	2.096
S(2)-N(2)	1.633(11)	1.614(14)	1.634(6)	1.635(6)	1.651(10)	1.63
N(1)-C(7)	1.332(17)	1.336(16)	1.341(9)	1.339(9)	1.32(1)	1.32
N(2)-C(7)	1.330(18)	1.383(17)	1.321(9)	1.332(9)	1.34(1)	1.31
C(1)-C(2)	1.381(18)	1.395(18)	1.367(10)	1.385(10)	1.365(7)	1.37
C(1)-C(6)	1.407(18)	1.409(17)	1.405(9)	1.402(9)	1.410(7)	1.37
C(2)-C(3)	1.351(19)	1.355(17)	1.393(10)	1.399(9)	1.385(8)	1.39
C(3)-C(4)	1.411(19)	1.43(2)	1.391(10)	1.374(9)	1.371(7)	1.42
C(4)-C(5)	1.39(2)	1.37(2)	1.380(10)	1.401(10)	1.376(8)	1.36
C(5)-C(6)	1.408(18)	1.405(18)	1.406(9)	1.388(10)	1.401(6)	1.38
C(6)-C(7)	1.506(19)	1.461(17)	1.488(9)	1.474(9)	1.472(7)	1.50

Table 4.2 Bond angles of 1 and 2 (°)

Atom No.	Angle (degrees)					
	(1)a	(1)b	(2)a	(2)b	<i>p</i> -ClC ₆ H ₄	Ph
N(1)-S(1)-S(2)	94.4(4)	94.5(5)	94.5(2)	94.1(2)	95.3(4)	93.0
N(2)-S(2)-S(1)	94.2(4)	94.8(5)	94.3(2)	94.6(2)	93.4(4)	94.1
C(7)-N(1)-S(1)	113.8(10)	115.2(10)	113.8(5)	114.4(5)	113.2(9)	116
C(7)-N(2)-S(2)	114.4(10)	114.8(10)	114.2(5)	114.3(5)	114.0(8)	115
C(2)-C(1)-C(6)	118.4(13)	119.4(12)	120.1(6)	119.9(6)	121.5(5)	121
C(2)-C(1)-Cl(1)	120.3(10)	119.0(10)	-	-	-	-
C(6)-C(1)-Cl(1)	121.3(10)	121.6(10)	-	-	-	-
C(3)-C(2)-Cl(2)	117.2(10)	117.4(10)	-	-	-	-
C(1)-C(2)-Cl(2)	119.5(11)	120.2(10)	-	-	-	-
C(1)-C(2)-Cl(1)	-	-	118.0(5)	118.2(5)	-	-
C(3)-C(2)-Cl(1)	-	-	121.1(5)	121.9(6)	-	-
C(4)-C(3)-Cl(1)	-	-	-	-	120.6(4)	-
C(5)-C(4)-Cl(1)	-	-	-	-	119.1(4)	-
C(1)-C(2)-C(3)	123.3(13)	122.4(12)	120.9(7)	119.9(6)	119.4(5)	120
C(4)-C(3)-C(2)	119.0(12)	118.5(12)	119.6(6)	120.4(6)	-	119
C(4)-C(3)-Cl(2)	-	-	119.0(5)	119.5(5)	-	-
C(2)-C(3)-Cl(2)	-	-	121.4(5)	120.1(5)	-	-
C(3)-C(4)-C(5)	119.8(12)	119.9(13)	120.1(7)	120.0(6)	119.7(5)	120
C(4)-C(5)-C(6)	119.9(12)	121.3(13)	120.2(7)	120.0(6)	120.9(4)	119
C(5)-C(6)-C(1)	119.6(12)	118.4(12)	119.0(6)	119.8(6)	119.1(5)	121
C(5)-C(6)-C(7)	115.8(12)	117.3(11)	120.5(6)	121.0(6)	121.3(5)	119
C(1)-C(6)-C(7)	124.7(12)	124.3(12)	120.5(6)	119.2(6)	121.6(5)	120
N(1)-C(7)-N(2)	123.1(13)	120.5(12)	123.2(6)	122.6(6)	123(1)	122
N(2)-C(7)-C(6)	115.6(12)	116.2(11)	119.4(6)	119.1(6)	116(1)	121
N(1)-C(7)-C(6)	121.2(12)	123.1(12)	117.4(6)	118.3(6)	119(1)	117
Twist Angle*	27.5	28	13.8	13.4	7	7

* Denotes the torsion angle between C(6) and C(7) based on the planes of both the dithiadiazolyl ring and the phenyl ring.

4.1.1 Structure of 2,3-dichlorophenyl-1,2,3,5-dithiadiazolyl (1)

A crystal suitable for x-ray analysis was produced by sublimation. First, the crude oil containing the dithiadiazolyl radical, prepared from the reduction of the respective dithiadiazolylium chloride, was purified by cold finger sublimation. The resulting needle-like crystals were carefully sublimed over a temperature gradient (temperature range of 95 °C - 25 °C, 10⁻³ torr) for approximately 48 hours. The resulting crystals were usually of poor quality, forming as microcrystalline bundles of highly twinned needles. Successive sublimations over several days yielded small quantities of small needle crystals suitable for x-ray analysis.

The asymmetric unit of **1** consists of two molecules and is monoclinic with a space group of P2₁/n. The molecules associate as dimer pairs with intradimer S...S distances of S1a...S1b and S1c...S1d, 3.203 Å; S2a...S2b and S2c...S2d, 3.130 Å (Figure 4.5). These distances are comparable to those observed for *cis*-cofacial dithiadiazolyl dimers (typically 3.0-3.2 Å).⁷ The dimers associate together in stacks parallel to the crystallographic b-axis. The interdimer distances (S1b...S1c, 4.098 Å; S2b...S2c, 4.168 Å) are considerably larger than those observed in regular dithiadiazolyl dimer structures (2.9 – 3.1 Å).⁷ This sort of association is surprising considering the twisted mode of association exhibited by 2,3-difluoro-1,2,3,5-dithiadiazolyl dimer^{1,3} (Figure 4.1). It might be expected that the addition of more bulky atoms to the phenyl ring would also cause a similar twisted motif. As in the α-phase of 3,5-dichloro-1,2,3,5-dithiadiazolyl (Chapter 3, page 84), the Peierls distortion is almost localised to the dithiadiazolyl ring with Cl...Cl between phenyl rings having almost constant intra- and inter-dimer contacts

(Cl1a...Cl1b and Cl1c...Cl1d, 3.640 Å; Cl2a...Cl2b and Cl2c...Cl2d, 3.674 Å; Cl1b...Cl1c, 6.656 Å; Cl2b...Cl2c, 3.628 Å).

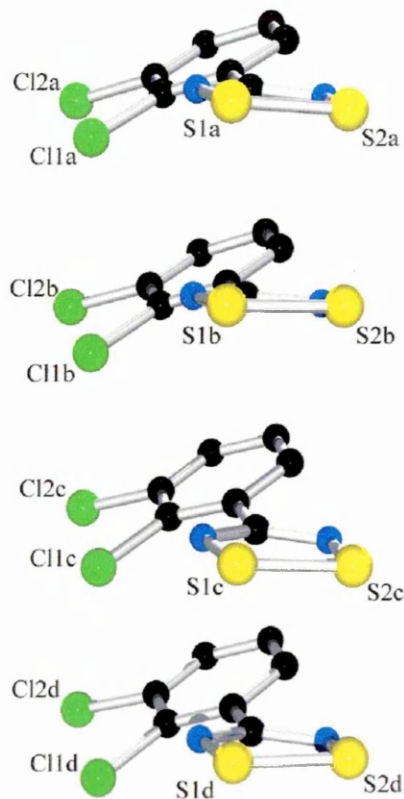


Figure 4.5 Orteplot of the stacking of **1**, with selected atoms labelled.

In addition to the intrastack S...S and Cl...Cl contacts, compound **1** also displays significant association between the stacks (i.e. in the *a* and *c* directions). Molecules in adjacent stacks are associated *via* a series of S...Cl contacts (Figure 4.6). Each interacting group lies at approximately 90° to each other with both chlorine atoms on the aromatic ring interacting with the sulfurs of the adjacent dithiadiazolyl (Cl1a...S2b, 3.608 Å; Cl2a...S2b, 3.627 Å; Cl2a...S1b, 3.481 Å). A further interaction is also observed between the chlorine in the *meta* position and a sulfur of the dithiadiazolyl ring (S1d...Cl2b, 3.563 Å). All of these S...Cl interactions lie within the range for the sum of

the van der Waals radii of sulfur and chlorine (3.5 Å - 3.7 Å)⁸ which suggests that the

S...Cl contacts within the molecule are relatively strong.

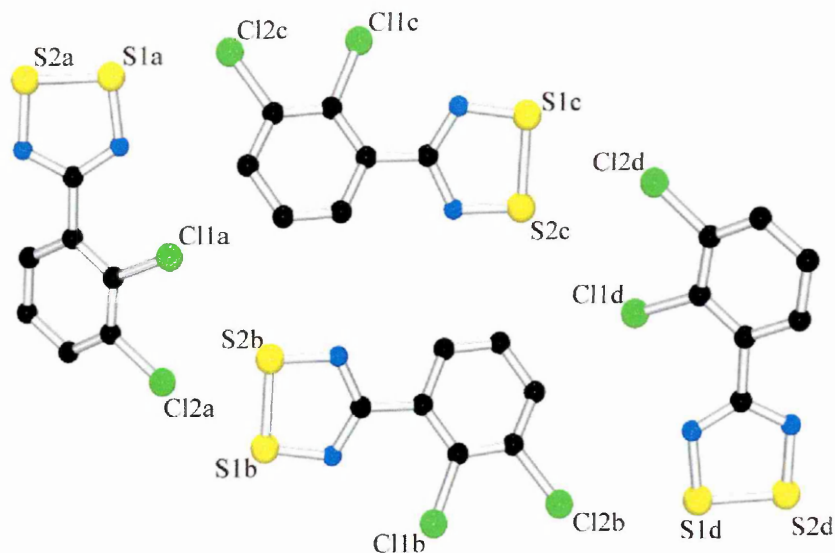


Figure 4.6 Ortep plot of the interactions of **1** within the *ac* plane, with selected atoms labelled.

Unlike the other dichlorophenyl dithiadiazolyl isomers shown in chapter 3 there would seem to be no Cl...Cl interactions in the *a* or *c* direction. Figure 4.7 shows the overall packing of **1**. Although not obvious initially, the whole structure can be viewed as a series of chains arranged in a herringbone fashion with each group interacting at an angle of approximately 90° to the adjacent group. Each adjacent chain is linked by one S...Cl interaction per molecule [Cl2b...S1d, 3.563 Å (Figure 4.6)] and is aligned anti-parallel to one another. The packing (Figure 4.7) again illustrates the ability of chlorine substituents to create a stacked structure and its ability, through electrostatic interactions, to form chains. Unfortunately, in this case the spin pairing within the molecule is the predominant feature and is almost certain to make the compound diamagnetic.

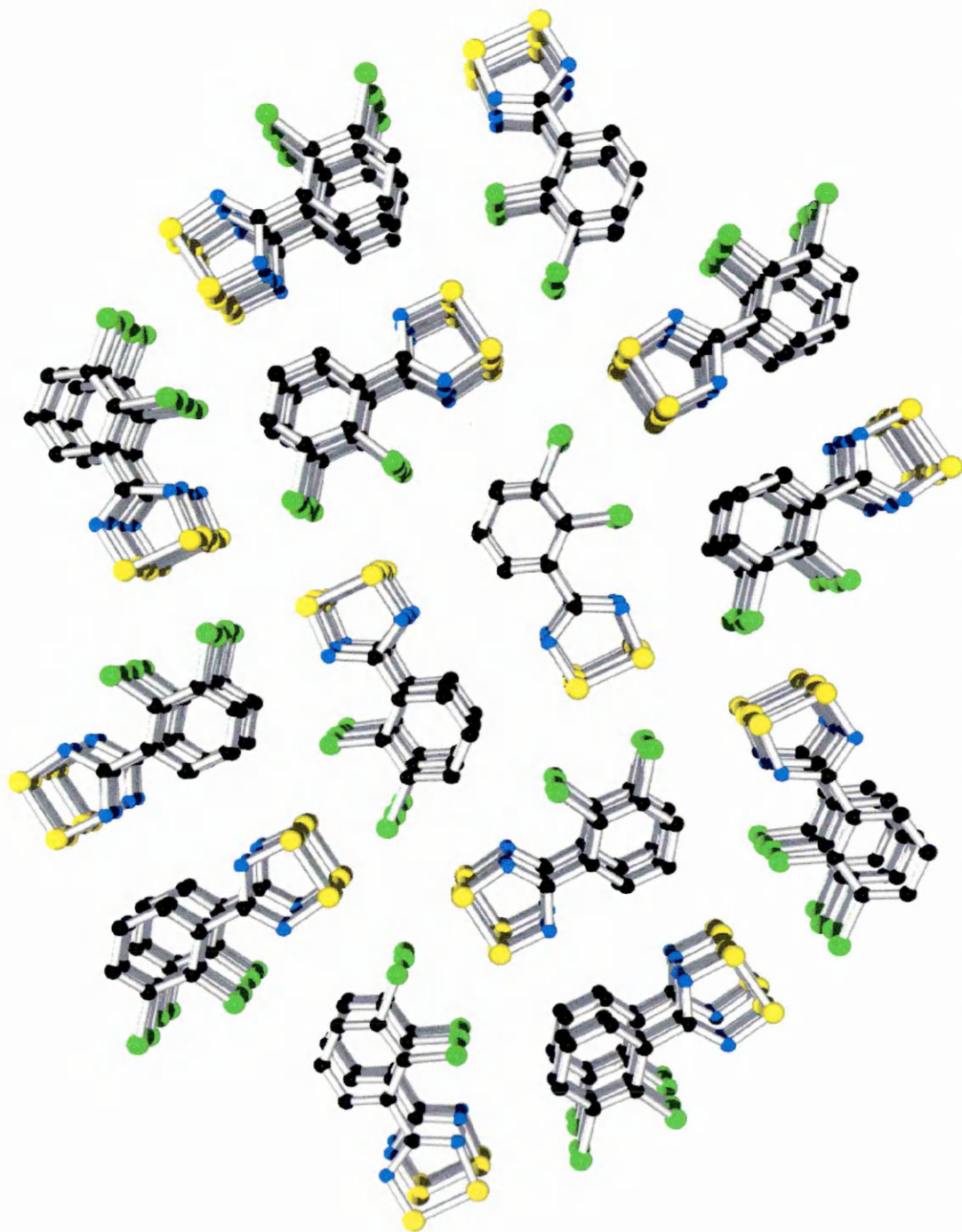


Figure 4.7 Ortep plot of the packing of 2,3-dichlorophenyl-1,2,3,3,5-dithiadiazolyl

4.1.2 X-ray Crystal Structure of 3,4-dichlorophenyl-1,2,3,5-dithiadiazolyl (2)

Crystals suitable for x-ray analysis were produced using a similar method to that described for **1** (Section 3.1.1, page 66). The gradient sublimation was completed using a temperature range 110-25 °C under a dynamic vacuum (10^{-3} torr). The resulting crystals were usually twinned and of poor quality but repeated sublimation over several days yielded small dark red crystals, suitable for crystallographic studies.

The asymmetric unit of **2** contains two molecules and is monoclinic with space group $P2_1/c$. The molecules also associate as dimer pairs with intradimer S...S distances of S1a...S1b and S1c...S1d, 3.125 Å; S2a...S2b and S2c...S2d, 3.207 Å (Figure 4.8) which are similar to those observed for *cis*-cofacial dithiadiazolyl dimers (typically 2.9 - 3.1 Å).⁷ The dimers associate in stacks parallel to the crystallographic *a*-axis. The interdimer distances are also considerably larger than those observed in regular dithiadiazolyl dimer structures (S1b...S1c, 4.103 Å; S2b...S2c, 4.033 Å). In a similar way to **1**, the Peierls distortion is almost localised to dithiadiazolyl rings with the intra and interdimer Cl...Cl contacts of the phenyl rings being almost constant (C11a...C11b and C11c...C11d, 3.628 Å; C12a...C12b and C12c...C12d, 3.569 Å; C11b...C11c, 6.589 Å; C12b...C12c, 3.672 Å).

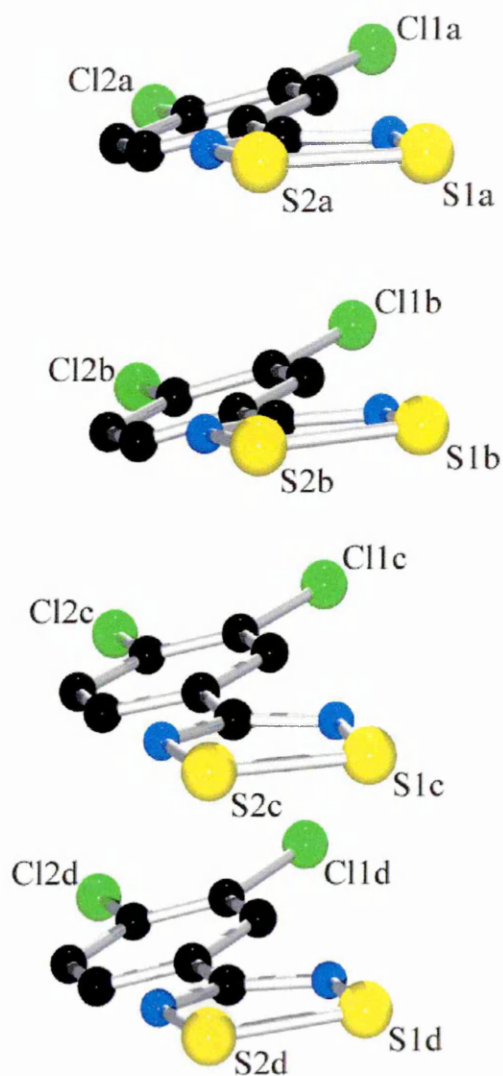


Figure 4.8 Ortep plot of the stacking of **2**, with selected atoms labelled.

Within the plane parallel to the *b* and *c* axis the molecules are linked into chains through electrostatic S...Cl interactions (Figure 4.9). There is significant interaction between both of the chlorine atoms with both of the sulfur atoms of the dithiadiazolyl ring (Cl2b...S1a, 3.351 Å; Cl1c...S2a, 3.328 Å).

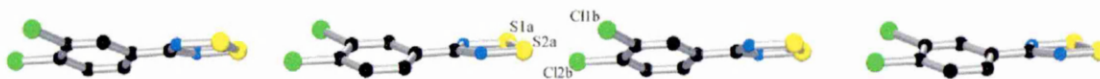


Figure 4.9 Ortep plot of the chain structure of **1**.

As well as the interactions within the chains of **2** there are further Cl⋯Cl, S⋯S and S⋯Cl interactions that hold the chains together [S2a⋯S2b, 3.338 Å; Cl2b⋯S1c, 3.646 Å; Cl2c⋯Cl2d, 3.474 Å (Figure 4.10)].

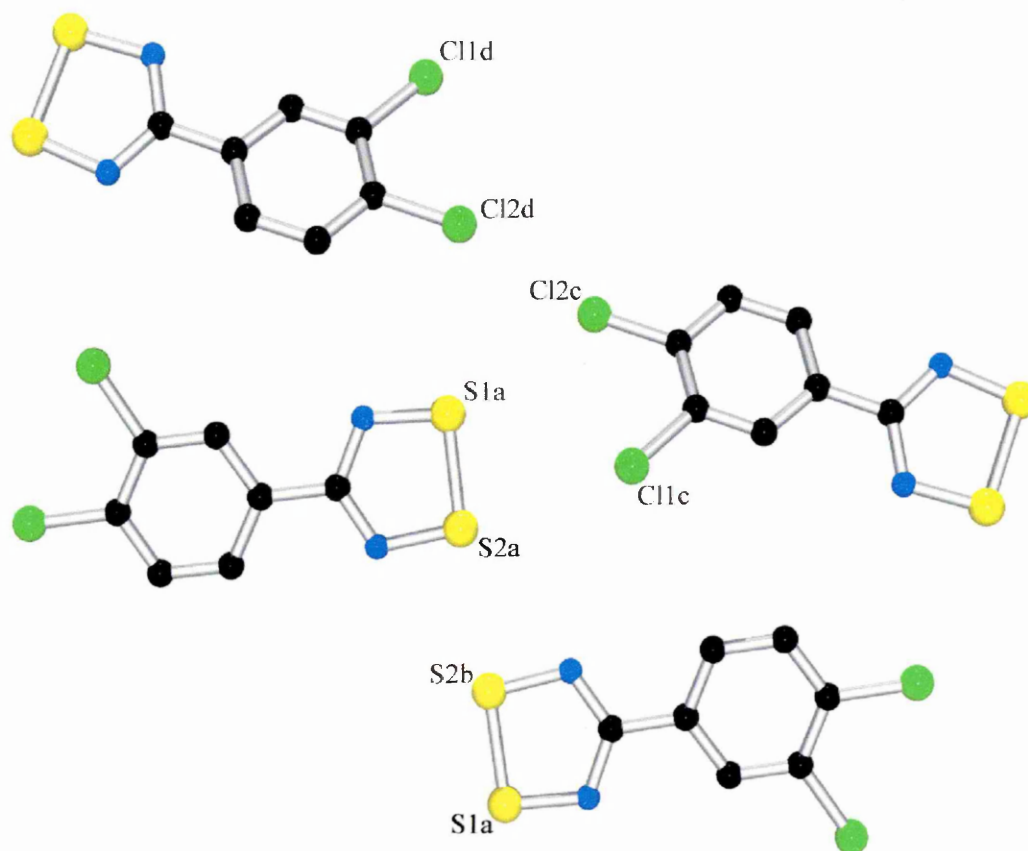


Figure 4.10 Ortep plot of the chain linkage interactions in **2**.

Figure 4.11 shows the overall packing of **2**. The chains are arranged in a herringbone fashion. Each adjacent chain is aligned anti-parallel to its neighbour. There is a striking similarity between the structure of **2** and that of 3,4-difluorophenyl-1,2,3,5-dithiadiazolyl¹ (Figure 4.2), although the absence of S⋯N linkages between adjacent chains in **2** should be noted. In addition, the halogen-halogen interaction observed between the chlorine atoms in the *para* position of **2** is not observed for the fluorinated molecule. The structure again shows the ability of chlorine to interact, firstly to produce a stacking motif, and secondly, to form a chain. The prominence of the Cl⋯Cl interaction within the plane is also an important factor in the overall packing of the molecules.

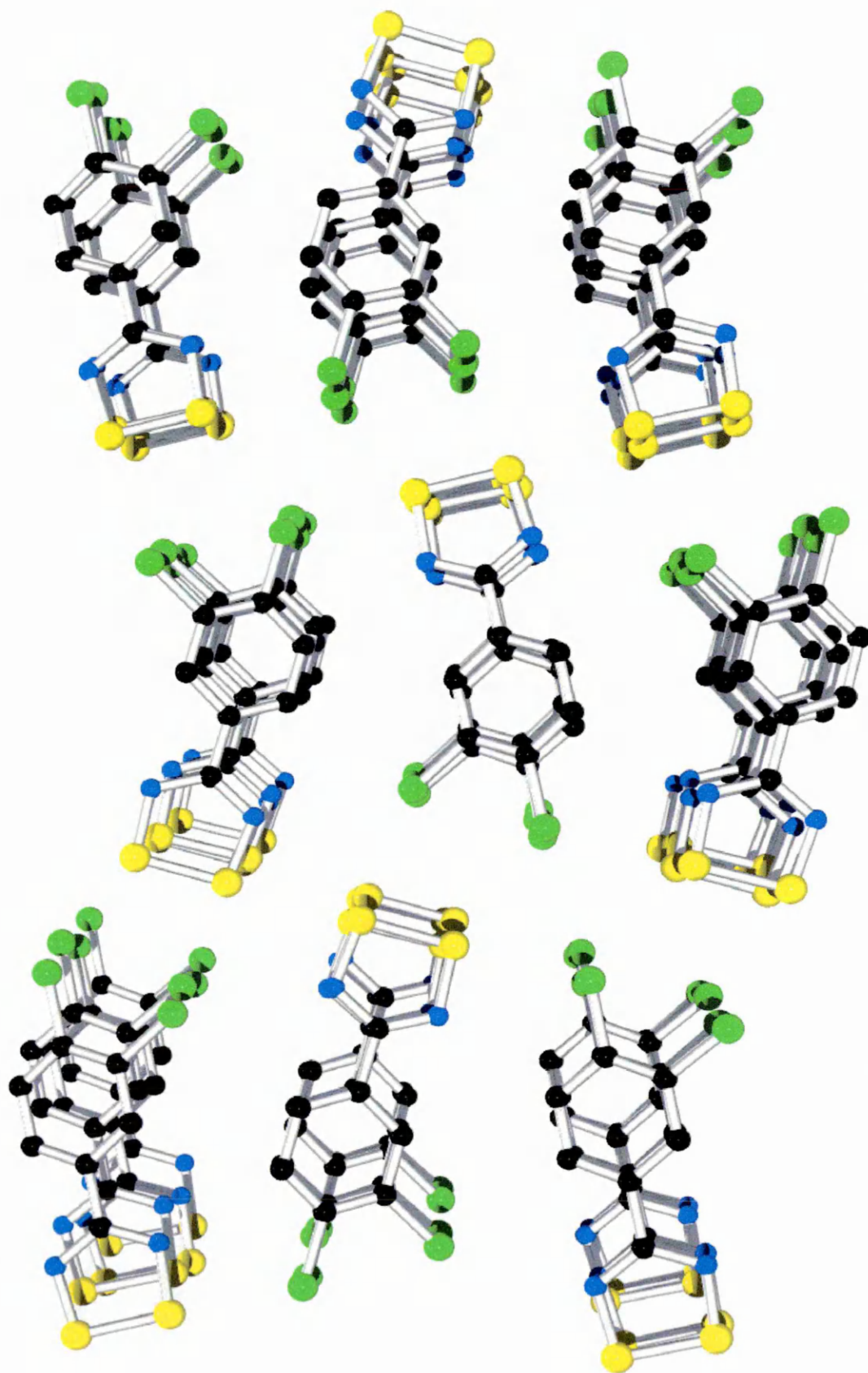


Figure 4.11 Ortep plot of the packing of 3,4-dichlorophenyl-1,2,3,5-dithiadiazolyl

4.2 Conclusions

Although the two compounds presented in this chapter are of little interest either magnetically or electronically, they illustrate the effects of chlorine substituents on the molecular packing of dithiadiazolyls. The use of chlorine in place of previously reported fluorinated derivatives has made a marked difference on the overall structure of the compounds under investigation. In addition, observations on the extent of electrostatic S...Cl interactions to form chains of radical units may also have future use in the development of molecular magnets.

4.3 References

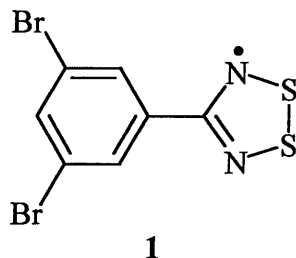
- 1 A.J. Banister, A.S. Batsanov, O.G. Dawe, J.A.K. Howard, J.E. Davies, J.M. Rawson and J.N.B. Smith, *Phosphorus, Sulfur, and Silicon*, 1997, **124**, 553.
- 2 L. Beer, A.W. Cordes, D.J.T. Myles, R.T. Oakley and N.J. Taylor, *Cryst. Eng Comm.*, 2000, 20.
- 3 A.J. Banister, A.S. Batsanov, O.G. Dawe, P.L. Herbertson, J.A.K. Howard, S. Lynn, I. May, J.N.B. Smith, J.M. Rawson, T.E. Rogers, B.K. Tanner, G. Antorrena and F. Palacio, *J. Chem. Soc., Dalton Trans.*, 1997, 2539.
- 4 A.M.T. Bell, J.N.B. Smith, J.P. Attfield, J.M. Rawson, K. Shankland and W.I.F. David, *New J. Chem.*, 1999, **23**, 565.
- 5 R.T. Boéré and K.H. Mook, *Z. Anorg. Allg. Chem.*, 1994, **620**, 1589.
- 6 A. Vegas, A. Pérez-Salazar, A.J. Banister and R.G. Hey, *J. Chem. Soc., Dalton Trans.*, 1980, 1812.
- 7 J.M. Rawson, A.J. Banister and I. Lavender, *Adv. Heterocycl. Chem.*, 1995, **62**, 137.
- 8 S.C. Nyburg and C.H. Faerman, *Acta. Cryst.*, 1985, **B41**, 274.

Chapter 5

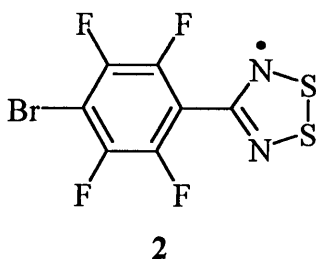
The Structure and Physical Properties of 3,5-dibromophenyl- 1,2,3,5-dithiadiazolyl

5.0 Introduction

This chapter describes the crystallographic characterisation of 3,5-dibromophenyl-1,2,3,5-dithiadiazolyl (**1**). An investigation of the physical properties of **1** in the solid state and in solution is also presented.



The use of bromine substituents has not been extensively studied in dithiadiazolyl chemistry although its steric bulk will inevitably have a marked effect on the association of the dithiadiazolyl ring systems in the solid state. The idea behind the strategy stemmed from the structural study of 3,5-dichlorophenyl-1,2,3,5-dithiadiazolyl (Chapter 3, Page 77) which associates in uniformly spaced stacks. Theoretical studies indicate that Br...Br interactions, like Cl...Cl interactions, should direct the structures of polybrominated aromatic molecules towards stacked motifs.¹ Moreover, it was hoped that the greater size of bromine would increase the distance between neighbouring molecules within the stacks. A recent communication showed that the addition of bromine to the *para* position of a per-fluorinated phenyl dithiadiazolyl (**2**)² could produce a compound that retains its paramagnetic nature in the solid state. It is thought that its low dimensionality leads to the absence of any long-range magnetic order.



5.1 X-Ray Crystal Structure

An Ortep structural plot of the asymmetric unit of **1** shown in Figure 5.1. Bond lengths and angles for **1** are listed in Tables 5.1 and 5.2 together with data for $(\text{Ph} \overline{\text{CNSSN}})_2^3$ and **2**² for comparative purposes. The full crystallographic data for **1** can be found in appendix 8.

The molecular structure of **1** is, as expected, similar to the molecular structure of most previously published aryl substituted dithiadiazolyls. Within each molecule, the aryl and dithiadiazolyl rings are essentially coplanar with a slight torsion angle between the dithiadiazolyl ring and the aryl ring of 7.4° and 5.5° (two molecules in the asymmetric unit). This value is similar to that observed for aryl substituents not possessing a large substituent in the *ortho* position (eg $\text{Ph} \overline{\text{CNSSN}}$ torsion angle = 7°).

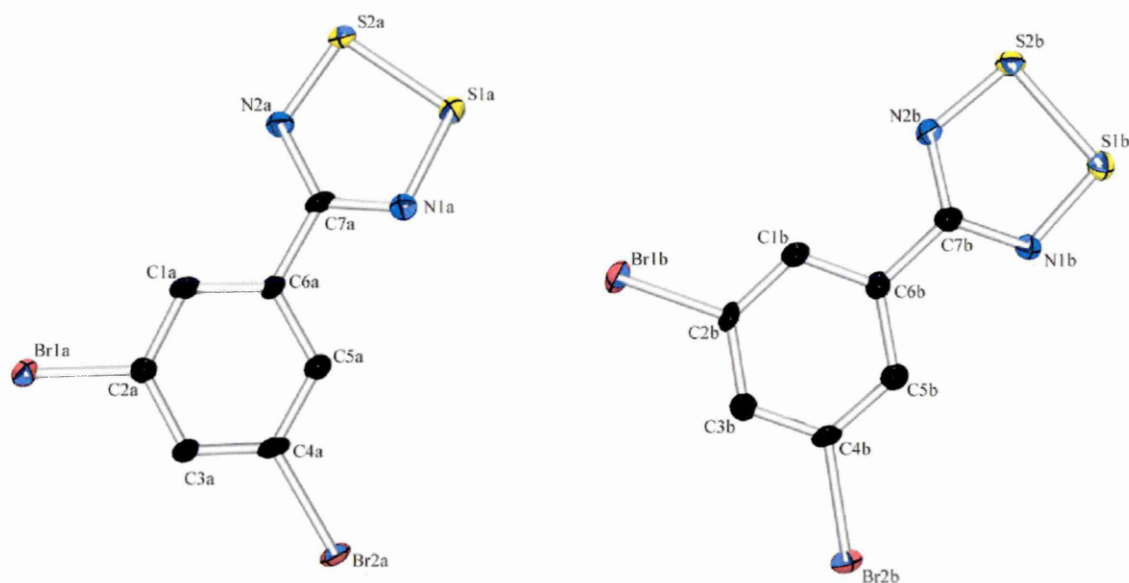


Figure 5.1 Ortep plot of 3,5-dibromophenyl-1,2,3,5-dithiadiazolyl (**1**)

Table 5.1 Bond lengths of 1 (Å).

Atom Numbers	Bond Distance (Å)			
	(1)a	(1)b	(2)	Ph. $\overline{\text{CNSSN}}$
Br(1)-C(2)	1.896(4)	1.891(3)	-	-
Br(2)-C(4)	1.893(4)	1.897(4)	-	-
Br(1)-C(3)	-	-	1.885	
S(1)-N(1)	1.638(3)	1.643(3)	1.640(8)	1.63
S(1)-S(2)	2.0914(13)	2.0963(14)	2.070(4)	2.096
S(2)-N(2)	1.633(3)	1.623(3)	1.624(9)	1.63
N(1)-C(7)	1.333(5)	1.327(5)	1.317(14)	1.32
N(2)-C(7)	1.349(5)	1.343(5)	1.327(12)	1.31
C(1)-C(2)	1.390(5)	1.386(5)	1.385	1.37
C(1)-C(6)	1.400(5)	1.407(5)	1.373	1.37
C(2)-C(3)	1.387(5)	1.378(5)	1.378	1.39
C(3)-C(4)	1.399(5)	1.399(5)	1.369	1.42
C(4)-C(5)	1.388(5)	1.381(5)	1.373	1.36
C(5)-C(6)	1.403(5)	1.402(5)	1.379	1.38
C(6)-C(7)	1.466(5)	1.494(5)	1.497	1.50

Table 5.2 Bond angles of **1** (°)

Atom Numbers	Angle (degrees)			
	(1)a	(1)b	(2)	Ph. $\overline{\text{CNSSN}}$
N(1)-S(1)-S(2)	94.67(12)	94.09(12)	93.7(4)	93.0
N(2)-S(2)-S(1)	94.55(12)	94.70(12)	95.5(3)	94.1
C(7)-N(1)-S(1)	113.9(3)	114.0(3)	113.9(7)	116
C(7)-N(2)-S(2)	113.9(3)	114.1(3)	112.8(7)	115
N(1)-C(7)-N(2)	118.9(3)	123.1(3)	124.0(9)	122
N(1)-C(7)-C(6)	116.8(3)	119.6(3)	117.5(3)	117
N(2)-C(7)-C(6)	120.3(3)	117.3(3)	118.4(1)	121
C(3)-C(2)-Br(1)	118.0(3)	118.4(3)	-	-
C(1)-C(2)-Br(1)	119.6(3)	119.9(3)	-	-
C(5)-C(4)-Br(2)	118.2(3)	120.4(3)	-	-
C(3)-C(4)-Br(2)	119.8(3)	117.6(3)	-	-
C(4)-C(3)-Br(1)	-	-	121.5(9)	-
C(2)-C(3)-Br(1)	-	-	119.6(8)	-
C(1)-C(2)-C(3)	122.3(3)	121.7(3)	119.5(0)	120
C(4)-C(3)-C(2)	117.7(3)	118.0(3)	118.7(1)	119
C(3)-C(4)-C(5)	121.9(3)	122.0(3)	121.5(1)	120
C(4)-C(5)-C(6)	118.9(3)	118.9(3)	120.8(2)	119
C(5)-C(6)-C(1)	120.3(3)	120.6(3)	116.9(9)	121
C(1)-C(6)-C(7)	120.9(3)	119.0(3)	120.5(1)	120
C(5)-C(6)-C(7)	118.8(3)	120.4(3)	122.4(7)	121
C(6)-C(1)-C(2)	118.9(3)	118.8(3)	122.4(6)	119
Twist Angle*	7.4	5.5	51.8	7

The unit cell of **1** contains eight molecules of $(\text{Br}_2\cdot\text{C}_6\text{H}_3\cdot\overline{\text{CNSSN}})_2$, two halves of which are in the asymmetric unit. Figure 5.2 shows the association of two dimers within the unit cell. The mode of association within each dimer is *cis*-cofacial, which is the most common motif for dithiadiazolyl radicals. The intradimer distances are short (S1a \cdots S1b, 3.180 Å; S2a \cdots S2b, 2.999 Å) lying within the normal range for dithiadiazolyl dimers (3.0 - 3.2 Å).⁴ Unlike many other dithiadiazolyls, the individual molecules within a dimer do not lie co-planar to each other. Instead, the steric repulsion causes the molecules to twist with respect to each other. The bromine contacts within the dimer are considerably longer than those of sulfur (Br1a \cdots Br1b, 3.966 Å; Br2a \cdots Br2b, 4.270 Å), which might be expected because of the larger size of bromine compared to sulfur. In fact the Br \cdots Br contacts within the dimer fall outside that of the sum of the van der Waals radii (3.72 Å)⁵ so can be classed as having no interaction with each other. To a lesser extent, this type of twisted dimer has also been observed for Ph. $\overline{\text{CNSSN}}$ ³ but the effect in **1** is much larger. The dihedral angle S-S to S-S are 6.56° and 17.6° for Ph. $\overline{\text{CNSSN}}$ and **1** respectively.

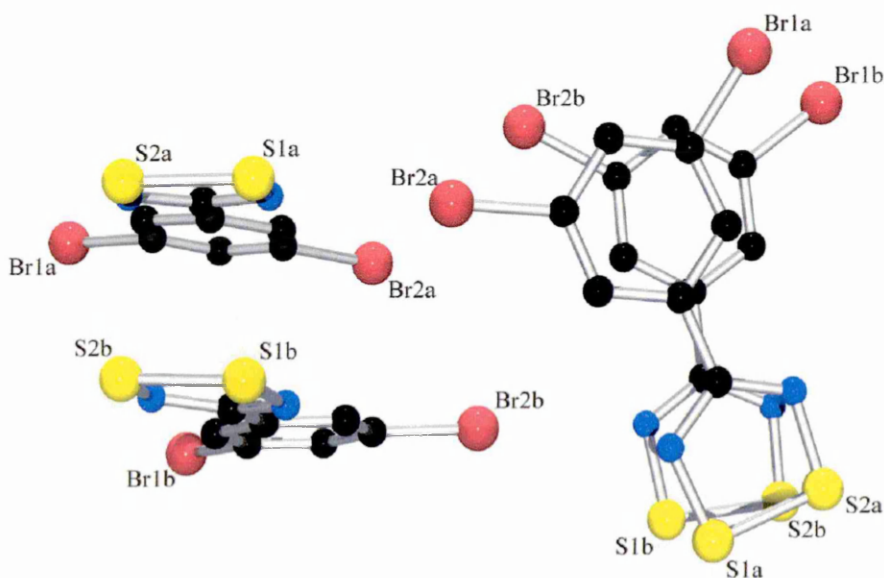


Figure 5.2 Ortep plot of the dimerisation of **1**

Each dimer pair shown in Figure 5.2 is associated as a stack of two dimers aligned in antiparallel directions (Figure 5.3). They are related *via* a 2-fold rotation and a glide plane in the *c*-direction. Although forming part of a stack of four individual dithiadiazolyl molecules, they are not joined by any close interactions. The reason for this packing arrangement is likely to be due to the steric repulsion of the large bromine atoms between adjacent dimers. This type of association was also observed for *p*-NC.C₆H₄. $\overline{\text{CNSSN}}$ ⁶ (Figure 5.4). In this case, the electrostatic attraction of the more negative nitrile group to the sulfur of the layer above may be the controlling factor of the packing of the molecules.

Perpendicular to the stack of two dimers is a second pair of dimers, which associate in an identical stack (Figure 5.3). The separate stacks are attached together by weak Br \cdots S interactions (3.310 Å in comparison to the sum of the van der Waals radii of 3.75 Å).⁵ The association of the dimers perpendicular to each other shows no close Br \cdots Br contacts. The apparent attractive nature of chlorine observed in earlier chapters (chapters 3 and 4) does not occur for bromine atoms, which appear to repel each other in the solid state.

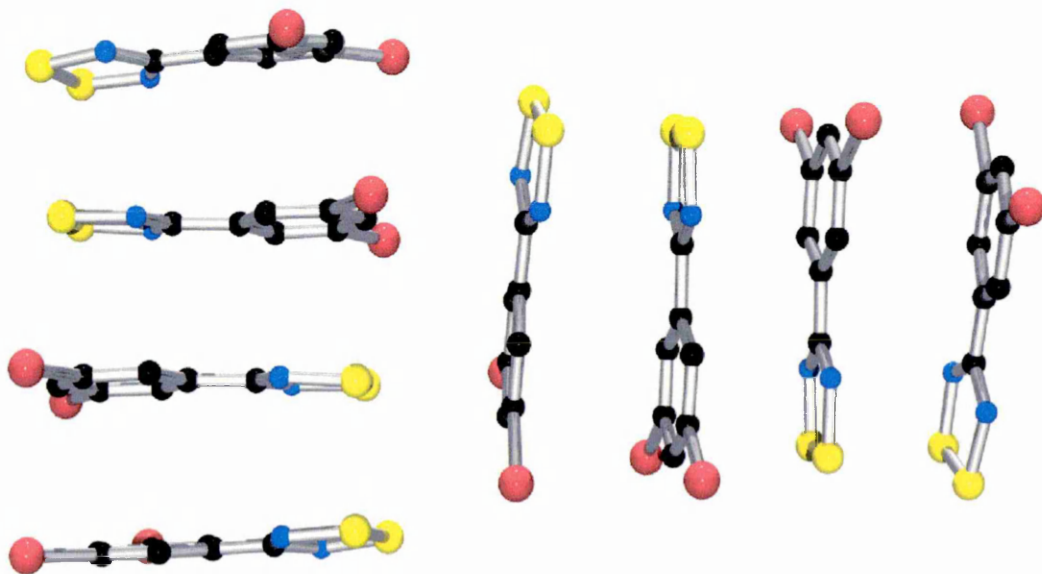


Figure 5.3 Orteplot of the interactions of 1

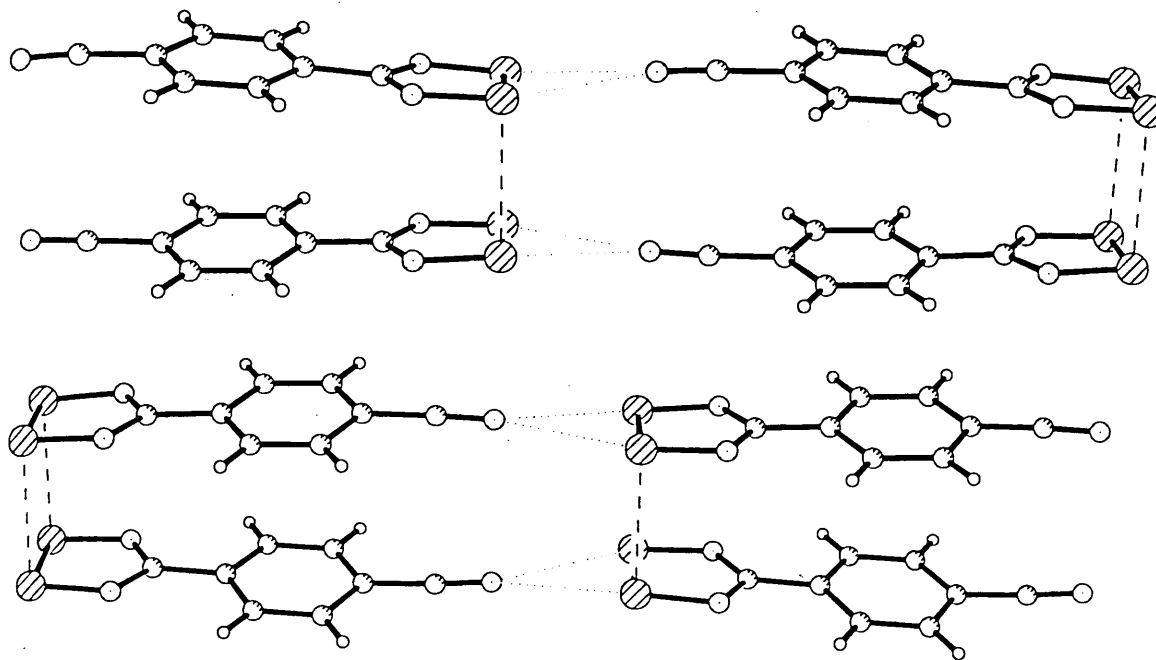


Figure 5.4 The crystal structure of $p\text{-CN.C}_6\text{H}_4.\overline{\text{CNSSN}}$ ⁶

The interactions observed in Figures 5.2 and 5.3 are repeated for every stack of two dimers within the structure. This creates an overall packing structure (Figure 5.5) with dithiadiazolyl units lying in two distinct planes. It is unclear why the molecules pack in this way, but it could be due to the directional nature of halogen interactions.⁷

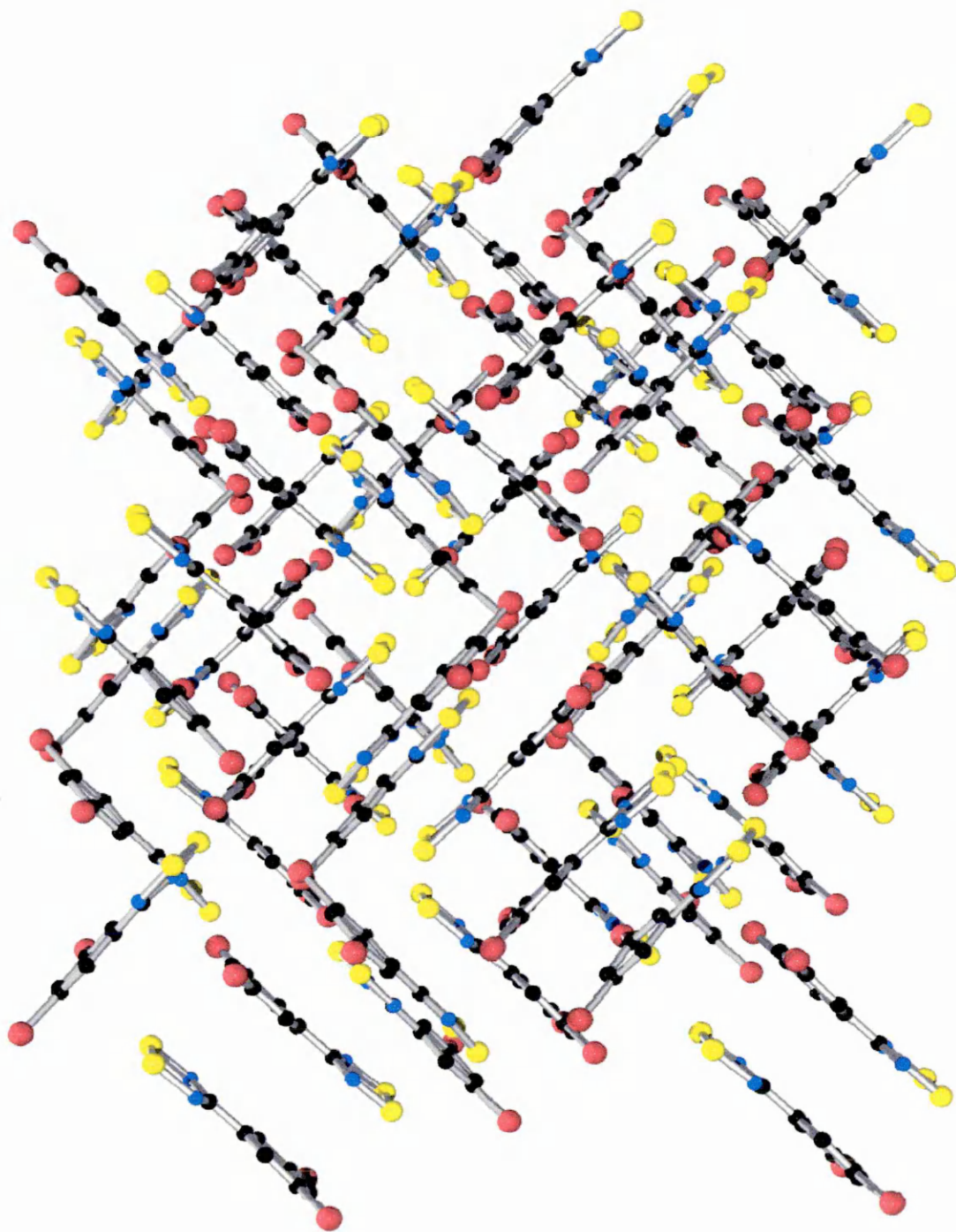


Figure 5.4 Ortep plot the packing of 3,5-dibromophenyl-1,2,3,5-dithiadiazolyl

5.2 Electron Paramagnetic Resonance Study

Compound **1** has been studied by electron paramagnetic resonance (EPR) spectroscopy. The properties of the monomeric radical were investigated by analysis of a frozen glass sample in dimethyl formamide.

5.2.1 Frozen Glass Studies

Solution samples were prepared by the dissolution of a few milligrams of **1** in approximately 0.5 ml of DMF. The resulting solution was treated with a drop of toluene to aid the formation of a satisfactory 'glass' when analysed. The solution was added to a quartz tube, which was sealed prior to analysis.

As expected for the solution, the spectra observed, and values obtained, were very similar to previous studies on dithiadiazolyls. The aim of the frozen glass study was to gain accurate information about the unpaired electron when the interactions between adjacent radical centres are at a minimum. This in turn leads to spectra exhibiting the properties of the monomer. Table 5.3 shows the calculated g-factors and where applicable the values for hyperfine splitting for **1** (K-band) and Ph. $\overline{\text{CNSSN}}$.⁸

	1	Ph. $\overline{\text{CNSSN}}$
Temperature	105 K	176 K
g_x	2.00875	2.0021
g_y	2.0023	2.0078
g_z	2.0219	2.0218
a_y/G	14.0	

Table 5.3 Frozen glass study of **1** and Ph. $\overline{\text{CNSSN}}$.

The spectrum has a peak ratio pattern of 1:2:3:2:1 (from two equivalent nitrogen-14 nuclei), which is typical for 1,2,3,5-dithiadiazolyl radicals. The calculated g-values are also typical for a radical species with significant unpaired spin density. Unfortunately, a suitable crystal for analysis could not be grown and so no crystal data could be recorded. Figure 5.6 shows the EPR frozen glass spectrum of **1**, including a computer generated simulation.

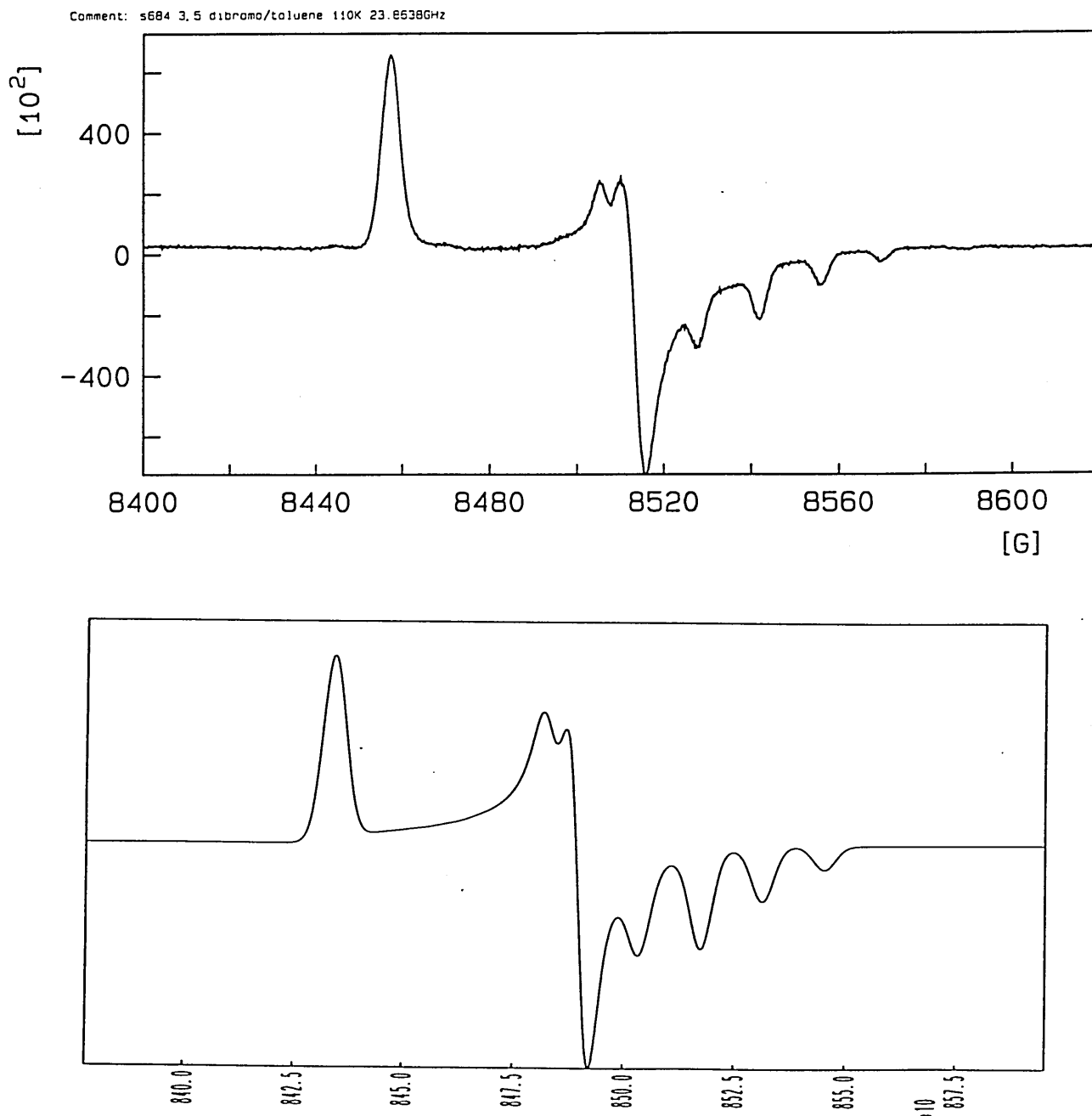


Figure 5.6 K-band EPR frozen glass spectrum of **1** at 105 K (top) and a computer generated simulation (bottom).

5.3 Conclusions

From the results reported in this chapter, it is clear that bromine atoms can have a significant effect on the dimerisation of dithiadiazolyls. The slightly twisted mode of association within the dimer is more pronounced than previously observed in the phenyl derivative, but is much less than the twisted conformations reported previously.⁹ The observed structural features clearly result from the large steric bulk of the bromine atoms.

5.4 References

- 1 (a) G.R. Desiraju and R. Parthasarathy, *J. Am. Chem. Soc.*, 1989, **111**, 8725; (b) V.R. Pedireddi, D.S. Reddy, B.S. Goud, D.C. Craig, A.D.Rae and G.R. Desiraju, *J. Chem. Soc., Perkin Trans. 2*, 1994, 2353.
- 2 G. Antorrena, J.E. Davies, M. Hartley, F. Palacio, J.M. Rawson, J.N.B. Smith and A. Steiner, *Chem. Commun.*, 1999, 1393.
- 3 A. Vegas, A. Pérez-Salazar, A.J. Banister and R.G. Hey, *J. Chem. Soc., Dalton Trans.*, 1980, 1812.
- 4 J.M. Rawson, A.J. Banister and I. Lavender, *Adv. Heterocycl. Chem.*, 1995, **62**, 137.
- 5 S.C. Nyburg and C.H. Faerman, *Acta. Cryst.*, 1985, **B41**, 274.
- 6 A.W. Cordes, R.C. Haddon, R.G. Hicks, R.T. Oakley and T.T.M. Palstra, *Inorg. Chem.*, 1992, **31**, 1802.
- 7 G.R. Desiraju and R. Parthasarathy, *J. Am. Chem. Soc.*, 1989, **111**, 8725.
- 8 S.A. Fairhurst, K.M. Johnson, H. Sutcliffe, K.F. Preston, A.J. Banister, Z.V. Hauptman and J. Passmore, *J. Chem. Soc., J. Chem. Soc., Dalton Trans., Trans.*, 1986, 1465.
- 9 (a) H.-U. Höfs, J.W. Bats, R. Gleiter, G. Hartmann, R. Mews, M. Eckert-Maksic, H. Oberhammer and G.M. Sheldrick, *Chem. Ber.*, 1985, **118**, 3781; (b) A.J. Banister, M.I. Hansford, Z.V. Hauptman, S.T. Wait and W. Clegg, *J. Chem. Soc., Dalton Trans.*, 1989, 1705; (c) W.V.F. Brookes, N. Burford, J. Passmore, M.J. Schriver and L.H. Sutcliffe, *J. Chem. Soc., Chem. Commun.*, 1987, 69; (d) A.J. Banister, A.S. Batsanov, O.G. Dawe, P.L. Herbertson, J.A.K. Howard, S. Lynn, I. May, J.N.B. Smith, J.M. Rawson, T.E. Rogers, B.K. Tanner, G. Antorrena and F. Palacio, *J. Chem. Soc., Dalton Trans.*, 1997, 2539; (e) A.J. Banister, A.S. Batsanov,

O.G. Dawe, J.A.K. Howard, J.E. Davies, J.M. Rawson and J.N.B. Smith,
Phosphorus, Sulfur, and Silicon, 1997, **124**, 553.

Chapter 6

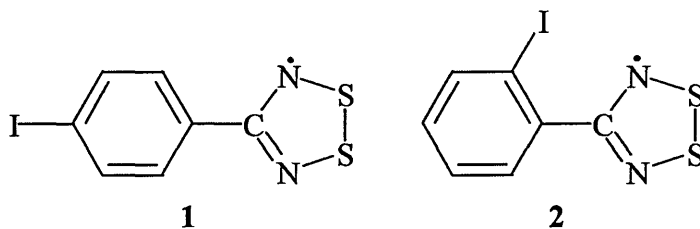
The Synthesis, Structure and Physical

Properties of Iodophenyl-

1,2,3,5- Dithiadiazolyl Radicals

6.0 Introduction

This chapter describes the characterisation of two iodophenyl dithiadiazolyls **1** and **2** and the synthesis of their respective cyano starting products. Compound **1** was successfully crystallised and its crystal structure determined. An investigation of the physical properties of **1** in the solid state and in solution is also discussed. The crystal structure of **2** has not been determined because the compound purifies as a viscous oil.



The use of iodophenyl derivatives in dithiadiazolyl radicals has not previously been investigated although the steric bulk of the iodine group would almost certainly have a marked effect on the association of the dithiadiazolyl radicals in the solid state. The idea behind the strategy stemmed from the structure of *p*-iodobenzonitrile,¹ and the cyanogen halides, XCN (X = Cl, Br, or I),² which assemble in chains through dipolar X...CN interactions (N...I distance = 3.18 Å, c.f. van der Waals contact distance, 3.65 Å). In the case of *p*-iodobenzonitrile, alternate chains run in opposite directions. Other work has shown that association of monomeric dithiadiazolyl radicals³ into supramolecular chains can facilitate bulk magnetic properties⁴ (i.e. *p*-CN.C₆F₄. $\overline{\text{CNSSN}}^{\bullet}$).

6.1 Synthesis of *para* and *ortho*-Iodobenzonitrile

Para- and *ortho*-iodobenzonitrile were prepared by the following reaction sequence (Scheme 6.1). The appropriate benzoyl chloride was initially added to a concentrated ammonia solution and, after stirring, the product was filtered and washed to yield *p*- or *o*-iodobenzamide as a white solid in almost quantitative yield. The dehydration of the amide derivative was completed using phosphorus pentoxide in an evacuated, cold finger, sublimation vessel (Figure 6.1). On heating white crystals of the corresponding nitrile formed on the sublimation finger and no further purification was required.

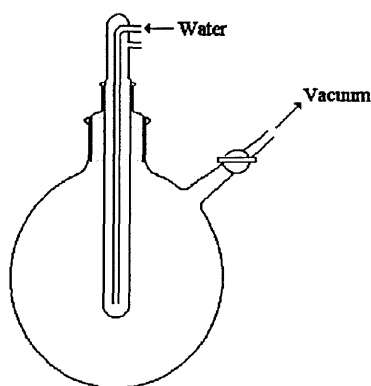
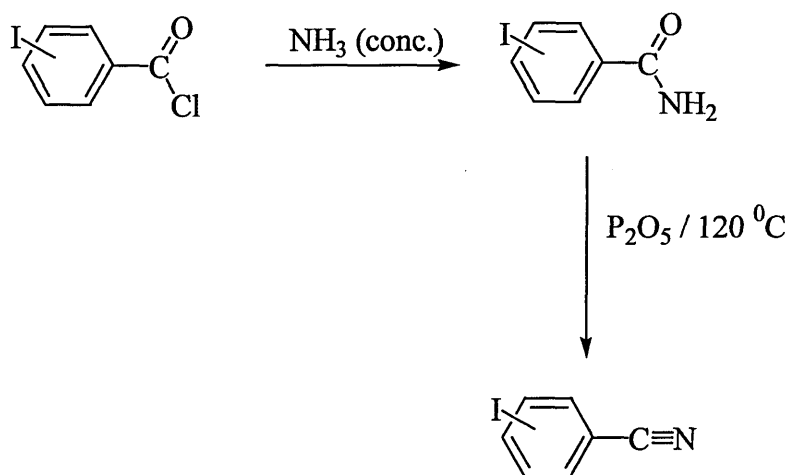


Figure 6.1 Cold finger sublimation vessel



Scheme 6.1 Synthetic route for *p*- and *o*-iodobenzonitrile

The subsequent conversion of the iodobenzonitrile into the dithiadiazolyl radical was completed using the standard methodology outlined in chapter 2. Purification of the

radicals was completed by vacuum sublimation. Compound **1**, after sublimation onto a cold finger, crystallised in a gradient sublimer as dark red/black blocks, suitable for x-ray and EPR crystal analysis. In contrast, compound **2** forms as a viscous purple/ red oil. The reason for this would seem to lie in the steric hindrance caused by the iodine group in the *ortho* position. A similar effect was observed for a tertiary butyl derivative, which also hinders dimerisation of the dithiadiazolyl ring.⁵

6.2 X-ray Crystal Structure of *p*-iodophenyl-1,2,3,5-dithiadiazolyl

An Ortep plot of the asymmetric unit is shown in Figure 6.2. The bond lengths and angles in **1** are listed in Tables 6.1 and 6.2 together with data for $(\text{Ph}\overline{\text{CNSSN}})_2$ ⁶ and *p*-iodobenzonitrile¹ for comparative purposes. The full crystallographic data for compound **1** can be found in appendix 9.

The molecular structure of **1** is, as expected, similar to the molecular structures of most other aryl substituted dithiadiazolyls. Within each molecule the aryl and dithiadiazolyl rings are essentially coplanar with a slight torsion angle between the dithiadiazolyl ring [root mean square (r.m.s.) $\Delta = 0.0077 \text{ \AA}$] and the aryl ring (r.m.s. $\Delta = 0.0089 \text{ \AA}$) of 8° . This value is similar to that observed for aryl substituents not possessing a bulky substituent in the *ortho* position (eg $\text{Ph}\overline{\text{CNSSN}}$ torsion angle = 7°).

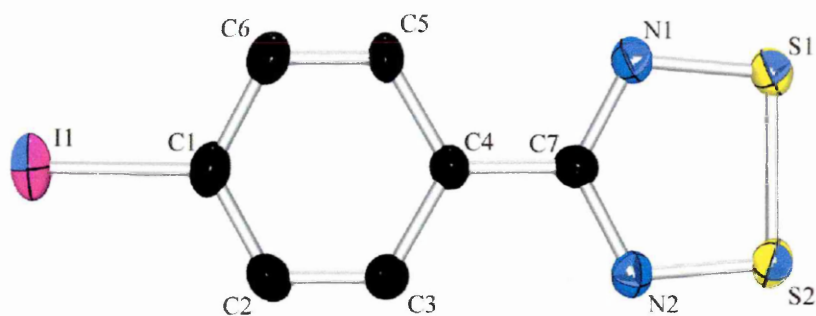


Figure 6.2 Ortep plot of **1** (*p*-iodophenyl-1,2,3,5-dithiadiazolyl)

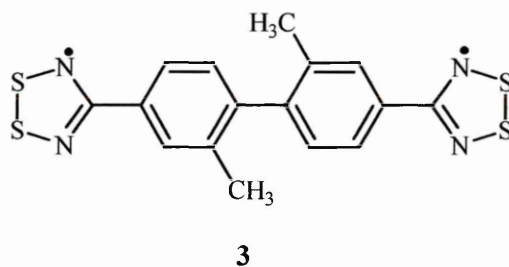
Table 6.1 Bond lengths of **1** (Å).

Atom Numbers	Bond Distance (Å)		
	(1)	<i>p</i> -IC ₆ H ₄ CN	Ph. $\overline{\text{CNSSN}}$
I(1)-C(1)	2.094(6)	2.064	-
S(1)-N(1)	1.635(5)	-	1.63
S(1)-S(2)	2.098(2)	-	2.096
S(2)-N(2)	1.629(5)	-	1.63
N(1)-C(7)	1.337(7)	-	1.32
N(2)-C(7)	1.347(6)	-	1.31
C(1)-C(2)	1.371(7)	1.407	1.39
C(1)-C(6)	1.388(8)	1.407	1.42
C(2)-C(3)	1.376(8)	1.385	1.37
C(3)-C(4)	1.398(8)	1.401	1.37
C(4)-C(5)	1.410(7)	1.401	1.38
C(5)-C(6)	1.365(7)	1.385	1.36
C(4)-C(7)	1.464(7)	1.370	1.50

Table 6.2 Bond angles of **1** (°)

Atom Numbers	Angle (degrees)		
	(1)	<i>p</i> -IC ₆ H ₄ CN	Ph. $\overline{\text{CNSSN}}$
N(1)-S(1)-S(2)	94.45(18)	-	93.0
N(2)-S(2)-S(1)	94.26(17)	-	94.1
C(7)-N(1)-S(1)	114.6(4)	-	116
C(7)-N(2)-S(2)	114.8(4)	-	115
N(1)-C(7)-N(2)	121.9(5)	-	122
N(1)-C(7)-C(4)	119.4(5)	-	117
N(2)-C(7)-C(4)	118.7(5)	-	121
C(2)-C(1)-I(1)	120.6(4)	121	-
C(6)-C(1)-I(1)	118.4(4)	121	-
C(1)-C(2)-C(3)	119.7(5)	121.2	120
C(2)-C(1)-C(6)	120.9(5)	118.0	119
C(4)-C(3)-C(2)	121.2(5)	120.1	121
C(3)-C(4)-C(5)	117.3(5)	119.5	121
C(4)-C(5)-C(6)	121.5(5)	120.1	119
C(5)-C(6)-C(1)	119.2(5)	121.2	120
C(3)-C(4)-C(7)	121.3(5)	120.25	120
C(5)-C(4)-C(7)	121.4(5)	120.25	119
Twist Angle*	8	-	7

Like the majority of dithiadiazolyl compounds **1** associates as dimers in the solid-state. However, the mode of association is unusual. Two molecules of **1** come together in a *trans*-cofacial manner across an inversion centre (Figure 6.3). This is only the second example of a dithiadiazolyl adopting this mode of association, the first [2,2'-dimethyldiphenylene radical (**3**)] was reported only recently.⁷ One of the heterocycles in **3** associates in a *trans*-cofacial manner, the other heterocycle is un-associated resulting in a paramagnetic material.



The interannular separation can be calculated to be the gap between two mid points of the heterocyclic rings. For **1** this value is 3.121 Å which is significantly shorter than that of **3** (3.24 Å). These compared favourably to the normal separation observed for dithiadiazolyl dimers, showing *cis*-cofacial and *trans*-antarafacial modes of association (3.0 - 3.2 Å). However, the interdimer S⋯S contacts for **1** (S1a⋯S1b and S2a⋯S2b, 3.696 Å) are significantly longer than the normal S⋯S distance in dithiadiazolyl dimers (S⋯S contacts typically 3.0 – 3.2 Å). In **3** similar interdimer S⋯S distances are observed [6.68(2) Å]. Each dimer pair also has two sets of S⋯N interactions (N1a⋯S1b and N2a⋯S2a, 3.152 Å; N2a⋯S2b and N1b⋯S1a 3.116 Å). The asymmetry of these interactions is due to further interactions between one sulfur atom and an iodine atom of an adjacent molecule (*vide infra*).

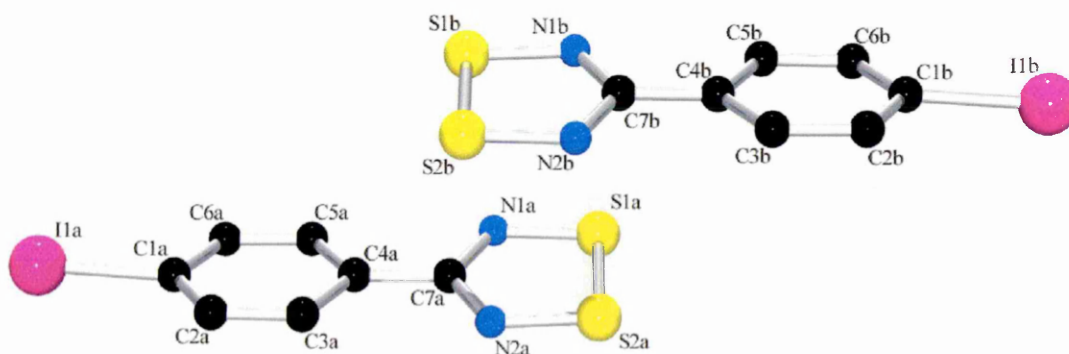
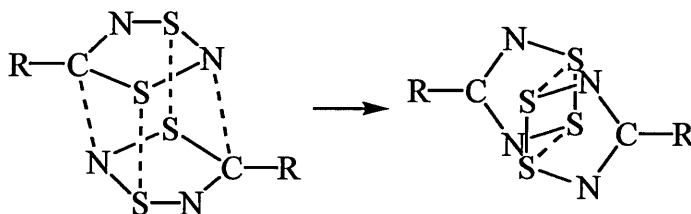
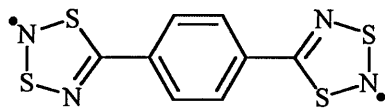


Figure 6.3 ORTEP plot of the *trans*-cofacial association of **1**.

As noted by Oakley and co-workers,⁷ the *trans*-cofacial mode of dimerisation adopted by **1** and **3** lies close to the transition state for the proposed photochemical isomerisation of 1,3,2,4- to 1,2,3,5-dithiadiazolyl (Scheme 6.2).^{5,8,9} Indeed the molecular structures of **1** and **3** show many similarities with that of 5,5'-(1,4-phenylene)bis(1,3,2,4-dithiadiazolyl) **4**,⁸ which contains short S⋯S (3.214 Å) and S⋯N (3.346 Å) interactions between parallel dithiadiazolyl rings. The *trans*-cofacial mode of dimerisation observed in **1** is unusual and I speculate that the molecules dimerise in this way to alleviate steric hindrance between the two iodine atoms that would occur if the molecules associated in a *cis*-cofacial manner. However, it is less obvious why *trans*-antarafacial or twisted geometries are disfavoured in this instance. In this study, the correlation between **1** and **4** is limited to a purely structural comparison. Further work should include theoretical studies to determine what factors prevent the molecules of **1** from sliding to give a *trans*-antarafacial geometry.



Scheme 6.2 Photochemical isomerisation of 1,2,3,4- to 1,2,3,5- dithiadiazolyl.^{5,8}



4

Each molecule of **1** is linked through a weak interaction between an iodine atom of one molecule and a sulfur atom of an adjacent molecule (Figure 6.4). The I⋯S contact (I1⋯S2, 3.82 Å) is significantly longer than a conventional S-I bond¹⁰ but is within the sum of the van der Waals radii of iodine and sulfur (3.4 – 4.1 Å depending on orientation of the contact vector relative to the bond).¹¹ The second I⋯S contact (I1⋯S1, 4.068 Å) is

at the limit of the van der Waals radii and could only be described as a very weak interaction. Every molecule within the chain is connected to an adjacent chain by *trans*-cofacial association (Figure 6.3). Therefore, each half of a dimer pair is a member of a separate chain running in the opposite direction. Adjacent molecules within the chains occupy orthogonal positions creating chains with a ‘zig-zag’ alignment. This type of arrangement has also been observed for $(p\text{-ClC}_6\text{H}_4\overline{\text{CNSSN}})_2$ ¹² (Figure 3.1, page 61) although the association of the dimers is *via* a *cis*-cofacial manner.

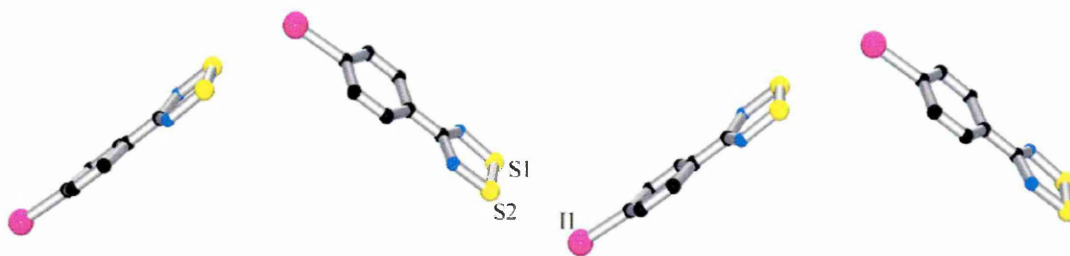


Figure 6.4 Ortep plot of the ‘zig-zag’ chains formed by **1**.

The overall packing of **1** shows a ‘herringbone’ arrangement (Figure 6.5) with adjacent chains along the plane of the rings running in the same direction and are linked by one $\text{S}\cdots\text{N}$ interaction ($\text{S2}\cdots\text{N1}$, 3.425 Å) on each side of the heterocycle. The structure is in contrast to that of *p*-iodobenzonitrile¹ that forms linear chains.

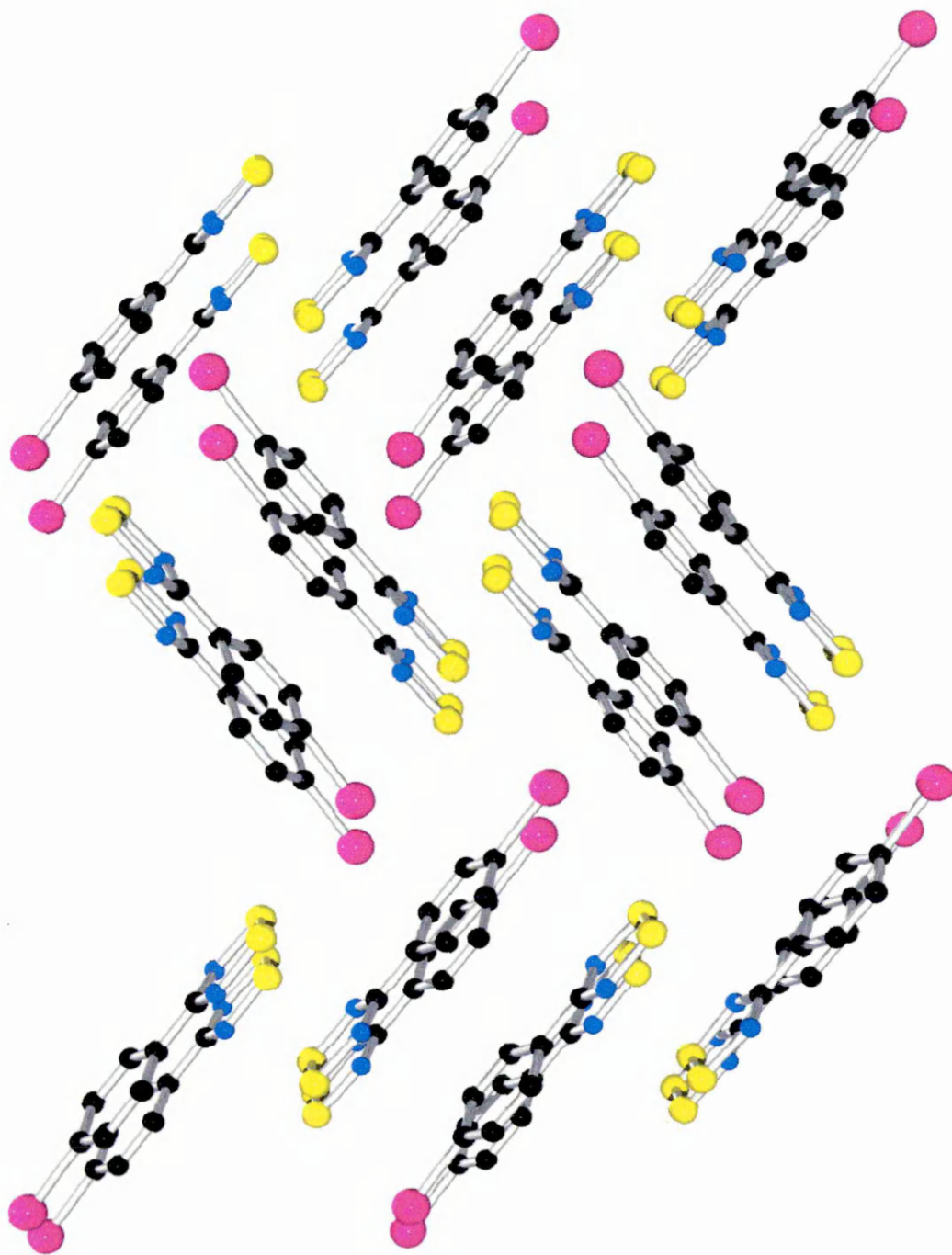


Figure 6.5 Ortepe plot of the packing of 1

6.3 EPR Study of *p*-Iodophenyl-1,2,3,5-dithiadiazolyl

The novel mode of dimerisation of **1** in the solid state makes analysis by EPR desirable. The *trans*-cofacial-associated dimer has never been studied by EPR and information regarding the role of the free radical within this conformation could be gained from solid state measurements. Compound **1** has been studied using frozen glass and single crystal EPR measurements (Spectra not included as analysis is in progress).

6.3.1 Frozen Glass Studies

Solution samples were prepared by the dissolution of a few milligrams of **1** in approximately 0.5 ml of DMF. The resulting solution was treated with a drop of toluene to aid the formation of a satisfactory 'glass' when analysed. The solution was added to a quartz tube, which was sealed prior to analysis.

The frozen glass study showed a spectrum of well-resolved peaks at 105 K but at room temperature the resolution was greatly reduced. The analysis of the frozen glass can be used in conjunction with the crystal measurements in order to identify features belonging to the unpaired electron. This will in-turn help to identify features due to the intermolecular interactions within the crystal. Table 6.3 shows the calculated *g*-factors and where applicable the values for hyperfine splitting for **1** (K-band) and Ph. $\overline{\text{CNSSN}}$.¹³

Table 6.3 Frozen glass study of **1** and Ph. $\overline{\text{CNSSN}}$

	1	Ph. $\overline{\text{CNSSN}}$
Temperature	105 K	176 K
<i>g</i> _x	2.00875	2.0021
<i>g</i> _y	2.0023	2.0078
<i>g</i> _z	2.0219	2.0218
<i>a</i> _y / <i>G</i>	14.0	

The spectrum has a peak ratio pattern of 1:2:3:2:1 (from two equivalent nitrogen-14 nuclei), which is typical for 1,2,3,5-dithiadiazolyl radicals. The calculated g-values are also typical for a radical species with significant unpaired spin density. Figure 6.6 shows the EPR frozen glass spectrum of **1**, including a computer generated simulation.

Receiver	Signal Channel	Field	Microwave
Receiver Gain : 2.00e+04	Conversion : 163.84 ms	Center Field : 8510.00 ^{8456.6} G	Frequency : 29.8643000 GHz
Phase : 0.0 deg	Time Const : 1.28 ms	Sweep Width : 220.00 G	Power : 3.62e+00 mW
Harmonic : 1	Sweep Time : 167.772 s	Resolution : 1024 points	
Mod Frequency : 100 0000 kHz	Scale : 17		
Mod Amplitude : 1.000 G			

Comment: s684 3,5 dibromo/toluene 110K 23.8638GHz

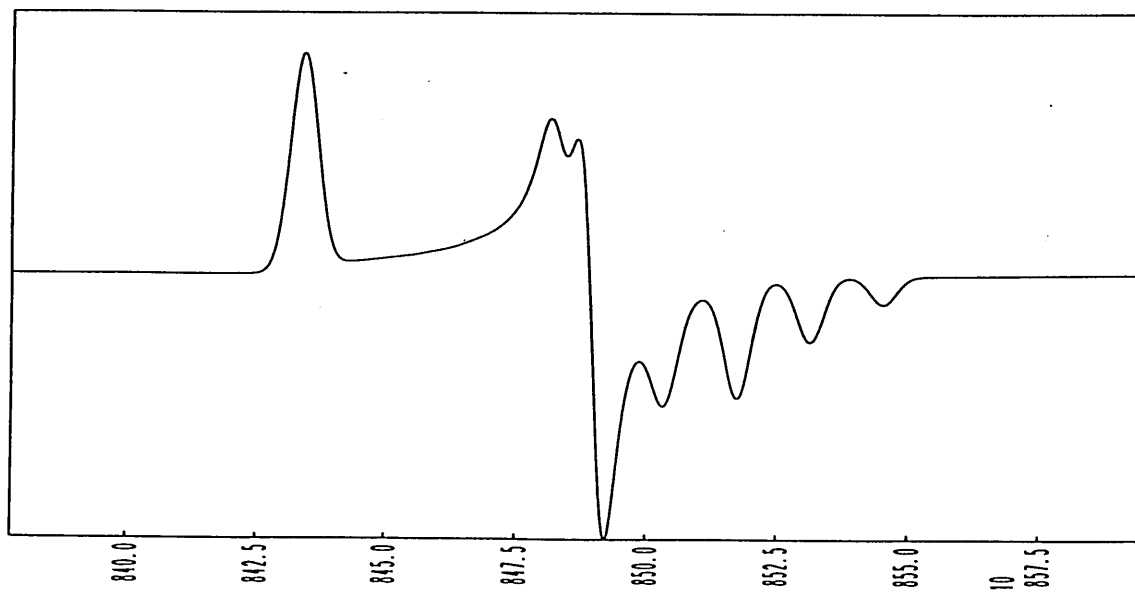
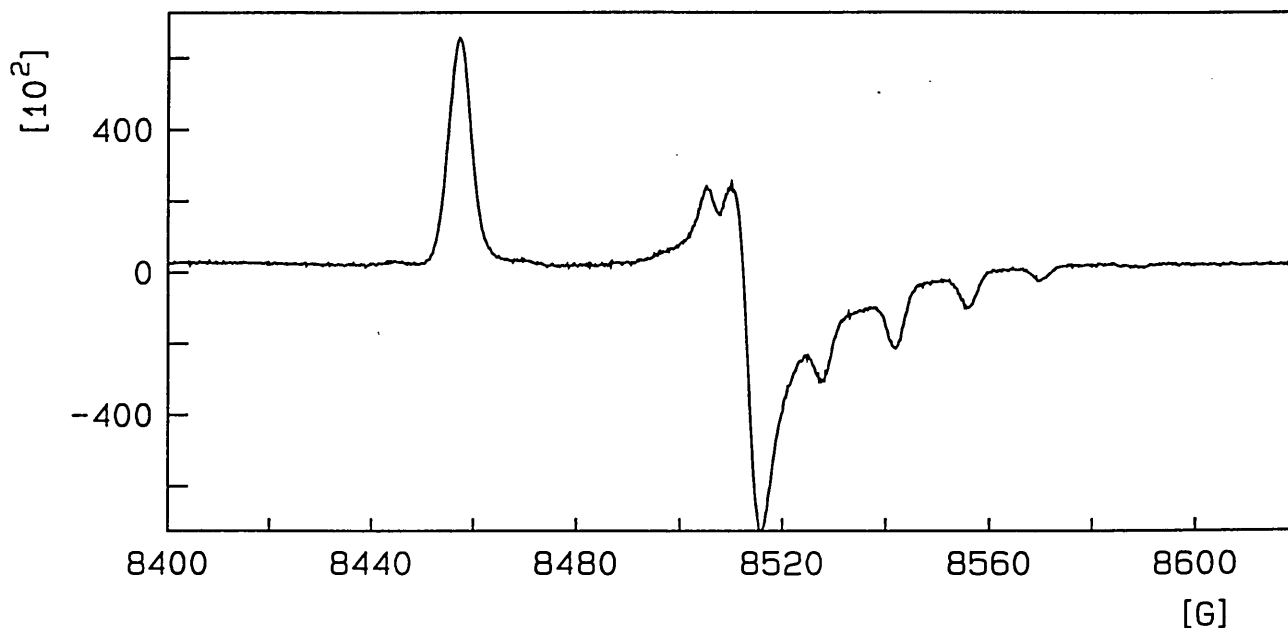
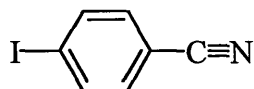


Figure 6.6 K-band EPR frozen glass spectrum of **1** (top), and a computer simulated spectrum (bottom)

6.4 Experimental

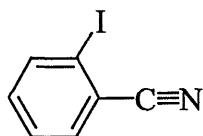
6.4.1 Preparation of *p*-Iodobenzonitrile



Finely powdered *p*-iodobenzoyl chloride (5.32 g, 0.02 mol) was slowly added to ice cold 0.880 ammonia solution (20 ml). The mixture was stirred for two hours and allowed to warm to room temperature. The resulting precipitate, *p*-iodobenzamide, was filtered, washed with water and dried. The *p*-iodobenzamide was then transferred to a 250 cm³ round bottomed flask fitted with a side arm and stopcock, together with a cold-finger. An excess of phosphorus pentoxide was added to the flask and the reactants thoroughly mixed. The flask was heated *in vacuo* (130 °C). The final product, *p*-iodobenzonitrile was isolated directly onto the cold finger from the reaction mixture as white needles. Purification of the final product was achieved by further vacuum sublimation (2.68 g, 59% yield)

Mpt	124-126 °C
MS (EI)	228.9 (M ⁺), 102.0 (M ⁺ - I), 75.0
IR (KBr), $\nu_{\max}/\text{cm}^{-1}$	2225(C≡N), 1578, 1475, 1390, 1054, 1010, 894, 541
δ_{H} (250MHz, CDCl ₃ ; Me ₄ Si)	7.85 (2H, d, <i>J</i> 8.3 Hz), 7.37 (2H, d, <i>J</i> 8.3 Hz)
δ_{C} (250MHz, CDCl ₃ ; Me ₄ Si)	138.86, 133.53, 118.57, 112.09, 100.68

6.4.2 Preparation of *o*-Iodobenzonitrile



Finely powdered *o*-iodobenzoyl chloride (2.66 g, 0.01 mol) was slowly added to ice cold 0.880 ammonia solution (20 ml). The mixture was stirred for thirty minutes and allowed to warm to room temperature. The resulting white precipitate, *o*-iodobenzamide, was filtered, washed with water and dried. The *o*-iodobenzamide was then transferred to a 250 cm³ round bottomed flask fitted with a side arm and stopcock, together with a cold-finger. An excess of phosphorus pentoxide was added to the flask and the reactants thoroughly mixed. The flask was heated *in vacuo* (90 °C). The final product, *o*-iodobenzonitrile was isolated directly onto the cold finger from the reaction mixture as white needles. Purification of the final product was achieved by further vacuum sublimation (1.68 g, 73% yield)

Mpt	42-50 °C
MS (EI)	229.0 (M ⁺), 102.1 (M ⁺ - I), 75.0
IR (KBr), $\nu_{\max}/\text{cm}^{-1}$	2229(C≡N), 1582, 1465, 1395, 1053, 1009, 894, 541
δ_{H} (250MHz, CDCl ₃ ; Me ₄ Si)	7.93 (1H, dd, <i>J</i> 7.9 Hz + 0.8 Hz), 7.61 (1H, dd, <i>J</i> 7.7 Hz + 1.4 Hz), 7.47 (1H, td, <i>J</i> 7.7 Hz + 1 Hz), 7.30 (1H, td, <i>J</i> 6.0 Hz + 3.3 Hz)
δ_{C} (250MHz, CDCl ₃ ; Me ₄ Si)	139.91, 134.62, 134.05, 128.64, 120.1, 119.67, 98.74

6.5 Conclusions

From the results reported in this chapter, it is clear that the iodine atom has a marked effect on the supramolecular structure of the compounds. As anticipated, the iodine substituent facilitated the production of chains by interacting with a sulfur atom on an adjacent molecule. The mode of association of **1** is only the second example of a *trans*-cofacial association and as such little is known about the reasons why this structure is favoured over *trans*-antarafacial or twisted geometries. Further EPR investigation of the crystals of **1** are being investigated presently to gain more information on this little known conformation.

6.6 References

- 1 E.O. Schlemper and D.Britton, *Acta. Cryst.*, 1965, **18**, 419.
- 2 R.B. Heiart and G.B. Carpenter, *Acta. Cryst.*, 1956, **9**, 60.
- 3 (a) A.J. Banister, N. Bricklebank, W. Clegg, M.R.J. Elsegood, C.I. Gregory, I. Lavender, J.M. Rawson and B.K. Tanner, *J. Chem. Soc., Chem. Commun.*, 1995, 679; (b) A.J. Banister, N. Bricklebank, I. Lavender, J.M. Rawson, C.I. Gregory, B.K. Tanner, W. Clegg, M.R.J. Elsegood and F. Palacio, *Angew. Chem. Int. Ed. Engl.*, 1996, **35**, 2533.
- 4 (a) F. Palacio, G. Antorrena, M. Castro, R. Burriel, J.M. Rawson, J. Nicholas, B. Smith, N. Bricklebank, J. Novoa and C. Ritter, *Physical Review Letters*, 1997, **79**, 2336; (b) P.J. Langley, J.M. Rawson, J.N.B. Smith, M. Schuler, R. Bachmann, A. Schweiger, F. Palacio, G. Antorrena, G. Gescheidt, A. Quintel, P. Rechsteiner and J. Hulliger, *J. Mater. Chem.*, 1999, **9**, 1431.
- 5 W.V.F. Brookes, N. Burford, J. Passmore, M.J. Schriver and L.H. Sutcliffe, *J. Chem. Soc., Chem. Commun.*, 1987, 69.
- 6 A. Vegas, A. Pérez-Salazar, A.J. Banister and R.G. Hey, *J. Chem. Soc., Dalton Trans.*, 1980, 1812.
- 7 T.M. Barclay, A.W. Cordes, N.A. George, R.C. Haddon, M.E. Itkis and R.T. Oakley, *Chem. Commun.*, 1999, 2269.
- 8 C. Aherne, A.J. Banister, A.W. Luke, J.M. Rawson, and R.J. Whitehead, *J. Chem. Soc., Dalton Trans.*, 1992, 1277.
- 9 (a) N. Burford, J. Passmore and X. Sun, *Phosphorus, Sulfur and Silicon*, 1994, **93-94**, 487; (b) N. Burford, J. Passmore and M.J. Schriver, *chem J. Chem. Soc., Chem. Commun.*, 1986, 141. (c) J. Passmore and X.Sun, *Inorg. Chem.*, 1996, **35**, 1313.

-
- 10 N. Bricklebank, P.J. Skabara, D.E. Hibbs, M. Hursthouse and K.M.A. Malik, *J. Chem. Soc., Dalton Trans.*, 1999, 3007.
 - 11 S.C. Nyburg and C.H. Faerman, *Acta. Cryst.*, 1985, **B41**, 274.
 - 12 R.T. Boéré and K.H. Moock, *Z. anorg. allg. Chem.*, 1994, **620**, 1589.
 - 13 S.A Fairhurst, K.M. Johnson, H. Sutcliffe, K.F. Preston, A.J. Banister, Z.V. Hauptman and J. Passmore, *J. Chem. Soc., Dalton Trans.*, 1986, 1465.

Chapter 7

General Experimental

7.0 Introduction

Many of the reactions undertaken, and the compounds prepared, are sensitive to air and moisture. It was therefore necessary to complete most reactions, and store most products, under an inert atmosphere.

All air and moisture sensitive materials were handled under dry nitrogen in a glove box fitted with a phosphorus pentoxide drying column. Reactions were completed using standard vacuum line techniques. All the nitrogen used was oxygen free (BOC) and was dried further by passing over phosphorus pentoxide. All glassware was pre-dried (*c.a.* 130 °C) for at least six hours prior to use. Equipment utilised in sublimations was flame dried under vacuum, prior to use.

7.1 Physical Methods

7.1.1 Infra-red Spectroscopy

Infra red spectra were recorded as nujol mulls if they were thought to be unstable to air or moisture, or by KBr disc for normal analysis. The instrument used was an ATI Mattson Genesis series FTIR.

7.1.2 Mass Spectrometry

Mass spectra were recorded using a VG Micromass 7070F mass spectrometer, using EI or FAB ionisation. A direct insertion probe was used for samples. Air and moisture sensitive compounds were taken from a sealed tube and analysed as quickly as possible to minimise any decomposition.

7.1.3 ^1H and ^{13}C NMR Spectroscopy

^1H and ^{13}C nmr spectra were obtained on a Bruker AC250 nmr spectrometer. Samples were dissolved in a deuterated solvent in a nitrogen glove box and were analysed immediately.

7.1.4 Differential Scanning Calorimetry

Differential scanning calorimetry (d.s.c) measurements were undertaken using a Mettler-Toledo TA8000.

7.1.5 Electron Paramagnetic Resonance

Electron paramagnetic resonance (EPR or ESR) spectra were obtained in conjunction with Dr F. Mabbs at the University of Manchester (EPSRC cwEPR service centre). Solution and powder samples were analysed on a Bruker EMX and single crystal analysis was performed on a Bruker ESP300E.

7.1.6 Single Crystal X-Ray Diffraction

Single crystal x-ray crystallography was performed by Harry Adams and Sharon Spey at the University of Sheffield. Data collected were measured on a Bruker Smart CCD area detector with Oxford Cryosystems low temperature system. Measurements were corrected for Lorentz and polarisation effects and for absorption by semi-empirical methods based on symmetry-equivalent and repeated reflections. Structures were solved by direct methods and refined by full matrix least squares methods on F^2 . Scattering factors were inlaid from the program package SHELXTL¹ as implemented on the Viglen Pentium computer.

7.1.7 Elemental Analysis

Carbon hydrogen and nitrogen analysis was performed by Medac Ltd, Brunel Science Centre, Coopers Hill Lane, Englefield Green, Egham

7.1.8 Magnetic Measurements

Magnetic experiments were performed by Fernando Palacio, G Antorena and Michel Julier (Instituto de Ciencia de la Materia de Aragón, Universidad de Zaragoza). Magnetisation of the samples was measured using a SQUID magnetometer from Quantum Devices. The polycrystalline samples were transferred into gelatine capsules inside a glove box. The capsules were then topped with cotton wool. The contact between the capsules and air was reduced to less than 5 minutes.

7.2 Solvents

All solvents used were pre-dried and distilled before use. Solvents not freshly distilled were stored under nitrogen in flask equipped with a Teflon vacuum tap. Before storage, the solvent was de-gassed via a freeze-thaw cycle.

7.2.1 Diethyl ether (Fisher)

Refluxed with sodium metal and benzophenone (indicator) under a constant stream of nitrogen.

7.2.2 Tetrahydrofuran (Sigma-Aldrich)

Refluxed with potassium metal and benzophenone (indicator) under a constant stream of nitrogen.

7.2.3 Dichloromethane (Fisher)

Refluxed with phosphorus pentoxide (P_2O_5) for at least 4 hours under a constant stream of nitrogen.

7.2.4 Acetonitrile (Fisher)

Refluxed with CaH_2 under a constant stream of nitrogen.

7.2.5 Dimethylformamide

Purchased pre-dried from Sigma-Aldrich and degassed by passing nitrogen through the solvent just prior to use.

7.2.6 Toluene (Fisher)

Refluxed with sodium metal and benzophenone (indicator) under a constant stream of nitrogen.

7.3 Reagents

All the starting compounds were obtained from various chemical suppliers and used as received.

7.4 References

-
- 1 SHELXTL version, An integrated system for solving and refining crystal structures from diffraction data (Revision 5.1), Bruker AXS LTD

Overall Conclusions and Suggestions

The work in this thesis has shown that the use of mono- and poly- halogenated phenyl substituents can have a significant effect on the molecular packing of 1,2,3,5-dithiadiazolyl radicals. Dichlorophenyl groups clearly enhance the ability of 1,2,3,5-dithiadiazolyls to associate in stacks. Two types of stacking motif have been identified; (i) dimer stacks and (ii) π -stacks containing uniformly spaced radical units. The latter is unprecedented for neutral mono-functional dithiadiazolyl radicals. In contrast, bromine was shown to exhibit a large steric hindrance, distorting the *cis* cofacial dimer association to form a slightly twisted motif. Unlike chlorine there seemed to be little or no homonuclear interactions.

The molecular structure of iodophenyl derivatives exhibited significant steric hindrance producing one viscous oil (*ortho*-iodophenyl-1,2,3,5-dithiadiazolyl), common in highly steric hindered systems and a *trans* cofacial association (*para*-iodophenyl-1,2,3,5-dithiadiazolyl). Halogen...sulfur interactions, which link adjacent molecules into chains, have also been observed for the chlorine and iodine derivatives.

Further studies into the magnetic susceptibility and EPR signals of the compounds may uncover additional information about the interaction of the molecules. An investigation of further chlorophenyl derivatives containing a cyano substituent may promote the formation of chains while still retaining significant stacking properties. Studies of poly-halogenated derivatives containing different halogen atoms would also be of interest.

Appendix 1

Crystal data and structure refinement: 2,4-dichlorophenyl-1,2,3,5-dithiadiazolyl

Identification code	shu14m	
Empirical formula	C7 H3 Cl2 N2 S2	
Formula weight	250.13	
Temperature	150(2) K	
Wavelength	0.71073 Å	
Crystal system	Monoclinic	
Space group	P2 ₁ /n	
Unit cell dimensions	a = 15.026(8) Å	α = 90°.
	b = 3.629(2) Å	β = 91.212(9)°.
	c = 15.923(9) Å	γ = 90°.
Volume	868.2(8) Å ³	
Z	4	
Density (calculated)	1.914 Mg/m ³	
Absorption coefficient	1.171 mm ⁻¹	
F(000)	500	
Crystal size	0.20 x 0.15 x 0.04 mm ³	
Theta range for data collection	1.84 to 28.53°.	
Index ranges	-19 ≤ h ≤ 19, -4 ≤ k ≤ 2, -21 ≤ l ≤ 20	
Reflections collected	5221	
Independent reflections	2092 [R(int) = 0.0945]	
Completeness to theta = 28.53°	95.3 %	
Absorption correction	Semi-empirical	
Max. and min. transmission	0.9547 and 0.7995	
Refinement method	Full-matrix least-squares on F ²	
Data / restraints / parameters	2092 / 0 / 120	
Goodness-of-fit on F ²	1.001	
Final R indices [I > 2σ(I)]	R1 = 0.0717, wR2 = 0.1668	
R indices (all data)	R1 = 0.1027, wR2 = 0.1861	
Largest diff. peak and hole	0.945 and -0.800 e.Å ⁻³	

Table 2. Atomic coordinates ($\times 10^4$) and equivalent isotropic displacement parameters ($\text{\AA}^2 \times 10^3$)

for Shu14m. $U(\text{eq})$ is defined as one third of the trace of the orthogonalized U^{ij} tensor.

	x	y	z	$U(\text{eq})$
Cl(1)	8896(1)	-3815(3)	5889(1)	35(1)
Cl(2)	9162(1)	1573(4)	2801(1)	39(1)
S(1)	6297(1)	-3019(6)	7113(1)	72(1)
S(2)	5298(1)	-3656(6)	6191(1)	65(1)
N(1)	7081(3)	-2302(16)	6448(2)	55(1)
N(2)	5970(2)	-3098(15)	5414(2)	47(1)
C(1)	8359(3)	-2011(13)	5012(2)	31(1)
C(2)	8890(3)	-1114(14)	4347(2)	33(1)
C(3)	8495(3)	343(14)	3625(2)	34(1)
C(4)	7591(3)	867(14)	3555(2)	34(1)
C(5)	7070(3)	-155(15)	4222(2)	36(1)
C(6)	7431(3)	-1535(13)	4973(2)	32(1)
C(7)	6810(3)	-2422(16)	5647(3)	41(1)

Appendix 2

Crystal data and structure refinement: 2,5-dichlorophenyl-1,2,3,5,-dithiadiazolyl

Identification code	shu24m	
Empirical formula	C7 H3 Cl2 N2 S2	
Formula weight	250.13	
Temperature	150(2) K	
Wavelength	0.71073 Å	
Crystal system	Monoclinic	
Space group	P2 ₁ /c	
Unit cell dimensions	a = 3.6685(6) Å	α = 90°.
	b = 24.346(4) Å	β = 97.508(4)°.
	c = 10.1635(18) Å	γ = 90°.
Volume	900.0(3) Å ³	
Z	4	
Density (calculated)	1.846 Mg/m ³	
Absorption coefficient	1.130 mm ⁻¹	
F(000)	500	
Crystal size	0.23 x 0.05 x 0.02 mm ³	
Theta range for data collection	2.19 to 28.31°.	
Index ranges	-4 ≤ h ≤ 4, -31 ≤ k ≤ 32, -10 ≤ l ≤ 13	
Reflections collected	5974	
Independent reflections	2158 [R(int) = 0.0883]	
Completeness to theta = 28.31°	96.8 %	
Absorption correction	Semi-empirical from equivalents	
Max. and min. transmission	0.9778 and 0.7812	
Refinement method	Full-matrix least-squares on F ²	
Data / restraints / parameters	2158 / 0 / 118	
Goodness-of-fit on F ²	0.984	
Final R indices [I > 2σ(I)]	R1 = 0.0562, wR2 = 0.1112	
R indices (all data)	R1 = 0.0948, wR2 = 0.1249	
Largest diff. peak and hole	0.684 and -0.809 e.Å ⁻³	

Table 2. Atomic coordinates ($\times 10^4$) and equivalent isotropic displacement parameters ($\text{\AA}^2 \times 10^3$)

for shu24m. $U(\text{eq})$ is defined as one third of the trace of the orthogonalized U^{ij} tensor.

	x	y	z	$U(\text{eq})$
Cl(1)	4903(2)	2613(1)	3968(1)	27(1)
Cl(2)	-2694(2)	4413(1)	218(1)	30(1)
S(1)	4057(4)	3730(1)	7348(1)	59(1)
S(2)	4472(5)	4536(1)	6649(1)	66(1)
N(1)	3102(11)	3462(1)	5873(3)	41(1)
N(2)	3661(11)	4362(1)	5096(3)	42(1)
C(1)	2678(9)	3127(1)	2990(3)	21(1)
C(2)	1656(10)	3002(1)	1662(3)	25(1)
C(3)	17(10)	3393(1)	801(3)	25(1)
C(4)	-625(9)	3910(1)	1278(3)	24(1)
C(5)	346(10)	4041(1)	2602(3)	24(1)
C(6)	2048(10)	3648(1)	3491(3)	24(1)
C(7)	2999(11)	3827(2)	4890(3)	32(1)

Appendix 3

Crystal data and structure refinement: β -(3,5-dichlorophenyl-1,2,3,5-dithiadiazolyl)

Identification code	shunearm	
Empirical formula	C7 H3 Cl2 N2 S2	
Formula weight	250.13	
Temperature	150(2) K	
Wavelength	0.71073 Å	
Crystal system	Monoclinic	
Space group	C2/c	
Unit cell dimensions	a = 41.546(7) Å	$\alpha = 90^\circ$.
	b = 3.6280(6) Å	$\beta = 99.013(3)^\circ$.
	c = 36.326(6) Å	$\gamma = 90^\circ$.
Volume	5407.7(15) Å ³	
Z	24	
Density (calculated)	1.843 Mg/m ³	
Absorption coefficient	1.128 mm ⁻¹	
F(000)	3000	
Crystal size	0.38 x 0.17 x 0.07 mm ³	
Theta range for data collection	0.99 to 28.32°.	
Index ranges	-54 ≤ h ≤ 55, -4 ≤ k ≤ 4, -48 ≤ l ≤ 35	
Reflections collected	16227	
Independent reflections	6391 [R(int) = 0.1203]	
Completeness to theta = 28.32°	94.9 %	
Absorption correction	Semi-empirical from equivalents	
Max. and min. transmission	0.9252 and 0.6738	
Refinement method	Full-matrix least-squares on F ²	
Data / restraints / parameters	6391 / 0 / 352	
Goodness-of-fit on F ²	1.067	
Final R indices [I > 2σ(I)]	R1 = 0.0556, wR2 = 0.1314	
R indices (all data)	R1 = 0.0765, wR2 = 0.1540	
Largest diff. peak and hole	0.669 and -1.301 e.Å ⁻³	

Table 2. Atomic coordinates ($\times 10^4$) and equivalent isotropic displacement parameters ($\text{\AA}^2 \times 10^3$)

for shunearm. $U(\text{eq})$ is defined as one third of the trace of the orthogonalized U^{ij} tensor.

	x	y	z	$U(\text{eq})$
Cl(1A)	392(1)	5026(3)	497(1)	30(1)
Cl(2A)	1394(1)	10163(3)	1486(1)	54(1)
S(1A)	1701(1)	5298(5)	-474(1)	63(1)
S(2A)	2099(1)	5607(6)	-45(1)	67(1)
N(1A)	1432(1)	5737(12)	-196(1)	41(1)
N(2A)	1878(1)	6097(13)	286(1)	48(1)
C(1A)	1001(1)	5757(10)	342(1)	25(1)
C(2A)	798(1)	6237(10)	608(1)	26(1)
C(3A)	912(1)	7581(10)	963(1)	32(1)
C(4A)	1238(1)	8451(11)	1045(1)	35(1)
C(5A)	1450(1)	8019(11)	793(1)	34(1)
C(6A)	1331(1)	6651(11)	438(1)	29(1)
C(7A)	1555(1)	6150(13)	164(1)	35(1)
Cl(1B)	-2043(1)	-5369(3)	2869(1)	32(1)
Cl(2B)	-1048(1)	-757(3)	2201(1)	28(1)
S(1B)	-2777(1)	-1421(5)	1091(1)	52(1)
S(2B)	-2388(1)	-1039(4)	789(1)	46(1)
N(1B)	-2542(1)	-1962(12)	1489(1)	36(1)
N(2B)	-2106(1)	-1481(12)	1154(1)	35(1)
C(1B)	-2111(1)	-3588(10)	2143(1)	25(1)
C(2B)	-1895(1)	-3902(10)	2473(1)	25(1)
C(3B)	-1567(1)	-3063(10)	2497(1)	26(1)
C(4B)	-1458(1)	-1878(10)	2175(1)	23(1)
C(5B)	-1664(1)	-1492(9)	1840(1)	21(1)
C(6B)	-1993(1)	-2351(10)	1826(1)	22(1)
C(7B)	-2224(1)	-1909(11)	1474(1)	26(1)
Cl(1C)	379(1)	-617(3)	4652(1)	28(1)
Cl(2C)	1147(1)	4496(3)	3710(1)	27(1)
S(1C)	-699(1)	3302(6)	3061(1)	63(1)
S(2C)	-400(1)	3805(5)	2652(1)	59(1)
N(1C)	-399(1)	2899(13)	3406(1)	42(1)
N(2C)	-61(1)	3489(12)	2945(1)	38(1)
C(1C)	149(1)	1258(10)	3941(1)	25(1)
C(2C)	423(1)	949(10)	4212(1)	23(1)

C(3C)	732(1)	1896(10)	4145(1)	24(1)
C(4C)	762(1)	3186(10)	3792(1)	23(1)
C(5C)	497(1)	3549(10)	3511(1)	24(1)
C(6C)	189(1)	2603(10)	3590(1)	24(1)
C(7C)	-104(1)	3008(12)	3299(1)	32(1)

Appendix 4

Crystal data and structure refinement: α -(3,5-dichlorophenyl-1,2,3,5-dithiadiazolyl)

Identification code	far1m	
Empirical formula	C7 H3 Cl2 N2 S2	
Formula weight	250.13	
Temperature	150(2) K	
Wavelength	0.71073 Å	
Crystal system	Triclinic	
Space group	P-1	
Unit cell dimensions	a = 7.2484(8) Å	$\alpha = 80.518(2)^\circ$
	b = 20.842(2) Å	$\beta = 84.323(2)^\circ$
	c = 36.499(4) Å	$\gamma = 84.933(2)^\circ$
Volume	5397.3(10) Å ³	
Z	24	
Density (calculated)	1.847 Mg/m ³	
Absorption coefficient	1.130 mm ⁻¹	
F(000)	3000	
Crystal size	0.50 x 0.11 x 0.08 mm ³	
Theta range for data collection	0.99 to 28.28°	
Index ranges	-9 ≤ h ≤ 9, -23 ≤ k ≤ 26, -35 ≤ l ≤ 48	
Reflections collected	32963	
Independent reflections	23629 [R(int) = 0.0626]	
Completeness to theta = 28.28°	88.1 %	
Absorption correction	Semi-empirical from equivalents	
Max. and min. transmission	0.9150 and 0.6019	
Refinement method	Full-matrix least-squares on F ²	
Data / restraints / parameters	23629 / 0 / 1405	
Goodness-of-fit on F ²	1.104	
Final R indices [I > 2σ(I)]	R1 = 0.0682, wR2 = 0.1778	
R indices (all data)	R1 = 0.0972, wR2 = 0.2022	
Largest diff. peak and hole	1.660 and -1.120 e.Å ⁻³	

Table 2. Atomic coordinates ($\times 10^4$) and equivalent isotropic displacement parameters ($\text{\AA}^2 \times 10^3$)

for far1m. $U(\text{eq})$ is defined as one third of the trace of the orthogonalized U^{ij} tensor.

	x	y	z	$U(\text{eq})$
Cl(1A)	10006(2)	2278(1)	6511(1)	34(1)
Cl(2A)	7449(2)	4246(1)	5498(1)	26(1)
S(1A)	9151(2)	820(1)	4981(1)	37(1)
S(2A)	9025(2)	1612(1)	4550(1)	36(1)
N(1A)	9029(7)	1266(2)	5312(1)	30(1)
N(2A)	8880(7)	2156(2)	4826(1)	31(1)
C(1A)	9372(6)	2140(2)	5817(1)	23(1)
C(2A)	9313(7)	2571(3)	6066(1)	25(1)
C(3A)	8734(6)	3225(2)	5975(1)	24(1)
C(4A)	8199(6)	3433(2)	5619(1)	21(1)
C(5A)	8249(6)	3023(2)	5355(1)	21(1)
C(6A)	8830(7)	2367(2)	5461(1)	22(1)
C(7A)	8906(7)	1913(2)	5189(1)	24(1)
Cl(1B)	5084(2)	2138(1)	6462(1)	36(1)
Cl(2B)	2483(2)	4184(1)	5498(1)	26(1)
S(1B)	3597(2)	781(1)	4929(1)	36(1)
S(2B)	3477(2)	1586(1)	4503(1)	36(1)
N(1B)	3667(7)	1217(2)	5262(1)	31(1)
N(2B)	3543(6)	2118(2)	4785(1)	28(1)
C(1B)	4320(6)	2053(2)	5769(1)	24(1)
C(2B)	4339(7)	2464(3)	6028(1)	26(1)
C(3B)	3808(7)	3123(2)	5950(1)	24(1)
C(4B)	3225(6)	3365(2)	5599(1)	23(1)
C(5B)	3186(6)	2970(2)	5330(1)	20(1)
C(6B)	3723(6)	2306(2)	5418(1)	22(1)
C(7B)	3648(7)	1862(2)	5144(1)	25(1)
Cl(1C)	3967(2)	2707(1)	3710(1)	25(1)
Cl(2C)	5690(2)	4215(1)	4669(1)	25(1)
S(1C)	4332(2)	5814(1)	2673(1)	38(1)
S(2C)	4251(2)	6402(1)	3088(1)	37(1)
N(1C)	4392(7)	5130(2)	2964(1)	30(1)
N(2C)	4335(7)	5791(2)	3431(1)	30(1)
C(1C)	4242(6)	4006(2)	3521(1)	22(1)
C(2C)	4391(6)	3471(2)	3800(1)	21(1)

C(3C)	4845(6)	3521(2)	4157(1)	21(1)
C(4C)	5152(6)	4132(2)	4229(1)	20(1)
C(5C)	5018(6)	4680(2)	3961(1)	21(1)
C(6C)	4564(6)	4615(2)	3606(1)	20(1)
C(7C)	4421(7)	5205(2)	3320(1)	25(1)
CI(1D)	8981(2)	2706(1)	3711(1)	24(1)
CI(2D)	10656(2)	4269(1)	4638(1)	23(1)
S(1D)	8819(2)	5788(1)	2632(1)	36(1)
S(2D)	8700(2)	6395(1)	3037(1)	36(1)
N(1D)	9115(6)	5116(2)	2931(1)	26(1)
N(2D)	8986(7)	5798(2)	3385(1)	29(1)
C(1D)	9201(6)	4005(2)	3502(1)	20(1)
C(2D)	9380(6)	3479(2)	3786(1)	20(1)
C(3D)	9849(6)	3549(2)	4138(1)	20(1)
C(4D)	10118(6)	4171(2)	4197(1)	20(1)
C(5D)	9922(6)	4715(2)	3927(1)	21(1)
C(6D)	9443(6)	4631(2)	3575(1)	19(1)
C(7D)	9171(7)	5211(2)	3282(1)	24(1)
CI(1E)	1252(2)	7100(1)	2196(1)	25(1)
CI(2E)	2721(2)	9101(1)	2855(1)	28(1)
S(1E)	1219(2)	9776(1)	777(1)	31(1)
S(2E)	1024(2)	10559(1)	1078(1)	30(1)
N(1E)	1462(7)	9214(2)	1143(1)	28(1)
N(2E)	1285(6)	10090(2)	1475(1)	25(1)
C(1E)	1451(6)	8330(2)	1829(1)	19(1)
C(2E)	1608(6)	7919(2)	2164(1)	21(1)
C(3E)	2016(6)	8145(2)	2484(1)	22(1)
C(4E)	2265(6)	8805(2)	2457(1)	22(1)
C(5E)	2123(6)	9232(2)	2129(1)	21(1)
C(6E)	1703(6)	8995(2)	1812(1)	20(1)
C(7E)	1482(6)	9449(2)	1463(1)	20(1)
CI(1F)	6240(2)	7095(1)	2207(1)	25(1)
CI(2F)	7727(2)	9077(1)	2885(1)	28(1)
S(1F)	6640(2)	9781(1)	801(1)	33(1)
S(2F)	6556(2)	10553(1)	1106(1)	34(1)
N(1F)	6730(6)	9214(2)	1165(1)	27(1)
N(2F)	6623(6)	10080(2)	1504(1)	27(1)
C(1F)	6506(6)	8326(2)	1850(1)	19(1)
C(2F)	6609(6)	7916(2)	2187(1)	21(1)
C(3F)	6977(6)	8129(2)	2509(1)	23(1)

C(4F)	7266(6)	8781(2)	2489(1)	21(1)
C(5F)	7204(6)	9211(2)	2159(1)	21(1)
C(6F)	6808(6)	8981(2)	1838(1)	18(1)
C(7F)	6708(7)	9444(2)	1487(1)	21(1)
Cl(1G)	7415(2)	5742(1)	366(1)	24(1)
Cl(2G)	4038(2)	7293(1)	1302(1)	24(1)
S(1G)	4926(2)	3603(1)	1966(1)	36(1)
S(2G)	4347(2)	4209(1)	2370(1)	35(1)
N(1G)	5243(7)	4198(2)	1618(1)	30(1)
N(2G)	4585(6)	4881(2)	2074(1)	27(1)
C(1G)	6193(6)	5289(2)	1078(1)	21(1)
C(2G)	6381(6)	5835(2)	804(1)	21(1)
C(3G)	5743(6)	6451(2)	872(1)	22(1)
C(4G)	4902(6)	6517(2)	1222(1)	19(1)
C(5G)	4689(6)	5989(2)	1505(1)	21(1)
C(6G)	5334(6)	5369(2)	1429(1)	21(1)
C(7G)	5065(7)	4790(2)	1719(1)	25(1)
Cl(1H)	2473(2)	5773(1)	332(1)	24(1)
Cl(2H)	-978(2)	7294(1)	1280(1)	25(1)
S(1H)	521(2)	3598(1)	1916(1)	37(1)
S(2H)	-87(2)	4187(1)	2331(1)	37(1)
N(1H)	629(7)	4207(2)	1575(1)	29(1)
N(2H)	-63(7)	4868(2)	2039(1)	29(1)
C(1H)	1322(6)	5309(2)	1043(1)	20(1)
C(2H)	1441(6)	5860(2)	771(1)	19(1)
C(3H)	779(6)	6472(2)	841(1)	20(1)
C(4H)	-70(7)	6525(2)	1194(1)	21(1)
C(5H)	-228(7)	5991(2)	1476(1)	21(1)
C(6H)	466(7)	5383(2)	1395(1)	22(1)
C(7H)	329(7)	4793(2)	1683(1)	26(1)
Cl(1I)	2413(2)	2132(1)	1464(1)	35(1)
Cl(2I)	4912(2)	4184(1)	502(1)	25(1)
S(1I)	6068(2)	789(1)	-76(1)	36(1)
S(2I)	6234(2)	1596(1)	-501(1)	36(1)
N(1I)	5440(7)	1224(2)	256(1)	31(1)
N(2I)	5623(7)	2128(2)	-221(1)	29(1)
C(1I)	3891(6)	2050(2)	770(1)	24(1)
C(2I)	3406(7)	2465(3)	1027(1)	26(1)
C(3I)	3686(6)	3121(2)	955(1)	24(1)
C(4I)	4484(6)	3368(2)	601(1)	19(1)

C(5I)	4982(6)	2975(2)	330(1)	19(1)
C(6I)	4696(6)	2309(2)	416(1)	21(1)
C(7I)	5263(7)	1866(2)	137(1)	25(1)
CI(1J)	7345(2)	2296(1)	1506(1)	35(1)
CI(2J)	9962(2)	4248(1)	489(1)	27(1)
S(1J)	10448(2)	814(1)	-15(1)	37(1)
S(2J)	10642(2)	1602(1)	-449(1)	36(1)
N(1J)	10011(7)	1270(2)	313(1)	31(1)
N(2J)	10257(7)	2153(2)	-179(1)	29(1)
C(1J)	8752(7)	2145(2)	816(1)	24(1)
C(2J)	8352(7)	2581(3)	1064(1)	25(1)
C(3J)	8700(6)	3236(2)	971(1)	23(1)
C(4J)	9499(7)	3442(2)	612(1)	22(1)
C(5J)	9926(7)	3024(2)	352(1)	21(1)
C(6J)	9543(6)	2366(2)	456(1)	20(1)
C(7J)	9957(7)	1907(2)	185(1)	24(1)
CI(1K)	2007(2)	2890(1)	2803(1)	25(1)
CI(2K)	5154(2)	883(1)	2149(1)	27(1)
S(1K)	1886(2)	218(1)	4225(1)	31(1)
S(2K)	2366(2)	-564(1)	3923(1)	30(1)
N(1K)	2221(6)	779(2)	3858(1)	27(1)
N(2K)	2796(6)	-97(2)	3529(1)	26(1)
C(1K)	2471(6)	1658(2)	3171(1)	19(1)
C(2K)	2755(6)	2067(2)	2833(1)	20(1)
C(3K)	3574(6)	1841(2)	2516(1)	22(1)
C(4K)	4142(6)	1179(2)	2541(1)	21(1)
C(5K)	3905(6)	757(2)	2874(1)	20(1)
C(6K)	3036(6)	1000(2)	3189(1)	19(1)
C(7K)	2684(7)	541(2)	3542(1)	21(1)
CI(1L)	7000(2)	2923(1)	2799(1)	26(1)
CI(2L)	10132(2)	949(1)	2113(1)	27(1)
S(1L)	7332(2)	231(1)	4200(1)	33(1)
S(2L)	7915(2)	-542(1)	3895(1)	33(1)
N(1L)	7510(7)	798(2)	3835(1)	29(1)
N(2L)	8165(6)	-69(2)	3498(1)	27(1)
C(1L)	7524(6)	1686(2)	3154(1)	19(1)
C(2L)	7756(6)	2107(2)	2819(1)	21(1)
C(3L)	8580(6)	1893(2)	2495(1)	23(1)
C(4L)	9149(6)	1237(2)	2512(1)	21(1)
C(5L)	8957(6)	802(2)	2841(1)	20(1)

C(6L)	8138(6)	1033(2)	3162(1)	19(1)
C(7L)	7919(7)	566(2)	3515(1)	22(1)

Appendix 5

Supporting data for magnetic measurement plots

Figure 3.25 $M(T)$ at 10,000 Oe (no Correction) Curie-Weiss fit for 3

T (K)	M(emu/mol) exp.	M(emu/mol) theor.	T (K)	M(emu/mol) exp.	M(emu/mol) theor.
1.7900	10.966	10.855	26.030	-0.80600	-0.68578
2.0000	9.8683	9.7492	28.030	-0.87966	-0.75876
2.2000	8.9398	8.8626	30.030	-0.93891	-0.82214
2.4000	8.0817	8.1032	32.020	-0.98694	-0.87744
2.6000	7.4029	7.4455	34.020	-1.0122	-0.92657
2.8000	6.7909	6.8703	36.020	-1.0050	-0.97031
3.0000	6.2540	6.3631	38.030	-1.0126	-1.0097
3.2000	5.7856	5.9123	40.020	-1.0375	-1.0448
3.4000	5.3659	5.5092	42.020	-1.0515	-1.0768
3.6000	4.9928	5.1465	44.010	-1.0624	-1.1057
3.8100	4.6471	4.8029	46.040	-1.0845	-1.1327
4.0000	4.3479	4.5203	48.020	-1.1159	-1.1568
4.2000	4.0849	4.2482	50.080	-1.1778	-1.1799
4.3900	3.8283	4.0107	55.010	-1.2871	-1.2282
4.5900	3.9127	3.7804	59.910	-1.3650	-1.2684
4.7900	3.6897	3.5678	65.150	-1.4230	-1.3047
4.9900	3.4844	3.3711	70.240	-1.4588	-1.3349
5.5200	3.0170	2.9141	75.310	-1.4846	-1.3608
6.0200	2.6481	2.5523	80.240	-1.5048	-1.3830
6.5200	2.3305	2.2429	85.450	-1.5233	-1.4036
7.0100	2.0682	1.9802	90.520	-1.5387	-1.4214
7.5000	1.8295	1.7502	95.600	-1.5525	-1.4373
8.0100	1.6208	1.5393	100.60	-1.5646	-1.4515
8.4900	1.4397	1.3629	110.69	-1.5866	-1.4761
9.0300	1.2669	1.1860	120.68	-1.6042	-1.4965
9.4800	1.1381	1.0533	130.91	-1.6206	-1.5141
9.9700	1.0083	0.92201	140.96	-1.6322	-1.5289
10.980	0.78204	0.68703	151.03	-1.6427	-1.5418
11.990	0.59960	0.49040	161.10	-1.6504	-1.5531
12.990	0.45897	0.32497	171.18	-1.6551	-1.5631
14.000	0.35385	0.18123	181.23	-1.6581	-1.5719
15.000	0.15081	0.057499	191.29	-1.6565	-1.5798
16.000	0.040661	-0.051131	201.35	-1.6499	-1.5869
17.010	-0.056705	-0.14817	221.50	-1.6213	-1.5993
18.010	-0.14443	-0.23376	241.67	-1.5479	-1.6096
19.010	-0.22459	-0.31051	261.78	-1.4181	-1.6182
20.010	-0.30067	-0.37975	281.93	-1.1696	-1.6257
22.030	-0.60930	-0.50076	302.08	-0.85876	-1.6322
24.030	-0.71557	-0.60085			

Figure 3.26 $M(T)$ at 10,000 Oe (no correction) Curie-Weiss fit for 1

Isotherm at 3K	
H/T	M-diamag. (emu/mol)
0.0000	-0.0035224
33.333	0.092119
66.667	0.18120
100.00	0.26907
133.33	0.35631
166.67	0.44147
200.00	0.52641
233.33	0.61363
266.67	0.69768
300.00	0.77688
333.33	0.86576
666.67	1.6982
1000.0	2.4988
1333.3	3.2954
1666.7	4.0830
2000.0	4.8676
2333.3	5.6481
2666.7	6.4196
3000.0	7.1897
3333.3	7.9489
4000.0	9.4298
4666.7	10.870
5333.3	12.300
6000.0	13.650
6666.7	14.965
7333.3	16.171
8000.0	17.363
8666.7	18.540
9333.3	19.626
10000	20.665
10667	21.614
11333	22.524
12000	23.372
12667	23.966
13333	24.925
14000	25.841
14667	26.527
15333	27.238
16000	27.393
16667	28.041

Isotherm at 1.8K	
H/T	M-diamag. (emu/mol)
0.0000	-0.015222
55.556	0.13622
111.11	0.27649
166.67	0.41596
222.22	0.55232
277.78	0.69118
333.33	0.82917
388.89	0.96749
444.44	1.1058
500.00	1.2464
555.56	1.3772
1111.1	2.7210
1666.7	4.0304
2222.2	5.3273
2777.8	6.6015
3333.3	7.8464
3888.9	9.0842
4444.4	10.301
5000.0	11.483
5555.6	12.625
6666.7	14.828
7777.8	16.893
8888.9	18.773
10000	20.520
11111	22.094
12222	23.532
13333	24.827
14444	25.992
15556	27.082
16667	27.971
17778	28.765
18889	29.464
20000	30.100
21111	30.560
22222	30.958
23464	34.361
24444	34.300
25556	32.921
26667	33.617
27778	35.407

Figure 3.27 M(H/T) (low temperature) diamagnetism removed Brillouin fit for 3

T (K)	M*T/H (emu.K/Oe.mol) exp.	M*T/H (emu.K/Oe.mol) theor.	T (K)	M*T/H (emu.K/Oe.mol) exp.	M*T/H (emu.K/Oe.mol) theor.
1.7900	0.0022713	4.8229e-27	26.030	0.0023862	0.41726
2.0000	0.0023182	4.9222e-24	28.030	0.0023631	0.53239
2.2000	0.0023458	1.0462e-21	30.030	0.0023538	0.65232
2.4000	0.0023531	9.0344e-20	32.020	0.0023560	0.77285
2.6000	0.0023727	3.9038e-18	34.020	0.0024173	0.89218
2.8000	0.0023838	9.7958e-17	36.020	0.0025853	1.0073
3.0000	0.0023930	1.5919e-15	38.030	0.0027005	1.1169
3.2000	0.0024027	1.8181e-14	40.020	0.0027421	1.2182
3.4000	0.0024101	1.5534e-13	42.020	0.0028203	1.3120
3.6000	0.0024176	1.0424e-12	44.010	0.0029059	1.3970
3.8100	0.0024269	6.1845e-12	46.040	0.0029385	1.4751
4.0000	0.0024283	2.6297e-11	48.020	0.0029137	1.5430
4.2000	0.0024392	1.0450e-10	50.080	0.0027288	1.6054
4.3900	0.0024369	3.4431e-10	55.010	0.0023964	1.7230
4.5900	0.0025867	1.0836e-09	59.910	0.0021433	1.8021
4.7900	0.0025926	3.0933e-09	65.150	0.0019525	1.8535
4.9900	0.0025983	8.1046e-09	70.240	0.0018541	1.8782
5.5200	0.0026163	7.3733e-08	75.310	0.0017931	1.8844
6.0200	0.0026312	4.1130e-07	80.240	0.0017483	1.8774
6.5200	0.0026427	1.7514e-06	85.450	0.0017039	1.8598
7.0100	0.0026575	5.8971e-06	90.520	0.0016659	1.8356
7.5000	0.0026642	1.6866e-05	95.600	0.0016269	1.8065
8.0100	0.0026781	4.3739e-05	100.60	0.0015904	1.7745
8.4900	0.0026849	9.6258e-05	110.69	0.0015066	1.7047
9.0300	0.0026996	0.00021073	120.68	0.0014301	1.6332
9.4800	0.0027121	0.00037720	130.91	0.0013373	1.5609
9.9700	0.0027228	0.00066813	140.96	0.0012762	1.4925
10.980	0.0027502	0.0018355	151.03	0.0012083	1.4275
11.990	0.0027845	0.0042202	161.10	0.0011644	1.3664
12.990	0.0028340	0.0084156	171.18	0.0011582	1.3091
14.000	0.0029072	0.015201	181.23	0.0011719	1.2558
15.000	0.0028103	0.025113	191.29	0.0012667	1.2059
16.000	0.0028214	0.038791	201.35	0.0014655	1.1594
17.010	0.0028339	0.056904	221.50	0.0022468	1.0754
18.010	0.0028425	0.079417	241.67	0.0042252	1.0017
19.010	0.0028480	0.10665	261.78	0.0079747	0.93719
20.010	0.0028455	0.13862	281.93	0.015593	0.88000
22.030	0.0024529	0.21704	302.08	0.026098	0.82914
24.030	0.0024202	0.31083			

Figure 3.28 M(H/T) (low temperature) diamagnetism removed Brillouin fit for 1

T (K)	M(emu/mol) exp.	M(emu/mol) theor.
1.7900	11.469	11.186
2.0000	10.323	10.116
2.2000	9.3566	9.2460
2.4000	8.4718	8.4920
2.6000	7.7477	7.8322
2.8000	7.1121	7.2501
3.0000	6.5532	6.7327
3.2000	6.0574	6.2697
3.4000	5.6152	5.8531
3.6000	5.2252	5.4761
3.8000	4.8699	5.1334
4.0000	4.5449	4.8205
4.2000	4.2600	4.5337
4.4000	3.9981	4.2698
4.6300	4.1111	3.9913
4.8100	3.8888	3.7899
5.0300	3.6653	3.5612
5.4700	3.2556	3.1535
5.9700	2.8590	2.7565
6.4900	2.4990	2.4031
6.9600	2.2192	2.1254
7.4800	1.9611	1.8559
7.9800	1.7339	1.6275
8.4700	1.5375	1.4282
8.9700	1.3549	1.2458
9.4900	1.1896	1.0753
9.9700	1.0558	0.93277
11.000	0.81502	0.66679
11.990	0.62894	0.45216
12.990	0.48764	0.26711
14.000	0.39007	0.10595
15.020	0.14256	-0.035666
16.000	0.027788	-0.15533
17.000	-0.077205	-0.26370
18.010	-0.17276	-0.36133
19.010	-0.25901	-0.44809
20.010	-0.34119	-0.52643
22.030	-0.49081	-0.66355
24.020	-0.92774	-0.77664

T (K)	M(emu/mol) exp.	M(emu/mol) theor.
26.030	-1.0328	-0.87370
28.030	-1.1167	-0.95675
30.030	-1.1836	-1.0290
32.020	-1.2355	-1.0920
34.030	-1.2569	-1.1484
36.020	-1.2412	-1.1980
38.020	-1.2287	-1.2428
40.000	-1.2380	-1.2828
42.020	-1.2517	-1.3198
44.020	-1.2539	-1.3530
46.050	-1.1658	-1.3839
48.070	-1.0419	-1.4121
50.060	-1.0119	-1.4376
55.020	-1.5086	-1.4934
60.070	-1.5621	-1.5408
65.130	-1.7019	-1.5809
70.190	-1.7787	-1.6154
75.320	-1.8194	-1.6456
80.200	-1.8458	-1.6708
85.440	-1.8653	-1.6946
90.530	-1.8824	-1.7152
95.570	-1.8966	-1.7334
100.61	-1.9095	-1.7498
110.69	-1.9315	-1.7781
120.65	-1.9507	-1.8015
130.88	-1.9662	-1.8218
140.90	-1.9805	-1.8389
151.06	-1.9912	-1.8538
161.12	-1.9973	-1.8668
171.17	-2.0026	-1.8783
181.24	-2.0030	-1.8885
191.29	-1.9995	-1.8976
201.34	-1.9861	-1.9058
221.49	-1.9650	-1.9200
241.64	-1.9157	-1.9319
261.79	-1.8534	-1.9419
281.90	-1.8070	-1.9505
302.00	-1.7640	-1.9580

Figure 3.29 χT (T) (diamagnetism removed) "dimere" fit for 3

Isotherm at 3K	
H/T	M-diamag. (emu/mol)
0.0000	-0.0053634
33.333	0.096128
66.667	0.18915
100.00	0.27941
133.33	0.37004
166.67	0.45949
200.00	0.54797
233.33	0.63714
266.67	0.72366
300.00	0.81429
333.33	0.89981
666.67	1.7536
1000.0	2.5879
1333.3	3.4131
1666.7	4.2285
2000.0	5.0414
2333.3	5.8445
2666.7	6.6359
3000.0	7.4255
3333.3	8.2004
4000.0	9.7367
4666.7	11.221
5333.3	12.667
6000.0	14.057
6666.7	15.391
7333.3	16.684
8000.0	17.911
8666.7	19.093
9333.3	20.205
10000	21.245
10667	22.241
11333	23.172
12000	24.055
12667	24.880
13333	25.657
14000	26.359
14667	27.056
15333	27.683
16000	28.250
16667	28.778

Isotherm at 1.8K	
H/T	M-diamag. (emu/mol)
0.0000	-0.016279
55.556	0.14278
111.11	0.28937
166.67	0.43548
222.22	0.58005
277.78	0.72313
333.33	0.86533
388.89	1.0071
444.44	1.1515
500.00	1.2887
555.56	1.4316
1111.1	2.8181
1666.7	4.1669
2222.2	5.5034
2777.8	6.8194
3333.3	8.1022
3888.9	9.3704
4444.4	10.613
5000.0	11.818
5555.6	12.998
6666.7	15.246
7777.8	17.343
8888.9	19.286
10000	21.073
11111	22.700
12222	24.179
13333	25.505
14444	26.700
15556	27.760
16667	28.708
17778	29.543
18889	30.272
20000	30.912
21111	31.479
22222	31.970
23333	32.396
24444	32.767
25556	33.083
26667	33.346
27778	33.568

Figure 3.30 χT (T) (diamagnetism removed) “dimere” fit for 1

T (K)	M*T/H (emu.K/Oe.mol) exp.	M*T/H (emu.K/Oe.mol) theor.	T (K)	M*T/H (emu.K/Oe.mol) exp.	M*T/H (emu.K/Oe.mol) theor.
1.7900	0.0024378	0.0022513	26.030	0.0029080	0.0022513
2.0000	0.0024947	0.0022513	28.030	0.0028964	0.0022513
2.2000	0.0025315	0.0022513	30.030	0.0029020	0.0022513
2.4000	0.0025492	0.0022513	32.020	0.0029284	0.0022513
2.6000	0.0025734	0.0022513	34.030	0.0030393	0.0022513
2.8000	0.0025934	0.0022513	36.020	0.0032735	0.0022513
3.0000	0.0026110	0.0022513	38.020	0.0035027	0.0022513
3.2000	0.0026264	0.0022513	40.000	0.0036482	0.0022513
3.4000	0.0026402	0.0022513	42.020	0.0037746	0.0022513
3.6000	0.0026551	0.0022513	44.020	0.0039446	0.0022513
3.8000	0.0026676	0.0022513	46.050	0.0045323	0.0022513
4.0000	0.0026780	0.0022513	48.070	0.0053265	0.0022513
4.2000	0.0026922	0.0022513	50.060	0.0056971	0.0022513
4.4000	0.0027052	0.0022513	55.020	0.0035293	0.0022513
4.6300	0.0028989	0.0022513	60.070	0.0035312	0.0022513
4.8100	0.0029047	0.0022513	65.130	0.0029186	0.0022513
5.0300	0.0029251	0.0022513	70.190	0.0026063	0.0022513
5.4700	0.0029569	0.0022513	75.320	0.0024897	0.0022513
5.9700	0.0029904	0.0022513	80.200	0.0024399	0.0022514
6.4900	0.0030172	0.0022513	85.440	0.0024327	0.0022515
6.9600	0.0030410	0.0022513	90.530	0.0024223	0.0022517
7.4800	0.0030751	0.0022513	95.570	0.0024221	0.0022522
7.9800	0.0030993	0.0022513	100.61	0.0024193	0.0022531
8.4700	0.0031233	0.0022513	110.69	0.0024187	0.0022572
8.9700	0.0031439	0.0022513	120.65	0.0024042	0.0022668
9.4900	0.0031693	0.0022513	130.88	0.0024061	0.0022874
9.9700	0.0031962	0.0022513	140.90	0.0023882	0.0023244
11.000	0.0032615	0.0022513	151.06	0.0023990	0.0023874
11.990	0.0033319	0.0022513	161.12	0.0024596	0.0024842
12.990	0.0034263	0.0022513	171.17	0.0025229	0.0026253
14.000	0.0035561	0.0022513	181.24	0.0026638	0.0028215
15.020	0.0034434	0.0022513	191.29	0.0028783	0.0030819
16.000	0.0034845	0.0022513	201.34	0.0032993	0.0034161
17.000	0.0035238	0.0022513	221.49	0.0040972	0.0043406
18.010	0.0035610	0.0022513	241.64	0.0056605	0.0056435
19.010	0.0035948	0.0022513	261.79	0.0077650	0.0073503
20.010	0.0036194	0.0022513	281.90	0.0096696	0.0094580
22.030	0.0036552	0.0022513	302.00	0.011658	0.011949
24.020	0.0029359	0.0022513			

Appendix 6

Crystal data and structure refinement: 2,3-dichlorophenyl-1,2,3,5-dithiadiazolyl

Identification code	shu13h	
Empirical formula	C7 H3 Cl2 N2 S2	
Formula weight	250.13	
Temperature	150(2) K	
Wavelength	0.71073 Å	
Crystal system	Monoclinic	
Space group	P2 ₁ /n	
Unit cell dimensions	a = 7.2936(14) Å	α = 90°.
	b = 13.572(3) Å	β = 101.468(3)°.
	c = 17.910(4) Å	γ = 90°.
Volume	1737.5(6) Å ³	
Z	8	
Density (calculated)	1.912 Mg/m ³	
Absorption coefficient	1.170 mm ⁻¹	
F(000)	1000	
Crystal size	0.44 x 0.28 x 0.28 mm ³	
Theta range for data collection	1.90 to 28.36°.	
Index ranges	-9 ≤ h ≤ 9, -17 ≤ k ≤ 18, -18 ≤ l ≤ 23	
Reflections collected	11155	
Independent reflections	4145 [R(int) = 0.1670]	
Completeness to theta = 28.36°	95.5 %	
Absorption correction	Semi-empirical from equivalents	
Max. and min. transmission	0.7353 and 0.6270	
Refinement method	Full-matrix least-squares on F ²	
Data / restraints / parameters	4145 / 0 / 236	
Goodness-of-fit on F ²	1.219	
Final R indices [I > 2σ(I)]	R1 = 0.1625, wR2 = 0.3651	
R indices (all data)	R1 = 0.1919, wR2 = 0.3733	
Extinction coefficient	0.0021(8)	
Largest diff. peak and hole	1.907 and -1.413 e.Å ⁻³	

Table 2. Atomic coordinates ($\times 10^4$) and equivalent isotropic displacement parameters ($\text{\AA}^2 \times 10^3$)

for shu13h. $U(\text{eq})$ is defined as one third of the trace of the orthogonalized U^{ij} tensor.

	x	y	z	$U(\text{eq})$
Cl(1A)	2695(4)	7715(2)	2544(2)	17(1)
Cl(2A)	4136(5)	9466(2)	3629(2)	18(1)
S(1A)	2270(5)	6395(3)	258(2)	21(1)
S(2A)	1658(6)	7545(3)	-533(2)	22(1)
N(1A)	2947(16)	7130(8)	990(6)	15(2)
N(2A)	2270(20)	8411(8)	102(6)	21(3)
C(1A)	3521(19)	8768(10)	2181(7)	16(3)
C(2A)	4164(19)	9550(10)	2655(7)	17(3)
C(3A)	4838(18)	10391(10)	2409(7)	16(3)
C(4A)	4864(18)	10494(11)	1627(8)	20(3)
C(5A)	4190(20)	9737(10)	1124(8)	18(3)
C(6A)	3524(19)	8863(10)	1398(8)	17(3)
C(7A)	2850(20)	8084(10)	809(8)	19(3)
Cl(1B)	7732(4)	7719(2)	2596(2)	18(1)
Cl(2B)	9153(5)	9423(3)	3728(2)	20(1)
S(1B)	7927(5)	6416(3)	346(2)	20(1)
S(2B)	7406(5)	7552(3)	-459(2)	21(1)
N(1B)	8405(18)	7159(9)	1078(7)	19(2)
N(2B)	7670(20)	8426(10)	164(7)	27(3)
C(1B)	8572(19)	8790(9)	2255(7)	16(2)
C(2B)	9191(19)	9555(10)	2763(7)	16(3)
C(3B)	9825(18)	10421(9)	2536(8)	16(2)
C(4B)	9920(19)	10539(11)	1750(8)	21(3)
C(5B)	9348(18)	9789(10)	1244(7)	16(3)
C(6B)	8683(19)	8894(10)	1483(7)	16(2)
C(7B)	8213(19)	8118(9)	912(7)	14(2)

Appendix 7

Crystal data and structure refinement 3,4-dichlorophenyl-1,2,3,5-dithiadiazolyl

Identification code	shu23a	
Empirical formula	C7 H3 Cl2 N2 S2	
Formula weight	250.13	
Temperature	150(2) K	
Wavelength	0.71073 Å	
Crystal system	Monoclinic	
Space group	P2 ₁ /c	
Unit cell dimensions	a = 7.1961(13) Å	α = 90°.
	b = 11.779(2) Å	β = 97.245(3)°.
	c = 20.874(4) Å	χ = 90°.
Volume	1755.2(5) Å ³	
Z	8	
Density (calculated)	1.893 Mg/m ³	
Absorption coefficient	1.158 mm ⁻¹	
F(000)	1000	
Crystal size	0.31 x 0.28 x 0.21 mm ³	
Theta range for data collection	1.97 to 28.26°.	
Index ranges	-9<=h<=9, -15<=k<=10, -27<=l<=26	
Reflections collected	10344	
Independent reflections	4089 [R(int) = 0.0835]	
Completeness to theta = 28.26°	93.7 %	
Absorption correction	Semi-empirical from equivalents	
Max. and min. transmission	0.7930 and 0.7153	
Refinement method	Full-matrix least-squares on F ²	
Data / restraints / parameters	4089 / 0 / 235	
Goodness-of-fit on F ²	1.138	
Final R indices [I>2sigma(I)]	R1 = 0.0848, wR2 = 0.1894	
R indices (all data)	R1 = 0.1146, wR2 = 0.2001	
Largest diff. peak and hole	0.774 and -0.704 e.Å ⁻³	

Table 2. Atomic coordinates ($\times 10^4$) and equivalent isotropic displacement parameters ($\text{\AA}^2 \times 10^3$) for SHU23A. $U(\text{eq})$ is defined as one third of the trace of the orthogonalized U^{ij} tensor.

	x	y	z	$U(\text{eq})$
Cl(1A)	5002(2)	2170(2)	1131(1)	28(1)
Cl(2A)	6410(3)	4585(2)	698(1)	29(1)
S(1A)	6274(3)	2218(2)	4439(1)	30(1)
S(2A)	6546(3)	3940(2)	4679(1)	27(1)
N(1A)	6157(9)	2434(5)	3664(3)	28(1)
N(2A)	6525(9)	4359(5)	3932(3)	28(1)
C(1A)	5734(9)	2972(6)	2334(3)	21(1)
C(2A)	5732(10)	3221(6)	1694(3)	23(1)
C(3A)	6355(9)	4272(6)	1501(3)	21(1)
C(4A)	6867(9)	5105(6)	1962(3)	22(1)
C(5A)	6858(10)	4871(6)	2609(3)	23(1)
C(6A)	6275(9)	3800(6)	2805(3)	21(1)
C(7A)	6329(9)	3528(6)	3503(3)	22(1)
Cl(1B)	22(2)	2143(1)	1263(1)	25(1)
Cl(2B)	1554(3)	4562(2)	892(1)	26(1)
S(1B)	636(3)	2033(2)	4561(1)	27(1)
S(2B)	1025(3)	3737(2)	4831(1)	26(1)
N(1B)	745(9)	2279(5)	3794(3)	26(1)
N(2B)	1161(9)	4186(5)	4097(3)	27(1)
C(1B)	646(9)	2872(6)	2488(3)	22(1)
C(2B)	748(9)	3147(6)	1849(3)	22(1)
C(3B)	1418(9)	4214(6)	1692(3)	19(1)
C(4B)	1952(10)	4997(6)	2167(3)	22(1)
C(5B)	1846(9)	4725(6)	2815(3)	22(1)
C(6B)	1183(9)	3669(6)	2976(3)	21(1)
C(7B)	1037(10)	3368(6)	3653(3)	22(1)

Appendix 8

Crystal data and structure refinement 3,5-dibromophenyl-1,2,3,5-dithiadiazolyl

Identification code	shu8a
Empirical formula	C7 H3 Br2 N2 S2
Formula weight	339.05
Temperature	150(2) K
Wavelength	0.71073 Å
Crystal system	Monoclinic
Space group	C2/c
Unit cell dimensions	a = 15.0126(12) Å $\alpha = 90^\circ$ b = 16.3582(13) Å $\beta = 113.9450(10)^\circ$ c = 16.9218(14) Å $\gamma = 90^\circ$
Volume	3798.0(5) Å ³
Z	16
Density (calculated)	2.372 Mg/m ³
Absorption coefficient	8.925 mm ⁻¹
F(000)	2576
Crystal size	0.45 x 0.45 x 0.30 mm ³
Theta range for data collection	1.94 to 28.36°.
Index ranges	-20 ≤ h ≤ 20, -21 ≤ k ≤ 21, -11 ≤ l ≤ 21
Reflections collected	12343
Independent reflections	4539 [R(int) = 0.0493]
Completeness to theta = 28.36°	95.3 %
Absorption correction	Semi-empirical
Max. and min. transmission	0.1749 and 0.1078
Refinement method	Full-matrix least-squares on F ²
Data / restraints / parameters	4539 / 0 / 235
Goodness-of-fit on F ²	1.109
Final R indices [I > 2σ(I)]	R1 = 0.0354, wR2 = 0.0939
R indices (all data)	R1 = 0.0452, wR2 = 0.1101
Largest diff. peak and hole	1.146 and -1.941 e.Å ⁻³

Table 2. Atomic coordinates ($\times 10^4$) and equivalent isotropic displacement parameters ($\text{\AA}^2 \times 10^3$) for Shu8a. $U(\text{eq})$ is defined as one third of the trace of the orthogonalized U^{ij} tensor.

	x	y	z	$U(\text{eq})$
Br(1A)	8735(1)	3063(1)	-3278(1)	21(1)
Br(2A)	4890(1)	4057(1)	-3910(1)	22(1)
S(1A)	7739(1)	6267(1)	-297(1)	22(1)
S(2A)	9172(1)	5864(1)	65(1)	19(1)
N(1A)	7301(2)	5734(2)	-1193(2)	22(1)
N(2A)	8905(2)	5241(2)	-754(2)	19(1)
C(1A)	8249(3)	4249(2)	-2283(2)	18(1)
C(2A)	7876(3)	3735(2)	-2997(2)	17(1)
C(3A)	6885(3)	3667(2)	-3500(2)	17(1)
C(4A)	6253(3)	4140(2)	-3267(2)	20(1)
C(5A)	6593(3)	4655(2)	-2553(2)	18(1)
C(6A)	7601(3)	4716(2)	-2064(2)	15(1)
C(7A)	7957(3)	5254(2)	-1306(2)	17(1)
Br(1B)	5094(1)	6497(1)	-1097(1)	25(1)
Br(2B)	1044(1)	6926(1)	-2881(1)	21(1)
S(1B)	2470(1)	9679(1)	669(1)	21(1)
S(2B)	3991(1)	9556(1)	1234(1)	22(1)
N(1B)	2316(2)	8978(2)	-70(2)	19(1)
N(2B)	4016(2)	8828(2)	592(2)	20(1)
C(1B)	3959(3)	7595(2)	-560(2)	18(1)
C(2B)	3933(3)	7021(2)	-1189(2)	16(1)
C(3B)	3076(3)	6823(2)	-1877(2)	20(1)
C(4B)	2219(3)	7208(2)	-1935(2)	18(1)
C(5B)	2218(3)	7782(2)	-1337(2)	19(1)
C(6B)	3101(3)	7981(2)	-649(2)	16(1)
C(7B)	3136(3)	8625(2)	-11(2)	17(1)

Appendix 9

Crystal data and structure refinement

p-iodophenyl-1,2,3,5-dithiadiazolyl

Identification code	shu6m	
Empirical formula	C7 H4 I N2 S2	
Formula weight	307.14	
Temperature	150(2) K	
Wavelength	0.71073 Å	
Crystal system	Monoclinic	
Space group	P2 ₁ /n	
Unit cell dimensions	a = 5.7193(7) Å	α = 90°.
	b = 8.6096(11) Å	β = 97.054(2)°.
	c = 18.320(2) Å	χ = 90°.
Volume	895.26(19) Å ³	
Z	4	
Density (calculated)	2.279 Mg/m ³	
Absorption coefficient	3.984 mm ⁻¹	
F(000)	580	
Crystal size	0.20 x 0.10 x 0.10 mm ³	
Theta range for data collection	2.24 to 28.31°.	
Index ranges	-7<=h<=7, -10<=k<=11, -19<=l<=24	
Reflections collected	5746	
Independent reflections	2139 [R(int) = 0.0771]	
Completeness to theta = 28.31°	95.5 %	
Absorption correction	Semi-empirical	
Max. and min. transmission	0.6914 and 0.5030	
Refinement method	Full-matrix least-squares on F ²	
Data / restraints / parameters	2139 / 0 / 109	
Goodness-of-fit on F ²	0.995	
Final R indices [I>2σ(I)]	R1 = 0.0478, wR2 = 0.1016	
R indices (all data)	R1 = 0.0756, wR2 = 0.1125	
Largest diff. peak and hole	1.772 and -1.464 e.Å ⁻³	

Table 2. Atomic co-ordinates ($\times 10^4$) and equivalent isotropic displacement parameters ($\text{\AA}^2 \times 10^3$)

for shu6m. $U(\text{eq})$ is defined as one third of the trace of the orthogonalized U^{ij} tensor.

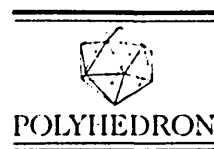
	x	y	z	$U(\text{eq})$
I(1)	7036(1)	1808(1)	2402(1)	39(1)
S(1)	5942(2)	-4301(2)	6110(1)	30(1)
S(2)	2376(2)	-4381(2)	5673(1)	29(1)
N(1)	6676(8)	-3079(5)	5494(3)	27(1)
N(2)	2700(8)	-3205(5)	4996(3)	26(1)
C(1)	6244(9)	405(6)	3273(3)	28(1)
C(2)	4087(10)	-299(7)	3249(3)	32(1)
C(3)	3633(9)	-1266(7)	3812(3)	30(1)
C(4)	5371(9)	-1606(5)	4395(3)	23(1)
C(5)	7564(9)	-855(5)	4402(3)	22(1)
C(6)	7997(9)	138(6)	3853(3)	29(1)
C(7)	4902(9)	-2654(6)	4990(3)	24(1)



PERGAMON

www.elsevier.nl/locate/poly

Polyhedron 19 (2000) 1163–1166



Modification of the solid state structures of dithiadiazolyl radicals: crystal structure of *p*-iodophenyl-1,2,3,5-dithiadiazolyl

Neil Bricklebank^{a,*}, Stephen Hargreaves^a, Sharon E. Spey^b

^a Division of Chemistry and Materials Research Institute, Sheffield Hallam University, City Campus, Sheffield S1 1WB, UK

^b Department of Chemistry, University of Sheffield, Western Bank, Sheffield S3 7HF, UK

Received 4 January 2000; accepted 27 March 2000

Abstract

The solid state structure of the 1,2,3,5-dithiadiazolyl *p*-IC₆H₄CN₂SSN (**3**) is described. The molecules associate in dimer pairs, across an inversion centre, in an unusual *trans*-cofacial manner. The separation between the heterocyclic rings is 3.121 Å. The intradimer sulfur contacts (3.696 Å) are larger than those observed in dithiadiazolyls that associate in the more usual *cis*-cofacial manner. Individual *p*-IC₆H₄CN₂SSN molecules are linked into zigzag chains through weak I⋯S interactions (3.82 Å); each half of a [*p*-IC₆H₄CN₂SSN]₂ dimer is a member of separate chains that run in opposite directions. ©2000 Elsevier Science Ltd. All rights reserved.

Keywords: Dithiadiazolyl radicals

1. Introduction

In recent years, 1,2,3,5-dithiadiazolyl (DTDA) radicals have been studied as building blocks for the design and synthesis of molecular magnets [1–5] and conductors [6–9]. The steric and electronic effects of the substituent R can be used to modify the molecular structure and hence the physical behaviour of the radical. In the solid state the majority of DTDA radicals associate as spin-paired dimers through the formation of out-of-plane intermolecular S⋯S interactions (Fig. 1) with a typical intermolecular separation in the range 3.0–3.2 Å. Crystal engineering of DTDA has focused on obtaining materials in which the radicals are aligned into infinite chains or stacked in columns; one of the principal tools used to achieve this has been to use nitrile groups as structure-influencing supramolecular synthons [1,2,8,9]. The idea behind this strategy stemmed from the structure of *p*-iodobenzonitrile [10] and the cyanogen halides [11], which associate as ribbon-like chains through weak X⋯CN interactions. Similarly, cyano-functionalised DTDA (e.g. compounds **1** and **2**) also associate as chains through CN⋯S interactions [1,2,8].

Halogen atoms can also have a marked effect on the molecular packing, although only fluorinated systems have received extensive study [1–4,12,13]. Partial fluorination of the aryl

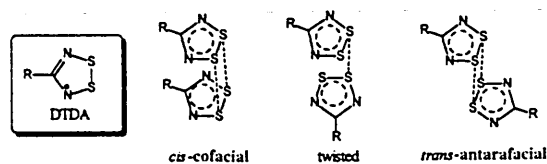


Fig. 1. Modes of dimerisation for DTDA radicals.

group can lead to the disruption of the dimerisation process: for example, [2,3-F₂C₆H₃CN₂SSN]₂ associates as an unusual twisted dimer [12], whereas 2,5-F₂C₆H₃CN₂SSN assembles in uniform stacks with an unusually long interannular spacing [3.54(3) Å] [12]. Total fluorination results in more dramatic changes: both *p*-NCC₆F₄CN₂SSN (**2**) [1–3] and *p*-BrC₆F₄CN₂SSN [4] do not associate as dimers and consequently are paramagnetic at room temperature. The latter compound associates in columns, whereas the combination of fluorine atoms and a nitrile group in compound **2** leads to a compound that assembles with a chain-like structure [1,2]. Upon cooling to below 36 K, one polymorph of compound **2** undergoes a transition to a weakly ferromagnetic state [3]. This is the highest ferromagnetic ordering temperature reported to date for a non-metallic molecular magnet.

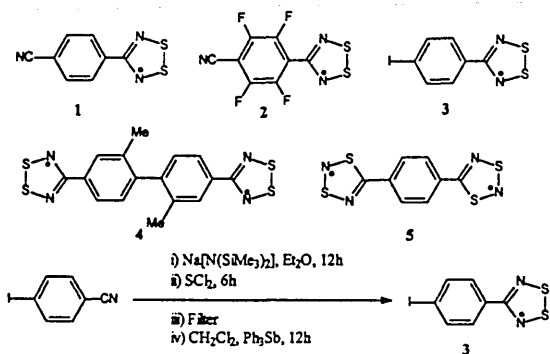
We are currently investigating the effect of the heavier halogen atoms on the supramolecular structures of dithiadiazolyl radicals. As part of this work, we decided to make *p*-iodophenyl-DTDA (**3**). In particular, we were keen to determine the structure-influencing properties of the iodine

* Corresponding author. Tel.: +44-114-225 4931; fax: +44-114-225 3066; e-mail: n.bricklebank@shu.ac.uk

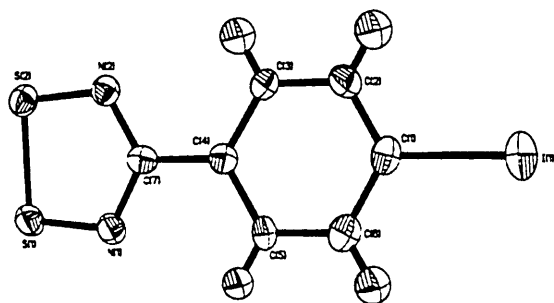
atom and to see whether it would also promote the assembly of the molecules into chains, as is observed for *p*-iodobenzonitrile and cyano-functionalised DTDAs (**1** and **2**).

2. Results and discussion

Compound **3** was prepared from *p*-iodobenzonitrile using a slightly modified version of the proven metal amidine route (Scheme 1). We have found that sodium bis(trimethylsilyl)amide gives slightly higher yields with iodo-, bromo- and chloro-substituted aromatic nitriles than lithium bis(trimethylsilyl)amide, which is usually employed in dithiadiazolyl synthesis [14]. Crystals suitable for X-ray diffraction were grown by vacuum sublimation as described in Section 4. The asymmetric unit of compound **3** (Fig. 2) contains one molecule of unexceptional geometry. The bond lengths and angles of the heterocycle (Table 1) are similar to those of other members of this class [14]. Within each molecule the aryl and dithiadiazolyl rings are essentially coplanar with a slight twist angle between the dithiadiazole ring [root mean square (r.m.s.) $\Delta = 0.0077 \text{ \AA}$] and the aryl ring [r.m.s. $\Delta = 0.0089 \text{ \AA}$] of 8° . However, compared with other DTDAs, the mode of association in compound **3** is unusual. Two *p*-IC₆H₄CN₂SSN molecules associate in a *trans*-cofacial manner across an inversion centre (Fig. 3). The only other example of a DTDA radical adopting this mode of association is the 2,2'-dimethylbiphenylene radical (**4**),



Scheme 1.



[14]. Indeed, the molecular structures of compounds **3** and **4** show many similarities with that of 5,5'-(1,4-phenylene)bis(1,3,2,4-dithiadiazolyl) (**5**), which contains short S...S (3.214 Å) and S...N (3.346 Å) interactions between parallel CN₂S₂ rings [15].

Individual *p*-IC₆H₄CN₂S₂N molecules in compound **3** are linked in a chain-like motif through a weak interaction between the iodine atom and one of the sulfurs of an adjacent molecule [$d(I1 \cdots S2) = 3.82$ Å]. The I...S distance is significantly longer than a conventional S–I bond [16] but is within bonding contact when compared with the sum of the van der Waal's radii of iodine and sulfur (which lies in the range 3.4–4.1 Å, depending on the orientation of the contact vector relative to the bonds) [17]. The distance between the iodine atom and the other sulfur atom of the disulfide bond [$d(I1 \cdots S1) = 4.068$ Å] is long and lies at the limit of the van der Waal's radius for a I...S contact, indicative of a very weak interaction. Each half of a [*p*-IC₆H₄CN₂S₂N]₂ dimer is a member of separate chains that run in opposite directions. Adjacent molecules within the molecular chains occupy orthogonal positions such that the chains have a 'zigzag' alignment (Fig. 4). Analogous Cl...S interactions are seen in the structure of [*p*-ClC₆H₄CN₂S₂N]₂, although in this derivative the molecules dimerise in a *cis*-cofacial manner [18]. The zigzag arrangement of the molecules in compound **3** contrasts with DTDAAs **1** and **2** and the parent *p*-iodobenzonitrile, all of which form linear chains.

In addition, it is well known that compounds containing carbon–iodine bonds can undergo metal-catalysed coupling reactions, with carbon–carbon bond formation. Thus, it is possible that compound **3** could be utilised in similar reactions, providing a new synthetic route to biphenyl-bis(dithiadiazolyl) derivatives.

3. Conclusions

From the results reported here we see that the iodine atom has a marked effect on the supramolecular structure of compound **3**. As anticipated, the iodine substituent promotes the assembly of the molecules into chains by interacting with the sulfur atom of an adjacent molecule. The *trans*-cofacial mode of dimerisation observed in compound **3** is unusual, and we speculate that the molecules dimerise in this way to alleviate steric hindrance between two iodine atoms that would occur if the molecules associated in a *cis*-cofacial manner. However, it is less obvious why the *trans*-antarafacial or twisted geometries are disfavoured in this instance.

4. Experimental

All reactions and manipulations were carried out under an atmosphere of dry nitrogen using standard double-manifold and glove box techniques. Solvents were dried, distilled and degassed prior to use. *p*-Iodobenzoyl chloride (Aldrich),

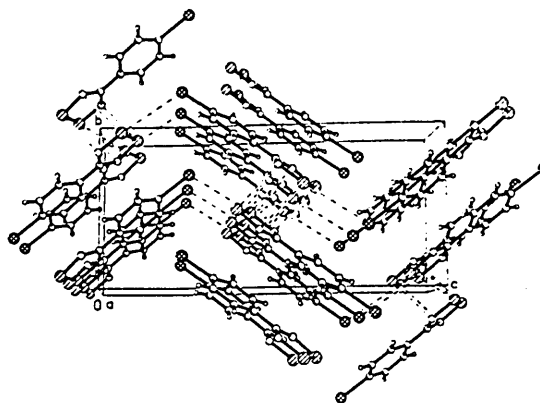


Fig. 4. Molecular packing of compound **3** parallel to crystallographic *a*-axis.

sodium bis(trimethylsilyl)amide (Aldrich), triphenylantimony (Aldrich), phosphorus pentoxide (Fisher) and sulfur dichloride (Fluka) were all obtained commercially and used as received.

4.1. *p*-Iodobenzonitrile

Finely powdered *p*-iodobenzoyl chloride (5.32 g, 0.02 mol) was slowly added to ice-cold 0.880 ammonia solution (20 ml). The mixture was then stirred for 2 h and allowed to warm to room temperature. The resulting precipitate, *p*-iodobenzamide, was filtered, washed with water and dried. The *p*-iodobenzamide was then transferred to a 250-cm³ round-bottom flask fitted with a side-arm and stopcock, together with a cold finger. An excess of phosphorus pentoxide was added to the flask and the reactants were thoroughly mixed. The flask was then heated in vacuo (130°C). Under these conditions the *p*-iodobenzonitrile product sublimes directly from the reaction mixture onto the cold finger as white needles. The *p*-iodobenzonitrile is then recovered and purified by a further vacuum sublimation (2.68 g, 59% yield; m.p. 124–126°C, lit. 124–125°C) [9]. ν_{\max} (cm⁻¹): 2225 (C≡N), 1578, 1475, 1390, 1054, 1010, 894, 541. δ_{H} (250 MHz; CDCl₃; Me₂Si): 7.85 (2H, d, *J* 8.3 Hz) 7.37 (2H, d, *J* 8.3 Hz). δ_{C} (250 MHz; CDCl₃; Me₂Si): 138.86, 133.53, 118.57, 112.09, 100.68. *m/e* 228.9 (m⁻), 102.0, 75.0.

4.2. 4-Iodophenyl-1,2,3,5-dithiadiazolyl

Sodium bis(trimethylsilyl)amide (1.673 g, 0.01 mol) and *p*-iodobenzonitrile (2.29 g, 0.01 mol) were stirred together in diethyl ether (50 cm³) at room temperature for 18 h. Sulfur dichloride (1.3 cm³, 0.02 mol) was slowly added, with cooling in an ice-bath, to produce an immediate orange precipitate which was stirred for 12 h, filtered off, washed with diethyl ether (3 × 10 cm³) and pumped to dryness. The crude product was then reduced in situ by adding dichloromethane (50 cm³) and triphenylantimony (0.176 g, 0.0005 mol). After 12 h, the dichloromethane was removed in vacuo. The residue was placed in a gradient sublimator (25–120°C, 10⁻³ torr). Under

these conditions, the product forms as deep red–black blocks (0.56 g, 18% yield; m.p. 172.5°C). Found: C, 27.13; H, 1.32; N, 9.05. $C_7H_4IN_2S_2$ requires: C, 27.37; H, 1.31; N, 9.12%. ν_{\max} (cm^{-1}): m/e 307.1 (m^+), 261.1, 229.1, 180.0, 134.1, 102.1, 77.9.

4.3. Crystal data

$C_7H_4IN_2S_2$ ($M = 307.14$) crystallises as deep red blocks; crystal dimensions $0.20 \times 0.10 \times 0.10$ mm. Monoclinic, $a = 5.7193(7)$, $b = 8.6096(11)$, $c = 18.320(2)$ Å, $\beta = 97.054(2)^\circ$, $U = 895.26(19)$ Å³, $Z = 4$, $D_c = 2.279$ Mg m⁻³, space group $P2_1/n$ (a non-standard setting of $P2_1/c$, C_{2h}^2 , No. 14), Mo K α radiation ($\lambda = 0.71073$ Å), μ (Mo K α) = 3.984 mm⁻¹, $F(000) = 580$. Data collected were measured on a Bruker Smart CCD area detector with Oxford Cryosystems low-temperature system. Cell parameters were refined from the setting angles of 111 reflections (θ range 2.24–28.31°). Reflections were measured from a hemisphere of data collected of frames each covering 0.3 degrees in omega. Of the 5746 reflections measured, all of which were corrected for Lorentz and polarisation effects and for absorption by semi-empirical methods based on symmetry-equivalent and repeated reflections (minimum and maximum transmission coefficients of 0.5030 and 0.6914), 1474 independent reflections exceeded the significance level $|F|/\sigma(|F|) > 4.0$. The structure was solved by direct methods and refined by full-matrix least-squares methods on F^2 . Hydrogen atoms were placed geometrically and refined with a riding model and with U_{iso} constrained to be 1.2 times U_{eq} of the carrier atom. Refinement converged at a final $R = 0.0478$ ($wR_2 = 0.1125$, for all 2139 data, 109 parameters, mean and maximum δ/σ 0.000, 0.000) with allowance for the thermal anisotropy of all non-hydrogen atoms. Minimum and maximum final electron density was -1.464 and 1.772 e Å⁻³. A weighting scheme $w = 1/[\sigma^2(F_o^2) + (0.0587P)^2 + 0.00P]$, where $P = (F_o^2 + 2F_c^2)/3$ was used in the latter stages of refinement. Complex scattering factors were taken from the program package SHELXTL [19] as implemented on a Viglen Pentium computer.

Supplementary data

Supplementary data are available from the CCDC, 12 Union Road, Cambridge CB2 1EZ, UK (fax: +44-1223-336033; e-mail: deposit@ccdc.cam.ac.uk) on request, quoting the deposition number 137/938.

Acknowledgements

We would like to thank Sheffield Hallam University for a studentship (S.H.), the Royal Society for an equipment grant (N.B.) and the Royal Society of Chemistry Research Fund and the Nuffield Foundation for financial support (N.B.).

References

- [1] A.J. Banister, N. Bricklebank, W. Clegg, M.R.J. Elsegood, C.I. Gregory, I. Lavender, J.M. Rawson, B.K. Tanner, *J. Chem. Soc., Chem. Commun.* (1995) 679.
- [2] A.J. Banister, N. Bricklebank, I. Lavender, J.M. Rawson, C.I. Gregory, B.K. Tanner, W. Clegg, M.R.J. Elsegood, F. Palacio, *Angew. Chem., Int. Ed. Engl.* 35 (1996) 2533.
- [3] F. Palacio, G. Antorrena, M. Castro, R. Burriel, J.M. Rawson, J.N.B. Smith, N. Bricklebank, J. Novoa, C. Ritter, *Phys. Rev. Lett.* 79 (1997) 2336.
- [4] G. Antorrena, J.E. Davies, M. Hartley, F. Palacio, J.M. Rawson, J.N.B. Smith, A. Steiner, *Chem. Commun.* (1999) 1393.
- [5] T.M. Barclay, A.W. Cordes, N.A. George, R.C. Haddon, M.E. Itkis, R.T. Oakley, *Chem. Commun.* (1999) 2269.
- [6] A.W. Cordes, R.C. Haddon, R.T. Oakley, *Adv. Mater.* 6 (1994) 798.
- [7] C.D. Bryan, A.W. Cordes, R.M. Fleming, N.A. George, S.H. Glarum, R.C. Haddon, R.T. Oakley, T.T.M. Palstra, A.S. Perel, L.F. Schneemeyer, J.V. Waszczak, *Nature* 365 (1993) 821.
- [8] A.W. Cordes, R.C. Haddon, R.G. Hicks, R.T. Oakley, T.T.M. Palstra, *Inorg. Chem.* 31 (1992) 1802.
- [9] A.W. Cordes, C.M. Chamchoumis, R.G. Hicks, R.T. Oakley, K.M. Young, R.C. Haddon, *Can. J. Chem.* 70 (1992) 919.
- [10] E.O. Schlemper, D. Britton, *Acta Crystallogr.* 18 (1965) 419.
- [11] R.B. Heiart, G.B. Carpenter, *Acta Crystallogr.* 9 (1956) 60.
- [12] A.J. Banister, A.S. Batsanov, O.G. Dawe, P.L. Herbertson, J.A.K. Howard, S. Lynn, I. May, J.N.B. Smith, J.M. Rawson, T.E. Rogers, B.K. Tanner, G. Antorrena, F. Palacio, *J. Chem. Soc., Dalton Trans.* (1997) 2539.
- [13] A.M.T. Bell, J.N.B. Smith, J.P. Attfield, J.M. Rawson, K. Shankland, W.I.F. David, *New J. Chem.* (1999) 565.
- [14] A.J. Banister, I. Lavender, J.M. Rawson, *Adv. Heterocycl. Chem.* 62 (1995) 137.
- [15] A.J. Banister, J.M. Rawson, W. Clegg, S.L. Birkby, *J. Chem. Soc., Dalton Trans.* (1991) 1099.
- [16] N. Bricklebank, P.J. Skabara, D.E. Hibbs, M. Hursthouse, K.M.A. Malik, *J. Chem. Soc., Dalton Trans.* (1999) 3007.
- [17] S.C. Nyburg, C.H. Faerman, *Acta Crystallogr., Sect. B* 41 (1985) 274.
- [18] R.T. Boere, K.H. Moock, M. Parvez, *Z. Anorg. Allg. Chem.* 620 (1994) 1589.
- [19] SHELXTL. An integrated system for solving and refining crystal structures from diffraction data (revision 5.1), Bruker AXS Ltd.